ANALYSIS OF

ELASTIC ARCHES

THREE-HINGED, TWO-HINGED,
AND HINGELESS

OF

STEEL, MASONRY,

AND

REINFORCED CONCRETE

BY

JOSEPH W. BALET
Consulting Engineer

NEW YORK
THE ENGINEERING NEWS PUBLISHING COMPANY
LONDON
ARCHIBALD CONSTABLE & COMPANY, LIMITED,
10 ORANGE STREET, LEICESTER SQUARE, W. C.
1908

ROBERT DRUMMOND COMPANY, PRINTERS, NEW YORK

PREFACE.

THE application of the elastic theory to the analysis of the stresses in arches, particularly in the case of the fixed or hingeless masonry arch, is exceedingly limited, notwithstanding the acknowledged fact that it is the only exact and reliable method of procedure. The reason is that, as usually presented, its application to the solution of a problem involves much labor, and the practi'ing engineer finds it difficult to devote the time and the concentrated study which its use demands.

This book is presented to the engineering profession as an exposition of a new system of treating the subject. By its use the stresses are obtained with absolute certainty, and the process of application is so clear and simple that the author is confident it will be found preferable to the forms of analysis now in general use.

Two steps are preliminary to its application:

The first is the special graphical construction employed in defining the exterior forces, their relations to each other, and their combination into force diagrams. This makes possible a clear conception of the problem as applied to each element of the arch. It is a marked advance over the usual procedure, as it presents to the eye a picture of the exterior forces, and shows clearly all the features of the analysis and their mutual dependence.

The second step is due to the discovery that there is a characteristic common to all arches of the same type, this characteristic being expressed by the intersection locus and the tangent curves used for the resolution of the exterior forces into their components. This makes possible an investigation to determine how the characteristic changes with the change in the form of the arch; and little effort is then required to present this relation in a graphical form, from which conclusions applicable to the solution of the problem can readily be derived. The second step in the solution is derived from the algebraic equations which define the elastic theory, and it would be difficult to express anything new thereon, or to put it in a clearer form than the one in which it has been presented by such scientists

as Winkler, Mohr, Müller-Breslau, Weyrauch, Sternberg, Grashof, Melan, and others. The author can only lay claim to a simple definition of the elastic theory as applied to the crescent-shaped arch, which compares favorably with the expressions for this same type of bridge given by the above-mentioned authorities. All these analytical expressions are compiled in the Appendix.

Where the author's method materially differs from those now generally used is, in the first place, in the graphical construction which defines the forces. He presents a method which applies to all problems, and which at the same time retains all the axiomatic truths of the elastic theory, without the necessity of approximations and assumptions that would throw doubt on its conclusions. This, however, was but one step in advance, and another was still necessary before the application of the elastic theory could attain that simplicity of execution so requisite for efficient designing.

It may generally be said that the stresses in the arch are defined by an intersection locus and tangent curves; when these are once found, the special graphical method is readily applicable.

All arches have their own loci and tangent curves; the author found, in addition, that they have a property in common, namely, the area enclosed by the arch axis and the straight line joining its ends. All changes in the form of the arch can be expressed in terms of this characteristic. This led at once to the conclusion that the characteristic, or the elements expressed by it, viz., the intersection locus and the tangent curves, could be reduced to a standard, and that any changes in form could be reduced to factors which referred to this standard.

The characteristic selected by the author is the parabola, since the expressions for its ordinates, its area, and its center of gravity are all in the simplest terms. All other forms of arches are expressed with reference to this standard. The manner in which this is done is fully explained in the book and analyzed in the Appendix, the only deviation being in the case of the spandrel-braced arch. The reason for this, as explained in Chapter III, Arts. 7 to 14, is that the arch axis is not well defined in such a structure. To surmount this difficulty the author had recourse to the laws of Maxwell, Castigliano, and others, as applied to the displacement theory, and with this assistance he was able to bring this arch within the scope of the standard method.

Chapter I discusses the various forces in the arch, and is in the nature of an introduction to prepare the reader for a clear understanding of the succeeding chapters.

Chapter II explains the special combinations of the forces, and, to interest the student, this explanation has not been put in algebraic form, but is demonstrated by computing graphically the stresses in three-hinged arches of various forms and materials.

Chapter III deals with two-hinged arches of various forms, Arts. 7 to 14 relating to the application of the displacement theory, and

Arts. 18 to 21 to the application of the elastic theory in its general form. This application is demonstrated by an analysis of the stresses in the Douro Bridge, showing the reasoning which guided the author in working out his method.

Chapter IV is devoted to what is known as the "stiff," or "fixed," arch, or, more properly, in the opinion of the author, as the "hingeless" arch.

The application of the elastic theory to the computation of stresses in this type of arch, and especially the masonry arch, is now recognized as the only reliable method. This opinion has been repeatedly expressed by many authorities on the subject; for instance, Mr. David A. Molitor, in the Transactions of the American Society of Civil Engineers, No. 834, July, 1898, says:

"In matters pertaining to the design of fixed (hingeless) masonry arches, it is safe to say that the method based on the theory of elasticity is the only one entitled to full confidence, and permitting of an analysis corresponding in accuracy with the knowable properties of the material. All other methods are too approximate to admit of close designing, such as the modern status of engineering science would generally demand.

"This modern and most exact method, however, is not free from criticism. While the fundamental principles of the theory are almost axiomatic, their final application to the solution of stresses is extremely complicated, so much so that few engineers can be credited with the patience and earnest endurance to master either the method or the solution of a problem to which it is applied.

"Therefore, unless the masonry arch can be so treated as to combine clearness, simplicity, undoubted accuracy, and economy in design with faultless construction, the field of usefulness of this class of structure will remain restricted, and such monuments as the Cabin John Bridge will continue to remain curiosities of rare production.

"This is not what the masonry arch deserves in view of its practically everlasting life, nominal cost of maintenance and naturally esthetic form, which latter should be a prime factor, though rarely given much consideration, in the choice of a bridge."

To this the author would add that, where natural conditions are favorable, an arch of masonry, and especially of reinforced concrete, can successfully compete with a steel structure as regards cost of construction. The cost of maintenance of the former is practically nil, and its life is measured by centuries, where that of the latter is only counted by years.

By the use of the method demonstrated in this book, the elastic theory as applied to masonry arches has been reduced to the simplest and clearest form for analyzing the stresses. For this purpose a masonry arch has been used as an example. The application of the elastic theory in its general form has been demonstrated by analyzing the stresses in the masonry arch over the Syra Valley, near Plauen, Saxony.

Chapter V treats of the distribution of the stresses in an arch rib of metal, stone, or reinforced concrete. Formulas have been appended to this chapter dealing with the stresses in columns of steel, stone and reinforced concrete, and with the stresses in reinforced-concrete beams and slabs. This part of the chapter is more in the nature of a memorandum than a treatise on these subjects, and for further information the reader is referred to the authorities cited.

Chapter VI (also in the nature of a memorandum) deals with wind stresses, the forces acting on the arch, and the good and bad qualities of the various types of arches. In preparing the latter, Schäffer and Melan were frequently consulted. No arch should be designed without a consideration of the principles presented in Arts. 6 and 7. In addition, some recommendations have been made regarding the stresses in piers and abutments, and at the end of the chapter tables have been added giving the standard loading of bridges according to American practice.

The Appendix (Chapters VII, VIII, and IX) is devoted to the algebraic deductions and expressions of the elastic theory as applied to arches, and (Chapter X) to the displacement theory.

JOSEPH W. BALET.

NEW YORK, November, 1907.

CONTENTS.

CHAPTER I.

THE ARCH RIB.

PAGE

The Exterior Forces of the Arch 1
The Application of the Elastic Theory 3
Components, Axial Force, Shearing Force 7
Line of Pressure 7
Line of Resistance 8
Intersection Locus and Tangent Curves 8
Maximum and Minimum Stresses 9
Division Lines 10
Loading Causing Maximum and Minimum Stresses in the Members of a Framed Arch 11

CHAPTER II.

THREE-HINGED ARCHES.

Three-Hinged Braced Arch 13
(Graphical determination of stresses.)
Three-Hinged Braced Roof-Truss 20
Three-Hinged Steel Arch Rib 22
(Flange stresses, web stresses, and deflections.)
Three-Hinged Arch Rib of Masonry, Concrete, or Reinforced Concrete 29
(Computation of stresses.)

CHAPTER III.

THE TWO-HINGED ARCH.

The Standard Diagram 36
Stress Analysis of the Two-Hinged Arch Rib 39
Temperature and Secondary Stresses 39
Deflections 42
Two-Hinged Arch Bridge (Curved I-Beam of Steel) 42
Computation of Stresses in a Two-Hinged Arch Rib of Parabolic Form—Example 45

PAGE
The Spandrel-Braced Two-Hinged Arch.... 51
The Williot Diagram.... 53
Correction of the Standard Intersection Locus.... 56
Computation of the Temperature Stresses.... 57
Two-Hinged Spandrel-Braced Arch with Curved Upper Chord.... 59
The Use of Deflection Angles for the Computation of the Intersection Locus. 60
Deflections of the Two-Hinged Spandrel-Braced Arch.... 64
Deflections of the Three-Hinged Spandrel-Braced Arch.... 67
Computation of Stresses in a Two-Hinged Spandrel-Braced Arch—Example. 70
Two-Hinged Arch with Variable Moment of Inertia.... 75
Crescent-Shaped Roof-Truss—Example.... 77

THE DOURO BRIDGE.

Computation of the Intersection Locus for the Two-Hinged Arch—General Method.... 84
Horizontal Forces.... 90
Deflections Caused by Vertical Forces.... 92
Deflections Caused by Horizontal Forces.... 96

CHAPTER IV.

HINGELESS ARCHES.

Introductory.... 100
Computation of Stresses: Vertical Loads.... 106
Horizontal Forces Acting in a Longitudinal Direction.... 118
Use of the Standard Diagram.... 120
Influence of Change of Form on the Arch.... 124

SYRA VALLEY BRIDGE.

Determination of the Intersection Locus and Tangent Curves for the Hingeless Arch—General Method.... 126
Horizontal Forces.... 140
Correction of the Intersection Locus and Tangent Curves.... 141
Analytical Computation of the Line of Pressure.... 154
Deflections of the Hingeless Arch and their Influence on the Erection... 159
Deflections of the Hingeless Arch Caused by Temperature Changes, Shrinkage of Masonry, and Yielding of the Abutments.... 163

CHAPTER V.

STRESSES IN ARCH SECTIONS—DISTRIBUTION OF STRESSES OVER AN IRREGULAR AREA UNDER NORMAL LOAD.

Stresses in a Bar Subjected to Compression and Bending.... 170
Distribution of the Stresses in an Arch Rib of Any Arbitrary Section—Example.... 174
Distribution of the Stresses in a Solid Arch Rib.... 175
Stresses in a Reinforced-Concrete Arch Section.... 178
Column Formulas for Stone and Reinforced Concrete.... 191
Column Formulas for Steel and Wood.... 196
Bending Moments and Shearing Forces in Beams.... 199
Longitudinal Stresses in a Reinforced Beam Subjected to Bending.... 202
Strength of Materials in Tension—Table XI.... 206
Ultimate Resistance of Materials to Compression—Table XII.... 206

CHAPTER VI.

STRESSES CAUSED BY LATERAL WIND PRESSURE.

PAGE
Standard System of Equivalent Loads (per Foot per Track) for Railway Bridges—Table XIII 213
Highway Bridges—Live Load per Square Foot—Table XIV 214
Highway Bridges—Electric Railway—Loads per Linear Foot of Track—Table XV 215
Impact Coefficients—Table XVI 216
Determination of the Type of Arch 218
Comparison of the Stresses and Deflections in the Three Types of Arches .. 210
The Abutments 227
The Intermediate Piers 229
Dimensions of Existing Arches 231
Dimensions of Wrought-Iron and Steel Arches and Roofs—Tables XVII and XVIII 232, 233
Dimensions of Masonry Arches—Table XIX 234–236

APPENDIX.

Notation 237

CHAPTER VII.

MATHEMATICAL ANALYSIS OF THE ELASTIC ARCH.

Relation Between the Exterior Forces and the Interior Stresses in the Arch 239
Analysis of the Change of Form of an Arch Rib 244
(Change in the length of the axis of a curved beam and in the length of its coördinates—Application of foregoing to the computation of the horizontal-thrust curve and the deflections caused by horizontal loads, vertical loads, and temperature changes for the three-hinged arch.)

CHAPTER VIII.

THE TWO-HINGED ARCH RIB.
(A Continuation of Chapter III.)

Computation of the Horizontal Thrust Caused by Vertical and Horizontal Forces, Temperature and Secondary (axial) Stresses 258
Special Equations for Determining the Horizontal Thrust 263
Deflections in Two-Hinged Arches 281

CHAPTER IX.

THE HINGELESS ARCH.
(A Continuation of Chapter IV.)

General Equations for Computing the Horizontal Thrust Caused by Vertical and Horizontal Loads, Temperature and Secondary (axial) Stresses 286

PAGE
Special Equations 296
Deflections.. 299

CHAPTER X.

ARCHED FRAMEWORKS.

ANALYSIS OF THE DISPLACEMENT THEORY FOR THE DETERMINATION OF STRESSES IN ARCHES.

Horizontal Thrust in the Two-Hinged Arch 302

INDEX.. 311

ANALYSIS OF ELASTIC ARCHES.

CHAPTER I.

THE ARCH RIB.

The Exterior Forces of the Arch. Application of the Elastic Theory.

The Exterior Forces of the Arch.—A curved beam is generated by moving the center of gravity of a plane figure along a curve of simple curvature, the plane maintaining a position at right angles to the curve during the motion. This curve will be called the axis of the beam, and the exterior forces must be located in the same plane in which the curve lies.

If the exterior forces are known, the interior forces in any section of the beam are known.

In Fig. II AB represents a portion of this curved beam. The origin of the coordinates is at the point A, and all abscissas measured to the right of A, and all ordinates measured upward from the line AB, are positive.

The angle which the tangent to the curve at any point (x, y) makes with the horizontal, or which the plane of section at this point makes with the vertical, is indicated by $\alpha°$.

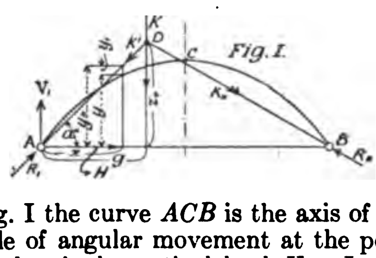

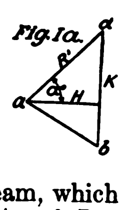

In Fig. I the curve ACB is the axis of the beam, which is assumed as capable of angular movement at the points A and B. This beam supports the single vertical load K. In Fig Ia a force polygon has

been drawn for the load K, and in Fig. I the reciprocal, or moment polygon, ADB, has been drawn, viz., $AD \parallel ad$, and $DB \parallel ab$.

From a well-known principle in graphics, the triangle ADB represents the moment polygon of a beam freely supported at A and B, and sustaining the single load K. At a point distant x from the support A this bending moment is equal to

$$\mathfrak{M} = y_{,,}H.$$

For the point (x, y) of the curved beam the moment is

$$M = y_{,}H = y_{,,}H - yH,$$

or

$$M = \mathfrak{M} - yH.$$

In Fig. I the segments AD and DB of the moment polygon are the components K' and K'' of the force K; they are held in equilibrium by the reactions $R_{,}$ and $R_{,,}$, and the exterior forces may be replaced by the reactions $R_{,}$ and $R_{,,}$ without disturbing the equilibrium of forces.

It is a well-known law in graphical statics that each segment of a closed moment polygon is the resultant of all the exterior forces. Fig. II shows on a large scale a portion of the arch from the support A to the point (x, y), the force $R_{,}$ of Fig. I corresponding to the sec-

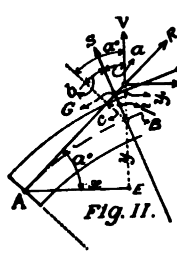

Fig. II.

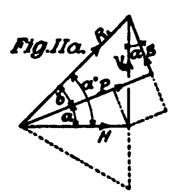

Fig. IIa.

tion-point (x, y) of the arch. This force $R_{,}$ may be resolved into a force P parallel to the tangent of the curve at the point (x, y), and a force S at right angles to this tangent; the force S is the shearing force. Or, the force R may be resolved into the vertical force V, which is equal to the vertical reaction at A, and the horizontal force H, which is equal to the horizontal thrust at A. The computation of these forces has been made in Fig. IIa, and, measured with the scale of forces, the lines P and S, and H and $V_{,}$, give the intensity of these forces.

Also, from Fig. IIa,

$$H = R_{,} \cos \alpha^{\circ} \quad \text{and} \quad S = R_{,} \sin b,$$

and from Fig. II,

$$c = y_{\prime} \cos \alpha^{\circ};$$

and

$$Hc = R_{\prime}c \cos \alpha^{\circ}, \quad \text{or} \quad Hy_{\prime} \cos \alpha^{\circ} = R_{\prime}c \cos \alpha^{\circ};$$

or

$$Hy_{\prime} = R_{\prime}c.$$

Similarly,

$$Pp = R_{\prime}c,$$

and

$$R_{\prime}c = Hy_{\prime} = Pp = M. \quad . \quad . \quad . \quad . \quad . \quad . \quad . \quad . \quad (1)$$

Fig. II*a* further gives

$$\left.\begin{aligned} P &= H \cos a + V_{\prime} \sin a, \\ S &= -H \sin a + V_{\prime} \cos a. \end{aligned}\right\} \quad . \quad . \quad . \quad . \quad . \quad . \quad . \quad (2)$$

The Application of the Elastic Theory.

The application of the elastic theory to arches is based on the assumption that an arch is a constrained curved beam, its ends being connected with rigid supports. These connections may be so made as to allow an angular movement at the points of connection, as in the "two-hinged arch," or the connection may be rigid, as in the "hingeless arch."

These two forms of arches belong to the class of girders whose stresses cannot be computed by the ordinary method of statics alone, as the equilibrium between the exterior forces and the interior stresses in the arch is dependent in part on its change of form; in other words, the interior stresses are dependent on the static equilibrium of the forces, the elastic equilibrium of the material, and the form of the arch.

When a third hinge is introduced, usually at the crown of the arch, this static indeterminateness ceases, the arch then being transformed into two curved beams, each freely supported at two points.

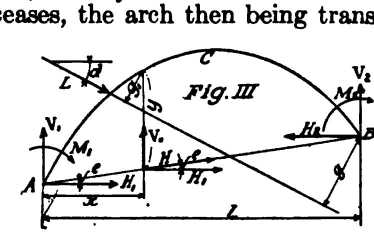

To illustrate the above let *ACB*, Fig. III, be the axis of an arch which can pivot around *B* and slide at *A*. This is equivalent to a beam freely supported at the ends. Let *L* be a single force acting on the beam. Under the influence of this force a pivotal motion will take place at *B*, a sliding motion at *A*, and a bending moment will be caused in the beam, which, for the point (x, y), will be

$$\mathfrak{M} = \frac{g}{l} xL - g_1 L. \quad . \quad . \quad . \quad . \quad . \quad . \quad . \quad . \quad . \quad (3)$$

The vertical reaction caused at A will be

$$V_1 = \frac{g}{l}L. \quad \ldots \ldots \ldots \quad (4)$$

No other exterior force is caused at A.

At B a vertical reaction will be caused

$$= V_2 = L \sin d - V_1,$$

and in addition a horizontal force

$$H_2 = L \cos d.$$

In a two-hinged arch no sliding motion can take place at A, and to change the beam into a two-hinged arch, a force H should be applied at A to push that end back into its former position.

The vertical component of this force is

$$V_{\prime\prime} = H \sin e.$$

The horizontal component is

$$H_1 = H \cos e, \quad \text{and} \quad V_{\prime\prime} = H_1 \frac{\sin e}{\cos e} = H_1 \tan e.$$

And the bending moment in the arch at the point (x, y) will be

$$\left.\begin{aligned} & M = \mathfrak{M} - yH_1 \\ \text{when} \quad & V_1 = \frac{g}{l}L + H_1 \tan e, \\ & V_2 = L \sin d - V_1, \\ \text{and} \quad & H_2 = L \cos d + H_1. \end{aligned}\right\} \quad \ldots \ldots \quad (5)$$

When the force L acts as indicated in Fig. III, $L \cos d$ is positive and H_1 may be negative.

If no hinges were provided at the supports, no angular movement could take place at A and B; and to change the two-hinged arch into a fixed arch, its ends should be bent back into their original positions, which requires a pair of forces at each support, each pair forming a moment (M_1 and M_2, Fig. IV).

These two moments act simultaneously on the arch and cause a bending moment at the point $(x, y) = \dfrac{M_1(l-x) + M_2 x}{l}$, and the total bending moment in the arch at the point (x, y) is

$$M_x = \mathfrak{M}_x + \frac{M_1(l-x) + M_2 x}{l} - yH_1, \quad \ldots \ldots \quad (6a)$$

$$\left.\begin{aligned} \text{when}\qquad & V_1=\frac{q}{l}L+\frac{M_2-M_1}{l}+H_x\tan e,\\ & V_2=L\sin d-V_1,\\ \text{and}\qquad & H_2=H_1+L\cos d. \end{aligned}\right\}\quad\ldots\ldots\quad(6b)$$

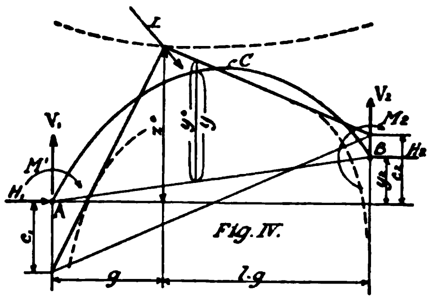

Fig. IV.

When more than one force acts on the arch, the equations (6*a*) and (6*b*) may be expressed in the general form:

$$M_x=\mathfrak{M}_x+\frac{M_1(l-x)+M_2x}{l}-yH_x, \quad \ldots\ldots \quad (6)$$

$$V_1=\frac{1}{l}\Sigma_0^l gL+\frac{M_2-M_1}{l}+H_x\tan e, \quad \ldots\ldots \quad (7)$$

$$V_2=\Sigma_0^l L\sin d-V_1, \quad \ldots\ldots \quad (8)$$

$$H_2=H_1+\Sigma_0^l L\cos d, \quad \ldots\ldots \quad (9)$$

$$V_x=\Sigma_0^x L\sin d-V_1, \quad \ldots\ldots \quad (10)$$

$$H_x=H_1+\Sigma_0^x L\cos d; \quad \ldots\ldots \quad (11)$$

and when the values of H, M_1, and M_2 are known, the resultant of the exterior forces for any point (x, y) of the arch can be found; from this the values of P and S in equations (2) are obtained, and from these the normal and shearing stresses in the arch may be computed.

In equations (6) to (9) the only known quantity is $\mathfrak{M}_x$, and for the fixed arch the three statically indeterminate quantities, M_1, M_2, and H_x, have to be ascertained.

For the two-hinged arch the values of M_1 and M_2 are equal to zero, and the statically indeterminate quantity H remains to be solved:

$$M_x = \mathfrak{M}_x - yH_x. \quad . \quad . \quad . \quad . \quad . \quad . \quad . \quad . \quad (12)$$

When the arch is also provided with a hinge at the crown, the bending moment at the center hinge caused by H is zero. For this same point the bending moment caused by the exterior forces is zero, the arch cannot resist bending at the hinge, and all the statically indeterminate quantities disappear:

$$M_x = Hy. \quad . \quad . \quad . \quad . \quad . \quad . \quad . \quad . \quad . \quad . \quad (13)$$

With the supports A and B at the same elevation and all the loads acting in a vertical direction, the equations (7) and (11) change into

$$V_1 = \frac{1}{l}\Sigma_0^l qL + \frac{M_2 - M_1}{l}, \qquad H_2 = H_x = H_1. \quad . \quad . \quad . \quad (14)$$

When all the loads act vertically, $\mathfrak{M}_x$, of equation (6), can be represented by a reciprocal polygon. This polygon should be drawn from a force polygon which has a pole distance equal to H_1 (see Fig. IV), and the end segments of the reciprocal polygon should intersect the verticals through A and B at a distance c above or below the point A, viz.,

$$c_1 = \frac{M_1}{H_1}, \quad . \quad . \quad . \quad . \quad . \quad . \quad . \quad . \quad . \quad . \quad . \quad (15)$$

and above or below B at a distance

$$c_2 = \frac{M_2}{H_2} = \frac{M_2}{H_1}. \quad . \quad . \quad . \quad . \quad . \quad . \quad . \quad . \quad . \quad (16)$$

The vertical ordinates of this reciprocal polygon, measured from the chord AB of the arc and multiplied by H_1, are equal to

$$\mathfrak{M}_x + \frac{M_1(l-x) + M_2 x}{l}.$$

The bending moment at the point (x, y) of the arch is equal to the product of H_1 multiplied by the difference between the ordinate y^0 of this reciprocal polygon and the ordinate y of the arch axis. Both ordinates are measured from the chord AB of the arc.

This law was first established by Winkler. (The analyses for the determination of the values H, M_1, and M_2 are given in the Appendix.)

Components, Axial Force, Shearing Force.

Components.—For a load the reactions at the supports and their points of application are known, and the axial force and its position in relation to the section-point (x, y) of the arch can be computed; when the graphical method is applied, the two segments of the reciprocal polygon (see Appendix) can be drawn in their proper positions relative to the arch axis. These two segments are the components of the load, and their point of intersection is on the load line. It should be observed that each component is held in equilibrium by a force (the reaction) acting at the support in a direction opposite to that of the component.

Axial Force.—In computing the stresses in an arch at a point (x, y) an imaginary section is made through the point, the portion of the arch to the left of the section is removed, and the forces are then found which will hold the remaining portion in equilibrium when acted on by a load.

The resultant of these forces is in equilibrium with the interior stresses of the arch. One of these forces acts parallel to the tangent to the arch at the point of section, and this is the axial force P_x previously mentioned.

Shearing Force.—The other force acts at right angles to the said tangent, and is the shearing force S_x.

Let the section be located between the left support and the load, and let the portion of the arch to the left of th section be removed (see Fig. IV). The remaining portion of the arch may be considered as a free body in equilibrium acted on by the load L or its components. Of these the right component is balanced by the right reaction, which is equal in magnitude and opposite in direction. The only forces remaining are the left component and the stresses in the arch, and the body can be in equilibrium only when this component is the resultant of the stresses in the arch.

Let the section be located between the load and the right support, and the portion of the arch to the left of the section be removed. The same reasoning will prove that in this case the right reaction is the resultant force which balances the stresses in the arch.

This reasoning applies in the same manner to a number of loads, and it should be observed that the resultant forre or forces which balance the stresses in the arch are those forces which are intersected by the plane of section. For this reason these forces are always referred to as the "forces in the section."

Line of Pressure.

A number of loads will form a reciprocal polygon, and, according to the properties of this polygon (which are demonstrated in any text-book on graphics), each of its sides is the resultant of all the exterior forces; and a curve drawn tangent to these sides is called the "line of pressure."

Line of Resistance.

Each side is resolved into its axial force P_x and its shearing force S_x; and the axial forces form a polygon which is tangent to a curve called the "line of resistance."

Where there is no shearing force the line of pressure and the line of resistance coincide.

Every arch has three lines which indicate the action of the exterior forces upon it, viz., the axis of the arch, the line of pressure, and the line of resistance.

From the foregoing paragraphs it will be seen that the line of pressure is defined by the exterior forces alone, and that this line represents the static equilibrium of the exterior forces mentioned at the beginning of the chapter. The position of the line of resistance in relation to the line of pressure is defined by the exterior forces and the curvature of the axis of the arch, and the positions of the line of pressure and the line of resistance in relation to the axis of the arch are defined by the curvature of the arch and the shape and material of the arch section; this is the meaning of the expression, "the elastic equilibrium of the material and of the form of the arch," at the beginning of this chapter.

Intersection Locus.

In a previous paragraph it was shown that a force can be resolved into its components, and that the intersection of the components must be on the load line. By giving different positions to the load a series of intersection points of the components is obtained, and a line drawn through these intersection points is called the "intersection locus."

Tangent Curves.

It has been shown above how the components of a force intersect the verticals through the points of support at a distance c above or below the points of intersection of the arch axis with these vertical lines. For each position of the load there is a corresponding point of intersection on the locus, and a point of intersection on the verticals. When the corresponding points of intersection on the locus are united with those on the verticals, a series of sides is obtained which form a polygon, and this polygon is tangent to a curve called the "tangent curve." For two- and three-hinged arches these tangent curves contract to a point which is the center of the hinge. The intersection locus of the three-hinged arch is defined by two straight lines, the prolongation of each passing through the abutment hinge and the crown hinge.

From this it follows that the direction and location of the components of a force may be obtained by drawing tangent lines to the two curves from the intersection point which the load line makes with the intersection locus (see Fig. IV).

Referring to the figure and equations (13) and (14),

$$c_1=\frac{M_1}{H_1} \quad \text{and} \quad c_2=y_2+\frac{M_2}{H_2}. \qquad (17)$$

Further, for any point of the left-hand component,

$$c_x=c_1+\frac{V_1}{H_1}x=\frac{M_1+V_1x}{H_1}. \qquad (18)$$

For any point of the right-hand component,

$$c_x=c_2-\frac{V_2}{H_2}(l-x)=\frac{M_2+H_2y_2-V_2(l-x)}{H_2}. \qquad (19)$$

And from equations (16) and (17) when $x=g$,

$$z^0=\frac{M_1+V_1g}{H_1}=\frac{M_2+H_2y_2-V_2(l-g)}{H_2}. \qquad (20)$$

For the two-hinged arch, $M_1=M_2=0$, and therefore $c_1=0$, $c_2=y_2$, the components pass through the hinges, and the tangent curves contract to a point which is the center of the hinge. The equations for the components are:

$$z_{x<g}=\frac{V_1}{H_1}x, \qquad (18a)$$

$$z_{x>g}=\frac{H_2y_2-V_2(l-x)}{H_2}, \qquad (19a)$$

and, if $x=g$,

$$z^0=\frac{V_1}{H_1}g=\frac{H_2y_2-V_2(l-g)}{H_2}. \qquad (20a)$$

Maximum and Minimum Stresses.

From equations (3) of Chapter V it follows that the normal stresses in a section of the arch rib are greatest in those fibers which are farthest from the axis of the arch.

This same chapter describes the meaning and value of the "core," the "core points" and the "core lines" in an arch rib. In Fig. V, let AB be an arch rib, the stresses of which are to be investigated for a section XX. The line O_1O_2 is the intersection locus, and the lines T and T_1 are the tangent curves. At this section N_1 and N_2 are the core points. Any force passing between the points N_1 and N_2 exerts com-

pression in all the fibers. Any force passing through N_2 exerts compression in the lower fibers, but exerts no stress in the upper fibers.

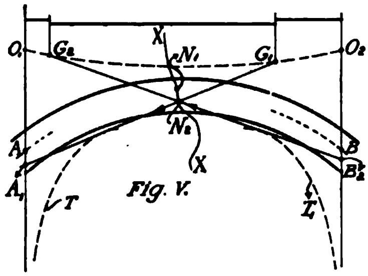

Fig. V.

Any force passing below N_2 exerts compression in the lower fibers and tension in the upper fibers.

The core point N_1 divides the section area similarly, but in an opposite sense.

To obtain maximum compression in the upper fibers, only the forces passing above the core point N_2 should be considered, and to obtain maximum tension in the upper fibers, only the forces passing below the core point N_2 should be considered.

In a previous paragraph it was shown that the resultant of all the forces in the section balances the stresses in the arch rib. In Fig. V, to the left of the plane of section XX, all the *reactions* of the loads are in the section, this being indicated by an arrow on the line G_2B_2. For all loads to the right of the section XX, all the *components* are in the section.

Now, for all loads placed between G_2 and the section line X, all the reactions in the section pass above the core point N_2. For all the loads placed between the section line XX and the point G_1, all the components pass above the core point N_2.

To obtain the maximum compression in the upper fibers of the arch rib at the section XX, the arch should be loaded only between G_1 and G_2.

The reactions of all loads between O_1 and G_2 pass below the core point N_2. For all loads between G_1 and O_2 the components pass below the core point N_2.

To obtain the maximum tension in the upper fibers of the arch rib at the section XX, the arch should be loaded from O_1 to G_2 and from G_1 to O_2, the space between the points G_1 and G_2 being left unloaded.

Division Lines.

The lines G_1A_1 and G_2B_2 divide the intersection locus into the distances which separate the two forms of loading which produce maximum and minimum stresses in the upper fibers; these two lines are called "division lines."

To obtain the maximum and minimum stresses in the lower fibers, the core point N_1 is the point at which the division lines should intersect.

Maximum Shear.—In Fig. VI AB is the arch rib, O_1O_2 the intersection locus, and UU a tangent to the axis of the arch at the section X. The line A_1G_1 is a tangent to the curve T and is drawn parallel to the line UU. From the equations at the bottom of page 2 it

follows that the shear $S = R \sin c$. In this case R is either the component or the reaction of a load placed on the arch, and the angle c is the angle which either force makes with the tangent to the axis of the arch. The sine of any angle which is measured upward from a line parallel to this tangent is positive, and when measured downward is negative.

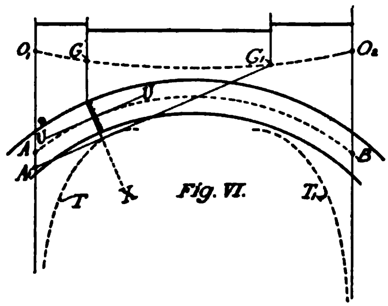

In Fig. VI the reactions of any load placed between O_1 and G are in the section, and the components are in the section for any load placed between G and O_2.

Now the sine is positive for the angle which the components make with the tangent, for any load which is placed between G and G_1; and to obtain maximum compressive shear the arch should be loaded from the point G to the point G_1.

The sine is negative for the angle which the components make with the tangent, for any load placed between G_1 and O_2; the sine is also negative for the angle which the reactions make with the tangent, for any load which is placed between G and O_1.

To obtain maximum tensile shear the arch should be loaded from O_1 to G and from G_1 to O_2, and the stretch from G to G_1 should be left unloaded.

Loading which Causes Maximum and Minimum Stresses in the Members of a Framed Arch.

The foregoing is applicable to the framed arch as well as to the arch rib.

In Fig. VII the line AB is the arch axis, the line O_1O_2 is the intersection locus, and the lines T and T_1 are the tangent curves.

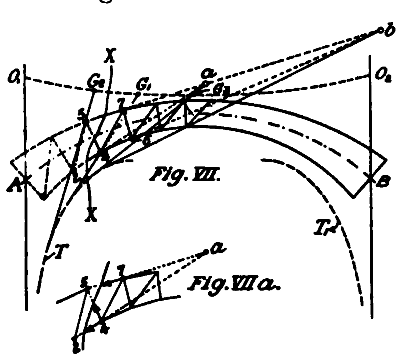

To find the loading which will cause maximum or minimum stresses in the members, an imaginary section XX is drawn, which intersects the members 2–4, 4–5, and 5–7, and the portion of the arch to the left of the section is supposed to be removed. As Fig. VIIa shows, the forces 2–4, 4–5, and 5–7 should balance the exterior forces in the section.

According to the moment theory of Ritter, the center of moments for the member 5–7 is at the intersection of the other two forces in the

section, or the point 4. Around this point as a fulcrum the moments of the forces 2–4 and 4–5 are equal to zero. The moment of the member 5–7 around this fulcrum must then be in equilibrium with the moment of the exterior forces in the section around this same fulcrum.

The moments of all the exterior forces passing above the point 4 are negative, and the moments of all the exterior forces passing below 4 are positive.

The point 4 must therefore be the point through which the division line passes, and in Fig. VII this line is drawn from the point 4 as a tangent to the tangent curve T.

This division line intersects the intersection locus at G_1, and all forces situated between O_1 and G_1 will cause compression in 5–7, all forces between G_1 and O_2 causing tension in the same member.

Similarly for the stresses in 2–4 and 4–5, the lines 5–G_2 and aG_3 being their respective division lines.

It will be understood that the point a is the point of intersection of the two forces 5–7 and 2–4.

To find the fulcrum for the diagonal 4–7, the two chords 4–6 and 5–7 are prolonged to a point of intersection b.

When the two chords are parallel and cannot intersect, the method explained in connection with Fig. VI is to be applied.

CHAPTER II.

THREE-HINGED ARCHES.

1. Three-Hinged Braced Arch.—SINGLE LOAD ON ARCH.—RESOLUTION OF LOADS.—A three-hinged braced arch with parabolic lower chord and horizontal upper chord is shown in Fig. 1. The hinges are located at A, B, and C, the end hinges A and B being at the same elevation.

Suppose this arch, which for the present is assumed weightless, to be loaded with a single load, II, at panel point 5. As is well known, the reactions produced at A and B must pass through the hinges (A and B–C respectively) and must intersect on the load line II.

The reactions, then, are R_2 at A, and R'_2 at B, and in value they are equal and opposite to the components 2 and 2′ of the load II. These components, of course, are found by a simple triangle of forces (heavy lines in Fig. 1a).

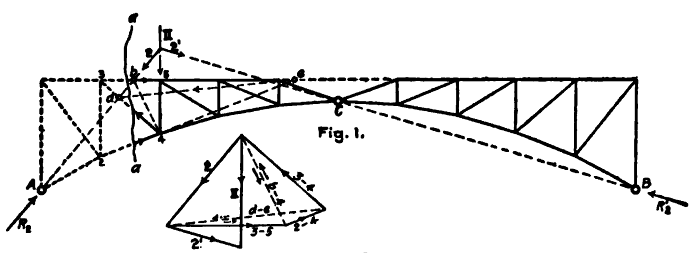

Fig. 1.

Fig. 1a.

STRESSES.—In order to find the stresses which this load produces in any member of the frame, a section is passed through the member in question, cutting the arch into two separate parts. The line aa represents such a line of section, cutting the three members 3–5, 3–4, and 2–4. Consider now the right-hand part of the arch as a free body in equilibrium. The external forces on it are:

1, the load II, or in place thereof its components 2 and 2′;
2, the reaction R'_2, and
3, the three stresses in the members cut by the section aa.

Now, load component $2'$ and reaction R'_2 are equal and opposite; hence they balance. The remaining forces are: the load component 2 and the stresses 3–5, 3–4, and 2–4. These four forces are in equilibrium. The force 2 and stress 3–5 intersect at b, while 3–4 and 2–4 intersect at 4; then these two pairs of forces have equal and opposite resultants acting in the line $b4$. Fig. 1a shows how this well-known principle gives graphically the three unknown stresses. Drawing $b4$ and 3–5 parallel to their action lines, their directions result as shown in Fig. 1a. Then, taking the reversed direction of $b4$ as the resultant of 2–4 and 3–4, these latter two forces are similarly found in direction and intensity.

Or, instead of pairing the force 2 with stress 3–5, we may combine it with one of the other stresses. Thus, 2 and 3–4 intersect at d, while 3–5 and 2–4 intersect at e. Then the equal and opposite resultants are on the line de, and this (instead of $b4$) may be used in Fig. 1a to determine the unknown stresses (see line de in Fig. 1a).

Or, again, taking moments about the intersection of two of the four forces, say about point 4, the moment of load component 2 must be equal and opposite to the moment of 3–5. This determines 3–5 at once, without involving the determination of the other two forces. To find 2–4 the center of moments would be at 3, and to find 3–4 the center of moments would be at e.

All of these methods give the same result. The first is the most convenient for computing the stresses in the chords, the second for computing the stresses in the web members, and the third is of value where the intersection of the forces with the member to be computed falls outside the drawing-board.

The principles above explained may be applied to any number of loads just as conveniently as to a single load. The procedure, in case of more than one load, appears to the author to be novel, and to have value because of its simplicity, especially as it treats partial loading (live loads) very much more simply than do the graphical methods hitherto used.

Consider first the usual case of dead load, i.e., the structure fully loaded with equal loads at all panel points.

(a) Dead-load Stresses.—Fig. 2 shows the same arch, loaded at all panel points with equal loads: O, I, II, . . . X. Each load is resolved into its two components, as was done with the single load of Fig. 1. One diagram, Fig. 2a, gives all the components. It should be remembered that there is a reaction equal and opposite to each of these components.

In Fig. 2b these components are added graphically by drawing the load components 0 to 9 from F to D, parallel to their lines of action and equal to their values as found from Fig. 2a. Note that load component 10 equals zero, since $10'$ is vertical. It is then obvious that the straight line FD resents the left-hand reaction, in intensity and direction; also th line ED is the horizontal thrust. If the broken line FD is followed from F towards D, it represents the various

components which are held in equilibrium by the reactions at the left-hand hinge A. The right-hand half of the diagram in Fig. 2*b* is symmetrical with the left half; but it is convenient to let the right half represent the right-hand reactions, while the left half represents the left-hand load components. The arrows used in Fig. 2*b* correspond to this convention.

Now, to find the stresses in any member, as in the bottom-chord section 4–6, pass a section *aa* to cut this member, and suppose the left-hand portion removed, so that the portion shown in full lines is to be considered as a free body. The forces acting on this body are:

1, the loads III to X, or their components, 3, 3′, to 10, 10′,

2, the reactions R'_0 to R'_{10}, and

3, the stresses in the members cut—5–7, 5–6, and 4–6.

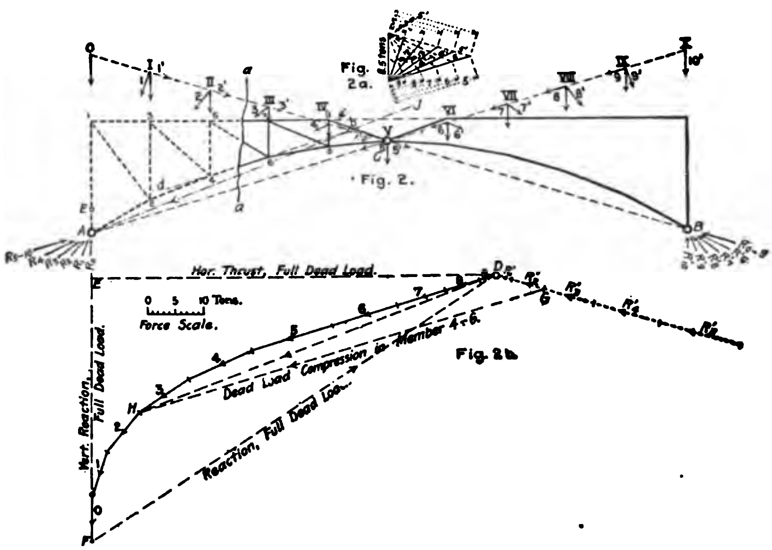

It will be seen that the load components 3′ to 10′ are balanced by the equal and opposite reactions R'_3 to R'_{10}, so that the only forces to be considered are: load components 3 to 10, reactions R'_0 to R'_2, and the unknown stresses. Referring to Fig. 2*b*, it appears that load components 3 to 10 and reactions R'_0 to R'_2 form a continuous line in the load diagram, so that their resultant is given by closing line GH in Fig. 2*b*. It is now necessary to find where this resultant acts in Fig. 2.

Since the load components 3 to 10 all pass through the left-hand hinge A, their resultant must also pass through A. But the direction of this resultant is given by line DH in the force diagram; therefore AJ, parallel to DH, is its line of action. Also R'_1 and R'_2 act

on the line BC in Fig. 2. The combined resultant GH then acts at the intersection of AJ and BC, that is, at the point b, and has a direction parallel to GH, viz., bd in Fig. 2.

The three unknown stresses are in equilibrium with the force GH acting on the line bd. But Fig. 2 shows that bd coincides with member 4–6. Hence the stress in 4–6 equals GH and is opposite in direction, that is, 4–6 is in compression. The stresses in 5–7 and in 5–6 are each equal to zero.

It will be remembered that a parabolic line is the curve of equilibrium for uniform vertical loading. A three-hinged arch, whose lower chord is on a parabola passing through the hinges, will therefore have no stress in the web members, under a uniform dead load. This checks with the result just found, that the dead-load stresses in 5–7 and 5–6 are zero.

The dead-load stresses in all the other members of the structure are found in exactly the same manner and require no further explanation. One diagram, Fig. 2, suffices for all members, obviously.

The proper selection of the forces acting on the section in each case can be made by the following rule: "All load components directed toward the section, whether belonging to the portion of the structure which was removed or on the portion retained, will be used in Fig. 2b to obtain the resultant. Those lying on the portion retained are used in their proper direction as load components; those on the portion removed are used in the opposite direction as reactions."

The procedure for finding live-load stresses is precisely the same, only that for each member it must be preceded by the determination of the position of loading which gives maximum stress in that member. The method of ascertaining this position is well known. The following summary of the determination of typical live-load stresses therefore omits detailed explanations, and gives only the successive steps in the procedure.

(*b*) Live-load Stresses.—Position of Loads.—For members 5–7, 5–6, and 4–6, the section aa (Fig. 3) is used, as before; the left-hand portion of the truss is supposed to be removed.

For member 5–7 the fulcrum is at panel point 6. The "forces in the section" * for a fully loaded bridge are 1′, 2′, 3, 4, 5, . . . 10; of these, 1′, 2′, 3 and 4 (1′ and 2′ being considered reversed) have a negative moment around 6; while 5, 6, 7, 8 and 9 have a positive moment. Then the loadings for the maximum and minimum stresses in 5–7 are:

$$5\text{–}7 \begin{cases} \text{Max. compression, I to IV loaded.} \\ \text{Max. tension, V to IX loaded.} \end{cases}$$

* This term is used to denote the forces directed *towards* the section, as by the rule above given. In accordance with that rule 1′ and 2′ will be mentioned when R'_1 and R'_2 are meant.

For member 5–6 the fulcrum is at d, Fig. 3. The forces 1′, 2′, 5, 6, . . . 9 have positive moment around d, while 3 and 4 have negative moment. Then the loading for 5–6 is:

$$5\text{–}6 \begin{cases} \text{Max. tension,} & \text{III and IV loaded.} \\ \text{Max. compression,} & \text{remaining panel points loaded.} \end{cases}$$

For member 4–6 the fulcrum is at panel point 5. Since 1′ and 2′ have negative moment, while 3 to 9 have positive moment, the loading is:

$$4\text{–}6 \begin{cases} \text{Max. tension,} & \text{I and II loaded.} \\ \text{Max. compression,} & \text{III to IX loaded.} \end{cases}$$

As an example of stress in a vertical, 4–5 is considered. The section for this purpose is on bb, the fulcrum at d. The "forces in the section" are different from those for section aa, being now 1′, and 2 to 9. Here 2, 3, and 4 have negative moment, while 1′ and 5 to 9 have positive moment. Then the loading is:

$$4\text{–}5 \begin{cases} \text{Max. tension,} & \text{I, V, and VI to IX loaded.} \\ \text{Max. compression,} & \text{II, III, IV loaded.} \end{cases}$$

Stresses.—For stresses in 5–7, see Figs. 3 and 3a. I, II, III, IV are loaded, and the forces in the section are 1′, 2′, 3, 4. Forces 3 and 4 have the resultant DE, passing through hinge A, line AJ; forces 1′ and 2′ pass through hinges B and C. Hence the resultant acts at the intersection e of AJ and BC. In Fig. 3a draw 1′ and 2′ to scale as line FD; then FE is the desired resultant in direction and intensity, acting on line ef in Fig. 3. The resultant ef is in equilibrium with 5–7, 5–6, and 4–6. It intersects 5–7 at g, while 5–6 and 4–6 intersect at 6; then the resultant of ef and 5–7 acts on line $g6$. Drawing FG in Fig. 3a parallel to $g6$ gives EG as the maximum compression in 5–7.

For maximum tension, V to IX are loaded, and the forces are 5, 6, 7, 8, 9, whose resultant HD in Fig. 3a passes through hinges A and C. Line AC intersects 5–7 at h, and line $h6$ is the resultant of HD with 5–7. Then HK, parallel to $h6$, gives DK as the maximum tension in 5–7. It will be observed that

$$DK = EG,$$

hence with the bridge fully loaded the stress in 5–7 is zero. This fact has been noted before, and checks the computation.

Stress in 5–6.—Maximum tension, III and IV loaded; forces in the section are 3 and 4. Their resultant (see Figs. 4 and 4a) is $D E$, acting through hinge A, hence on line AJ parallel to DE. AJ intersects 5–6 at k, while 5–7 and 4–6 intersect at d. Then dk is the direc-

tion of the resultant of *DE* with 5–6, and *FE* (parallel to *dk*) gives *FD* as the maximum tension in 5–6.

For maximum compression I, II, and V to IX are loaded, and the forces in the section are 1′, 2′, 5, 6 to 9. Their resultant is *GD*. Since 1′ and 2′ act on *BC* in Fig. 4, and 5 to 9 act on *AC*, the resultant passes through their intersection *C* and has the direction *CK*, parallel to *GD*. *CK* intersects 5–6 at *m*, while 4–6 and 5–7 intersect at *d*. Their joining line *md* is the direction of the resultant of *GD* with the stress 5–6; then *GF* parallel to *dm* gives *DF* as the maximum compression in 5–6. As for the preceding member, the maximum live-load stresses are equal and opposite.

Stress in 4–6.—For maximum tension, I and II are loaded, and the forces in the section are 1′ and 2′, both of which act on the line *BC*. *BC* intersects 4–6 (prolonged) at *n* (Fig. 5), while 5–7 and 5–6 intersect at 5; hence *n*5 is the direction of their resultant. In Fig. 5*a*, *ED* is the external force, and *FD* parallel to *n*5 is the resultant of this force with 4–6. Then *FE* parallel to 4–6 gives the maximum tension in 4–6.

For maximum compression III to IX are loaded, and the forces in the section are 3 to 9, all of which act through hinge *A*. Their resultant *DG* in Fig. 5*a* must also act through hinge *A*, hence acts on line *AJ*, intersecting 4–6 (prolonged) at *p*. But 5–6 and 5–7 intersect at 5, so that *p*5 is the direction of the resultant of *DG* with 4–6. Drawing *HG* parallel to *p*5, and *HD* parallel to 4–6, determines point *H*, which gives *HD* as the maximum compression in 4–6.

For this member, of course, the live-load stresses are not equal and opposite, since the full-load stress is not zero, but equals line *GH* in Fig. 2*b*.

The computation for a web vertical, such as 4–5, is precisely similar to the above; it is to be remembered that in the web verticals the full-load stress is not zero, but equal to a panel load, so that the maximum live-load stresses must differ by that amount.

Attention may be called to the fact that for maximum stress in 8–10 the bridge is to be fully loaded; but for maximum stress in 9–10 the bridge is loaded on one half only. In finding the live-load stress in 9–10, the resultant force on the section is to be resolved along 8–10 and 9–10. Since only two members are cut, the four-force method of resolution employed in the preceding does not apply, but the simple triangle of forces is sufficient.*

(*c*) Analytical Calculation.—Though every calculation described in the preceding paragraphs has been executed graphically, the method is convenient also for analytical computation, being much simpler than any of the systems hitherto employed. Thus, in Fig. 1, the locations of the points *A*, *B*, *C*, O, I, II, etc., are known, and from them the horizontal and vertical angles of deflection of the

---

* Up to this point the chapter consists of an article by the author, published in *Engineering News*, Oct. 20, 1904.

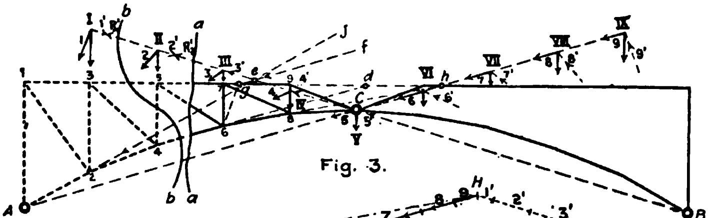
Fig. 3.

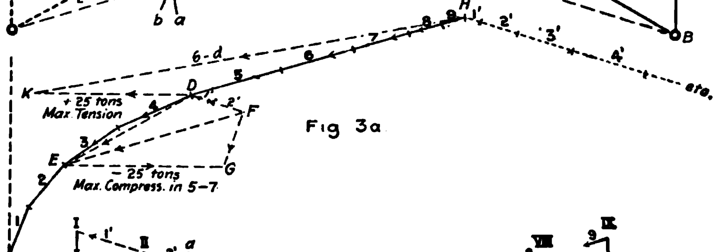

Fig 3a

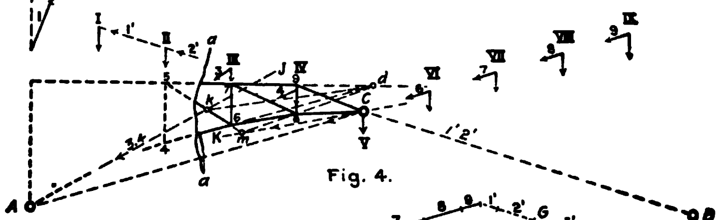
Fig. 4.

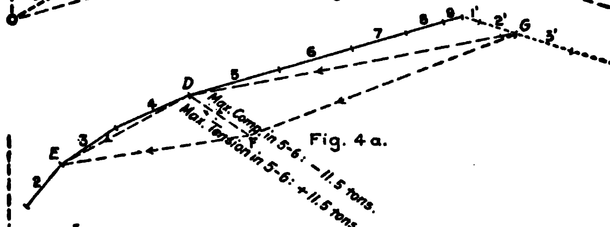

Fig. 4 a.

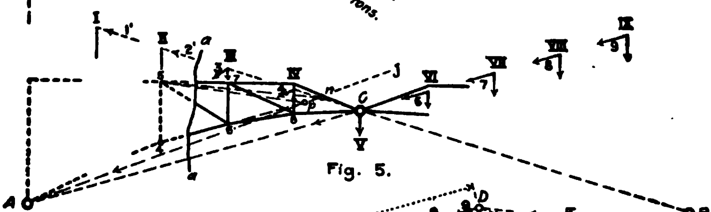
Fig. 5.

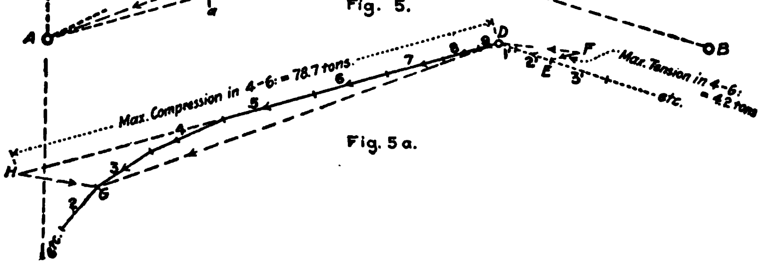

Fig. 5 a.

load components 0, 1, 2, etc., and 0′, 1′, 2′, etc., may be calculated. The amount of each component may then be computed and the broken line of the force diagram (Fig. 2) may be calculated in the same manner as the line of a survey, calling F the origin, and assuming the line FE as the north line. Each of the successive points of the broken line may then be defined by latitude and departure, and any one conversant with the methods pursued in plotting and computing a survey will find no difficulty in computing the stresses.

(*d*) To compute the deflections of the arch under a load, see the computation of the "Deflections of the Two-Hinged Spandrel-Braced Arch," Art. 13, Chap. III.

The three-hinged spandrel-braced arch makes a stiff bridge; the deflections caused by the live load and changes in temperature, however, are considerably larger than those of the two-hinged braced arch, but the slight excess of metal necessary for its construction is well compensated for by its superior rigidity. (See further explanation under "Two-Hinged Spandrel-Braced Arch," Chap. III.)

2. Three-Hinged Braced Roof-Truss.—This is a favorite form of arch for roof-trusses of long span.

Fig. 1*A* shows such a roof-truss, which has been built for the Pennsylvania R.R. trainshed in Jersey City, N. J. Its span from A to B is 253 feet, and its rise is 90 feet.

The dead-load was assumed as	30	pounds per square foot.
The wind pressure (vertical projection)	35	" " " "
The snow-load (horizontal projection)	17	" " " "

A two-hinged crescent-shaped roof-truss has been analyzed in detail in Chapter III, and these paragraphs will only point out where the computations of the stresses in these two types of arches differ; for that part where the computation is the same for both arches, the author refers to Art. 17, Chap. III.

Assume a horizontal force G to act on the arch. The portion CB of the arch acts as a simple beam, supported at C and B. The support at C is not direct, being given by the curved column AC which is hinged at A. Now, any reaction (caused by the force G) at C must pass through the hinge A, and the component of the force G must then act in an opposite direction to this reaction. This component intersects the load line at D, which is the point where the components intersect. For the same reason a force J acting on the half-truss AC will produce the point D' as the point of intersection of the components J' and J''.

Maximum and Minimum.—Suppose the dotted portion of the arch to the left of the section-line a–a to be removed.

The wind acts at an angle to the horizontal, and the wind pressure, acting at a panel point, is resolved into a horizontal force, such as G or J, and a vertical force, such as g or j; each of these forces can be resolved into its components, as the drawing indicates.

The load IV represents a snow load concentration, and 4 and 4′ are its components. The components of all the loads indicated on

the drawing are in the section. For the top chord 4–6 the panel point 7 is the fulcrum and Am is the division line. Now, all vertical forces similar to IV acting to the left of m will have components or reactions (like 4) which tend to turn in a negative direction about 7 as a fulcrum, or they will have negative moments. The components of the forces J and j will have negative moments, but those of G and g will be positive. The components of a snow load to the left of m and those of the wind pressure from left to right have the same sign, but a snow load to the right of m and the wind pressure from right to left will cause moments of an opposite sign.

The fulcrum for the bottom chord 5–7 is at the panel point 4, and the fulcrum for the diagonal 4–7 is at the point of intersection n of the two chords 4–6 and 5–7. The foregoing is sufficient to indicate the conditions of maximum and minimum loading for these members, and that the variation in the stresses must be large.

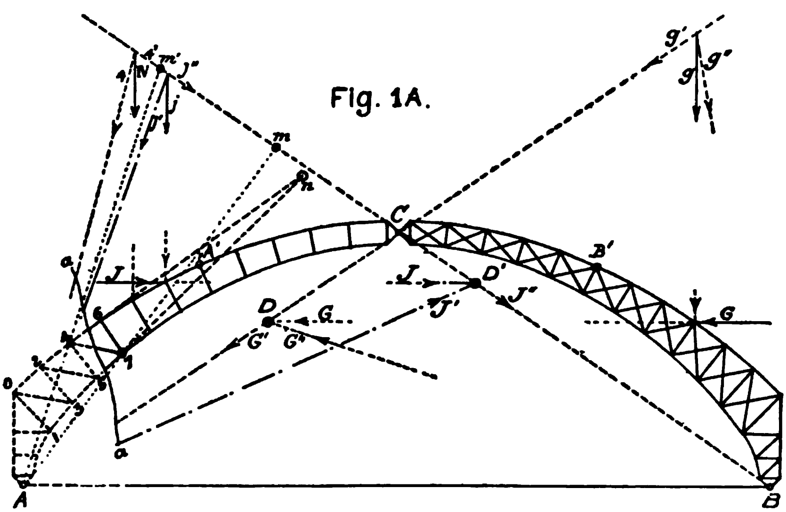

Fig. 1A shows a double system of web members. To find the stresses, the framework should be separated into its two single systems, viz., A, 1, 0, 3, 2, etc., and A, 0, 1, 2, 3, 4, etc. Each system resists one-half of the load, and the stresses should be added; or, the supposition can be made that the diagonals resist only tensile stresses, and when compressive stress is found in a diagonal, it should not be considered, the opposite diagonal being computed in its stead. The first method is usually preferred for roof-trusses, their web members being shaped to resist either compression or tension.

With this introduction and the detailed example of the computation of stresses in the braced arch, it should not be difficult to compute the stresses in the roof-truss. (See Art. 17, Chap. III.)

When the arch is supported on rollers at A, and the points A and B

are held in position by a tie-rod, the stress in this rod can be measured directly from the force diagrams (as in Fig. 2*b*, etc.) for different forms of loading.

3. Three-Hinged Steel Arch Rib.—Fig. 6 represents the outline of a solid-rib arch, of parabolic form, hinged at crown and springing line, and subject to loading at the panel points O, I, II, . . . X, which are spaced 10.45 ft. apart. The arch has a span of 107 ft. c. to c. of end hinges, and a rise of 16.6 ft. c. to c. of hinges. These dimensions and the panel length have been so chosen as to bring the end panel points O and X a short distance within the hinges, in order to illustrate the effect of such a condition. The rib consists of a plate web with flanges of two angles and cover-plates. Its depth, as represented in Fig. 6, is 3.6 ft. between centers of flanges.

It is desired to find the flange stresses and the transverse web-shear at various sections of the rib, under such a distribution of loading as will give the maximum stresses at these sections.

The dead load on the arch amounts to 8 tons per panel, the live load to 8.5 tons per panel.

Using the latter for the graphical work, the resolution diagram Fig. 6*a* is drawn, which gives the components of each load acting along the lines passing through the hinges. These components are shown in Fig. 6 by 1 and 1′ for load I, 2 and 2′ for load II, etc., the right-hand components being reversed to represent the reactions at hinge *B*, as explained in the preceding chapter for the three-hinged braced arch.

In Fig. 6*b* half of these components are brought together in proper sequence to form a force diagram.

(*a*) Flange Stresses.—By means of the latter diagram the flange stresses are found in the manner described generally in the previous article.

As an example, the procedure for finding the flange stresses in section *ZZ* will be given, as follows:

For the bottom-chord section 2–4 (Fig. 6) the center of moments is at the top-chord point 3. The "forces in the section" are 0′, 1′, 2, 3, . . . 10. Of these, the forces 0′, 1′, 2, and 3 have negative moment and produce tension in 2–4, while the forces 4, 5, . . . 10 have positive moment and produce compression in 2–4. Hence, for maximum tension in 2–4, load O, I, II, and III; for maximum compression, load IV, V, . . . X.

For the top-chord section 1–3 the fulcrum is at the bottom-chord point 4 (the same line of section being used). Forces 0′, 1′, 2, 3, and 4 have negative moment, etc., and

For maximum tension in 1–3, O, I, II, III, and IV should be loaded;

For maximum compression, load V, VI, . . . X.

Stresses in 2–4.—For tension, load O, I, II, and III, giving as forces in the section 0′, 1′, 2, and 3. In Fig. 7*a*, the forces 0′ and 1′ are drawn from the upper end of force 3, and the closing line *HF* represents their resultant. Now, the resultant of 2 and 3 (line *JF*) must act

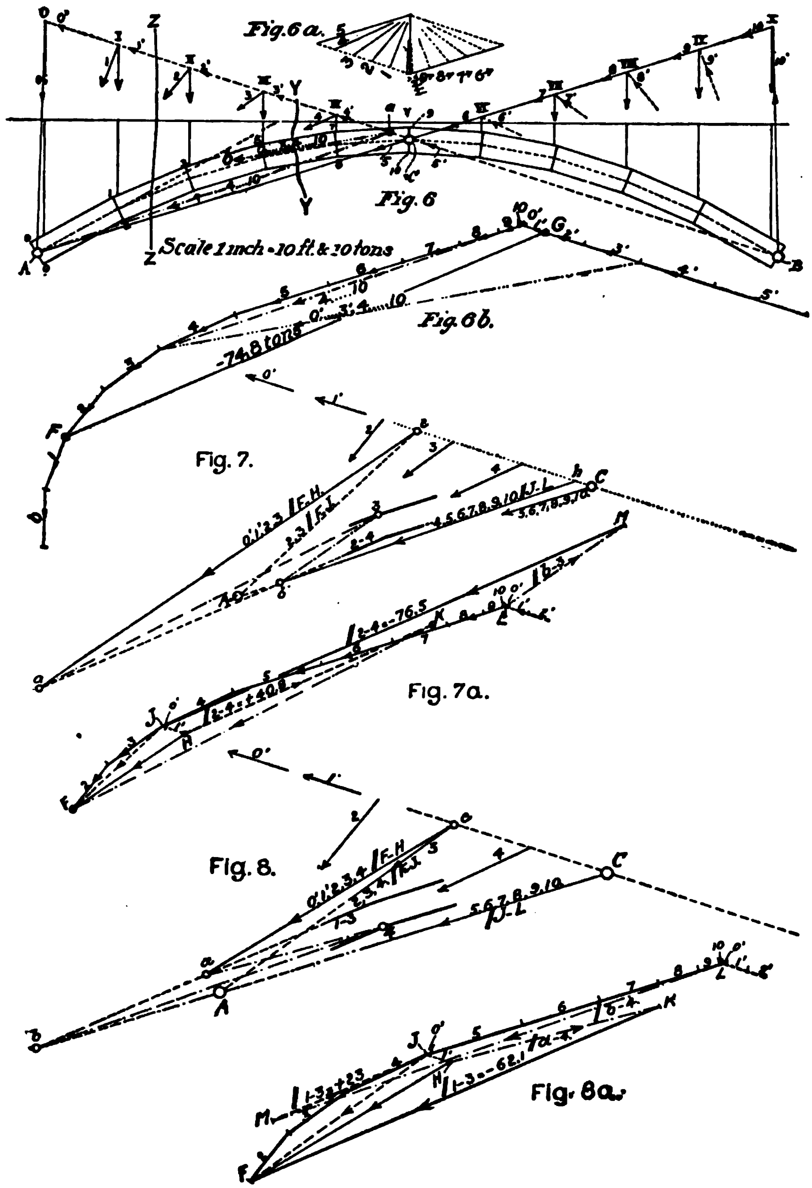

Fig. 6 a.

Fig. 6

Fig. 6 b.

Fig. 7.

Fig. 7 a.

Fig. 8.

Fig. 8 a.

through the hinge A in the arch diagram, Fig. 7, while the resultant of 0′ and 1′ (line HJ in Fig. 7a) must pass through the hinges B and C. The intersection of these two lines (point c in Fig. 7) is in the line of action of the resultant HF, whence this force acts on the line ca drawn parallel to HF. The resultant ca intersects the line of flange 2–4 produced at a. Since panel point 3 is the fulcrum, and the force ca is in equilibrium with the stress in 2–4, their resultant must pass through panel point 3 and hence must act on the line $a3$ in Fig. 7. Then, in Fig. 7a, drawing FK parallel to $a3$ and HK parallel to the member 2–4, the intersection K is found, and HK is the tension in flange 2–4.

The graphical work for finding the compression in 2–4 is shown in Figs. 7 and 7a; the work for finding the stresses in 1–3 is shown in Figs. 8 and 8a.

The resulting stresses are:

in Fig. 7a, max. compression in 2–4 = length JM;
in Fig. 8a, max. tension in 1–3 = length JM;
max. compression in 1–3 = length FK.

A check on the work up to this point for full load gives:

Bottom-flange stress	$= -76.5 + 40.8$	$= -35.7$ tons
Top-flange stress	$= -62.1 + 23$	$= -39.1$ "
	Total thrust	$= -74.8$ tons

This must check with the line FG in Fig. 6b, which gives directly the total force for full load.

The dead-load stresses in the chords are, of course, full-load stresses, and they may be found from the values just tabulated by reducing the stresses -35.7 and -39.1 in the ratio of the dead-load panel load to the live-load panel load—in this case 8 : 8.5 tons. This gives

Dead-load compression in bottom chord	$= -33.6$ tons
" " " top chord	$= -36.8$ "
Total	$= -70.4$ tons

The maximum and minimum chord stresses at section Z–Z are then:

Bottom chord,	$-33.6 - 76.5$	$= -110.1$ tons
and	$-33.6 + 40.8$	$= +\ 7.2$ "
Top chord,	$-36.8 - 62.1$	$= -\ 98.9$ "
and	$-36.8 + 23$	$= -\ 13.8$ "

The stresses in all the chord members of the arch are summarized in Table I, page 27.

It will be seen that the dead-load compression is greater in the top chord than in the bottom chord, which indicates that the line of pressure in the arch does not coincide with the neutral axis. (See line *ab*, section *YY*, Fig. 6.) This may seem surprising, in view of the fact that the parabola is the curve of equilibrium for uniform vertical loading. It is apparent from Fig. 6, however, that the loading is not uniform horizontally, since full panel loads come on the arch at O and X, points which are not directly over the hinges, and therefore introduce the effect of loading beyond the springing lines. As a result, the line of pressure touches the neutral axis only at the hinges, and lies above it at all points between the abutments and the center hinge.

(*b*) Web Stresses.—Shear is the force tending to buckle the web. Its value at right angles to the neutral axis is desired.

In the graphical work for determining shear, the tangents to the neutral axis at the various sections are required. These lines may be obtained in various ways, but it is most convenient if they have already been found in drawing the line of the neutral axis. This procedure, in case of a parabolic rib, is illustrated in Fig. 9. *A*, *B*, and *C*

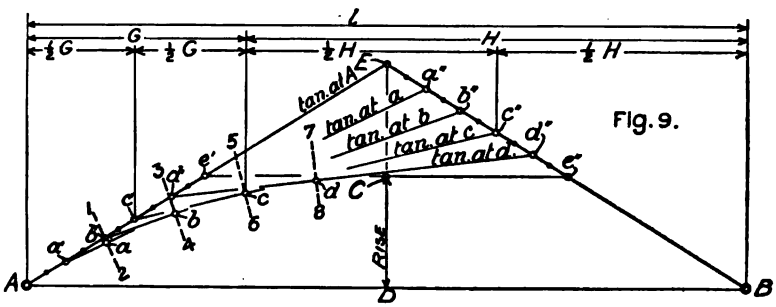

Fig. 9.

are the known locations of the hinges. Draw $DE = 2 \times DC$. Then EA and EB are tangents to the parabola at A and B. To obtain the tangent at any point c, which divides the span into the parts G and H: halve the distances G and H and drop verticals at the middle points intersecting EA and EB at c' and c'', respectively. Connect c' and c''; this is the desired tangent to the parabola at c, and any other tangent may be drawn in a similar manner. The construction for four intermediate tangents in the half-arch is shown in Fig. 9, omitting some of the elementary construction lines. Note that, for uniform spacing of the panel points a, b, c, d, the construction points a', b', c', d' are uniform subdivisions of $Ae' = \frac{1}{2}AE$, and a'', b'', c'', d'' are uniform subdivisions of $Ee'' = \frac{1}{2}EB$.

In Fig. 10 the line ZZ represents a section passed through the arch near the panel points 1 and 2. It is desired to find the shear in this section. The load components are, as before, 0 and 0′, 1 and 1′, etc. In the case of section ZZ, the "forces in the section" are 0′, 1, 2, 3,

. . . 10. By drawing a line $a'a''$ (see also Fig. 9) parallel to the tangent at panel point 1–2, it becomes evident at once which of the forces act downward along the section and which upward. It will be seen that forces 1, 2, and 3 produce positive shear, whereas 0′, 4, 5, . . . 10 produce negative shear. Hence (see Fig. 6),

For maximum positive shear, load I, II, III.
" " negative " " O, IV, V, . . . X.

In the force diagram (Fig. 10*a*), draw through point E the line DF parallel to the tangent to the arch at panel point 1–2. For maximum positive shear, the "forces in the section" are 1, 2, and 3; their axial component is, evidently, DE, and their shear component is DG (acting on the free end of the right-hand arch portion in a direc-

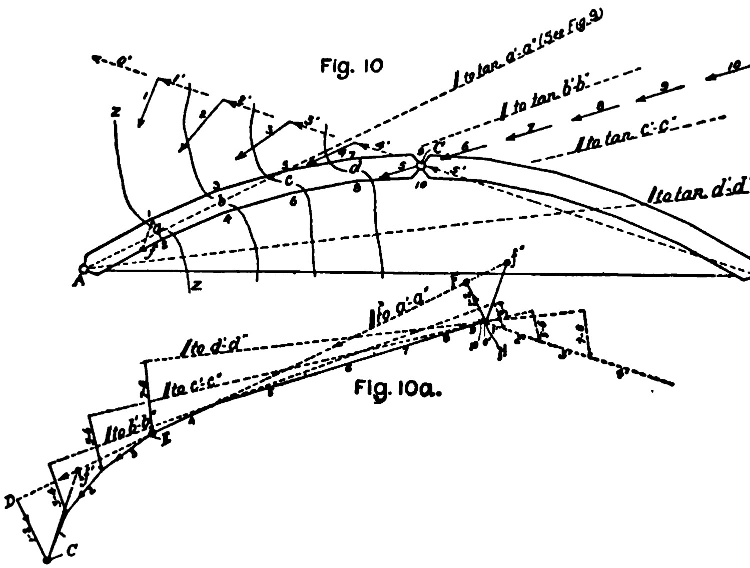

Fig. 10

Fig. 10a.

tion opposite to that shown in Fig. 10*a*). For maximum negative shear the "forces in the section" are 0′, 4, 5, . . . 10, their axial component is EF and their shear component is FH. The shears thus found (10.8 tons positive shear—compression in the hypothetical member 1–2, Fig. 10, and 7.2 tons negative shear—tension in 1–2) combine to give a full-load shear of 3.6 tons.

Reduced by the ratio 8:8.5, this gives a dead-load shear of 3.4 tons (compression in 1–2).

The maximum dead- and live-load shears on the section in question are then:

Positive. . . . . $-10.8-3.4=-14.2$ tons
Negative. . . . . $+\ 7.2-3.4=+\ 3.8$ "

In the force diagram, Fig. 10a, are drawn all the lines necessary to carry out this shear analysis for the four sections 1–2, 3–4, 5–6, and 7–8. The results are included in Table I.

If the arch rib has an open web in place of the solid plate, the procedure needs only very slight modification. If, in Fig. 10, the web system at panel 1–2 consists of the diagonal $1f$ and the vertical 1–2, the line Gf' in Fig. 10a, drawn parallel to member $1f$, and intersecting the line DE at f', gives Gf' as the maximum tension in member $1f$, and Hf'' is the maximum compression. The stresses in member 1–2 are those already found.

In general, if the web is an open one, the most unfavorable loading must be determined separately for each member by drawing the imaginary line of section and noting carefully the "forces in the section" and their direction with respect to the axis. Thus, if the web diagonal $1f$ were replaced by one of opposite slope, the analysis above described for the stress in member 1–2 would be changed, as the line of section would then have to pass to the right of panel point 1.

If the chords are not parallel, as in Fig. 1A, the chords in the imaginary section are brought to an intersection, and this point of intersection forms the fulcrum for the lever-arm of the web members in the section. Joining this point of intersection to the abutment hinge produces a line, and the process for finding the stresses is exactly that described and shown in Figs. 5, 5a, etc.

TABLE I Summary of Stresses in the THREE-HINGED-RIB ARCH BRIDGE.
Outline of Arch Parabolic; Span 107 ft c to c; Rise 16.6 ft. c to c; Panel length 10.45 ft.
Dead-Load Panel-load 8 tons; Live-Load Panel-load 8.5 tons

CHORD STRESSES					
Live-Load Stresses	0-1	1-3	3-5	5-7	7-9
TOP-CHORD max.	-62.2	-62.1	-62.1	-46.4	
TOP-CHORD min.	+10.	+23.	+25.3	+19	
TOP-CHORD full-load	-42.2	-39.1	-36.8	-36.4	-37.5
	0-2	2-4	4-6	6-8	8-10
BOTTOM CHORD max.	-64.3	-76.5	-69.1	-51.5	
BOTTOM CHORD min.	+27.8	+40.8	+33.7	+17.9	
BOTTOM CHORD full load	-36.5	-35.7	-36.4	-33.6	-31.5
Dead-Load Stresses					
TOP-CHORD	-39.7	-36.8	-34.6	-34.2	-35.3
BOTTOM-CHORD	-34.3	-33.6	-33.3	-31.6	-29.7
Combined Stresses					
TOP-CHORD	-91.9	-98.9	-96.7	-79.6	-72.8
BOTTOM-CHORD	-98.6	+ 7.2 or -110.1	-102.4	-83.1	-62.2
WEB-STRESSES					
Live-Load Stresses	1-2	3-4	5-6	7-8	
max.	-10.8	-8.2	-9.3	-11.7	
min.	+7.2	+4.2	+5.	+7.4	
full-load	-3.6	-4	-4.3	-4.3	
Dead-Load Stresses	-3.4	-3.8	-4.1	-4.1	
Combined Stresses					
max.	-14.2	-12.	-13.4	-15.8	
min.	+3.8	+0.4	+0.9	+3.3	

(c) The deflections in the three-hinged arch rib caused by live loads and temperature changes are proportionately larger than those

in either the two-hinged arch rib or the three-hinged braced arch, and where rigidity is specially desired, any of the other types of arches should receive the preference. This subject is specially treated in the following paragraphs and in Chapter III.

In Art. 5, Chap. III, another method for finding the stresses is given, which can also be applied to the arch described in Art. 3 of this chapter.

TABLE II.

Live-load Stresses						
Top chord	member	0-1	1-3	3-5	5-7	7-9
Stresses	maximum	-40.9t.	-53.6t	-56.4t	-44.8t.	-38.4t
	minimum	+10.3	+10.8	+21.9	+10.3	+3.7
	full load	-38.6t.	-36.8t	-34.8t	-34.5t	-34.7t
Bottom chord	member	0-2	2-4	4-6	6-8	8-10
Stresses	maximum	-62.8t	-63.7t	-61.9t	-48.8t	-21.2t
	minimum	+21.9	+24.9	+23.9	+12.8	-13.6
	full load	-40.9	-38.8	-38.	-36.	-34.8
The above figures are for live load only, and for the dead load the figs in the 2nd column should be reduced by 8 ton + 8.5 ton		Dead-load Stresses				
	top chord	-36.3t	-34.6t	-32.4t	-32.4t	-32.6t
	bot. chord	-38.5	-36.5	-35.7	-33.9	-32.7
Max load Stresses	top chord	-40.9 - 36.3 = -85.2t.	-88.2t	-88.8t.	-77.2t.	-70.1t
	bot. chord	-62.8 - 38.5 = -101.3	-100.2	-97.6	-82.7	-67.5
Shears	live load	1-2	3-4	5-6	7-8	9-10
	maximum	-9.8t	-8.2t	-9.3t	-11.7t	-12.7t
	minimum	+5.8	+4.2	+5.2	+7.7	+8.7
	full load	-4. t	-4t	-4.1t	-4. t	-4. t.
dead load		-4.8+0.8 = -3.8	-3.8	-3.8	-3.8	-3.8
Max. load Shear	maximum	-9.8-3.8 = -13.6t	-12.2t	-13.4t	-15.7t	-16.7t.
	minimum	+5.8-3.8 = +2.	+0.4	+1.3	+3.9	+4.9

TABLE III.

Stresses for an assumed horizontal thrust of 10 Tons Ht = 14.5 tons Hs = 4.7 tons										
	0-1	0-2	1-3	2-4	3-5	4-6	5-7	6-8	7-9	8-10
In the Chords	-14.4	+23.3	-27.1	+36.3	-37.4	+47.2	-40.3	+50.	-41	+51.2
Shear	1-2 = 4.8		3-4 = 4.		5-6 = 2.9		7-8 = 1.8		9-10 = 0.6	
Stresses from dead load	-34.3	-38.5	-34.6	-36.5	-32.4	-35.7	-32.4	-33.9	-32.6	-32.7
" " live "	-40.9	-62.8	-53.6	-63.7	-56.4	-61.9	-44.8	-48.8	-38.4	-34.8
St×14.5+10 temperature	-20.9		-33.3		-59.2		-58.5		-59.5	
Ss = 4.7+10 load Stress	-6.8	+11.0	-12.7	+17.0	-17.6	+22.2	-19.0	+23.5	-19.3	+24.1
Total.	-112.9	-90.3	-140.2	-83.2	-160.6	-75.4	-154.7	-59.2	-149.8	-93.4
dead load		-38.5		-36.5		-35.7		-33.9		-32.7
live "		+21.9		+24.9		+23.9		+12.8		-13.6
temperature		+33.8		+52.6		+68.4		+72.5		+74.3
load Stress		+11.0		+17.0		+22.2		+23.5		+24.1
Total		+28.2		+58.0		+78.8		+79.9		+52.1
Shears live & dead	-13.6		-12.2		-13.4		-15.7		-16.7	
	-7		-5.8		-4.2		-2.6		-0.9	
	-2.3		-1.9		-1.9		-0.8		-0.3	
	-22.9		-19.9		-19.0		-19.1		-17.9	
		90.3		83.2		78.8		74.9		52.1
		21.1		43.5		56.6		49.4		32.5
Construction St tons	-112.9	111.4	140.2	126.7	160.6	135.3	154.7	119.3	149.8	84.6
Net area □ inch	18.8	18.8	18.8	18.8	23.3	18.8	23.3	18.8	23.3	18.8
Stresses per □ inch	5.96	6.07	7.45	6.7	8.53	7.19	8.22	6.35	7.96	4.5

4. The Three-Hinged Arch Rib of Masonry, Concrete or Reinforced Concrete.—This type of arch owes its origin principally to the difficulty thus far experienced in computing the stresses in the hingeless arch with absolute certainty. The stresses in this arch are statically defined, and no recourse need be had to the elastic theory or to any empirical method of computation. With the application of the author's method for the computation of stresses in the hingeless arch, however, this particular advantage is lost.

One advantage which it does possess is that a yielding of the abutments does not materially affect the stresses in the arch, and, in a case where this is to be expected, the use of this arch is to be recommended.

(*a*) In a structure of this kind, the maximum and minimum stresses are found somewhat differently from the method followed for a plate-girder rib. The live load is only a small fraction of the dead load, and a reversal of stresses rarely takes place; but a large variation in the stresses of the extreme fibers of the arch rib may occur.

In Fig 11 is shown an arch rib of concrete, in which the full line *AC* represents the center of pressure in the arch resulting from the dead load. Now, assume the portion to the left of *Z–Z* to be removed.

(In Chapter V it is shown that the points *b* and *c*, at one-third and two-thirds respectively of the height *ad*, are the core points, and any force applied in *b* does not cause stress in the extreme fibers of the arch at *d*.)

The center of pressure in the arch rib is at *e*, the force *K* being the resultant of all the dead-load components of the arch at that point.

This point *e* is situated in this case within the middle third, and the force *K* will exert compression in every fiber of the arch rib. This compression is greatest at *a* and least at *d*. To change the compression at *a* into tension, this force *K* should shift downward from *e* to a point below *c*.

This can only be accomplished by some form of application of the live load; the live load, however, is small compared with the dead load, and in this case no form of loading can produce such a reversal of stress in *a*. Moreover, any force passing below *c* will diminish the stress at *a* which the computation will prove.

Any force passing above the point *c* will exert compression at *a*, and:

1. Any component or reaction passing above *c* increases the compression at *a*.

Any force passing above *b* will exert tension at *d*. To reduce the stress at *d* to zero, the point of application *e* of the force *K* should shift to *b*, and if by some form of loading it could shift upward above *b*, tension would result at *d*.

2. Any component or reaction of the live load passing above *b* causes the center *e* to shift and may produce a reversal of stress at *d*.

(*b*) Stresses in the Three-Hinged Concrete Arch Rib.—Such an arch has three hinges, viz., one at the crown, and one at each abutment. All these hinges are located in the axis of the arch and,

except in special cases, the arch is symmetrical with respect to the crown hinge, and the abutment hinges are situated in the same horizontal plane.

In Fig. 11 the left half of such an arch rib is shown; its span from center to center of abutment hinges is 106 feet, and the rise of the axis is 11.7 feet.

This half-arch is divided into eight vertical strips having the same width, and all figures are for an arch ring 1 foot wide.

The dead load of each strip, including the weight of the rib, the filling, and the paving, is represented by the forces I, II, III, etc.,

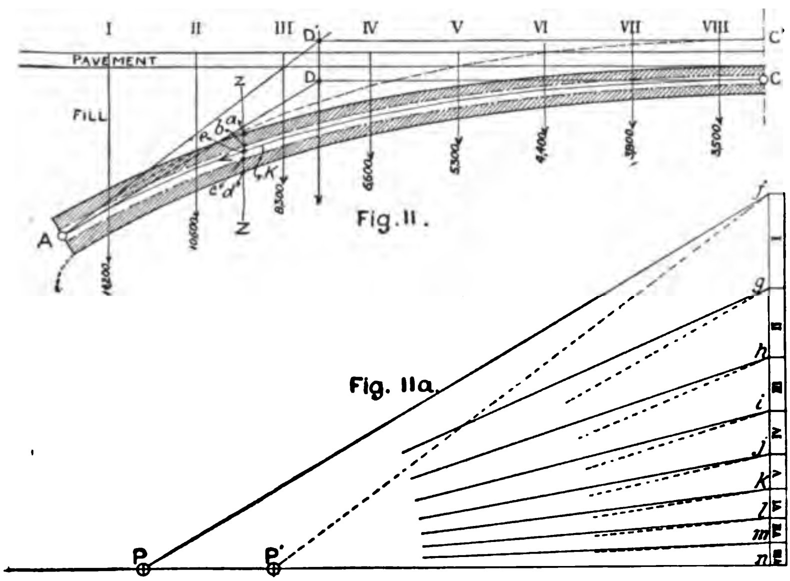

Fig. 11.

Fig. 11a.

which forces pass through the centers of gravity of their particular strips.

The live load is assumed as 100 pounds per square foot, which makes the panel loads at I, II, III, etc., 700 lbs. In addition to this a 16-ton road-roller is assumed to produce an equivalent concentrated load of 3,000 lbs., which load is so placed that it produces maximum or minimum stresses in the arch.

To find the line of pressure, the same method may be used which is described for the three-hinged braced arch; but the relation between the live and dead loads is not a constant ratio; for instance, at I the dead load is 14,200 lbs. and the live load 700 lbs., and at VIII these values are 3,500 lbs. and 700 lbs. respectively; and this method would be more laborious than the one which follows.

In Fig. 11*a* the forces I, II, etc., are drawn to scale in their proper sequence, and a trial pole P' is assumed.

The reciprocal polygon must pass through the hinges, and one starting point A of same is known. With the trial pole P' the dotted line AC' is drawn in Fig. 11, viz., AI parallel to $P'f$, I–II parallel to $P'g$ . . . , VIII C' parallel to $P'n$. The lines AI and VIII C' are drawn to an intersection at D', which is the point through which the resultant of all the parallel forces from I to VIII passes. The pole P' in Fig. 11*a* may be shifted to the right or to the left, and each new location of P' will produce a reciprocal polygon AC'. The end rays AI and VIII C' of all these polygons intersect on the line $D'D$.

Amongst all these polygons is one which passes through the points A and C. The end ray VIII C of this polygon is known; it is parallel to $P'n$ of Fig. 11*a* and passes through the point C, and, drawing this line, it is found to intersect the line DD' at the point D. The other end ray must then be the line AD, and, drawing in Fig. 11*a* a line Pf parallel to this line, the intersection point P of the two lines fP and nP must be the true pole of the force polygon.

With this pole a new reciprocal polygon AC is drawn in Fig. 11, viz., AI parallel to Pf, I–II parallel to Pg . . . , VIII C parallel to Pn. Measuring the rays Pf, Pg, etc., in Fig. 11*a* with the scale of forces gives the pressure in the arch in Fig. 11 from A to I, from I to II, etc. The location of the line of pressure can also be obtained from Fig. 11.

The line AC thus obtained may deviate considerably from the neutral axis of the arch rib, and corrections in the form of the arch should be made until the line AC practically coincides with the neutral axis.

In Fig. 11 the upper and lower thirds of the arch rib are cross-hatched, and the middle third is left blank to show clearly the line of pressure.

(*c*) Maximum and Minimum Stresses Caused by the Live Load.—In Fig. 12 the middle third of the half-arch AC is shown. The straight lines EC and AC pass through the hinges, and a live load of 700 lbs. is placed at each panel point I, II, . . . XVI. The loads from IX to XVI are not shown, their components all coinciding with the line AC, and the reactions of these loads not being used in the computation of the stresses. As previously indicated, the live-load forces I, II, etc., are resolved into their components and reactions in Fig. 12*a*, and the broken line of forces FGH is drawn in Fig. 12*b*.

The arch is to be investigated at the section line ZZ, at which section the point b is in the upper and the point c in the lower side of the middle third of the arch rib (the core points).

Any force passing below the point c exerts tension in the extreme upper fibers of the arch, and, conversely, any force passing above this point exerts compression.

In the section are the reactions 1′ and 2′ and the components 3, 4, 5, . . . 16; of these forces, 1′, 2′, 3, 4, 5, and 6 pass above the point c. In the section is also the dead-load force $P'K'$, which is equal to the ray between II and III in Fig. 11.

Concentrated Load.—That position for the road-roller load of 3,000 lbs. is to be found which will produce maximum compression in

the upper fibers. If a load were placed at I, its reaction would be in the section and its relative value would be equal to 1′, Fig. 12*b*. If it were placed at II, its relative value would be 2′, both of these forces passing at the same distance above the point *c*; and the maximum value is obtained when the load is placed at II. If the load were placed at III, its component would be in the section, its equivalent value would be 3, Fig. 12*b*, and its distance from the point *c* would be less than that of 2′. Now, as to the magnitude of the forces, the component 3 is nearly three times as large as the reaction 2′, while the distance of 2′ from *c* is about two and one-half times as great as the distance of 3 from *c*.

If the load is shifted to the right of II, the distance of the reaction from the point *c* remains the same, and the magnitude of the force increases very little; therefore, shifting to the right of II will not produce a maximum stress.

If the load is shifted to the left of III, the magnitude of the component will not increase, but its distance from *c* will increase, and the farther the load is shifted to the left of III, the greater will be the stresses in the upper side of the arch resulting from this load. There is, however, a limit to the shifting of the load to the left, because, if the load is shifted so far that its reaction is in the section, the stress in the upper fibers of the arch will not be a maximum.

To obtain the maximum stress in the upper fibers the concentrated load is placed at an infinitely small distance to the right of the section, or, in practice, at the section.

The concentrated load of 3,000 lbs. placed at the section will produce a component of 3,100 lbs.

Now, the forces in the section are:

1, the reactions 1′, 2′, and the components 3, 4, 5, and 6;

2, the dead-load force $P'K'$;

3, the component (=3,100 lbs.).

In Fig. 12*b* the resultant of the components 3, 4, 5, and 6 is equal to the line LM, and the line Ad in Fig. 12, drawn parallel to LM, intersects the reactions 1′ and 2′ at d. At the top of the line LM in Fig. 12*b* are drawn the forces 1′, 2′, equal to MN, and the line LN is the resultant of forces 1′, 2′, 3, 4, 5, and 6. The line de in Fig. 12 is drawn parallel to LN in Fig. 12*b*, its magnitude being 3,900 lbs.

This line intersects the concentrated-load component at the point e (Fig. 12), through which the resultant of all the live-load forces passes. The computation has been made in Fig. 12 and the line ef is this resultant (parallel to $e'f'$). This force ef intersects the dead-load force $P'K'$ (prolonged) at g, and this is the point through which the resultant of all the forces passes.

Fig. 12*c* is of similar construction to Fig. 11*a*, and the ray PK is equal to the magnitude of the force $P'K'$ of Fig. 12. At the point K in Fig. 12*c* the force KF is added by drawing this line parallel to gf of Fig. 12, and the line PF in Fig. 12*c* is then the resultant of all the forces (=106,200 lbs.). Drawing in Fig. 12 a line gF', parallel to

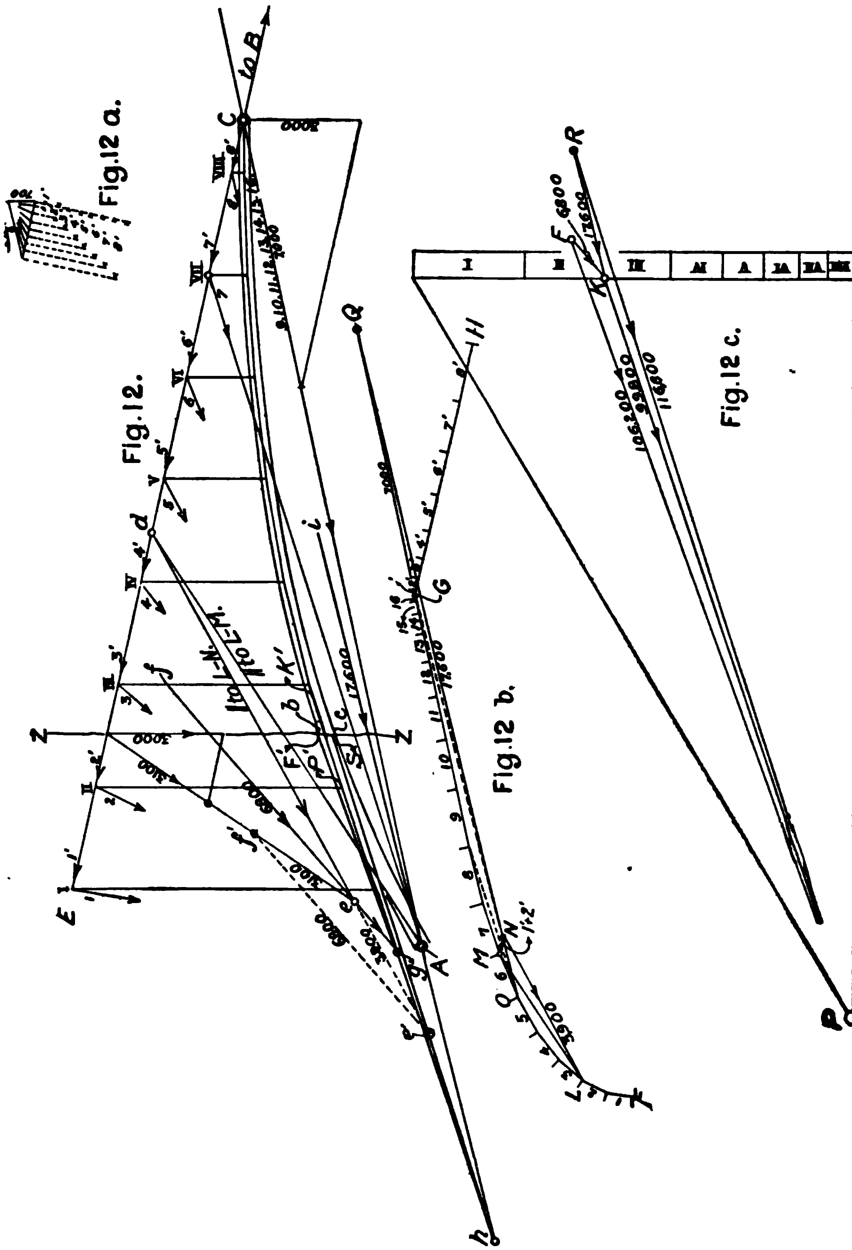

Fig. 12 a.

Fig. 12.

Fig. 12 b.

Fig. 12 c.

PF of Fig. 12*c*, gives the point of intersection *F'* with the section line *ZZ*. This point *F'* is located above the upper-third part of the arch rib, and tensile stresses will result in its extreme lower fibers.

Maximum Tension in the Extreme Lower Fibers of the Arch.—To obtain this, the point *b* (Fig. 12) is the core point, and all forces passing above this point will produce tension in the lower fibers.

These forces are the reactions 1', 2', the components 3, 4, and 5, and the road-roller.

The difference between this form of loading and the former one is the component 6, and the computation will show a very slight increase in the eccentricity of the force *gF'*, and a reduction in this force or in *PF* of 1,200 lbs. The net result is a very slightly increased stress in the extreme lower fibers.

Maximum Compression in the Extreme Lower Fibers of the Arch.—To obtain this stress, the point *b* is the core point, and all forces passing below this point will exert compression in the lower fibers, viz., the components 6, 7, . . . 16.

Road-Roller.—The farther the component passes below the point *b* and the greater its intensity, the greater will be the stress in the lower fibers.

The maximum possible distance from *b* to the component occurs when this component passes through the hinges *A* and *C*, and a comparison with Fig. 12*b* shows that the components 8 and 9 are the greatest of all the components. Consequently, maximum compression in the lower fibers results when the concentrated load is placed at the hinge *C*.

In Fig. 12 the resultants of the components 6, 7, . . . 16 and of the load at *C* all pass through the hinge *A*. In Fig. 12*b* all these forces are added and their resultant is the line *OQ*; and in Fig. 12 the line *hi* is drawn through the hinge *A* and parallel to *OQ* of Fig. 12*b*.

The force *P'K'* (prolonged) intersects the force *hi* at *h*, and through this point passes the resultant of all the forces. In Fig. 12*c* the resultant *OQ* of Fig. 12*b* is added to *PK*, viz., *KR*, and the line *PR* is the resultant of all the forces.

A line drawn parallel to *PR* through the point *h* in Fig. 12 gives the line *hS* intersecting the section-line *ZZ* at *S*.

The figure shows that this point is situated well inside the middle third.

To complete the foregoing the distribution of the stresses over the section is computed according to the explanation and analysis given in Chapter V, Art. 3 *et seq.*

(*d*) COMPUTATION OF THE STRESSES ON THE ARCH RIB.

The height of the arch rib = 35 ins.
The force *gF'* = 106,200 lbs.
Distance from the top = 9.56 ins.
Distance above the center = 7.94 ins.

The force hS $=116,800$ lbs.
Distance from the top $=21.94$ ins.
Distance below the center $=4.44$ ins.
Area of section $=35\times12$ $=420$ sq. ins.

The force $gF'=106,200$ lbs.
If the force acted at the center of the section, the pressure per square inch would be $106,200\div420$ $=253$ lbs.
The distance of the force from the axis of the arch is 7.94 ins., or, reduced to the height of an arch equal to unity, $\frac{7.94}{35}$ $=0.233$ unit.
Extreme fiber compressive stress in units $=(0.233\times6)+1$ $=2.40$ units compression.
Extreme fiber unit tensile stress $=2.40-2$ $=0.40$ unit tension.
Maximum compression in upper fibers $=2.40\times253$ $=607$ lbs. per sq. in.
Maximum tension in lower fibers $=0.40\times253=101$ lbs. per sq. in.

The force $hS=116,800$ lbs.
Unit pressure per sq. in. $=116,800\div420$ $=278$ lbs.
Eccentricity, in units, $=\frac{4.44}{35}$ $=0.127$
Maximum fiber stress $=(0.127\times6)+1$ (compression) $=1.762$ units.
Minimum fiber stress (compression) $=2-1.762=0.238$ unit.
Maximum compression in lower fibers $=1.762\times278$ $=490$ lbs. per sq. in.
Minimum compression in upper fibers $=0.238\times278$ $=66$ lbs. per sq. in.

These figures show that the stress in the extreme upper fibers of the rib varies from 607 lbs. to 66 lbs. (compression), and in the extreme lower fibers from 490 lbs. compression to 101 lbs. tension.

A special chapter is devoted to the theory of stresses, and reinforced concrete, as employed in arches, is fully described and analyzed in the chapter dealing with the hingeless arch.

The above-described arch would not be a safe structure, and its dimensions should be increased or reinforcing bars put in.

Compare these stresses with those of the fixed solid-rib arch of the same span and rise, and also with those of this same arch after the axis has been changed.

CHAPTER III.

THE TWO-HINGED ARCH.

1. The Standard Diagram.— As was shown in Chapter I, the stresses in the two-hinged arch are not statically defined. In the Appendix the two-hinged arch is analyzed and the conclusion reached that the stresses are dependent on

(1) The manner in which the forces are applied. (When the intensity, location, and direction of these forces are known, their resultant is defined by the static law.)

(2) The curvature of the arch axis.

(3) The form of the arch rib (the moment of inertia and the area of the arch rib).

Factors (2) and (3) are elements of the arch and are independent of the manner of loading; they define its flexibility and can be expressed as follows:

"The stresses in the two-hinged arch are defined by the static law governing the exterior forces and the elastic law governing the form and material of the arch."

From this it follows that the stresses in the arch are not only dependent on the exterior forces, but that a change in the curvature or a change in the sectional area of the arch rib influences them, and that each particular curvature of the axis, or each particular form of the arch rib, requires its own analysis for the determination of its stresses.

Many scholars have defined the relation between these factors in algebraic form, and it is due to the efforts of Winkler, Mohr, Müller-Breslau, Melan, and others that at the present time this relation is known with absolute certainty and precision; their results in connection with those of the author have been compiled in the Appendix.

As stated in the Preface, the algebraic forms expressing this relation are complex and laborious, and their comprehension and application require a special education; their use is therefore very limited. In the following articles the author explains this relation in such a manner that it can be easily comprehended by any engineer.

The description of the three-hinged arch has shown that the components of a force are determined when their point of intersection

on the load line is known. The same is true of the two-hinged arch. The line on which this point of intersection is located in the three-hinged arch is composed of two straight lines, each passing through an abutment hinge and intersecting at the crown hinge; or, concisely stated: the intersection locus of the three-hinged arch is defined by the hinges. The intersection locus of the two-hinged arch is defined by the hinges, the curvature of the axis, and the form of the arch rib.

As previously stated, each arch will have its own algebraic expressions defining this line. There is, however, a relation between the intersection-locus lines of different two-hinged arches, and this relation can be expressed in algebraic form or by simple graphical construction.

This reduces the application of the elastic theory from intricacy to simplicity, because, if by a simple construction the intersection locus of one arch can be changed to satisfy the conditions of another arch, a standard diagram of the intersection locus may then be drawn which, by means of correction, may be made to satisfy the conditions for any arch.

As the Appendix shows, and as specially demonstrated in Article 18 of this chapter (which deals with the general method for computing the intersection locus as applied to the Douro Bridge), the change in the moment of inertia of the arch must be very considerable to influence the intersection locus. Except in special cases, which are described under separate articles in this chapter, the intersection locus of the standard diagram may be applied to the two-hinged flat arch without appreciable error.

The influence of a change in the curvature of the axis upon the intersection locus is more pronounced. Still, the change of the standard diagram to satisfy this condition is very simple.

The standard diagram refers to a two-hinged arch whose axis is a parabola.

The rise of this axis = 1, and

One-half the span of the axis = 1.

The moment of inertia of the arch rib increases from the crown to the hinges in the same ratio as the secant of the angle which the arch axis makes with the horizontal.

A two-hinged arch which satisfies these conditions is chosen for this purpose, because its algebraic deductions are the simplest, and its analysis is given in the Appendix (Art. 2, Chap. VIII).

For a vertical force [see equation (85) of the Appendix]

$$z_0 = \frac{8}{5}\,\frac{l}{1+k-k^2}. \qquad (1)$$

For a horizontal force [see equation (88) of the Appendix]

$$x_0 = \frac{k}{2}\Big[5(1-k-2k^2+4k^3)-8k^4\Big]. \qquad (1a)$$

The standard diagram for the vertical forces is shown in Fig. 14, and for the horizontal forces in Fig. 13.

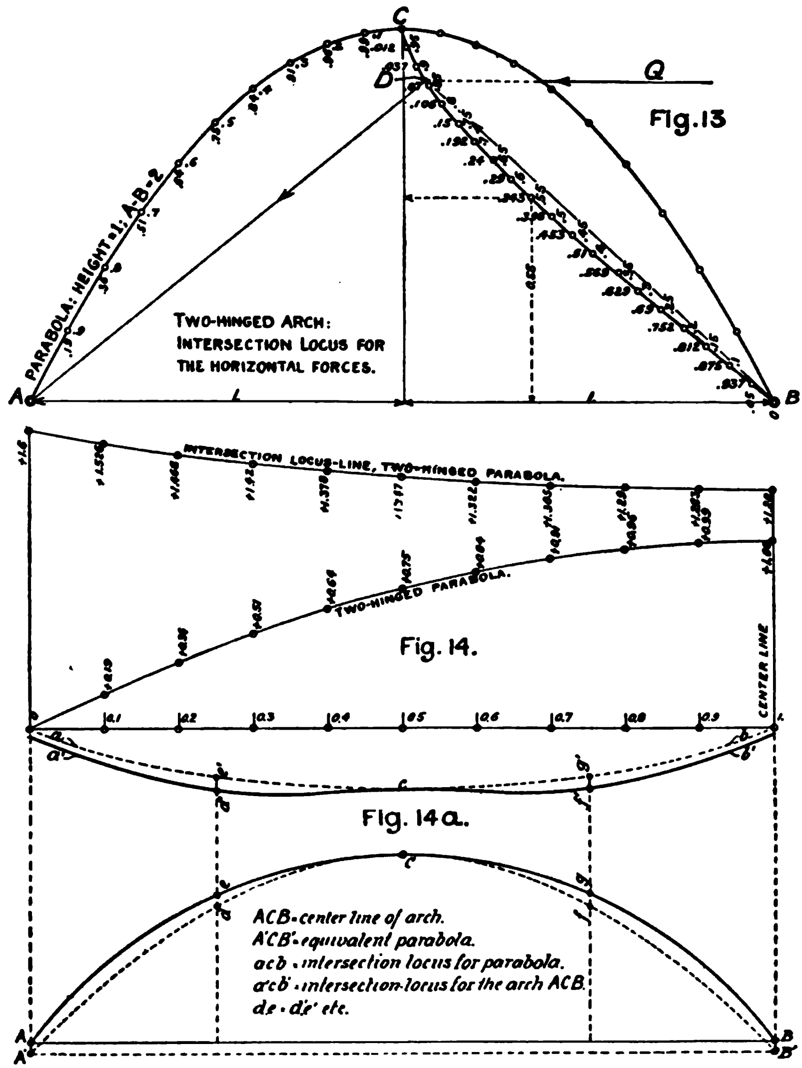

(*a*) To correct the diagram of Fig. 14 for an arch axis which is not a parabola, the following method will be sufficiently accurate:

Compute the area enclosed by the axis of the arch and the X-axis. Then compute the rise of a parabola having the same area and same

span. Use this parabola in conjunction with equation (85) of the Appendix, or with the ordinates of Fig. 14 to compute the ordinates of the intersection locus. This intersection locus is then to be used with the *actual arch* (not the substituted parabola), to find the worst positions of load and the maximum stresses.

The stresses thus found will be in error by an amount not exceeding three parts in one thousand for an arch whose rise is not greater than one-tenth of the span; in other words, the method is exact for nearly all practical purposes.

If greater accuracy is required where the rise exceeds one-tenth of the span, the following method may be used (see Fig. 14*a*): Compute the intersection locus *acb* for a parabola of equal area, as just described. Draw this parabola $A'CB'$ to coincide with the actual arch ACB at the crown. Deduct from each ordinate of the intersection locus the difference between the ordinates of the actual arch and the parabola ($de=d'e'$), where the latter lies below the arch curve; or, add the difference where the parabola lies above it. If this corrected intersection locus $a'cb'$ is used in connection with the actual arch ACB to find the stresses, the results will be correct within 6 parts in 1,000, even for a semicircular arch.

(*b*) The intersection locus for the horizontal forces (see Fig. 13) can also be used for a two-hinged arch whose axis is not a parabola.

A correction may be made to the intersection locus in the same manner as that described for the vertical forces; this, however, would be a refinement which is not necessary. Horizontal forces are caused by either the conjugate pressure of a spandrel filling, in case such a construction is followed (the author does not know of any example), or the wind pressure. As elsewhere mentioned, the intensity and direction of these forces is rather indefinite, and the error resulting from this indefinite knowledge will be very much greater than that resulting from the slight inaccuracy of the intersection locus. This point is clearly demonstrated in Art. 18 of the present chapter. (See also Art. 2 (*h*), Chap. VIII.)

2. Stress Analysis of the Two-Hinged Arch Rib.—After the intersection locus has been found, the procedure for finding the positions of loading and the stresses is practically identical with that described for the three-hinged arch. One or two slight differences occur, but these will cause no difficulty. The resolution of the loads into their reaction components (as in Fig. 6*a* for the three-hinged arch) cannot be done by a single diagram, but is best effected by a triangle of forces drawn directly on the load line (see Figs. 15 and 15*a*) where it cuts the intersection locus. In drawing the force diagram, Fig. 15*a*, the right-hand portion of the curve will form a broken line, instead of a straight line as for the three-hinged arch. In all other respects the work follows exactly the procedure already described.

3. Temperature and Secondary Stresses.—The stresses produced in a two-hinged arch by changes of temperature and by the

shortening due to compression may be treated together, since their effects are analogous, the shortening due to compression being of nearly the same kind as that due to lowered temperature.

If the ends of the arch were free to move, no stresses would be caused by a change of temperature; the ends, however, are held by the hinges A and B, which will cause a horizontal pull with a

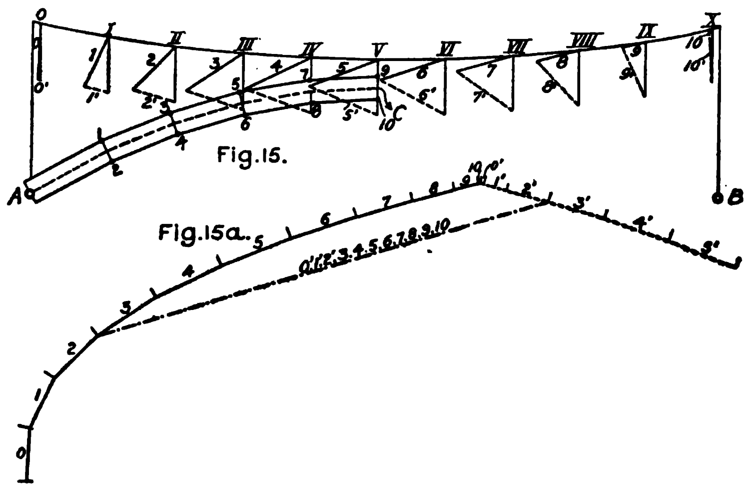

decrease in temperature, and a horizontal thrust with an increase in temperature.

The horizontal thrust caused by temperature changes * is

$$H_t = \frac{15EIwt}{8f^2}, \quad \dots\dots\dots \quad (2)$$

where E = coefficient of elasticity of material;
I = average moment of inertia of arch rib;
t = degrees above or below normal temperature;
w = coefficient of linear expansion of material for a change of temperature of one degree;
f = rise of arch.

The horizontal thrust caused by compression † is

$$H_n = -\frac{15nI}{8f^2}, \quad \dots\dots\dots \quad (3)$$

in which n = axial thrust per sq. in. in arch above the normal (if the arch is erected so as to have the calculated dead-load stresses under dead load, then n = axial thrust caused by the live-load temperature and compressive stresses).

* See Equation (93), Chapter VIII. † See Equation (92), Chapter VIII.

It should be remembered that the latter stress can be largely obviated by erecting the arch longer than the span and springing it into place, thus creating in the arch a compensating initial stress equal to the one caused by the live load.

The moment of inertia should be computed at different points of the arch and the average result used. The stresses caused by the live load should be computed at different points, using the maximum stresses, and the average result should be used.

The best method is to obtain the stresses in the various sections of the arch rib for a horizontal thrust of 10 tons, and by means of the slide-rule transform these to the actual horizontal reactions; it will require two or more trials before the true value for H_n is obtained.

The procedure for finding the stresses caused by $H=10$ tons in any section of the arch is shown in Figs. 16 and 16*a*, as follows:

The chords (3–5 and 4–6) are brought to an intersection with H, and H is the resultant of 3–5 and a–6. In Fig. 16*a* draw FH

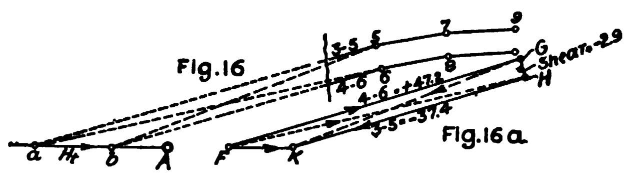

parallel to a–6 in Fig. 16, and KH parallel to 3–5 in Fig. 16—both on a base $FK=10$ tons. Then $KH=37.4$ tons (tension for an increase in temperature and compression for a decrease in temperature) is the stress in 3–5 due to a thrust of 10 tons. The same computation is performed for 4–6, and joining G and H gives the shear in the web. This is also a means of checking the calculation, since GH should be at right angles to FG and KH.

In Table III all these stresses are tabulated, and, combined with the live- and dead-load stresses of Table II, they give the maximum and minimum stress in each member.

Comparison of Tables II and III will render further explanation unnecessary.

Analytical Calculation.—See Art. 1 (*c*), Chap. II, for a convenient method.

Horizontal Forces.—The two-hinged arch rib as described in the preceding paragraphs is seldom used for roof-trusses. This chapter, however, would be incomplete if it did not indicate a method for finding the stresses in the arch caused by horizontal loads, and in Fig. 13 is shown the intersection locus CDB for the horizontal forces acting on the right half CB of a parabolic arch ACB. The moment of inertia of this arch increases from the crown to the hinges directly as the secant of the angle which the curve makes with the horizontal.

For an arch of any other curvature the same reductions can be made that are described for Figs. 14 and 14*a*.

(*a*) THE STRESS ANALYSIS FOR HORIZONTAL FORCES is explained in Arts. 16 and 17 of this chapter, which are devoted to the two-hinged crescent-shaped arch. (See foot-note, page 280.)

4. Deflections.—This subject is specially treated in Art. 20. The following is a simple and approximately correct method for computing the deflection of the crown of an arch:

Assume the camber to be computed for the purpose of erection.

Find the sectional areas and the stresses in the arch at different points, and from these compute an average stress and an average area; from the data thus obtained determine the amount of shortening of the arch axis, and thus the length of the arch axis when the falsework is removed.

The length of the parabola=

$$s=\tfrac{1}{2}l\left[1+\frac{2}{3}\left(\frac{f}{\frac{1}{2}l}\right)^2-\frac{2}{5}\left(\frac{f}{\frac{1}{2}l}\right)^4 \text{ etc.}\right].$$

For all practical purposes it is sufficiently accurate to assume

$$s=\tfrac{1}{2}l\left[1+\frac{2}{3}\left(\frac{f}{\frac{1}{2}l}\right)^2\right].$$

Find the value of s from this equation, add the shortening of the arch axis as found above, and call this length s' ($s'=s+\Delta s$).

Substituting s' for s and solving for f',

$$f'=\tfrac{1}{2}l\sqrt{\frac{3s'}{l}-\frac{3}{2}},$$

and is the rise of the arch axis when the arch is resting on the falsework. With this rise compute or draw a new parabola which will be the axis for the arch when resting on the falsework.

5. Two-Hinged Arch Bridge Made by Bending a Rolled Steel Shape.—Though the caption may indicate a repetition of former paragraphs, the method used for the computation of stresses differs from the one previously employed.

By bending an I-beam a graceful arch may be cheaply obtained for spanning a small opening. For computing the stresses in such an arch rib the method previously described is only partially applicable. In such an arch rib there are no fulcrums for the chords or the web members, and the stresses in the arch rib are determined by the position of the line of pressure and the intensity of the forces, as shown in Chapter I and applied in Chapter II. Article 4.

(*a*) In Chapter I all stresses caused by vertical loads were found by assuming these loads to be concentrated at panel points; in the

following paragraphs the live and dead loads will be considered as uniformly distributed loads, the dead load being taken as a permanent load and the live load as a moving load. The computation of the stresses is made with the same facility with this form of loading as with panel loads; but before entering into a description of the method, an introductory explanation is necessary to determine the point of intersection with the intersection locus of a uniformly distributed load.

In Fig. 17 the line AB represents the deck of a bridge, and the points I, II, III, etc., are the panel points.

Now, suppose that a uniformly distributed load extends from A to B, and that this load is subdivided into the portions a, b, c, and d, said subdivisions corresponding to the panel lengths. The portion a of the load causes reactions in I and II. Now, the sum of these reactions is equal to the load a, and the resultant, which is in equilibrium with these reactions, is a force p, equal to a; the point of application of this resultant coincides with the center of gravity of the load. The same is true of the loads b, c, etc. Also, the force P, which passes through the center of gravity of the full load from A to B, must be the resultant of the reactions at I, II, III, etc., and these reactions may be replaced by this single load P for the purpose of computing the reactions at the abutments.

In Chapter II (Art. 4) the core points in an arch rib and their use have been mentioned, and in Chapter V [Art. 1 (a)], an analysis of their value and meaning has been given. In Fig. 18 an arch rib CD is shown, at the section ZZ of which the point d is the upper, and the point e the lower, core point. As previously demonstrated, any force passing below d exerts compression in the lower fibers of the arch, and any force passing above d exerts tension in these fibers, the line Cf representing the division line. All forces passing below this line exert compression in the lower fibers of the arch, and to obtain the greatest compression all forces to the right of f should be considered in the computation.

The points e and g are located on the line dividing the forces which cause maximum compression in the upper fibers.

In Fig. 17 the line CA represents the line Cf of Fig. 18, and JJ' is the intersection locus. A small portion a' of the moving load will cause panel loads or reactions at I and II, whose resultant will be equal to p'. Now, the panel load I can be resolved into its components, and IC represents the left-hand component of load I, IIC being the left-hand component of the load II. $A'C$ is the resultant of the components IC and IIC, and this resultant component passes below AC and will cause compression in the lower fibers of the arch. The smaller a' becomes, the nearer the resultant component $A'C$ will approach AC, and when a' becomes infinitely small, the component $A'C$ will coincide with AC. Therefore, to obtain maximum compression in the lower fibers of the arch, the load should extend from the point A to the right-hand support. This is true in both cases,

viz., where the load acts directly on the arch, and where this action is transferred at the panel points to the arch.

The next step in this discussion is to establish the fact that the resultant of any number of vertical, equidistant, and equal forces, such as V, VI, VII, VIII, and IX (see Fig. 18), intersects the intersection locus at the same point as the resultant of the components of these forces. This is true when these forces are all located on the right side or on the left side of the axis of symmetry, which in this case is a vertical line passing through the point h.

The necessity of this last condition is self-evident. Thus, assume two parallel vertical forces, respectively located at the same distance to the right and to the left of the point h. The figure then instantly shows that, though the resultant of these two forces passes through the point h of the intersection locus, the resultants of their components intersect on the same vertical line, but above the point h.

(*b*) In proof of the fact stated above the following computation, which will be readily understood, affords an example of the analytical computation of a force diagram similar to Fig. 15*a*.

A load p placed at V (Fig. 18) is resolved into its components VC and VD, and the horizontal thrust b' and the vertical reactions a' and c' are to be computed.

From two equal triangles

$$a:b=a':b', \quad \text{and} \quad a:(l-b)=c':b'.$$

Now $$b=kl \quad \text{or} \quad k=\frac{b}{l}, \quad \text{and} \quad a'+c'=p.$$

Substituting these values and reducing the above equations gives

$$a'=p(1-k), \qquad c'=pk, \qquad b'=\frac{a'b}{a}.$$

These equations are sufficient to compute the diagram Fig. 18*a*.

Example.—In Fig. 18 the rise of a parabolic arch is assumed as equal to 0.5, and the span $l=2$ units of length; and the computation is to be made for a load of one unit weight at each of the panel points V, VI, VII, VIII, and IX.

The ordinates of the intersection locus JJ' are obtained from Fig. 14 and the following table is arranged:

	$-l$	a	b	k	a'	c'	b'
V	2	0.6735	0.5	0.25	0.75	0.25	0.5581
VI	2	0.661	0.6	0.3	0.7	0.3	0.6487
VII	2	0.6525	0.7	0.35	0.65	0.35	0.7119
VIII	2	0.645	0.8	0.4	0.6	0.4	0.7442
IX	2	0.6415	0.9	0.45	0.55	0.45	0.7716
					$3.25=A$;	$1.75=A'$;	$3.4345=B$.

With these results the force diagram of Fig. 18*a* is plotted, in which A is the vertical reaction at C, A' the vertical reaction at D, and B the horizontal thrust. When these forces are plotted in Fig. 18, the sum of the resultants of the horizontal and vertical reactions at each support intersects the locus at VII. To prove this:

$$d':E=A:B, \qquad d':l-E=A':B;$$

or

$$d'=\frac{AA'l}{B(A+A')}=0.6525, \qquad E=0.7$$

In place of resolving each of the forces from V to IX into its components and drawing the force diagram of Fig. 18*a*, all these forces may be replaced by one force at VII, which force is equal to the sum of the five forces, and its intersection with the locus line will at once produce the resultant components.

In computing the components of a uniformly distributed live load, stress is laid once more on the requirement that all the load must be located either on the right or on the left of the center line. When a load overlaps this line, it should be divided into two loads, each reaching to the center line; the components of each load should be computed separately, and the components thus obtained should be combined to obtain the resultant component.

Another point which requires special notice is that in a paneled structure one-half of the load on the panels adjoining the abutments is directly supported by the hinge and the abutment, and for loads reaching to the abutments this length should be reduced by one-half of a panel length.

With this explanation the computation of stresses should present no difficulty. To relieve all uncertainty the foregoing explanation is illustrated by an example. It hardly needs mention that this method is also applicable to the three-hinged arch, or the two-hinged arch described in Article 2 of this chapter. The first step in the computation is to determine the curvature of the arch axis, and then the influence of the live load and the changes in temperature.

If desired, the secondary stresses may be considered, but in a small arch, like the one illustrated in the following example, the stresses in the material may not reach such considerable values as in larger arches; because, the mass in the bridge being relatively small as compared with that of the live load, safety dictates a large allowance for the impact of the live load, and this allowance will be sufficient to provide for the secondary stresses.

6. Example.—Computation of Stresses in a Two-Hinged Arch Rib of Parabolic Form.—The arch rib is formed of a 20-in. Pencoyd I-beam having the following properties: weight per foot, 68.4 lbs.; gross sectional area, 19 sq. ins., net area, 17.7 sq. ins.; moment of inertia, 1,146; radius of gyration, 7.76.

The span of the arch from hinge to hinge is 50 ft., and the rise of the neutral axis is 10 ft.

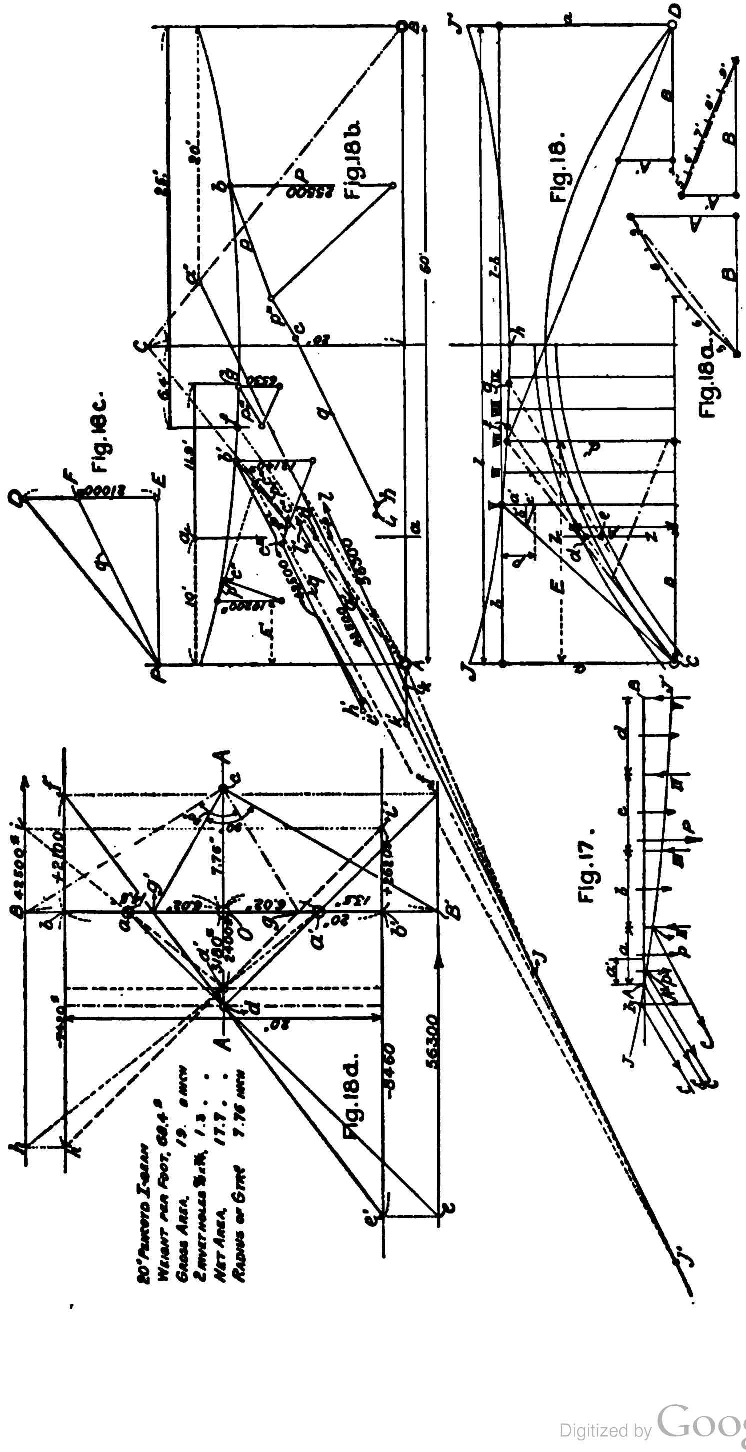
Fig. 18b.
Fig. 18c.
Fig. 18.
Fig. 18a.
Fig. 18d.
Fig. 17.

The deck of the bridge is composed of buckle-plates and granite paving. Dead load = 140 lbs. per sq. ft.

For the live load the tables of Chapter VI are used, and the computation is made for the heaviest highway traffic—class A = 112.5 lbs. per sq. ft. for a span of 50 ft.

The impact coefficient = 1.5, making a total of live load and impact = 170 lbs. per sq. ft.

The I-beams are placed 6 ft. c. to c., making the dead load per running foot of beam = 840 lbs. and the live load per running foot of beam = 1,020 lbs.

In Fig. 18 an arch of the above dimensions is drawn, and for the computation of stresses the core points only are of interest. The beam is to be investigated (see Fig. 18*b*) at a distance of 0.2 of the span from the supports, that is, at 10 ft. from the support *A*, and the upper and lower core points are indicated by the letters *d* and *e*.

Dead-Load Stresses.—In Fig. 18*b* the arch is omitted, as it is unnecessary for the computation of stresses and its lines would only lead to confusion; the core points *d* and *e* alone are shown.

The line of pressure for a uniformly distributed dead load is a parabola which coincides with the neutral axis of the arch. (For construction, see Fig. 9.)

In the center of the span twice the rise of the neutral axis (20 ft.) is plotted, which produces the point *C*, and the lines *AC* and *BC* are tangents to the curve at *A* and *B*.

[Figs. 11 and 11*a* show that the lines *Pn* and *Pf* (Fig. 11*a*) are parallel to the lines of pressure in the arch (Fig. 11) between *A*I and VIII*C*; and the intersection of these two lines produces the point *D*, which point is also the point of intersection of the resultant of all the vertical forces from I to VIII.]

In Fig. 18*b* these two lines are known, viz.: one is the tangent *AC* (or the line *PD* in the force diagram, Fig. 18*c*); the other is a horizontal line which is tangent to the axis at the crown of the arch, or the line *PE* parallel to the same in Fig. 18*c*. The length of the line *DE* must then represent the dead load of the arch from the hinge *A* to the center of the span in Fig. 18*b*. The dead load for one-half of the arch is $25\times840=21{,}000$ lbs. In Fig. 18*c* the point *P* is the pole of the force polygon, the line *PE* is the horizontal thrust, and the line *DE* is the vertical reaction caused by the dead load. As previously shown by Fig. 9, the points a' and a'' on the end tangents in Fig. 18*b* are points of the tangent $a'a''$. This tangent is also the location and direction of the line of pressure at the section *aa*, and its magnitude is found by drawing a line parallel to it in Fig. 18*c*, viz., the line *PF*. Summing up the results obtained, *The line $a'a''$ is the location of the line of pressure of the dead load at the section aa, and the line PF represents its magnitude.*

Live-Load Stresses. (Maximum compression in the lower fibers of the arch rib.)—The arch is loaded from the point *f* to the support *B*, and the left-hand components of any portion of this load

are in the section aa. This distance is indicated by a heavy line and is equal to 31.4 ft. This length overlaps the half-span by 6.4 ft., and the total load can be replaced by a load of $6.4 \times 1,020$ lbs. $= 6,530$ lbs. at g, and $25 \times 1,020 = 25,500$ lbs. at b. These two loads are resolved into their components p''' and p, the two components are added together, and a line which unites the points b and c is then equal to the magnitude and direction of the resultant of these two components, its point of location being at the hinge A. The line $a'a''$ was found to be the line of pressure of the dead load, and, prolonging the line $a'a''$ and drawing a line AJ parallel to the line cb, the live- and the dead-load resultant components will intersect at the point J. At the point c a line ch is drawn parallel to PF of Fig. 18c, and ch is measured from c equal to the line PF. A straight line joining the points h and b will be equal in direction and magnitude to the resultant of the live and dead loads, and a line Jk drawn parallel to hb will give the location of this resultant.

(*a*) TEMPERATURE STRESSES.—The equation $H_t = \frac{15EIwt}{8f^2}$ gives the horizontal thrust caused by temperature changes. In this equation

$$E = 29,000,000;$$
$$I = 1,145;$$
$$t = 60^\circ \text{ above or below normal;}$$
$$w = 0.000007 \text{ for } 1^\circ \text{ F.;}$$
$$f = 120 \text{ ins.;}$$

and
$$H_t = 1,820 \text{ lbs.}$$

This horizontal thrust is exerted at the hinge A.

Increasing or Decreasing Temperature.—The line bh is equal to the resultant of the live and dead loads, and in Chapter V (Arts. 2 and 3) it is explained that there are two causes which will increase the stresses in the extreme fibers, viz., an increase in the eccentricity of the force, or an increase in the force itself.

With an increase in the temperature a force will be exerted in the arch acting from right to left, that is, in the same general direction as the resultant due to the live and dead loads, and an increase in temperature will increase the magnitude of this resultant.

As regards eccentricity, the live- and dead-load resultant falls below the dead-load resultant Ja'' (this dead-load resultant is at the same time a tangent to the curve at the section aa), and an increase in the angle which $a'J$ and Jk make at J will increase the eccentricity. This occurs when hi is added to bh in a direction towards the left of h. But this is also the direction of the force when the temperature increases, and an increase in temperature not only increases the force, but it also increases the eccentricity of the force; and a line which joins the points b and i determines the magnitude and direction of the resultant of the live load, the

dead load, and the temperature stress. (For a full discussion of the effect which increasing eccentricity of a force has on the stresses in a beam, see Chapter V.)

The live- and dead-load resultant Jk intersects the horizontal thrust at k, and a line kl drawn parallel to bi gives the location of the final resultant. Its magnitude is 56,300 lbs., and its eccentricity below the neutral axis of the arch at the section $aa = 13.5$ ins.

This is the force which causes maximum compression in the lower fibers. It will not produce maximum tension in the upper fibers of the arch, because all components passing between the points d and e exert compression in the upper fibers, the line Aeg being the division line. All the forces to the right only of the point g should enter in the computation. In this case, however, the stress variations in the upper fibers are not nearly as large as they are in the lower fibers, and for this reason their computation may be omitted.

Maximum Compression in the Upper Fibers.—For this case the line Ag is the division line, and all the loads to the left of this line cause maximum compression. Part of the load is to the left of the section aa, and its right-hand reaction is in the section.

The live load is divided as follows:

$$10 \text{ (ft.)} \times 1{,}020 \text{ lbs.} = 10{,}200 \text{ lbs.} \quad (1)$$

and

$$11.9 \text{ (ft.)} \times 1{,}020 \text{ lbs.} = 12{,}140 \text{ lbs.} \quad (2)$$

The reaction of (1) $= p'$,
The component of (2) $= p''$;

and the two forces intersect at the point c''', which is the point of intersection of the resultant of these two forces. The reaction $c''c^{\text{IV}}$, which is equal to the force p', is added to the component $b'c''$, and a line joining the points b' and c^{IV} gives the direction and magnitude of the resultant of these two forces, or the resultant of the live load. A line $c'''J'$ drawn parallel to $b'c^{\text{IV}}$ through the point c''' gives the location of this resultant, which intersects the dead-load resultant at J'. To the line $b'c^{\text{IV}}$ is added the line $c^{\text{IV}}h'$, which is parallel to PF of Fig. 18*c* and of the same magnitude. Drawing $J'k'$ parallel to $b'h'$ gives the location of the resultant of the dead and live loads. This resultant intersects the temperature thrust at k', and, as the figure shows, this force has an eccentricity above the neutral axis of the arch at the section under consideration.

Now, an increase in temperature will increase the magnitude of the resultant, but it will decrease the angle formed at J' between the line $J'k'$ and the arch axis $J'a'$. (The tangent to the arch axis and the line of pressure of the dead load coincide, as demonstrated at the beginning of this article.) A decrease in temperature will decrease the magnitude of the resultant, but it will increase the angle, and consequently the eccentricity; and, in this case, the increased eccentricity will cause a maximum fiber stress in the

upper fibers of the arch. The horizontal thrust $h'i'$ is added from left to right to the resultant $b'h'$, and a line parallel to $b'i'$ is drawn through the point k', producing the line $k'l'$, which is the location of the force causing maximum compression in the upper fibers of the arch at the section aa. The magnitude of this force is 42,500 lbs., and its eccentricity above the neutral axis is 14.5 ins.

What was said in regard to the former system of loading is also true in this instance. In each case where the dead load is considerably less than the live load, four systems of loading should be investigated.

(b) DISTRIBUTION OF THE STRESS OVER THE CROSS-SECTION. A special article in Chapter V is devoted to this subject, but the foregoing calculation would not be complete without a computation of the stresses in the section, and it is therefore given here, referring for explanation to the chapter mentioned.

Force $\quad = 56{,}300$ lbs.
Eccentricity $= 13.5$ ins.

In Fig. 18d the height of the I-beam ($=20$ ins.) is measured off and the neutral axis AA is drawn through its center; a vertical axis BB' is also drawn, making O the point of origin.

To obtain the core points of the beam the radius of gyration ($=7.76$ ins.) is set off on the neutral axis to the right of the point O, and the core points a and a' can be found either by computation or graphically, viz.:

$$aO = \frac{(Oc)^2}{Ob'};$$

or, a right-angled triangle is drawn, which has for its hypothenuse the line ab' and for its height the radius of gyration Oc.

This method is very simple, and the construction lines are omitted for the sake of clearness.

The net area of the beam $=17.7$ sq. ins., and, if the load be uniformly distributed, the compression per square inch will be $\frac{56{,}300}{17.7} = 3{,}180$ lbs.

This 3,180 lbs. is measured off by the scale of forces, viz., Od, and a straight line is drawn through the core point a and the point d, intersecting the force at e; another line is drawn through the point d and the core point a' to an intersection with the force at f.

Perpendiculars ee' and ff' through the points e and f cut off the distances $b'e'$ and bf', equal respectively to the maximum compression and the maximum tension in the extreme fibers.

The same construction is employed for the force 42,500 lbs., and no further description is necessary.

In order to check the computation the right-angled triangle Bcg

has been drawn, giving the zero point g. The zero point g' is found in the same manner, and these points must be located on a straight line which connects f' with e' and h' with i'. The points g and g' are neutral points in the beam where no stress occurs for the respective positions of the force.

This diagram shows that the stress in the upper fibers varies from 7,420 lbs. compression to 2,100 lbs. tension, and in the lower fibers from 8,460 lbs. compression to 2,620 lbs. tension.

Magnitude of the Error Involved.—The locus of Fig. 14 is for a parabolic arch whose moment of inertia increases from the crown to the abutments in the same ratio that the secant of the angle which the axis makes with the horizontal increases from the crown to the abutment. In an arch with a uniform cross-section, if the section is sufficient to resist the stresses near the abutments, it is larger than is necessary at the crown. This is equivalent to diminishing the flexibility of the arch, making it more rigid than is needed; but the error is on the safe side. (See also the influence of the moment of inertia on the intersection locus, Art. 18.)

The forces $k'l'$ and kl in Fig. 18b should also be resolved into shear and axial stresses; such resolution has no material effect on the result, as the figure shows that the shear is very small. To investigate the beam for maximum and minimum shear, see Figs. 10 and 10a, Chapter II. The lateral bracing will strengthen the web sufficiently to withstand the shear, and any such computation is superfluous in this case.

Every pair of I-beams, however, should be connected by lateral bracing to make the structure rigid. But this belongs to the duties of the designer and it is not a subject for present consideration.

7. The Two-Hinged Spandrel-Braced Arch.— Among all the framed structures the two-hinged spandrel-braced arch is one of the most rigid, and, when the conditions of the locality provide natural abutments, it is at the same time the most economical.

Live loads and temperature changes will cause deflections, but, as compared with those of the three-hinged spandrel-braced arch, they are considerably less.

For spanning valleys the two-hinged spandrel-braced arch is one of the best forms of bridges that can be built, uniting beauty, rigidity, economy, and facility of erection. Though in many such localities this type of bridge has been built, there are numerous examples in existence where preference has been given to the cantilever, the suspension, or the truss bridge, when the arch, and especially the two-hinged spandrel-braced arch, should have been selected.

The reason for this neglect must be ascribed to the difficulty or the uncertainty in the determination of the stresses in arches of this type.

In the following paragraphs a method of computation will be illustrated which unites certainty with facility of application. It

is a combination of the elastic theory and the displacement theory. The elastic theory is used to compute the stresses in the structure, but the intersection locus is obtained by correcting the standard diagram of Fig. 14 by an empirical method which is derived from the application of the displacement theory. The temperature stresses are obtained by means of the displacement theory alone. (For the analysis of the displacement theory see Chap. X, Art. 1.)

To compute the stresses in an arch according to the elastic theory, the curvature of the arch axis should be known.

In other chapters it has been demonstrated that small deviations in this curve do not materially alter the intersection locus. In some arches the axis is not well defined. In such cases an axis must be assumed in order to make the computation of stresses possible, and this assumption may be considerably in error, resulting in the design of a defective arch.

The two-hinged spandrel-braced arch is of this character. The axis is not defined and the assumed axis may differ very considerably from the true one.

The following paragraphs will show how this difficulty is to be avoided:

The first point to be considered is the erection of the arch. The spandrel-braced arch is especially adapted for erection without falsework, the arch being built out as two cantilevers from the sides of the valley until the ends meet in the center. The top chord and the last diagonal of each projecting portion form the top chord of the cantilever during erection.

When the cantilevers meet, only the bottom chords are connected, after which all fastenings which were used to hold the cantilevers in place may safely be removed.

In this position the bottom chord will be flexible at the crown, and the arch will be a three-hinged spandrel-braced arch.

In case the bottom chord should be too rigid to allow sufficient movement at the crown, special provision should be made, by providing a temporary hinge and making the chords continuous after completion of the bridge.

Now, all lateral and wind braces and the floor system can be put in place, and the bridge can be completely finished except the connection of the top chord at the crown.

In this condition the arch will still be a three-hinged spandrel-braced arch, supporting its full dead load, and without temperature stresses.

When the top-chord connection is made, all the stresses in the arch will still be those caused by the dead load in a three-hinged arch. Now, however, temperature changes will cause stresses in the arch also the live load will exert itself (the bridge being completed), and therefore temperature stresses and live-load stresses are exerted in a two-hinged spandrel-braced arch.

This division can be adhered to in the computation of stresses,

and will simplify the method and reduce possible errors to a minimum.

In an arch of long span the dead load exerts the greatest stresses in the members, and these can be computed for a statically defined structure.

In addition a curve may be found for the neutral axis of the bottom chord of the arch, which coincides with the line of pressure in the arch resulting from the dead load. Then all the dead-load stresses in the arch will be resisted by the bottom chord, and only temperature changes and the live load will cause stresses in the web members and in the top chord.

No great error is committed when the dead load is assumed to be uniformly distributed over the arch; and to satisfy the condition of the previous paragraph, the axis of the bottom chord must be a parabola.

Usually the dead load increases slightly towards the abutments, and when this increase is known, or can be estimated, the bottom chord may be as easily designed with such a loading as if the latter were uniformly distributed.

Before taking up the computation of stresses, it will be necessary to consider the Williot Diagram, and also the construction of deflection angles in connection with their resultant force- and reciprocal-polygons. These will not only show the reader the method followed for obtaining the intersection locus, but they will assist him in the computation of stresses in special cases.

8. The Williot Diagram.—In Fig. 19A the bars AB and AC are two members of a truss. The point B of the bar AB is subject to a displacement from B to B', and the bar is subject to compression which shortens it by the length $A'_B A''_B$.

The point C of the bar AC is subject to a displacement to C', and the bar is subject to tension which lengthens it by $A'_C A''_C$.

It is now assumed that the bars move parallel to themselves, their new positions being $B'A'_B$ and $C'A'_C$. The changes in length result in bringing the point A'_B to A''_B, and the point A'_C to A''_C.

The two bars, however, are united at the point A, and the new position of the point A must be at the intersection of two arcs, one being drawn from the point B' as a center and with the radius $B'A''_B$, and the other from the point C' as a center and with the radius $C'A''_C$; the point of intersection of the two arcs is at A''', and the new position of the two bars is $B'A'''C'$.

The displacements of the bars, as well as their elongation or contraction, are so small as compared with their length that there is no significant difference between the arc and the tangent to the arc; the line $A'''A''_C$ is therefore taken as perpendicular to $A''_C C'$, or to AC, and the line $A'''A''_B$ perpendicular to $A'_B B'$, or to AB.

In the figure the polygon $A'''A''_C A'_C A A'_B A''_B A'''$ represents the various movements of the point A, as just described, and forms

a figure which can be drawn independent of the length of the bars. This affords a means of representing these movements on a greatly exaggerated scale, and it can then be applied to determine the movements or deflections of the panel points of any framed structure.

Fig. 19^B shows one-half of a braced arch, which is supported on rollers at A and is equivalent to a simple beam. Now, a vertical load placed on this arch will slide the point A toward the left, and if a horizontal force of sufficient intensity be applied at A, it will slide this point back into its former position. From Maxwell's theorem (see Appendix) a vertical load $=1$ applied, for instance, at the panel point 5 will cause a horizontal displacement at A, which is equal to the vertical displacement at the panel point 5 which would be caused by a horizontal force $=1$ applied at the point A.

This theorem may be used to compute the horizontal thrust caused by a vertical load.

The displacement theory provides the means of computing the changes in the lengths of the members of the truss, and the Williot Diagram is one of many methods for computin the displacement of the truss at the panel points caused by these changes in length; while Maxwell's law can be used to define the relation between the horizontal thrust and the deflectio s caused by any load.

Fig. 19 shows the arch. In Fig. 19d the distance ab represents a horizontal force $(=1)$ which is applied at A, and the Cremona Diagram of Fig. 19d is drawn which gives the stresses in the members of the arch caused by the force $ab=1$.

A table is now made similar to IV (Art. 14). The first column gives the index figures of the members; in this column each member is indicated by its two panel points and by a letter. The letter is used to indicate the elongation or contraction of each member in the Williot Diagram, and the figures indicate the panel points in said diagram.

The second column gives the length (s) of each member in inches.

The third column gives the sectional area (F) of each member in square inches.

The fourth column gives the stress (u') in each member caused by a horizontal force $=1$. These stresses are measured from the Cremona Diagram of Fig. 19d.

The fifth column gives the change in length of each member, the equation $E\Delta s=\frac{u_1 s}{F}$ being derived from equations (175) and (176) of the Appendix. In this case $P=0$, and H is equal to the horizontal force $=1$. When the force is equal to 1 ton, then $E=14.500$ (ton-inches) and the changes in length of the members should be divided by 14,500 to obtain the actual change.

(*a*) The Williot Diagram in Fig. 19^C is drawn to a scale of 1 in. $=200$ ins., and to determine the actual deflections, those obtained from the diagram should be multiplied by 200 and divided by 14,500; or the deflections shown in the diagram are 72.5 times larger than

the actual deflections which are caused by a horizontal thrust of 1 ton.

In Fig. 19^B the vertical at the crown of the arch does not contribute anything to the deflection, and for this reason it does not appear in the computation.

The panel point 10 is made the starting point of the diagram. The top chord a stretches 67.3 ins. $\div$ 14,500 (see Table IV). This 14,500 is a common divisor to all the members, and for convenience the figures of the table will be mentioned as if they were the actual changes in length. (See Fig. 19^C.)

This stretch of 67.3 ins. is measured in the direction of the top chord and to the left of 10.

The contraction of the diagonal b is 16.55 ins. and is measured in the direction of the diagonal to the right of 10. (Observe that + or tension is measured to the left or downward, and − or compression is measured to the right or upward.)

Perpendiculars are erected at the ends of a and b, which perpendiculars intersect at 9 in Fig. 19^C, and the location of 9 with reference to 10 shows the relative displacement of these two points.

MEMBERS c AND d.—The member c contracts 24.35 ins., and this contraction is plotted to the right of 10. The member d elongates 2.29 ins., and is plotted downward from 9; again, perpendiculars are erected at the ends of these two lines, which perpendiculars intersect at the point 8, and the position of 8 with reference to 10 gives the relative displacement between these two points, etc. (In Fig. 19^D the panel points 2 and 3 of the Williot Diagram have been shown on a larger scale.)

Finally, the panel points 1 and 0 are reached, and the location of these points with reference to 10 gives their relative displacements.

The line $A10$ is the center line, and a diagram for the right half of the arch would be similar to the one in Fig. 19^C were the plane in which the latter lies revolved through 180° on the axis $A10$.

If the full diagram were drawn, the relative horizontal displacement of the right-hand support with reference to the panel point 10 would be represented by a line equal to Ao measured to the left of A, and the displacement of the point A with reference to the right-hand support would then be equal to twice the length of the line $Ao = 2 \times \frac{1}{2}K = K$.

The vertical upward deflection at the panel point 3 caused by the horizontal load = 1 will be equal to the vertical ordinate of the point 3 above XX.

The vertical upward deflection at the panel point 5 will be equal to the vertical ordinate of the point 5 above XX, etc.

(b) Now a load equal to 1 placed at the panel point 3 will cause a horizontal displacement at A equal to the vertical ordinate $X3$. A horizontal force equal to 1 applied at A will cause a horizontal displacement at A equal to twice $Ao = K$.

To prevent the horizontal displacement at the point A which is

caused by the vertical force=1 placed at 3, a horizontal force of sufficient intensity should be applied at A to push A back a distance equal to $X3$.

The magnitude of this force H must then be equal to $\frac{X3}{K}$.

In the same manner it can be proved that the horizontal thrust caused by a vertical load placed at 5 is equal to $\frac{X5}{K}$.

Construction of the Intersection Locus.—In Fig. 19^E the ordinates $X3$, $X5$, $X7$, etc., have been plotted on the corresponding verticals I, II, III, etc. (the scale for these ordinates has been reduced to one-fourth of that of Fig. 19^C), and these ordinates are equal to the horizontal thrust. The line K is then the unit force, and $A'B'$ is the horizontal thrust curve.

These ordinates have also been plotted in Fig. 19^B on the axis AC, viz., $A3=X3$, $A5=X5$, etc., and verticals have been erected through these points. The line K has been plotted from A to D, and the line $CE=\frac{1}{2}K$.

The line DE cuts off ordinates on the verticals I, II, etc., which are equal to the reactions at A when the load K is placed respectively at I, II, etc.

These reactions have been transferred to the verticals erected at 3, 5, 7, etc., giving the points a', b', c', etc. The line Aa' is then the component for a load placed at I, and I is a point of the intersection locus; Ab' is the component for a load placed at II, and II is a point of the intersection locus, etc. The line FG which passes through all points similarly determined is the intersection locus.

The line $F'G'$ is the intersection locus which is plotted from the standard diagram (Fig. 14) for a parabola with a rise equal to CC'.

9. Correction of the Standard Intersection Locus.—Fig. 19^B shows that these two intersection loci coincide at the center of the span, and that the difference between their ordinates at A is equal to $\frac{4}{19.5}\times 1.3f=\frac{4}{15}f$, or to the depth of the arch at the crown divided by the depth of the arch at the abutments, this quotient being multiplied by 1.3 (which is a factor of the structure), and by f, or the rise of the bottom chord.

In Fig. 19^F the differences between the ordinates of the two lines FG and FG' have been plotted from the straight line AB, and are bounded by the dotted line BC. The line BC is so nearly straight that no material error is made in assuming it to be such. Applying this result to Fig. 19^B, the correction of the standard diagram for the purpose of computing the stresses in a two-hinged spandrel-braced arch is very simple, as may be seen from the following:

Plot the intersection locus of the standard diagram (Fig. 14) for an arch having a rise equal to that of the axis of the bottom chord. When the bottom chord does not form a parabola, first find the

equivalent parabola, and plot the intersection locus for a rise equal to that of the equivalent parabola (see Fig. 14). If necessary, this line may be corrected as described and shown in Fig. 14*a*.

Plot $\frac{t'}{t} \times 1.3f$ of Fig. 19^B as an ordinate from a straight line AB in Fig. 19^F, in which $AC = \frac{t'}{t} \times 1.3f$ ($= \frac{4}{15}f$ in this case). Draw the straight line BC, and plot the ordinates of the line BC upwards from the intersection locus $G'F'$ in Fig. 19^B; this will produce the intersection locus GF', which is to be used for the computation of the stresses in the arch.

All spandrel-braced arches for bridges are very similar in form, and the foregoing construction is generally applicable in the determination of the intersection locus. Its advantage is evident: it enables the designer to compute the stresses in the arch from the start, and with great accuracy. Any other method includes in its application the unknown quantity F, viz., the sections of the members, for which assumptions have to be made; and the computation has to be repeated until the assumptions and the results correspond. Any one who has computed the stresses in the spandrel-braced arch knows how laborious this operation is.

After the foregoing explanation the computation of the temperature stresses should be readily understood.

10. **Computation of the Temperature Stresses.**—When one end of the bridge is free to move horizontally, there will be no temperature stresses in the arch, and sliding will occur at A. When A is pushed back in place by a horizontal force, this force will represent the horizontal thrust caused by the change in temperature.

From this it follows that the computation of the temperature stresses requires the same procedure that was described in the foregoing paragraphs. Its application, however, differs slightly.

The construction of the Williot Diagram, like the construction of the Cremona Diagram, is subject to unavoidable errors in execution. In the computation of the intersection locus these errors are not serious so long as they are confined exclusively to the execution of the drawing. The purpose of the computation is to find the relation between the vertical deflections of the panel points and the horizontal displacement of the point of support, and the same errors will practically obtain in both, and therefore balance each other.

For the computation of temperature stresses, however, the actual displacements determine the stresses in the members. For this reason the magnitude of these displacements should be determined with great accuracy, and for this purpose the analytical method is better adapted.

The method of finding the temperature stresses is not a direct one.

First, the horizontal displacement is found which is caused by a unit horizontal force, say 10 tons.

The actual displacement of the support caused by a temperature change is computed under the supposition that the arch is a simple girder, free to move at A; then the ratio between the displacements is the same as between the forces. To illustrate: If the displacement caused by 10 tons $=D$, and that caused by a rise in temperature $=d$, then

$$H:10 \text{ tons}=d:D.$$

Taking the arch in Fig. 19 as an example, the distance ab of Fig. 19d is then equal to 10 tons, and all the stresses of column IV should be multiplied by 10. This has been done and the stresses are inserted in column VI, Table IV.

From equation (179a) of the Appendix,

$$-E\Delta l=\Sigma zPu.$$

There are no vertical forces in this case causing horizontal thrust; there is only a horizontal force causing stresses P in the members. Now $zu=\frac{u's}{F}$, the value of which was found before; these stresses are given in column V, and multiplying the figures in column V by those in column VI will give $\frac{Pu's}{F}$. These products are inserted in column VII, and the sum of all the figures in column VII $=\Sigma\frac{Pu's}{F}$ for one-half the span, or for the whole span,

$$\Sigma\frac{Pu's}{F}=11{,}247\times 2=E\Delta l.$$

Now E in inch-tons $=14{,}500$, and $\Delta l=22{,}494\div 14.500=1.556$ ins. is the horizontal displacement caused at A by a horizontal force of 10 tons.

Here the Williot Diagram can be checked, viz.: The line Ao (Fig. 19c), which is 72.5 times as large as one-half the displacement of the support A caused by a horizontal force of 1 ton, gives

$$1.556 \text{ ins.}\times\frac{72.5}{2\times 10}=5.64 \text{ ins.}$$

The maximum temperature above or below the normal is assumed to be 75° F.

The coefficient of linear expansion for steel per degree F. $=0.000007$.

The length of the bridge $=105\times 12=1{,}260$ ins.

If the bridge were free to move at A the horizontal displacement would be

$$0.000007\times 75\times 1{,}260=0.662 \text{ in.}$$

The horizontal thrust caused by a change in temperature of 75° will be

$$\frac{0.662}{1.556} \times 10 = 4.25 \text{ tons.}$$

To obtain the stresses in the members caused by this horizontal thrust, the stresses of column VI of Table IV (which are for a horizontal thrust of 10 tons) should be multiplied by $\frac{4.25}{10}$.

These stresses are inserted in column VIII of Table IV, and it will be understood that these stresses are for an *increase* in temperature of 75°.

For the computation of the temperature stresses it is necessary to assume the sections of the members.

In connection with this it should be remembered that the stresses caused by the dead and live loads can be accurately obtained from the computation.

The best method to follow is to compute the necessary areas of the members from the stresses caused by the dead and live loads, and to make the following additions:

To the sections of the top chord	110%
" " " " " bottom chord	9%
" " " " " diagonals	80%
" " " " " verticals	25%

With the sections thus obtained the temperature stresses should be computed, and the final results should be compared with these assumptions, corrections being made if necessary.

One trial will be found sufficient for computing the correct temperature stresses.

11. Two-Hinged Spandrel-Braced Arch with Curved Upper Chord.—The foregoing method will give accurate stresses in the two-hinged spandrel-braced arch with a horizontal upper chord. Roof-trusses and bridges, however, are often built in which the upper chord is curved. In this case three methods may be used for the correction of the intersection locus.

First Method.—When the hinge is located in the axis of the arch, the correction of the intersection locus may be made as illustrated and described in Article 1 of this chapter; the increase in the moment of inertia from the crown towards the abutments is neglected in this case, and as Article 18, etc. will show, this is an approximation which will produce an error in the stresses of the arch averaging from 0.5 to 4% on the side of safety. This error is distributed over the arch as follows: At the crown the stresses are slightly too large, and their increase toward the abutments depends on the ratio of increase in the height of the arch rib.

For the arch rib with parallel chords the error will be zero.

For the arch rib with a horizontal upper chord the error will reach its maximum value (9%) at the abutments, and for a curved upper chord the error must lie somewhere between zero and 9%.

It will be seen from the foregoing paragraphs that the error involved is not objectionable from the standpoint of practical engineering.

Second Method.—This should be preferably used for arches with a curved upper chord when the hinges are located in the axis of the bottom chord; it may, however, also be applied in place of the first method. Divide the height of the arch rib at the crown by its height at the hinges, this height in both cases being measured radially (*not* along the vertical ordinates); multiply this quotient by 1.3 times the rise of the arch (when the hinges are in the axis of the bottom chord take the rise of the bottom chord; when the hinges are in the axis of the arch, take the rise of the arch axis), and proceed according to Article 9 and Figs. 19^B and 19^F.

This method yields somewhat closer results than the one first described, but the stresses found are also too high. A correction of the intersection locus can be developed, similar to that shown in Fig. 38, for the stiff arch, but the author believes that the foregoing methods are sufficiently accurate for all practical bridge designing and that any further refinement would be superfluous.

The horizontal forces which result ordinarily from wind pressure can be resolved into their components by the use of the standard diagram of Fig. 13; this will give stresses that are in error, but the error will not exceed 5%. The wind pressure, however, is a factor which is based on assumptions that will vary a great deal more than 7% from the actual conditions, and for this reason any correction of the standard diagram is unnecessary.

Third Method.—The intersection locus for the vertical and horizontal forces may be obtained by the method described in Article 8 of this chapter. This method should preferably be employed in special cases, and then the use of deflection angles will give results of greater accuracy.

12. The Use of Deflection Angles for the Computation of the Intersection Locus.—The construction of the Williot Diagram may give sufficiently accurate results for the computation of deflections, but it is, nevertheless, subject to a cumulative error which may be as large as 12%. It should not be understood, however, that its use would result in an error in the computation of stresses equal to 12%. As was previously pointed out, the computation of the intersection locus is based on the ratio which exists between the vertical deflections of the panel points and the imaginary horizontal displacement of the support, and even a larger error than 12% in the deflections may give an accurate ratio.

The following is a more accurate method, but its use involves a much greater amount of labor:

From previous paragraphs and Figs. 19^B and 19^C it is seen that the horizontal thrust is derived from the deflections of the panel points where the forces are applied; this line of deflection may also be obtained from the angular deflections and the changes in length of the members.

If in Fig. $19^{H'}$ the top chord 1–3 and its deflection angle were plotted, and to this were joined the top chord and the deflection angle of 3–5, etc., the deflections at the panel points would be represented by a curve which is tangent to the polygon thus obtained.

Instead of using the top chord, the deflection angles 1, 2, 3, etc. of the web members may be plotted, and the resulting panel points will be located on the same deflection curve which was obtained by plotting the angular deflections of the top chord.

In proof of this (see triangle ABC, Fig. 19^G) assume the angle A to increase to $A+da$, and the angle B to $B+db$; then the angle C must decrease and it will become equal to $C-(da+db)$, and $(da+db)$ will be the deflection angle of the bar AC. If the bar AC be horizontal in its original position, it will deflect upward from a horizontal line drawn through A, and the deflection angle will be equal to $(da+db)$.

These deflection angles can be obtained very accurately and on a greatly exaggerated scale. In Fig. 19^G the three bars AB, BC, and AC form a closed polygon. The bar AC shortens under compression the distance AA'_C, the bar BC shortens the distance BB'_C, and the bar AB elongates the distance $B'B'_A$. First conceive the bar AB to be moved parallel to itself, assuming the position A'_CB', and then that the elongation of this bar takes place; the new position of B after these two displacements will be B'_A.

The bar BC shortens, and the new position of the point B on the bar BC will be the point B'_C. These two bars are connected, and to find the final position of the point B, an arc should be described with the bar $A'_CB'_A$ as a radius and the point A'_C as the center. In the same manner the bar B'_CC describes an arc around C as a center, and the intersection of these two arcs gives the point B''; and the new position of the bars is then indicated by the figure $A'_CB''C$. As before explained, the arcs and the tangents coincide, B'_AB'' is perpendicular to AB, and B'_CB'' is perpendicular to BC. It is clear from the figure that the arc (or perpendicular) B'_AB'' measures the angular displacement of the bar $A'_CB'_A$ (or of the bar AB), and that the angle which it subtends is negative; the figure shows that the angle at A has become smaller. The projection of this deflection angle on the bar BC is then equal to the line B'_Ab.

The figure shows that this angular displacement may be obtained without drawing the bars, the polygon $B'_CBB'B'_Ab$ being all that needs to be plotted.

To determine the angular deflection at the panel points of a framework, this polygon is drawn at the point where the angular deflection is to be computed, viz., at A, and the polygon $Acde$ completes the

computation. The lines Ag and ef are perpendiculars on BC, and $gf=B'_A b$.

[For the analytical computation of the deflection angle at A, let the changes in length of the bars be da', db', and dc':

$$\Delta A=\Delta c'b'=(da'-dc')\cot(a'c')+(da'-db')\cot(a'b').$$

Scale for Measuring the Angle.—Assume the line Ah to be the unit radius for measuring the angle gAf; then, if the side Af of the angle is prolonged and a perpendicular is erected on Ah at h which intersects Af at the point i, the line hi will be the measure of the deflection angle gAf at the unit radius Ah.

The same arch shown in Fig. 19 is redrawn in Fig. 19^H. The computation of the deflection angles for the web members is preferable, because it saves labor, and by drawing a simple moment polygon the horizontal displacement at A is also obtained, which is the unit of measurement for the deflections.

The angular deflections are first computed and two force polygons are drawn, in one of which the deflections are considered as horizontal forces, and in the other as vertical forces; reciprocal polygons are then drawn from these force polygons. The ordinates of these reciprocal polygons give the horizontal displacement at A and the vertical deflection at the panel points, and adding to these the change in the length of the bars completes the computation, all according to equation (181) of the Appendix:

$$H=\frac{\Sigma K_x g_{xa}+\Delta l}{g_{aa}}.$$

The use of angles and lines as forces in drawing force and moment polygons is explained in the Appendix (see two-hinged arch, page 261, etc., and also in Art. 10 of this chapter—Douro Bridge).

In Fig. 19^H the angular deflections of the web members are computed, and the change in the length of the bars for computing these deflections is again taken from column V of Table IV.

In plotting the changes in the length of the bars the scale used is 1 in. = 40 ins.

The computation needs no further explanation, but the positive and negative deflections should be carefully noted. In Fig. 19^G the deflection obtained is negative and is measured toward the right of the perpendicular which is drawn from the panel point A on the bar BC. If the deflection angle were positive it would be measured to the left of this line. This is a convenient way in which to determine the sign of the angle, and applying same to Fig. 19^H it is seen that all the deflection angles are negative except 5 and 7.* (In this figure p'' is the unit radius.)

*** The author wishes to lay stress on the fact that the sign of the deflection**

In Figs. 19^I and 19^J the deflection angles have been added in the two force polygons, the deflections V and VII being positive, and with the pole distance p' the reciprocal polygons of Figs. $19^{I'}$ and $19^{J'}$ have been drawn. The arch being symmetrical with respect to the center line, only one-half of these polygons need be drawn.

Scale.—For the purpose of comparison, it is desirable to have the same scale for Figs. 19^E, $19^{I'}$, and $19^{J'}$.

The Williot Diagram is drawn to a scale of 1 in. = 200 ins. The figures of column V, Table IV, are computed for a unit of 1 ton, or $E = 14{,}500$; and the ordinates of Fig. 19^E are one-fourth those of Fig. 19^C, or to a scale of 1 in. = 800 ins.

In Fig. 19^H the changes in the length of the members are plotted to a scale of 1 in. = 40 ins., and p'' is plotted equal to 50 ins. on a scale of 1 in. = 40 ins.

When p'' is the unit of measurement for the angles, and the pole distance p' is made equal to p'', then the ordinates of the reciprocal polygon of Fig. $19^{J'}$, divided by E, give the deflections at the panel points, expressed in the same units as those of Fig. 19^H, viz., 1 in. = 40 ins. The ordinates of Fig. 19^E are measured with a unit of 1 in. = 800 ins., and if in Figs. 19^J and 19^I the pole distance $p' = \frac{800}{40} \times p''$, then the ordinates of Fig. $19^{J'}$ can be measured with the same scale as the ordinates of Fig. 19^E. Figs. 19^I and 19^J would be too large for the illustration, and for this reason they have been considerably reduced.

In Fig. $19^{J'}$ AB is the horizontal-thrust curve when the force $= 1 = ab$ of Fig. $19^{I'}$.

This curve includes only the angular deflections, and the changes in the lengths of the bars should be added. To compute these a simple Williot Diagram (Fig. 19^K) of the web members only has been drawn, the changes in the lengths of the bars being again taken from Column V, Table IV. Only one-half of the diagram is to be drawn, as the diagram for the whole bridge is symmetrical with respect to the center line $A10'$.

This diagram is drawn to a scale of 1 inch = 40 inches, and that of Fig. $19^{J'}$ to a scale of 1 inch = 800 inches. The ordinates of Fig. 19^K measured from the line XX to the panel points 10′, 9, 7, etc., should be divided by 20 and the quotients added to the ordinates of the line AB; this will give the horizontal-thrust curve AB'.

To the horizontal force g'_{aa} should be added one-tenth of the line $A0$ (this is only one-half the displacement of the point of support), which is equal to g''_{aa}, making the unit force $K = ab + bc$.

---

angles 5 and 7 of Fig. $19^{H'}$ is *opposite* to the sign of all the other deflection angles, because authorities state as a law that the deflection angles of the web members all have the *same* sign, and they partially base further deductions on this assertion.

Though the error resulting from such an assumption may be small, its employment, nevertheless, is confusing to the practising engineer, who has no time to investigate it.

There is a difference of about 7% between Figs. 19^E and $19^{J'}$; but there is the same difference between the unit forces of these two figures, and both will give the same intersection locus.

The angular-deflection method commends itself for the accurate results it gives, though the first method is sufficiently precise for the computation of the intersection locus. The author would advise that the Williot Diagram be drawn two or three times in order to reduce the possible error.

When the arch is not symmetrical with respect to the center line, the diagrams of Figs. 19^C, 19^H, and 19^K should be plotted in full. When the hinges of the arch are not in the same plane, the lines 2, 4, 6, etc., of Fig. $19^{I'}$ are to be drawn parallel to the chord which unites the two hinges of the arch; and in Fig. 19^I the deflection angles are plotted as forces on a line which is parallel with this chord of the arch. In this case the lines drawn through the top-chord panel points in Fig. $19^{I'}$ do not coincide; the construction of the reciprocal polygon of Fig. $19^{I'}$, however, remains the same.

In this figure the segments of the reciprocal polygon come so close together that only one line is drawn where two segments should be shown; this would, however, make the figure unintelligible. Its appearance is worse than its result, as a high degree of accuracy may be obtained.

The method for obtaining the horizontal thrust in an arch by means of deflections is applicable to a framed arch of any shape. To apply the method the sectional areas of the members should be known; but the object of the computation is to find the sectional areas of the members, and this is the very factor which is assumed as known in this method! Various methods and approximations can be employed to simplify the preliminary computation; notwithstanding this, it remains laborious and complicated.

The author does not discuss these various methods, as the one which he presents for the correction of the intersection locus is simple and gives, in nearly all cases, results which are accurate or very nearly so, and in every instance as accurate as those obtained by employing the methods referred to in the preceding paragraph.

He would recommend, however, that a final computation be made by the method of angular deflections, which will not only be a check on the work, but will furnish diagrams which can be used to compute temperature deflections, the camber to be given to the bridge for erection purposes, and also the deflections caused by the live load.

These applications of the diagrams are explained in the following article.

13. Deflection of the Two-Hinged Spandrel-Braced Arch.—The deflections in the arch can be easily computed. (For analysis see Chapter X.) In the foregoing paragraphs the ratio between the horizontal thrust and the vertical load which causes this thrust was found from the deflections. This same process can be reversed to

find the deflections of the arch under a given loading, viz.: First find the deflections caused by a load acting on the arch when the assumption is made that the arch is a simple beam. Then find the deflections caused by a horizontal thrust at the support, this horizontal thrust being caused by the load.

The difference between these deflections must be the deflection of the arch.

The deflections caused by the horizontal thrust are given in Figs. 19^E and $19^{J'}$, and the unit of measurement needs only to be determined.

To find the deflections caused by a vertical load, assume in Fig. $19^{L'}$ a vertical upward reaction$=1$ ton at A, and draw the Cremona Diagram of Fig. 19^K. When the arch is symmetrical, one-half of the diagram is sufficient. In Table IV, Column IX, the stresses obtained from Fig. 19^K have been inserted.

To find the stresses in the members caused by a load of 1 ton which is placed, for instance, at 7: The reaction at $A=0.7$ ton, and that at $B=0.3$ ton.

The stresses to the left of the line XX are equal to those in Column IX (above the horizontal lines) multiplied by 0.7, and the stresses to the right of XX are equal to those in Column IX multiplied by 0.3; for example, the stress in $3–4=+1.358$ tons, and that in $3'–4'=+0.582$ ton; the stress in $7–9=7'–9'=0.3\times-9.02=-2.71$ tons; the stress in $6–8=+3.47$ tons, and in $6'–8'=+1.50$ tons, etc.

In Fig. $19^{L''}$ the deflection angles for the web members have been computed by using the values in Column X of Table IV (which are derived from Column IX, as explained in the preceding article for a load of 1 ton at the crown), and have been inserted in Column XI. The unit radius is the same as that in Fig. 19^H.

To find the deflection angles for a load placed at 7, the reaction at $A=0.7$ ton and that at $B=0.3$ ton.

The angles 1, 2, 3, 4, 5, and 6, as obtained from Column XI, should be multiplied by 0.7, and the angles 8, 9, 10, 9′, 8′, . . . , 1′ should be multiplied by 0.3.

The angle 7 is the only angle to be computed, and the sides of the triangle which affect it are 6–7, 6–8, and 7–8. Now, the changes in length of 6–7 and 6–8 are obtained by multiplying the values given in Column X by 0.7, and that of 7–8 by multiplying by 0.3.

In the example which is illustrated in Fig. $19^{M'}$ it is assumed that a load of 1 ton is applied at the crown of the arch. From the thrust curve of either Fig. 19^E or Fig. $19^{J'}$, it follows that $H=1.306$ tons, viz.: the ordinate CB' of Fig. $19^{J'}$ divided by the ordinate ac of Fig. $19^{I'}$.

For a load of 1 ton at the crown the reaction at $A=\frac{1}{2}$ ton, and to construct the force polygon the values in Column XI should be divided by two.

The thrust curve of Fig. $19^{J'}$ was found for a unit horizontal

thrust = 1 ton, the horizontal thrust caused by the load placed at the crown = 1.306 tons, and the ordinates of Fig. $19^{J'}$ should be multiplied by 1.306; or, the pole distance of Fig. 19^{M} should be 1.306 times smaller than that of Fig. 19^{J}, or the figures of Column XI, Table IV, should be divided by 2×1.306. The last course has been followed in Fig. 19^{M}, which is drawn on the same reduced scale used in Fig. 19^{J}.

From this force polygon has been drawn the reciprocal polygon AB.

In Fig. 19^{N} a simple Williot Diagram has been drawn for the changes in length of the web members, and, in order that the scale may correspond to that of Fig. $19^{J'}$, the figures of Column X, Table IV, have been divided by 2×1.306.

The ordinates of this diagram have been divided by 20 (see explanation of Fig. 19^{K}) and have been added to the ordinates of the thrust curve AB of Fig. $19^{M'}$, producing the line AB'. The line AB'' is the same as the line AB' of Fig. $19^{J'}$, and in Fig. $19^{M'}$ the ordinate $B'B''$ is the deflection of the arch at the crown caused by a load of 1 ton.

Scale of Measurement.—The ordinates of Fig. $19^{J'}$ or the line AB'' of Fig. $19^{M'}$ give the deflections in inches caused by a horizontal force of 1 ton, when they are divided by 18.125 $\left(=\frac{14{,}500}{800}\right)$.

The horizontal thrust caused by the load of 1 ton at the crown $=1.306$ tons and the ordinates of Fig. $19^{M'}$ give the deflections in inches when they are multiplied by the ratio $\frac{1.306}{18.125}=0.072$.

The ordinate $B'B''=1.58$ ins. and the deflection at the crown $=1.58\times0.072=0.114$ in.

Figs. 19^{L} to 19^{N} give the following results:

In Fig. $19^{L''}$ the elongations of the bars are plotted from Column X, Table IV, on a scale of 1 in. = 40 ins. The unit force is 1 ton, or $E=14{,}500$; the reaction due to a load of 1 ton at the crown = ½ ton.

The unit radius p'' is 50 ins. measured on a scale of 1 in. = 40 ins.

The pole distance p' of the force polygon is plotted = 1,000 ins. on a scale of 1 in. = 40 ins., or $\frac{p'}{p''}=20$.

The horizontal thrust is 1.306 tons, and the deflection angles are plotted to a scale of 1 in. = (40 ins. ÷ 1.306).

The deflections are then measured in inches multiplied by $\frac{40\times1.306}{14{,}500}\times20=0.072$, and the deflection at the crown is obtained as before = 0.114 in.

For a load placed at 7 in Fig. $19^{L'}$ it is necessary to draw the full force polygon, Fig. 19^{M}, the full reciprocal polygon, Fig. $19^{M'}$, and the full Williot Diagram, Fig. 19^{N}.

The deflections can also be computed by the application of equation (189), Chapter X.

The computation of the horizontal displacement of the crown, or of any other part of the arch under a vertical loading, may be performed according to the method set forth in a later article. [See equation (192), Chapter X.]

(*a*) Deflections Caused by a Change in Temperature and by a Yielding of the Abutments.—Yielding of the abutments affects the arch in the same manner as a reduction in temperature, consequently only the temperature changes need be described.

According to Art. 10, a change in temperature of 75° F. causes a thrust of 4.25 tons, and the ordinates in Figs. 19^E or $19^{J'}$, when multiplied by $\frac{4.25}{18.125}$, will give the deflections in inches. (The ordinates are for a horizontal thrust of 1 ton.)

14. Deflections of the Three-Hinged Spandrel-Braced Arch. (For the analysis and explanation of the principle underlying the following computations, see Chapter X.)

Suppose a load of 1 ton is again placed at the crown of the arch. From equation (195) it follows that the angular displacement a_c at the crown hinge is equal to $(\mathcal{H}_x - H_x)\frac{g_a}{f}$.

Now $\mathcal{H}_x$ is the horizontal thrust in the three-hinged arch which is defined by the ordinates of a triangle having its apex on the vertical line through the crown, and, from equation (21), Chapter VII,

$$\mathcal{H} = K\frac{l}{4f}.$$

Now $K=1$ ton, $l=105$ ft., and $4f=62$ ft.;

$$\therefore \mathcal{H} = \frac{105}{62} = 1.695.$$

H_x is the horizontal thrust in the two-hinged arch, and is equal to 1.306 (see Art. 13). In Fig. $19^{M'}$ the ordinates of the line AB'' represent H_x, the ordinates of the line AB''' represent $\mathcal{H}_x$, and the difference between the ordinates of these two lines is equal to $\mathcal{H}_x - H_x$.

The value of g_a should now be found.

For a horizontal thrust of 1 ton, $g_a = ac$ of Fig. $19^{I'}$, $=K$ of Fig. 19^E, and $1.306 \times K = g_a$.

$$f = 15.5 \text{ ft.} = 186 \text{ ins.}, \quad p'' \text{ of Fig. } 19^{L''} = 50 \text{ ins., and}$$

$$\frac{B''B'''}{f} = \frac{a_c}{k}, \quad \text{or} \quad a_c = B''B''' \times \frac{k^*}{f}.$$

* k (= 1.306) is a factor of the diagram, as explained in Art. 13.

Now, $B''B'''$ measures 0.95 in. actual length in Fig. $19^{M'}$, the pole distance p' of Fig. 19^{M} is 1.000 ins.; consequently

$$a_c = 0.95 \times 1,000 \times \frac{50}{186} \times 1.306 = 334,$$

and a_c is the angular deflection of the crown hinge when measured with the scale used in Figs. $19^{L''}$ and 19^{M}.

To compute the deflections in the three-hinged spandrel-braced arch:

First compute the thrust curve in a two-hinged arch for a vertical load=1 placed at the panel point of which the deflection is desired. (When this load is placed at the crown the line AB' of Fig. $19^{M'}$ will be this curve.)

Next compute the horizontal-thrust curve for the horizontal thrust caused by this vertical load (=1) in the *three-hinged* arch, but as if this thrust were acting in the two-hinged arch.

The difference between the ordinates of these two curves gives the partial deflection (or the deflection of an arch in which the abutments could approach each other a distance equal to a_c of the preceding article).

The top chord is then assumed to be parted in two at the crown, and this increases the deflection. (This is equivalent to forcing the abutments back into their original positions, as a result of which the crown sinks.) To obtain this:

Compute the horizontal-thrust curve for this same arch as a two-hinged arch, and also the horizontal-thrust curve of the three-hinged arch (these two lines are given in Fig. $19^{M'}$, viz., AB'' and AB''').

Now, for illustration, assume the line AB' of Fig. $19^{M'}$ to be the deflection curve of the three-hinged arch with the top chord gg' in position. The angular deflection at the crown hinge is found as described on a previous page. In Fig. 19^{O} this angular deflection has been plotted as the force of a force polygon with the same scale and pole distance p' as that of Fig. 19^{M}. From this force polygon of Fig. 19^{O} is drawn the reciprocal polygon (see Fig. $19^{M'}$), and the ordinate measured from the line AB^{IV} to the line AB' gives the deflection of the three-hinged arch at the crown.

(*a*) * For a full, uniformly distributed load when the hinges are located in the axis of the bottom chord, the deflection can be computed with sufficient accuracy for practical purposes by finding an average cross-section of the bottom chord and the average stress in this chord caused by the load. From these the modulus of contraction of the chord can be computed, and, assuming the two straight lines uniting the crown hinge with the abutment hinges to contract in the same ratio as the bottom chord, the problem resolves

* This method applies to the three-hinged spandrel-braced arch as well as to the three-hinged arch rib.

Table IV.

TWO-HINGED SPANDREL-BRACED ARCH.

Member.	Length in ins. s.	Area in sq. ins. F.	Stress for 1 ton at $A_1 = u'$ (tons).	Increase in length $E\Delta s = \frac{u's}{F}$.	$H = 10$ tons. Stress for 10 tons at $A_1 = P$ (tons).	$E\Delta s = \frac{Pu's}{F}$.	Temperature stresses in tons.	Reaction $= 1$. s''.	$\frac{s''s}{F}$.	Deflection angles.	$\frac{s}{F}$.
I.	II.	III.	IV.	V.	VI.	VII.	VIII.	IX.	X.	XI.	XII.
						Top Chord.					
t 0–1	126	8	+0.40	+ 6.30	+ 4	25.2	+ 1.7	− 1	− 15.75	 0	15.75
q 1–3	126	8	+1.03	+16.30	+10.3	167.8	+ 4.4	− 0.73	− 11.5	+ 0.5 I	15.75
m 3–5	126	8	+2.03	+32.00	+20.3	650	+ 8.6	− 2.17	− 34.2	+ 33.5 II	15.75
i 5–7	126	8	+3.26	+51.40	+32.6	1675	+13.9	− 4.88	− 76.9	+ 13.5 III	15.75
e 7–9	126	8	+3.93	+61.90	+39.3	2430	+16.7	− 9.02	−142	+ 95.5 IV	15.75
a 9–11	126	8	+4.27	+67.30	+42.7	2880	+19.2	−11.22	−176.5	+ 51.5 V	15.75
										+ 274 VI	
						Bottom Chord.					
s 0–2	143	24	−1.15	− 6.87	−11.5	79	− 4.9	0	0	+ 118 VII	5.96
o 2–4	137	24	−1.50	− 8.57	−15	128.5	− 6.4	+ 0.82	+ 4.68	+ 607 VIII	5.71
k 4–6	132	24	−2.13	−11.73	−21.3	240	− 9.1	+ 2.26	+ 12.42	+ 120 IX	5.5
g 6–8	128	24	−3.07	−16.35	−30.7	502	−13.1	+ 4.97	+ 26.55	+1120 X	5.34
c 8–10	127	24	−4.27	−24.35	−42.7	1040	−19.2	+ 9.03	+ 47.80	....	5.29
						Verticals.					
p 2–3	166	24	+0.57	+15.75	+ 5.7	89.8	+ 2.4	− 1.33	− 9.2	....	6.92
l 4–5	114	24	+0.61	+11.60	+ 6.1	70.8	+ 2.6	− 1.67	− 7.93	....	4.75
h 6–7	78	24	+0.54	+ 7.03	+ 5.4	38	+ 2.3	− 1.87	− 6.07	....	3.25
d 8–9	55	24	+0.25	+ 2.29	+ 2.5	5.7	+ 1	− 1.62	− 3.71	....	2.29
						Diagonals.					
r 1–2	208	6	−0.66	−22.85	− 6.6	151	− 2.8	+ 1.25	+ 43.30	....	34.66
n 3–4	168	6	−0.86	−24.10	− 8.6	207	− 3.7	+ 1.94	+ 54.30	....	28
j 5–6	148	6	−1.16	−28.70	−11.6	323	− 4.9	+ 3.2	+ 79	....	24.66
f 7–8	140	6	−1.35	−31.50	−13.5	425	− 5.7	+ 4.55	+106.2	....	23.33
b 9–10	136	6	−0.73	−16.55	− 7.3	121	− 3.1	+ 4.52	+102.5	....	22.66

itself into determining one side of a right-angled triangle, having given the hypothenuse and the remaining side. The hypothenuse is the contracted straight line uniting the crown and abutment hinge, and the known side of the triangle is equal to one-half the span; the remaining side is the rise of the loaded arch; and this deducted from the rise of the unloaded arch gives the deflection.

Temperature deflections can be obtained in the same manner.

In the three-hinged spandrel-braced arch the deflections caused by single panel loads may be computed direct from the stresses in the members by drawing a Williot Diagram, or by computing the deflection curve from the deflection angles. This, however, necessitates the computation of the values of u and s'', and also the deflection angles for each position of the load. In applying the method described in earlier paragraphs these values need be computed but once; they are then reduced according to the procedure given in Art. 13.

15. Example.—The arch shown in Fig. 1 is used, but without the center hinge.

In Fig. 19 one-half of the arch is shown, its span between the end hinges being 105 ft., its rise 15.5 ft., and its height at the crown 4 ft. The top chord is horizontal and the hinges are in the same plane.

In Fig. 19*a* the same arch is shown and the intersection locus is drawn by correcting the standard diagram of Fig. 14, the correction being shown in Fig. 19^B (see also Art. 9).

For the sake of clearness in illustrating the following computations, the intersection locus has been drawn farther above the top chord at the crown of the arch than the true locus.

In Fig. 19*a* the panel points have been indicated by short lines, indexed *O*, I, II, etc.

The line *OC* (Fig. 19*a*), which is the line of pressure in the arch caused by the dead load, must coincide with the neutral axis of the lower chord.

The panel loads resulting from the dead load are 8 tons per panel, and in Fig. 19*b* these loads are measured off in their proper order (it should be borne in mind that the reactions are each equal to 4.5 panel loads).

In the equilibrium polygon *OC* (Fig. 19*a*) the points *O* and *C* are known, and, as was described and illustrated in Figs. 11 and 11*a*, a trial pole P' is chosen in Fig. 19*b* and a trial polygon is drawn, from which the true pole *P* in Fig. 19*b* is found; this pole *P* will produce the polygon *OC* in Fig. 19*a* (as previously described).

The tangent method should not be used to obtain the neutral axis of the bottom chord, because the member 0–2 is not the direction of the end tangent, but is a tangent to the parabola at the center of the panel.

(*a*) Live-Load Stresses.—The live load is 8.5 tons per panel, or 0.81 ton per ft.

Maximum and Minimum Stresses (Fig. 19f)—Stress in 4–6: For this member the fulcrum is at 5 and the line $A5$ intersects the intersection locus at E. The section line is at ZZ. All loads to the left of E will have their reactions in the section, and all loads to the right of E will have their components in the section. All loads to the left of E cause tension in 4–6, and all loads to the right of E cause compression. The perpendicular through E divides the span in two lengths, one of 25.8 ft. and the other of 79.2 ft. The latter length overlaps the half-span by 26.7 ft. One-half of the load on each end panel is directly transmitted to the supports A and B, and the lengths of the loads which cause stresses in the arch are then 20.55 ft., 26.7 ft., and 47.25 ft.; and bisecting each of these lengths gives the points F'', F', and F, through which points pass the resultants of the respective loads.

For maximum compression in 4–6 the point F' is loaded with $26.7 \times 0.81 = 21.63$ tons, and the point F with $47.25 \times 0.81 = 38.27$ tons. The left-hand components of these two forces are equal to $F'G'$ and FG and intersect at A, through which point their resultant passes. To obtain the magnitude and direction of this resultant, the component $F'G'$ is added to FG, viz., Gg', and the line uniting g' with F gives the magnitude and direction of the resultant; and a line drawn parallel to $g'F$ through the point A gives the location of this resultant, which intersects 4–6 at the panel point 6. This resultant is resolved into a force directed toward the fulcrum 5, and the stress in 4–6. This resolution is effected as follows:

FD is drawn parallel to 5–6 and $g'D$ parallel to 4–6; the stress in 4–6 equals 68.2 tons compression. That the resultant intersects at the panel point 6 is accidental.

For maximum tension in 4–6 the load $F''h''$ is resolved into its reaction $F''G''$, which is in the section and intersects the prolongation of 4–6 at the point E'. This reaction is resolved into a force toward the fulcrum 5, viz., $E'5$, and the stress in 4–6. This resolution has been effected, $D''F''$ being the stress in 4–6, and equal to 3.8 tons tension. For a fully loaded bridge the stress from the live load would be $-68.2+3.8=64.4$ tons compression. Now, the dead-load stress is 70.6 tons compression, and the ratio of live load to dead load is as 8.5:8, or $\frac{8.5}{8} \times 70.6 = 75$ tons compression. The above figures give only 64.4 tons compression, which indicates that the center of pressure passes above 4–6, the difference between the two stresses being taken up by the top chord. It also indicates that the equilibrium polygon for the live load does not coincide with the equilibrium polygon of the dead load, and that a fully loaded bridge will have stresses in the top chord. In the three-hinged arch it was seen that a full load did not cause stresses in the top chord.

Stress in 5–7. (Fig. 19*g*).—To find the stresses in this member the fulcrum is located at the panel point 6, and a straight line passing

through A and 6 intersects the intersection locus at E; this point divides the span into two lengths—50.5 ft. and 54.5 ft. The section-line passes through the center of the third panel and is indicated by ZZ. All forces to the left of ZZ have their reactions in the section, and all forces to the right of ZZ have their components in the section. All the components to the right of E have a positive moment around the fulcrum 6, and all components or reactions to the left of E have a negative moment around this fulcrum.

To obtain maximum tension in 3–5 the bridge is loaded from E to B' with $[(50.5-5.25)\times 0.81=]$ 36.66 tons, and the resultant of this force passes through the point F, which bisects the distance EB' minus one-half of the end panel. Its component is equal to the line GF, which intersects the prolongation of the member 5–7 at the point a. The component is resolved into a force $a6$—which passes through the fulcrum 6—and the stress in 5–7; and drawing a line GD parallel to $a6$ and a line FD parallel to 5–7 gives the stress in 5–7 which is equal to 17.5 tons tension.

To find the maximum compression in 5–7 the bridge is loaded from A' to E, that is, for a distance of 54.5 ft., which overlaps the half-span by 2 ft. Of the remaining 52.5 ft. for the first $(26.25-4.25=)$ 22 ft. the reaction is in the section; for the remainder of the load the component is in the section $(22\times 0.81=17.82$ tons), and its resultant passes through the point F''.

Next to be considered is a load of 21.27 tons, having its component in the section and its resultant passing through the point F'''. Following this comes the load on the adjoining half of the span, viz., $2\times 0.81=1.62$ tons, the resultant of which passes through the point F'. The order of combining these two components with the reaction to find the resultant is not the best to follow. It is better to first combine the two components, and then combine the resultant thus found with the reaction. This order of combining the forces, however, would bring them too close together to be clearly indicated in a diagram.

The component $G'F'$ prolonged intersects the reaction $F''G''$ at the point b, and measuring these forces in their respective directions from the point b gives bd, which is equal to $F''G''$, and $bc=F'G'$.

The line dc is equal to the resultant of these two forces, and its point of application is the intersection point b, through which point a line be is drawn parallel to the line dc. This resultant intersects the component $F'''G'''$ at the point e, and measuring again the two forces in their respective directions from the point e gives eg equal to $F'''G'''$, and ef equal to dc. Joining the points g and f gives the magnitude and direction of the resultant of the three forces, and the intersection point e is the location of this resultant.

Through e a line parallel to gf gives the line ei, which is made equal in length to the line gf. The prolongation of ei intersects the member 5–7 at h, and the resultant is resolved into a force $h6$—which passes through the fulcrum 6—and the stress 5–7; and drawing

the line ij parallel to $h6$ and the line ej parallel to 5–7 gives the stress in 5–7, which is equal to 30 tons compression.

From the one form of loading the stress was found $= +17.5$ tons
From the other " " " " " " " $= -30.$ "

And for a full live load the stress is $= -12.5$ tons,
which is the equivalent of the discrepancy that was found in the bottom chord.

Stress in 5–6.—A section-line through 5–6 (see ZZ in Fig. 19) cuts the members 5–7 and 4–6, and they intersect each other at D (see Fig. 19c). This point of intersection is the fulcrum for 5–6. The line which passes through the hinge A and point D cuts the intersection locus at E, and the line which passes through B and D intersects the locus at E'. The section line passes somewhere between 5 and 7.

Maximum Compression in 5–6.—The reactions of the loads between A and E' have a positive moment around the fulcrum D, and the components of the loads between E and B also have a positive moment around the fulcrum D. The farther the section line is shifted to the right, the greater will be the load between the point of support A and the section line; and, consequently, the greater will be the resultant reaction of this load.

The section line cannot be shifted any farther than the panel point III; if it were shifted still farther to the right it would cut the members in the next panel. Therefore to obtain maximum compression in 5–6, the bridge should be loaded from O to III, and from E to X.

The resultant of the loads from E to X passes through the point F, its magnitude is [$0.81(44.4-5.25)=$] 31.71 tons, and its component is represented by the line FG.

The resultant of the load from O to III passes through the point F', its magnitude is [$0.81(31.5-5.25)=$] 21.27 tons, and its reaction is given by the line $F'G'$.

The component FG and the reaction $F'G'$ intersect at the point g, through which their resultant passes. The length of the line $F'G'$ is plotted from g as $f'g$, and the length of the line FG is measured from g as fg; then the line joining f and f' gives the magnitude and direction of this resultant, and the point g is its location. A line drawn parallel to ff' through the point g intersects the diagonal 5–6 at 6, and this line is resolved into a force $6D$, toward the fulcrum D, and the stress in the diagonal. To avoid confusion this resolution of forces has been made in Fig. 19c', the line $f'f$ being in direction and magnitude equal to the resultant. From the point f a line is drawn parallel to $6D$, and from f' a line parallel to the diagonal; the stress in 5–6 equals 10.6 tons compression.

Maximum Tension in 5–6.—To obtain this stress the remainder of the bridge is loaded from III to E (Fig. 19c). This has been shown in Fig. 19e, and the length of the load is equal to 21 ft. on

one side of the center line and 8.1 ft. on the other. The loads are respectively (21×0.81 ton=) 17.01 tons and (8.1×0.81 ton=) 6.55 tons, and the resultants of these loads pass through the points F' and F respectively. The fulcrum for 5–6 is again the point D, and, after the foregoing description, the figures require no explanation; the stress in 5–6 equals 10.6 tons tension.

Stress in the Vertical 4–5.—To obtain the stresses in 4–5 the section-line cuts the members 3–5, 4–5, and 4–6. The members 3–5 and 4–6 intersect again at D, and D is the fulcrum for 4–5 (see Fig. 19*c*). The same method of obtaining the maximum stress in 5–6 (which was given in the preceding paragraph) holds good for the member 4–5; and maximum tension is caused in 4–5 when the bridge is loaded from O to II and from E to X.

The reaction is equal to $F''G''$ and the component is equal to FG. The two forces intersect at g', and their magnitudes are measured off from g' in their proper directions, viz., $g'f''$ and $g'f'''$; and their resultant is equal to the line $f''f'''$.

A line drawn through the point g' parallel to $f''f'''$ intersects the vertical 4–5 at the point k, and the resultant is resolved into a force kD toward the fulcrum and the stress in the vertical 4–5. The computation has been made in Fig. 19*c''*, and the stress in 4–5 equals 4.3 tons tension. The stress caused by the other form of loading equals 11.6 tons compression and is indicated in Fig. 19*e*.

For a fully-loaded bridge the stress caused by the live load = +4.3 −11.6 = 7.3 tons compression.

Stress in the Vertical 4–5:

Minimum.

From dead load	− 8 tons
From live load	+ 4.3 "
Total minimum stress in 4–5 =	− 3.7 tons

Maximum.

From dead load	− 8 tons
From live load	−11.6 "
Total maximum stress in 4–5 =	−19.6 tons

Stress in the diagonal	5–6 = ±10.6 tons − 11.6 tons
Stress in the top chord	5–7 = +17.5 tons − 30 tons
Stress in the bottom chord	4–6 = (−68.2 − 70.6) = −138.8 tons

(*b*) The temperature stresses below are taken from Column VIII of Table IV, and are added to the above stresses to give maximum total stresses:

	Highest Temp.	Lowest Temp.
5–7, top chord	+13.9 tons	−13.9 tons
4–6, bottom chord	− 9.1 "	+ 9.1 "
4–5, vertical	+ 2.6 "	− 2.6 "
5–6, diagonal	− 4.9 "	+ 4.9 "

9 tons

2 "
5 "

ction
hord
nbers
terial
rding
nec-
the

on of

the
the

. the

om-
osely
and

a.—
aced
arch

ords
The
and
ared
een

uilt

sses
sing
are
In

ord-

hen
ord.
be

And the maximum combined stresses in the members are:

5–7, $\left(\begin{array}{l} \quad -30 \quad -13.9 \\ \text{or } +17.5+13.9 \end{array}\right)$	$+31.4$ tons	-43.9 tons
4–6, $(-138.8\ -9.1)$	-147.9 "	
4–5, $(-\ 19.6\ -2.6)$		-22.2 "
5–6, $(\pm\ 10.6\ \pm 4.9)$	$+\ 15.5$ "	-15.5 "

In the arch of Fig. 19 the top chord has a uniform cross-section consisting of two 8-in. channels (13.5 lbs. per ft.), the bottom chord is made from two 12-in. channels (40 lbs. per ft.), and the web members are two 6-in. channels (10 lbs. per ft.). While a small saving in material can be obtained by varying the sections at different points according to the stresses, the uniform sections adopted admit of simple connections, result in lower unit prices, and enhance the beauty of the structure.

For long spans this uniformity is not economical; a discussion of this subject, however, does not belong in this book.

The intersection locus obtained in Fig. 19^B can be used for the computation of the dead-load stresses as well as for those of the live load.

The advantages, however, of following the division used in the foregoing example are self-evident.

One, moreover, that is worthy of special mention is that the computed stresses and the actual stresses in the structure will closely correspond when the bridge is mounted as two cantilevers and completed as a three-hinged arch.

16. Two-Hinged Arch with Variable Moment of Inertia.— The foregoing articles have described an arch which might be placed under this head; the spandrel-braced arch, however, is not an arch rib in the true sense of the word, but a framework.

In many structures in which the arch rib is composed of chords and web members, the chords are anchored to the abutments. The rib may also increase in height from the crown to the abutments, and such an arch has the decided advantage of great rigidity as compared with the two-hinged type of the same dimensions. This has been specially described in the chapter dealing with the hingeless arch.

(*a*) Structures exist, however, in which this arch has been built with two hinges.

When, in such an arch, the hinges are located in the axis, the stresses can be computed by the application of the elastic theory, using the standard diagram of Fig. 14, and making such corrections as are necessary according to the method of Article 1, Chapter II. In this case the center line of the arch rib is the axis of the arch.

Also the correction of the intersection locus may be made according to the rules given in Article 11 of the same chapter.

The latter method, however, results in greater accuracy when applied to an arch having the hinges in the axis of the bottom chord. In making the correction the axis of the bottom chord should be

considered as the axis of curvature. Either of these methods may be used to compute the stresses in the structure, and the general method described in Article 18 may be applied as a check to the sections thus obtained.

(*b*) There is, however, a two-hinged arch which is very rigid, and which, in contradistinction to those thus far described, increases its moment of inertia from the hinges to the crown.

The crescent-shaped arch is of this type and is much favored for bridges, and particularly for roofs.

The analysis of the two-hinged arch is given in Chapter VIII, and in Article 18 of this chapter the application of this analysis is described.

In Article 2 (*d*) of Chapter VIII the analysis has been developed for such an arch when special conditions (there enumerated) are satisfied, and in Art. 18 it has been shown that, notwithstanding such special conditions, equations (95*a*) and (98) are general in their application.

These equations are [see Art. 2 (*d*), (*e*), Chap. VIII]:

$$\int_0^l y''dx = \int_0^l ydx$$

for vertical forces; when the arch axis is a parabola, equation (96) applies: $z_0 = \frac{8}{5}f$ for vertical forces, and equation (98), $x_0 = k(3 + k^2 - 6k)$ for horizontal forces.

With the last two equations the standard diagram of Fig. 20 is drawn for an arch in which the rise = 1 unit and the span = 2 units. Multiplying the ordinates of this diagram by one-half of the span and by the rise of the arch axis will give the intersection loci for the horizontal and vertical forces.

As stated before, the point of intersection of the load line with the intersection locus is also the point where the components of the load intersect.

The method described for the computation of stresses in Chapter II, Article 1, may be used, and each member of the structure may be investigated independently. In the case of a roof-truss the wind should be considered as pressing on either the full right half or the full left half of the truss; to treat the wind pressure as a moving load which may come on any one or more panels, but not on all, is in this case a refinement which has no place in practical engineering.

(*c*) If the arch is supported on rollers at one hinge, and the hinges are held in position by a tie-rod, the stress in this rod can be measured directly from the force diagrams for different forms of loading, as will be seen below.

As an example a roof-truss has been selected, and the method of computing the stresses can be applied to either the three-hinged or the two-hinged arched roof.

17. Example: Crescent-Shaped Roof-Truss. — Fig. 21 shows a roof for a railway station. Its axis is a parabola. The span from A to B is 110 ft., and the rise of the axis at C above AB is 36 ft. The depth of the arch rib at the crown is 8 ft. 3 ins., or

$$k=\frac{h}{y}=\frac{8.25}{36}=\frac{11}{48}.$$

The trusses are placed 25 ft. apart.

Wind pressure = 35 lbs. per sq. ft., its direction making an angle with the horizontal = 15°. This produces a pressure per sq. ft. of

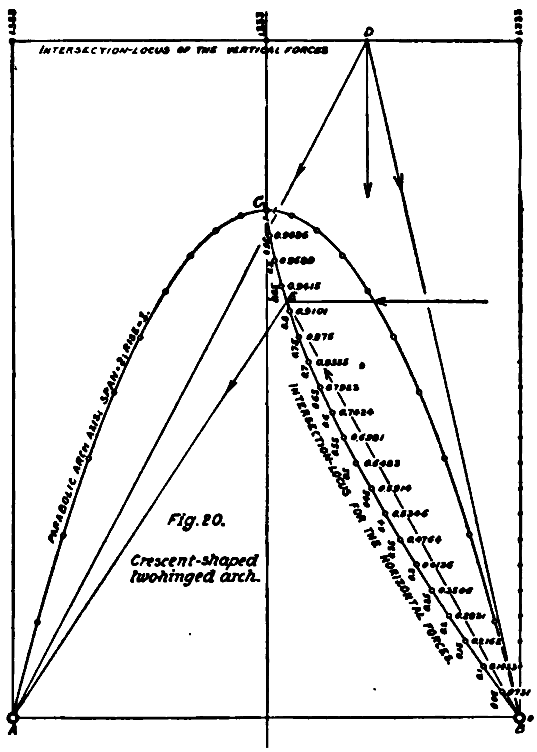

Fig. 20.

Crescent-shaped twohinged arch.

horizontal projection = 9 lbs., and a pressure per sq. ft. of vertical projection = 34 lbs.

Dead load = 30 lbs. per sq. ft. of horizontal projection.

Snow load = 17 " " " " " " "

and the stresses are computed for three cases:

The snow covering the roof (1) from 7 to the center;
(2) from the center to 7′;
(3) from 7 to 7′.

The weight of the trusses is 115 lbs. per lin. ft.

With the above data the panel loads are computed and the results indicated in Fig. 21.

The locus for the vertical forces is JJ' ($1.33 \times 36 = 48$ ft.).

The locus CB for the horizontal forces is obtained by multiplying

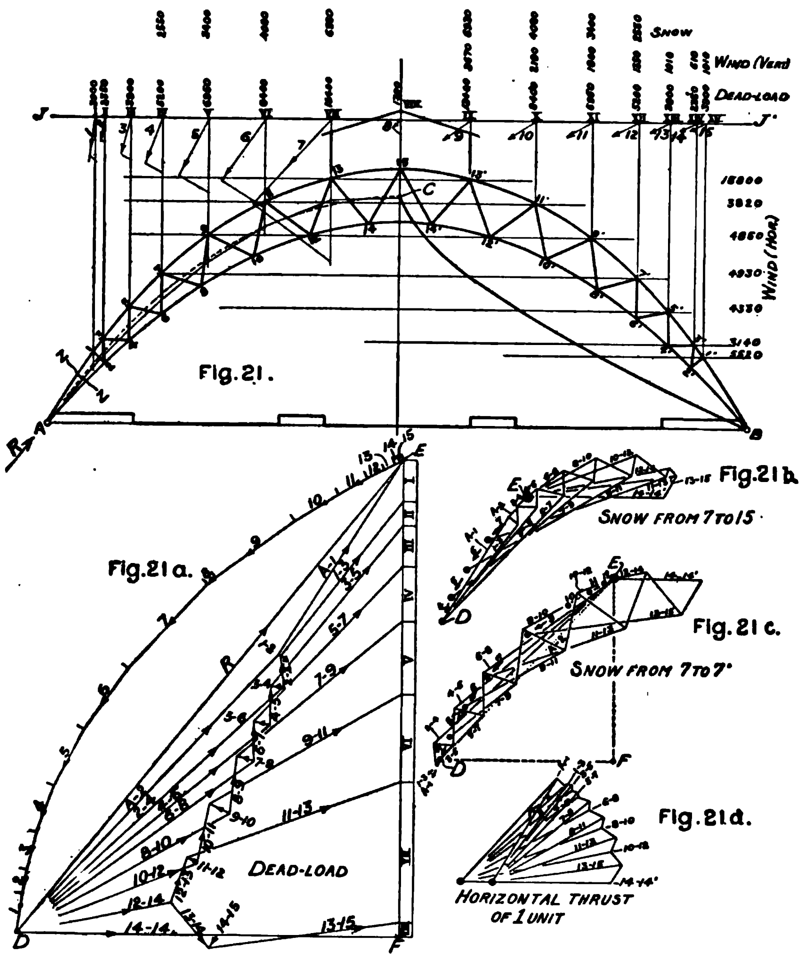

Fig. 21. Fig. 21 a. Fig. 21 b. Fig. 21 c. Fig. 21 d.

the horizontal ordinates in Fig. 20 by 55 ft., and the vertical ordinates by 36 ft.

(*a*) Stresses Caused by the Dead Load.—The dead loads at the panel points I, II, . . . , XV are resolved into their components 1, 2, etc. The components toward B are omitted, as they are not

required in the computations. It should be remarked that the components toward A of the loads from IX to XV are equal to the components toward B of the loads from I to VIII, and therefore that the resolution into components need only be made for the loads from I to VIII.

These components toward A are added in Fig. 21*a*, forming the broken line DE, and the straight line DE is equal to the resultant R of all these components, as previously explained. The reaction R at A is equal to this resultant, its direction being indicated by an arrow.

A section ZZ is made in Fig. 21, and the portion of the truss to the left of this section is removed. The forces in the section are R (the reaction) and the stresses in $A1$ and $A2$; these three forces are in equilibrium, and R must be the resultant of $A1$ and $A2$. The computation has been performed in Fig. 21*a*, and the directions of the arrows indicate that the forces in $A1$ and $A2$ are exerted against the portion ZZB of the truss and cause compression.

The remaining members of the truss have been computed in a similar manner in Fig. 21*a*, which is known as the "Cremona Diagram," and the results are entered in Table V.

In Fig. 21*a* the line DF is equal to the horizontal thrust caused by the dead load, and, using the point D as a pole, the reciprocal polygon $A \ldots C$ is drawn with a solid line in Fig. 21. The dotted line is the center line of the arch, and the distance between these two lines indicates how the center of pressure shifts above and below the neutral axis. This shows, for example, that the compression in 3–5 = 19,700 lbs., in 2–4 = 34,400 lbs., and in 4–6 = 31,000 lbs. It also affords a means of checking the Cremona Diagram by the moment method, as previously explained.

Another check upon the computation consists in independently determining the stress in any given member by the method described in Art. 1, Chap. II, for the three-hinged braced arch.

When the hinge A is supported on rollers and the hinges A and B are united by a tie-rod, the stress in this rod is equal to the line DF measured by the scale of forces.

(*b*) Stresses Caused by the Snow Load.—Where the roof has an inclination which makes an angle with the horizontal of more than 45°, no snow will rest; the snow loads are distributed as shown in Fig. 21.

Snow Covering the Roof from Panel Point 7 *to the Center.*—In the same manner as described for the dead load, the resultant DE in Fig. 21*b* for the snow load has been computed, and a Cremona Diagram has been drawn with these loads (see Fig. 21*b*).

The results are entered in Table V under the heading "Left Half."

Snow Covering the Roof between Panel Points 7 *and* 7′.—The resultant DE of the left-hand components (see Fig. 21*c*) is obtained according to the previously described method, and the Cremona Diagram is drawn.

The results are entered in Table V under the heading "Total."

Snow Covering the Roof from the Center to 7'.—These stresses are the differences between the stresses caused by the snow load on the left half and the total snow load. The computation of these stresses resolves itself into a simple deduction, and they are entered under the heading "Right Half" in Table V.

(*c*) Stresses Caused by a Change in Temperature and by the Secondary Stresses.—To obtain the temperature stresses, the horizontal thrust caused by changes in temperature must be computed [see equation (100), Art. 2 (*f*), Chap. VIII].

$$H_t = \tfrac{1}{2} twEk^2F,^*$$

where t = change in temperature = $\pm 60°$ F.;

w = coefficient of elongation for 1° F. $= \dfrac{7}{1{,}000{,}000}$;

E = modulus of elasticity of steel = 29,000,000;

$k = \dfrac{h}{y} = \dfrac{8.25}{36} = 0.229; \qquad k^2 = 0.0525;$

F = sectional area of one chord at the crown = 8.5 sq. ins.

Then

$$H_t = 2{,}720 \text{ lbs. (or, roughly, 2,800 lbs.).}$$

For the secondary stresses [see equation (101)],

$$H_n = -\tfrac{1}{2} nk^2F,$$

where n = stress per sq. in. of gross section caused by live-load, temperature, and secondary stresses = 1,300 lbs. (assumed for the purpose of illustration);

k and F as before. Then

$$H_n = \tfrac{1}{2} \times 1{,}300 \times 0.0525 \times 8.5 = 280 \text{ lbs.}$$

In these two equations F and n are values which are obtained from the final results of the computation; the value 280 lbs. can be obtained only by trial, for which reason the Cremona Diagram of Fig. 21*d* is drawn for a horizontal thrust equal to one unit. When the intensity of the horizontal thrust which is caused by a change in temperature or by the secondary stresses is computed, the stresses obtained from Fig. 21*d* are multiplied by these horizontal thrusts.

In the example the horizontal thrust caused by a temperature change of 60° is 2,800 lbs., and the stresses caused in the members by this thrust are inserted in Table V.

The secondary stresses are also inserted in this table.

* See Art. 20 (*b*) before applying this equation.

(*d*) **Stresses Caused by Wind Pressure.**—In Fig. 21*e* the wind is assumed to blow from right to left, and the vertical and horizontal pressures are considered independently in order to compute the reactions at *A* and *B*.

The points of intersection of the horizontal and the vertical forces with the intersection loci are indicated by black circles, the loci being left out to avoid confusion.

The vertical loads are resolved into their components: *d* in 9 and 9′, *e* in 10 and 10′, etc. The components 9, 10, 11, etc., are drawn in their proper sequence in Fig. 21*f*, forming the broken line *KM*; also the components 9′, 10′, etc., are drawn, forming the broken line *KL*. As a check on the computation *Ll* (the vertical reaction at *A*) plus *lM* (the vertical reaction at *B*) should be equal to the sum of all the vertical loads *de . . . j*. It should be specially noted that the directions of the forces are indicated by arrows, and great care should be exercised in this, as an error would produce extremely faulty results.

The horizontal loads are resolved into their components: *D* into 9 and 9′, *E* into 10 and 10′, etc.

The components 9, 10, 11, etc., toward *B* are added together in their proper sequence in Fig. 21*f*, forming the broken line *MN*; and to obtain the resultant of *NM* and *KM* the forces must follow in the same direction.

In the same manner the components toward *A* (as 9′, 10′, etc.) are drawn in their proper sequence in Fig. 21*f*, forming the line *LO*, and, as before, their direction must be a continuation of the broken line *LK*. And the line *NK* represents in magnitude and direction the resultant of all the components toward *B* of all the vertical and horizontal forces, and similarly the line *OK* is the resultant toward *A*.

As a check on the computation the line *Nm*, which represents the vertical reaction at *B*, must be equal to the line *On*, which is the vertical reaction at *A* of the horizontal forces.

Computation of the Stresses.—The reaction at *B* must be equal and opposite to the force *NK*, and the reaction at *A* must be equal and opposite to the force *KO*. These two reactions are added in their proper sequence in Fig. 21*g*, and a line which would unite the points *N* and *O* would be the resultant of these reactions, and would also be the resultant of the forces IX, X, . . . XV in Fig. 21*e*. This condition is indicated in Fig. 21*g* and forms a check on the computation, and the Cremona Diagram in Fig. 21*g* gives the stresses in all the members.

The drawing of this diagram furnishes another check on the computation, because, if the diagram is commenced at *B* with the reaction *NK*, it must meet the point *O* of the reaction *OK* at *A*, and any deviation from this point *O* shows the computation to be defective.

With the wind acting from left to right the Cremona Diagram

will be the reverse of Fig. 21g, and the stresses 5′–7′, 7′–9′, 6′–8′, 8′–9′, etc., will become equal to 5–7, 7–9, 6–8, etc.

If the arch shown in Fig. 21 is used for a highway or railroad bridge, as, for instance, the bridge over the Douro, the maximum and minimum stresses are obtained in the same manner as are those for the two-hinged spandrel-braced arch, and the intersection locus for the forces is obtained from Fig. 20.

For the maximum and minimum stresses of Table V, the cross-sections are determined by adding together the larger stress and ¾ of the smaller stress and allowing 16,000 lbs. per sq. in. of net section in the member for the combined stresses. This shows that the cross-sections of the chords increase very closely in the same ratio as does the secant which the arch makes with the horizontal; and with the variable loading shown in Figs. 21 to 21g the accuracy resulting from this assumption is striking.

(e) Tie-Rods.—When the hinges are kept in position by a tie-rod, the stress in this rod caused by the wind pressure acting on the right of the roof is equal to the line Ln (Fig. 21f) $=26{,}400$ lbs.

It is assumed that the hinge A rests on a roller bearing.

Now, the stress in this tie-rod (caused by the dead load) is 36,150 lbs. tension ($=DF$ of Fig. 21a), and the stress in the rod will be $27{,}600+36{,}150=63{,}750$ lbs. tension.

When the wind exerts pressure on the left side of the roof it causes 17,790 lbs. compression (line mM of Fig. 21f), and the stress in the rod will be 18,360 lbs. tension.

Also a full snow load causes a tension in the rod equal to the line DF of Fig. 21$c=16{,}250$ lbs.

When the condition of the roof-truss assumed for the computation is that at normal temperature and with the dead load, any change in the stresses or the length of the tie-rod will alter the span of the arch.

When the tie-rod is equally exposed to the changes in temperature with the roof, there will be no temperature stresses; but when the tie-rod is placed under the station platform, it is safe to assume that its temperature does not change, and the temperature stresses as previously computed can then be used.

The change in the length of the tie-rod caused by the variation in its stresses will influence the stresses in the arch.

When the stress in the tie-rod above or below the normal $=P$ and its area $=F$, its change in length will be equal to $\Delta l=\dfrac{Pl}{FE}$; from equation (99), Chap. VIII,

$$\Delta l=\frac{2Hl}{Ek^2F}=\frac{Pl}{FE},$$

and

$$H=\frac{Pk^2}{2}.$$

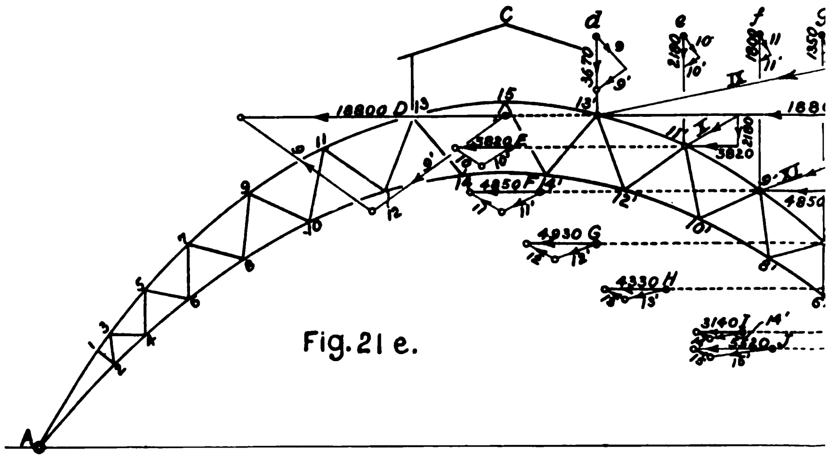

Fig. 21 e.

Fig. 21 f.

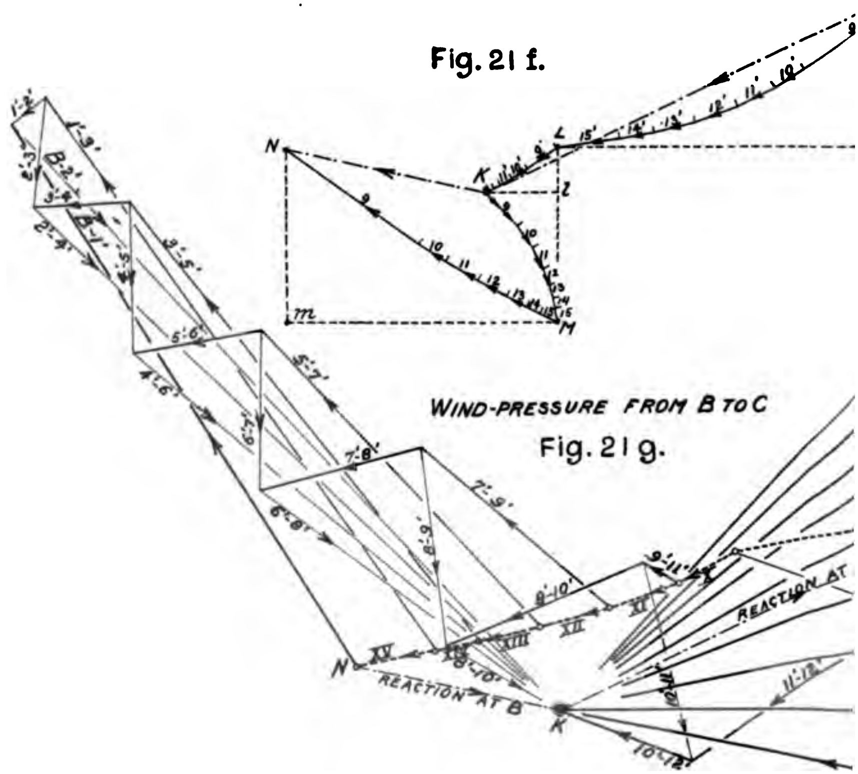

WIND-PRESSURE FROM B TO C

Fig. 21 g.

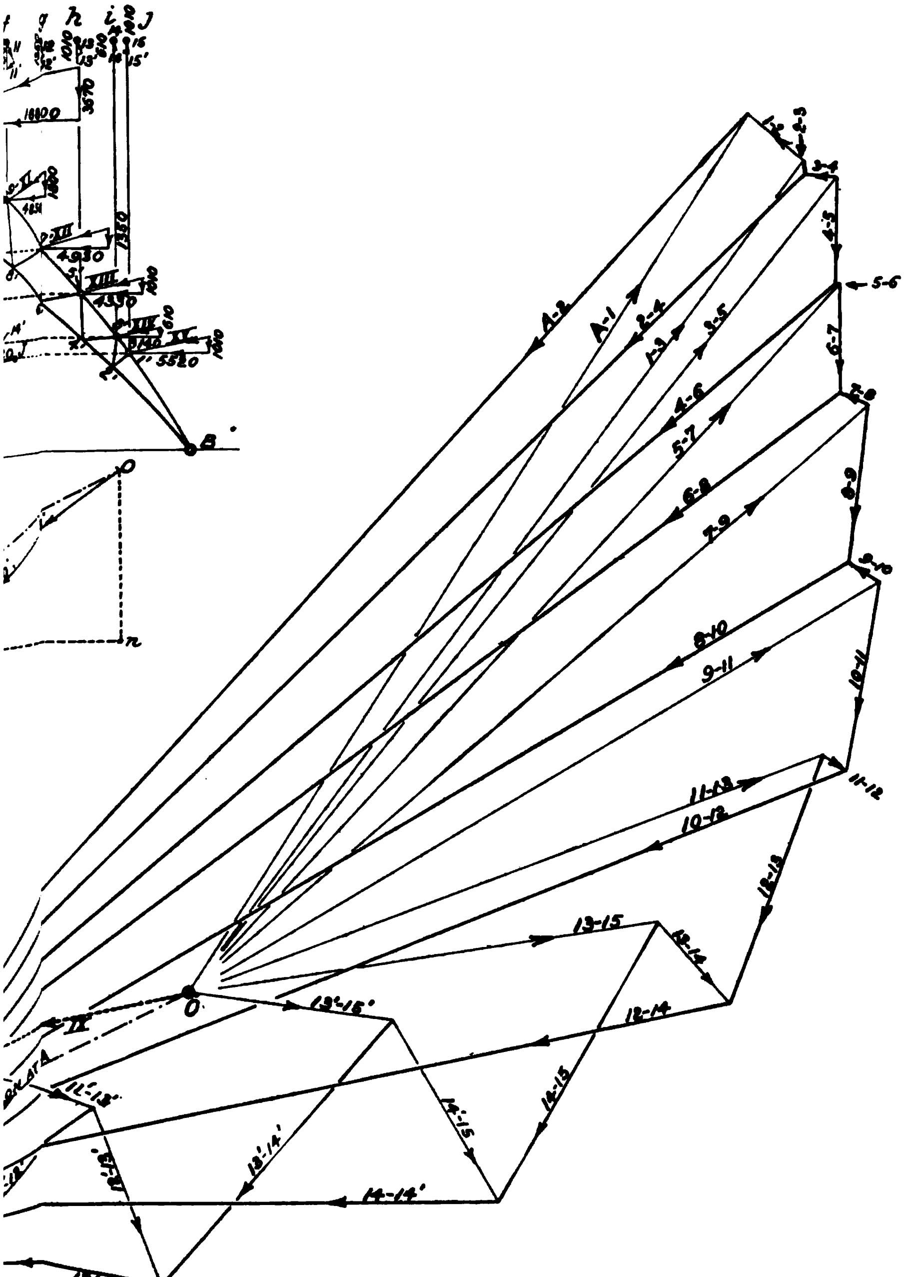

[*To face page 82.*

Now the wind will cause an additional stress of 27,600 lbs. tension or 17,790 lbs. compression, and a full snow covering will add an additional tension of 16,250 lbs. Or, with the wind blowing on the left side, the stress in the rod will be 17,790 lbs. below the normal stress.

With the wind blowing on the right side and a snow covering from 7 to 7′, there will be an increase of $27,600+16,250=43,850$ lbs. tension, and substituting these values for P in the above equation gives (when $k=\frac{11}{48}$),

$$H=-935 \text{ lbs.} \quad \text{and} \quad H=+2,290 \text{ lbs.},$$

which act respectively in the same manner as a rise or a drop in temperature. Multiplying the stresses obtained from the diagram (Fig. 21*d*) with the above values will give the stresses in the members.

[For deflections see Art. 4, Chap. III; also Art. 20 (*b*) *et seq.*]

Table V.

TWO-HINGED CRESCENT-SHAPED ROOF-TRUSS

	DEAD-LOAD	WIND		SNOW			TEMPERATURE		SEC'Y STRESS	MAX:	MIN.
		RIGHT TO LEFT	LEFT TO RIGHT	LEFT HALF	RIGHT HALF	TOTAL	RISE	FALL			
				TOP CHORD							
A-1	-21800	+73600	-45700	-11700	+12400	+700	+10900	-10900	-1090	-91190	+74010
1-3	-18700	+73000	-48000	-11600	+12300	+700	+10600	-10600	-1060	-89960	+76140
3-5	-19700	+73500	-39800	-14000	+12200	-1800	+11100	-11100	-1110	-85710	+75990
5-7	-20300	+67900	-28800	-16400	+10800	-5700	+10900	-10900	-1090	-77490	+68210
7-9	-20200	+63300	-17500	-17400	+9400	-8000	+11200	-11200	-1120	-67420	+62580
9-11	-20800	+56800	-2800	-18000	+7200	-10800	+11300	-11300	-1130	-54030	+53370
11-13	-21300	+47800	+12700	-17800	+4000	-13800	+11600	-11600	-1160	-51860	+40940
13-15	-18200	+33600	+14600	-14100	-600	-14700	+11500	-11500	-1150	-45550	+25750
				BOTTOM CHORD							
A-2	-36100	-104600	+56800	-2600	-21600	-24200	-12500	+12500	+1250	-176150	+34450
2-4	-34400	-104300	+51600	-1400	-21800	-23200	-12500	+12500	+1250	-173150	+30950
4-6	-31000	-100700	+39400	+1100	-20600	-19500	-12700	+12700	+1270	-163730	+23470
6-8	-27600	-96200	+26300	+4100	-19400	-15300	-12700	+12700	+1270	-154630	+16770
8-10	-23100	-90100	+9200	+7400	-17300	-9900	-12900	+12900	+1290	-142110	+7690
10-12	-18200	-83300	-10000	+10900	-14700	-3800	-13300	+13300	+1330	-128170	+7330
12-14	-15900	-70700	-29700	+13600	-10400	+3200	-13400	+13400	+1340	-109060	+12440
14-16	-19000	-52800	-52800	+12700	-4400	+8300	-13200	+13200	+1320	-88080	+8220
				WEB MEMBERS							
1-2	-300	-5000	+3100	+1200	-1400	-200	-1100	+1100	+110	-7690	+5210
2-3	-2900	-900	+7800	-1700	-300	-2000	+300	-300	-30	-5830	+6170
3-4	+1200	-2200	-6900	+1900	-100	+1800	-600	+600	+60	-6340	+3760
4-5	-3600	-7500	+10800	-1700	-1800	-3500	-600	+600	+60	-15140	+7860
5-6	+1600	-300	-9200	+2600	+200	+2800	-600	+600	+60	-5060	+8140
6-7	-3800	-7700	+11400	-2300	-1800	-4100	-500	+500	+50	-16050	+8150
7-8	+1600	-2300	-11900	+2900	+400	+3300	-1100	+1100	+110	-11290	+6110
8-9	-5400	-11300	+14200	-2200	-3000	-5200	-800	+800	+80	-22620	+9680
9-10	+2100	-2600	-15200	+3700	+700	+4400	-1500	+1500	+150	-14450	+8150
10-11	-5700	-13500	+14600	-2000	-3600	-5600	-900	+900	+90	-25610	+9890
11-12	+1000	+1900	-18300	+3400	+2200	+5600	-1500	+1500	+150	-18650	+10150
12-13	-4500	-18700	+13500	-800	-5000	-5800	-1300	+1300	+130	-30170	+10430
13-14	-5700	+7700	-24900	+900	+4300	+5200	-1500	+1500	+150	-31950	+8850
14-15	+1500	-22900	+15000	+2400	-6300	-3900	-1800	+1800	+180	-29320	+20880

THE DOURO BRIDGE, OPORTO.

18. Computation of the Intersection Locus for the Two-Hinged Arch.—General Method.—In Arts. 1 to 14 of this chapter the horizontal thrust is computed from an intersection locus which is drawn for a two-hinged parabolic arch rib whose moment of inertia increases from the crown to the hinges in the same ratio as the secant of the angle which the arch axis makes with the horizontal. In Art. 2 (*h*), Chap. VIII, the principle is explained on which is based the correction of this intersection locus for an arch of any other curvature.

Special cases, however, may present themselves in practice, and, as an example of such a case, the author has chosen the crescent-shaped arch bridge over the Douro, at Oporto, Portugal.

The conditions which are set forth in Art. 2 (*d*), Chap. VIII, are not satisfied in this arch, and it is specially adapted for demonstrating the influence of a variation in the moment of inertia upon the intersection locus.

A description of this bridge by T. Seyrig, its designer, may be found in "Mémoires et Comptes Rendus des Travaux de la Société des Ingenieurs Civils," Sept., 1898.

Fig. 22 is an elevation of this bridge, in which the span is 160 meters and the rise of the neutral axis 42.65 meters. (All dimensions given are in meters.) The bridge deck is supported by the arch at the points *D*, *E*, *F*, and *G*. In Figs. 22*a* and 22*b* the moments of inertia and the sectional areas of the arch have been plotted from the above description in the metric system. These figures show that the moment of inertia near the hinges is 0.246 $m.^4$, at the crown 4.696 $m.^4$, and that the sectional area near the hinges is 0.293 $m.^2$, and at the crown 0.228 $m.^2$.

The ordinates of the line *GJ* (Fig. 22*a*), measured from the axis *GL*, represent the moments of inertia of the arch, and are seen to vary widely. The line *GL* is equal to *AC*, or one-half the length of the arch axis, and the abscissas of the points on the line *GJ* correspond to the points x, y, of the arch axis measured along the curve.

The analysis of the two-hinged arch is given in Art. 1, Chap. VIII.

In applying equations (71) and (72) of the Appendix the approximation $v_m = \frac{I_0}{I_m} y_m$ (70) is sufficiently correct, and the panel lengths are all assumed to be equal to d_0. The ordinates of Fig. 22*a* represent the values of I_i; and I_0, or the average moment of inertia, should be computed. The graphical method is specially adapted for this purpose. (See Fig. 22*c*.) The computation is based on the principle of reducing the figure *abc* . . . *h* to a triangle having the same area and the same base; then one-half the height of the triangle is the desired average. Let *ab* be the axis and *cdefg* be the line uniting the ordinates, which are plotted in their proper sequence.

The average ordinate ak should be found. Unite e with g and draw fh (parallel to eg) to an intersection h with the line ia. The triangles egh and egf have the same base and the same height, and must therefore have the same area. The figure has now been changed into $abcdeh$, having the same area as the original figure. The same method is applied to the points d, e, h, etc., until finally the triangle abi is obtained, and one-half its height is equal to ak. (To make the computation only the intersection points on the line ai are marked; no other lines should be drawn, as they only confuse the computer.) This method has been applied in Fig. 22a; GLM is the desired triangle, and the distance NL is the average moment of inertia$=I_0$.

In the same manner the average area F_0 of the arch is obtained in Fig. 22b, the line GM representing the side of the equivalent triangle, and $OG=F_0$.

Construction of the Horizontal-Thrust Curve.—Vertical Forces.— Equation (62) of the Appendix gives the horizontal thrust

$$H=\frac{\int_0^b \frac{\mathfrak{M}}{I} y ds + EwtB\cos a - E\Delta l}{\int_0 \frac{y^2 ds}{I} + \frac{B}{F_0}\cos a}. \quad . \quad . \quad . \quad (62^A)$$

Equation (71) gives

$$\int_0^b \frac{\mathfrak{M}}{I} y ds = \int_0^l \frac{\mathfrak{M} y}{I_1} dx = \frac{d_0}{I_0}\Sigma_0^l \mathfrak{M}_m v_m, \quad . \quad . \quad . \quad (71^A)$$

and substituting for v_m the approximate value $v_m=\frac{I_0}{I_m}y_m$ gives

$$\int_0^b \frac{\mathfrak{M}}{I} y ds = \frac{d^0}{I_0}\Sigma_0^l \mathfrak{M}_m \frac{I_0}{I_m} y_m.$$

In the same manner is obtained

$$\int_0^b \frac{y^2 ds}{I} = \frac{d_0}{I_0}\Sigma_0^l y_m v_m. \quad . \quad . \quad . \quad . \quad . \quad . \quad (72^A)$$

The interpretation of these summations is given in Chap. VIII, Art. 1.

In equation (62^A) the term $EwtB \cos a$ represents the influence of the temperature, the term $E\Delta l$ the influence of a turning or shifting of the abutments, and the term $\frac{B}{F_0}\cos a$ the influence of the change in length of the axis of the arch (in this book termed "the secondary stress").

Neglecting the influence of temperature and shifting of the abutments, equation (62^A) may be written

$$H=\frac{\frac{d_0}{I_0}\Sigma_0^l \mathfrak{M}_m \frac{I_0}{I_m} y_m}{\frac{d_0}{I_0}\Sigma_0^l y_m v_m+\frac{B}{F_0}\cos a}=\frac{\Sigma_0^l \mathfrak{M}_m \frac{I_0}{I_m} y_m}{\Sigma_0^l y_m v_m+\frac{B\cos a}{F_0}\frac{I_0}{d_0}},$$

and if the denominator of this expression is made the unit of measurement, then

$$H=\Sigma_0^l \mathfrak{M}_m \frac{I_0}{I_m} y_m.$$

The computation, either graphically or analytically, is very easily performed; it consists in either drawing a reciprocal polygon, or computing the bending moment of a simple beam supporting the loads. The graphical method is here given, with an incidental explanation of the analytical method.

(a) Equation (73) of Chap. VIII gives the value of

$$\Sigma_0^l \mathfrak{M}_m v_m=K\left[(l-g)\Sigma_0^g\frac{x_m v_m}{l}+g\Sigma_g^l\frac{(l-x_m)v_m}{l}\right]. \qquad (73^A)$$

In Fig. $22d$ the axis ACB of the arch is shown and equation (73^A) is interpreted as follows with reference to this figure:

It is desired to find the horizontal thrust caused by a load K placed at 5.

The arch is divided into twenty equal panels whose centers are indicated by 1, 2, 3, etc.

Now, the first part of equation (73^A) means that loads v_1, v_2, v_3, v_4, and v_5, placed on a simple beam supported at A and B, will cause a reaction at B which is equal to $\Sigma_0^g\frac{x_m v_m}{l}$, and this reaction will cause a bending moment in the beam at 5, which is equal to $(l-x)\Sigma_0^g\frac{x_m v_m}{l}$.

The second part of this equation gives in the same manner the bending moment in the beam for all the loads from v_5 to $v_{1\prime}$, and the sum of these two bending moments is the total bending moment in the beam.

$$v_m=\frac{I_0}{I_m}y_m, \text{ and from Fig. } 22a,\ I_0=\text{ordinate } GO.$$

To facilitate the computation Fig. $22a$ should be so changed that the value of I_m is given to correspond with the panel centers 1, 2, 3, etc. For this purpose the lengths Aa, ab, bc, etc., of the

axis in Fig. 22*d* are plotted on the line GL in Fig. 22*a*, and perpendiculars are erected through these points intersecting the line GJ at the points a', b', c', etc.; and drawing lines through these points parallel to GL and to intersections with their corresponding panel centers, will determine the points 1, 2, 3, etc. The ordinate of the point 1 to the axis GL is the average moment of inertia for the panel 1; and the ordinate of the point 2 to the axis GL is the average moment of inertia for the panel 2, etc.

The ratio $\frac{I_0}{I_m}$ should now be computed. To make this division any arbitrary unit may be selected—in Fig. 22*a* the unit taken is equal to two panel lengths, or $he=1$.

The line $e8$ is drawn and gf parallel to it, and from equal triangles

$$\frac{gh}{h8}=\frac{hf}{1}; \quad \text{now,} \quad gh=I_0, \quad \text{and} \quad h8=I_m;$$

$$\therefore \frac{I_0}{I_m}=hf.$$

The next step is to compute the values of v_m:

$$v_m=\frac{I_0}{I_m}y_m.$$

For this purpose the point f of Fig. 22*a* is transferred to f' in Fig. 22*d*, a line is drawn uniting the points $e_{,}$ and 8, and the line $f'g_{,}$ is drawn parallel to $e'8$, and to an intersection with the panel center 8.

Now, $h_{,}8=y_m$, $h_{,}f_{,}=\frac{I_0}{I_m}$ (for the unit $h_{,}e_{,}$), and from similar triangles

$$g_{,}h_{,}=h'8\times\frac{h_{,}f_{,}}{h_{,}e_{,}}=y_m\times\frac{I_0}{I_m}.$$

The same procedure is followed for each panel center, and the ordinates so obtained define the line DE.

The foregoing explanation shows the simplicity of the computation and the special adaptability of the graphical method for that purpose.

The next step is to obtain the value of equation (73^A). For this the ordinates $a'a''$, $b'b''$, $c'c''$, etc., are plotted as the forces of a force polygon in Fig. 22*e* ($a'a''=1$, $b'b''=2$, etc.), and a pole distance is chosen.

The best results are usually obtained by making the pole distance p equal to about $\frac{1}{2}\Sigma v_m$. In Fig. 22*e* a reduction in the scale of the

figure has been required for illustrative purposes; in practice no such reduction is necessary.

With the pole P and the forces 1, 2, etc., the reciprocal polygon (in this case the moment polygon) ACB is drawn in Fig. 22E in the well-known manner, and the ordinates of this curve, measured from the axis AB, are equal to the horizontal thrust; for example, when the load K acts at the panel center 5, the ordinate H equals the horizontal thrust, and when the unit of measurement is established the problem is solved.

As stated on a preceding page, the unit of measurement is the value of the denominator, viz.:

$$\Sigma_0^l y_m v_m + \frac{B \cos a}{F_0} \frac{I_0}{d_0}.$$

This value is composed of two terms, and the second may be assumed as a constant.

The first term is the bending moment of a cantilever supporting the forces v_m, which act at the distance y_m from the point of support.

In Fig. 22e the forces 1, 2, etc., are equal to the ordinates v at 1, 2, etc. For the purpose of clearness these forces are shown on FG reduced to one-fifth their values.

To obtain the moment of the horizontal forces v the same force polygon with the same pole distance p has been reproduced in Fig. 22e', but with this difference: the forces v act horizontally.

From this force polygon the reciprocal polygon $A'C'B'$ has been drawn in Fig. 22E', and the line $A'B'$ is the moment of all the forces v, and is equal to $\Sigma_0^l y_m v_m$.

The constant should now be added. For this it should be remembered, from the graphical properties of the moment polygon, that the moment is equal to the ordinate of the moment polygon multiplied by the pole distance of its force polygon, and that the distance

$$B_{,}B_{,,} = \frac{B \cos a}{F_0 p} \frac{I_0}{d_0}.$$

Now,

$$\begin{aligned} B &= 185 \text{ m. (meters)}; \\ \cos a &= 0.525; \\ I_0 &= 2.78 \text{ m.}^4 = OG \text{ of Fig. } 22a; \\ F_0 &= 0.235 \text{ m.}^2 = OG \text{ of Fig. } 22b; \\ p &= 275 \text{ m.}; \\ d_0 &= \tfrac{1}{25} l = 8 \text{ m.} \end{aligned}$$

Also,

$$\begin{aligned} B_{,}B_{,,} &= 0.518 \\ A_{,}B_{,} &= 57.0 \\ \hline A_{,}B_{,,} &= 57.5+ \end{aligned}$$

and $A_{\prime}B_{\prime\prime}$ is the unit with which to measure the ordinates of Fig. 22E,

or $$H=\frac{27}{57.5}\times K=0.47K.$$

To obtain the intersection locus it is necessary to find the points of intersection of the component on its respective load line for successive positions of the load. This construction has been shown in Fig. 22d.

The distance FB equals K of Fig. 22E', and the points F and A in Fig. 22d are joined by a straight line; the line LG= line NM is equal to the reaction at B caused by the load K placed at 3′. The horizontal thrust caused by the load K is equal to MN of Fig. 22E.

This horizontal thrust has been plotted in Fig. 22d from the point B, viz., MB, and a perpendicular erected through the point M. A line LN is drawn through the point L and parallel with the line MB, and the intersection point N and the hinge B are two points of intersection of the component; and prolonging the line BN to an intersection with the load line 3′ gives a point of the intersection locus.

(*b*) The heavy solid line OP is the intersection locus for the vertical loads.

Figs. 22 to 22E' are for the purpose of illustrating the method of computation, and no especial pains have been taken to obtain accurate results, the original scale being 1 inch=20 meters. To show the great degree of accuracy which can be obtained by the graphical method, even with this scale, the author gives below the results obtained by Seyrig and also those obtained from the figures above mentioned.

TABLE VI.

	Equation (85).	Equation (95a).	H (Seyrig).	H (Figs. 22–22E).
Load at D	0.370K	0.370	0.370K	0.368K
" " E	0.645K	0.590	0.592K	0.603K
" " F	0.695K	0.640	0.631K	0.642K
" " G	0.730K	0.670	0.650K	0.658K

Equation (95a) of Chap. VIII gives for the ordinates of the intersection locus: $\int y''dx=\int ydx$. The intersection locus is the straight dash-and-dot line $O_{\prime}P_{\prime}$ in Fig. 22d, and as a means of comparison, the horizontal thrusts obtained by its use have been inserted in the foregoing table under the head "Equation (95a)."

The heavy dotted line $O''P''$ is the intersection locus obtained from equation (85) and the standard diagram of Fig. 14. A comparison of the values in the table shows that for practical purposes equation (95a) gives accurate results for the arch under consideration. This is of great importance in designing the crescent-shaped arch, as it enables the engineer to make his computations with absolute

certainty from the start, while the methods described in Figs. 22 to $22E'$ involve a great deal of labor and require in advance knowledge of the dimensions of the arch at various sections. The computation, however, is for the very purpose of determining these sections, from which it follows that preliminary assumptions have to be made by means of which computations may be effected; the results form a basis for further computations, upon which to make a second computation, and so on until the final result is in sufficient agreement with the assumptions. This is a laborious operation which, even with the graphical method here described, involves a great deal of time for an arch of the dimensions of the Douro Bridge.

The values in the table due to equation (85) are obtained by means of the intersection locus of a parabolic arch, whose moment of inertia increases from the crown to the supports in the same ratio as does the secant of the angle which the axis of the arch makes with the horizontal. This line $O''P''$ is indicated by heavy dots in Fig. 22*d*.

The table shows that this intersection locus causes an error in the center of the arch of 12%; this error is on the side of safety, but it is entirely too large to be incorporated into a design.

At the same time the table shows that the variation in the moment of inertia must be very large to have any appreciable effect on the horizontal thrust; and, with the exception of a few special cases, of which the Douro Bridge is an example, the intersection locus of Fig. 14 and equation (85), with the corrections as described in connection with Fig. 14*a*, give sufficiently accurate results for all practical purposes.

19. Horizontal Forces.—The graphical method described in Art. 18 not only gives the horizontal thrust for vertical loads, but also for horizontal loads.

From equation (75), Chap. VIII,

$$H_q=\frac{\Sigma_0^l\mathfrak{M}'_m v_m+Q\dfrac{I_0u}{F_0d_0}}{\Sigma_0^l y_m v_m+\dfrac{q\cos aI_0}{F_0d_0}}. \quad . \quad . \quad . \quad . \quad . \quad . \quad (75^A)$$

In this equation the denominator is the same as in the equation for vertical forces, and its value is equal to the line $A_,B_{,,}$ of Fig. $22E'$.

From equation (76),

$$\Sigma_0^l\mathfrak{M}'_m v_m=Q\left[\frac{q}{l}\Sigma_0^l(l-x)v_m-\Sigma_0^u(q-y)v_m\right]. \quad . \quad . \quad (76^A)$$

As explained in Chap. VIII, $\frac{1}{l}\Sigma_0^l(l-x)v_m$ is the vertical reaction at A of a beam of the span l which is loaded with the vertical forces v_m.

$\frac{q}{l}\Sigma_0^l(l-x)v_m$ = the moment caused by this force when it acts in a horizontal direction (see Fig. 22*I*).

$\Sigma_0^u(q-y)v_m$ = the negative moment caused by the forces v_m acting in a horizontal direction on the beam between the support A and the panel center 5 (Fig. 22*d*), or the whole expression is represented by the difference between the lines $A_{,,}C'$ and DC'' in Fig. 22*E'*.

To this should be added the value of $\frac{I_0u}{F_0d_0p}$. Now

$$I_0 = 2.78 \text{ m.}^4;$$

$$u = 36 \text{ m.};$$

$$F_0 = 0.235 \text{ m.}^2;$$

$$d_0 = 8 \text{ m.};$$

$$p = 275 \text{ m.}$$

$\therefore \frac{I_0u}{F_0d_0p} = 0.1935$, a value so small that it disappears in the drawing.

The horizontal thrust is then equal to H_1 when $A_{,}B_{,,}$ is the unit of measurement in Fig. 22*E'*.

$$H_1 = \frac{21.7}{57.5} = 0.38Q,$$

and to obtain the abscissa OR of the intersection locus,

$$0.38 \times 160 = 60.8 \text{ meters.} \quad \text{(See Fig. 22}d\text{.)}$$

The heavy line COB is the intersection locus thus computed for the horizontal forces.

The heavy dash-and-dot line is the intersection locus for the crescent-shaped arch of Fig. 20 and equation (98) of Chap. VIII. This gives

$$H_1 = 0.361Q,$$

which contains an error of 4½ per cent. and is a maximum at this point; towards the crown and the hinges it decreases to zero. For H_2 the reverse is the case and the average error is about 1½ per cent.

Horizontal forces are usually caused by wind pressure, which is a force subject to wide variations in direction and intensity, and a 1½ per cent. error is insignificant when compared with the error that may be made in assuming a particular intensity for the wind pressure on a roof.

The heavy dotted line is the intersection locus of equation (88) of Chap. VIII, or of Fig. 13 of the standard diagram. Even this intersection locus may be used for the computation of wind stresses and yet produce sufficiently accurate results.

20. Deflections Caused by Vertical Forces (General).—Equations (111), (113), (114), (115*a*), (112*a*), (113*a*), (114*a*), (116), and (117) of Chap. VIII are:

$$M\frac{I_0}{I_{\prime}}+\frac{I_0}{r\cos a}\left(\frac{P}{F}-Ewt\right)=\text{o}; \quad . \quad . \quad . \quad . \quad (111^A)$$

$$-EI_0\Delta y=\frac{x'}{l}\int_0^l \text{o}(l-x)dx-\int_0^{x_{\prime}}\text{o}(x_{\prime}-x)dx+C_1; \quad (113^A)$$

$$EI_0\Delta x=\frac{y_{\prime}}{l}\int_0^l \text{o}(l-x)dx-\int_0^{x_{\prime}}(y_{\prime}-y)dx+C_2; \quad . \quad (114^A)$$

$$\left.\begin{aligned} C_1&=I_0\left(\frac{H}{F_0}-Ewt\right)y_{\prime};\\ C_2&=-I_0\left(\frac{H}{F_0}-Ewt\right)x_{\prime};\end{aligned}\right\} \quad . \quad . \quad . \quad . \quad . \quad (115_a{}^A)$$

$$EI_0\Delta a_0=\mathfrak{D}_A, \quad . \quad . \quad . \quad . \quad . \quad . \quad . \quad . \quad (112_a{}^A)$$

$$-EI_0\Delta y=M\text{o}_v+C_1. \quad . \quad . \quad . \quad . \quad . \quad . \quad (113_a{}^A)$$

$$EI_0\Delta x=M\text{o}_h+C_2; \quad . \quad . \quad . \quad . \quad . \quad (114_a{}^A)$$

$$\text{o}=H\left[\left(\frac{\mathfrak{M}}{H}-y\right)\frac{I_0}{I_{\prime}}+c\right]; \quad . \quad . \quad . \quad . \quad . \quad (116^A)$$

$$c=\left(1-\frac{EF_0wt}{H}\right)\frac{I_0}{F_0\, r\cos a} \quad \text{when} \quad P=H. \quad . \quad . \quad (117^A)$$

When the values of o are assumed to be forces acting on a beam, then $\frac{1}{l}\int_0^l \text{o}(l-x)dx$ is the vertical reaction $\mathfrak{D}_A$ of these forces at the support A.

$\frac{x_{\prime}}{l}\int_0^l \text{o}(l-x)dx$ is the bending moment in the beam caused by this reaction $\mathfrak{D}_A$.

$\int_0^{x_\prime} \mathfrak{o}(x_\prime - x)dx$ is the negative bending moment caused by the forces $\mathfrak{o}$ which act between the support A and the point $x_\prime$. C_1 is a constant.

The whole expression of equation (113^A) is then the bending moment at the point $x_\prime$ of a simple beam supporting the loads $\mathfrak{o}$.

Equation (114^A) has the same significance when $\mathfrak{D}_A$ and $\mathfrak{o}$ are considered as acting in a horizontal direction, and when the values of the forces $\mathfrak{o}$ are known, the problem resolves itself into the simple construction of a moment polygon.

Equation (116^A) is composed of two parts:

(1) $\frac{\mathfrak{M}}{H}\frac{I_0}{I_\prime}+c$, in which $\frac{\mathfrak{M}}{H}$ is the moment polygon of a single load and is drawn from a force polygon with the pole distance H. The ordinates of this moment polygon are to be multiplied by the ratio $\frac{I_0}{I_\prime}$, and to the ordinates thus obtained the value of c is to be added.

(2) This part, $y\frac{I_0}{I_\prime}$, has been obtained before, being $=v_m$ of Art. 18(a), and is represented by the ordinates of the line DE in Fig. 22d.

In substituting the two values of $\mathfrak{o}$ in equation (113^A) or (114^A) there results for each equation two moment polygons, and the deflection is the difference of the ordinates between these two polygons.

The substitution of the value $y\frac{I_0}{I_\prime}$ [Art. 18 (a)] in equations (113^A) and (114^A) produces the horizontal-thrust curves of Figs. 22e, 22E, 22e', and 22E', and their construction is fully described in the article mentioned.

The value of $\frac{\mathfrak{M}}{H}\frac{I_0}{I_\prime}$ should now be found.

Suppose the deflections of the arch are required for a vertical load K, acting at the panel center 5 [Art. 18 (a)]. When the value of K is equal to $A_\prime B_{\prime\prime}$ of Fig. 22E', its horizontal thrust is equal to H in Fig. 22E, and the force polygon has been drawn in Fig. 22f, from which the moment polygon ABC has been drawn in Fig. 22F; the ordinates of this polygon measured from AB to the line ACB are equal to the bending moment $=\frac{\mathfrak{M}}{H}$.

Next, the value of $\frac{\mathfrak{M}}{H}\frac{I_0}{I_\prime}$ should be determined.

The points f and e of Fig. 22a are reproduced on the axis AB of Fig. 22F, and a line fg is drawn parallel to a line uniting the points e and 8; from similar triangles,

$$hg = h8 \times \frac{hf}{he}.$$

Now, $h8 = \frac{\mathfrak{M}}{H}$, $hf = \frac{I_0}{I_{\prime}}$, as formerly obtained, and $he = 1$;

$$\therefore\ hg = \frac{\mathfrak{M}}{H}\,\frac{I_0}{I_{\prime}}.$$

All the panel centers are similarly computed, and the ordinates so obtained determine the line DE of Fig. 22F.

The value of c should be added to these ordinates $\left(c = \frac{I_0}{F_0 r \cos a}\right)$; the effects of temperature changes will not be considered at this time.

Substituting in this equation,

$$c = \frac{2.78}{0.235 \times 96.5 \times 0.525} = 0.24 \text{ (approx.)};$$

and this value is nearly constant for all the ordinates and should be added to those of Fig. 22F by drawing a line parallel to AB and above it at a distance $=0.24$; this distance, however, is so small that it is unnoticeable in the scale of the drawing.

The ordinates of the line DE of Fig. 22F have been plotted in Fig. 22g. For the purpose of clearness this figure has been drawn to a scale which is one-fifth of that for Fig. 22F. For the force polygon the same pole distance is used as that in Fig. 22e, and with this force polygon the moment polygon $AC'B$ has been drawn in Fig. 22E.

The ordinates included between the curves ACB and $AC'B$ represent the vertical deflections of the arch caused by the load K, when measured with the proper scale. Not only this, but from the law of reciprocal action, the deflection at 5 is known for any position of the load; for instance, when a load is placed at D, the deflection at 5 will be upward and equal to Dd. For a load placed at E the deflection at 5 will be downward and equal to Ee, etc., and the line $AC'B$ may be termed the influence line of the deflections.

(*a*) Horizontal Displacement Caused by Vertical Forces.—To obtain the horizontal displacement caused by the vertical load K, Fig. 22g is reproduced in Fig. 22g'; the moment polygon $A'C'''B'$ has been drawn in Fig. 22E' and requires no further explanation.

Unit of Measurement.—The differences between the ordinates of the moment polygons as obtained from the figures are equal to $EI_0\Delta y$ and $EI_0\Delta x$ [(113$_a$A) and [(114$_a$A)]. For the load at 5 the ordinate H of Fig. 22E is equal to the horizontal thrust when $A_{\prime}B_{\prime\prime}$ (in Fig. 22E') is the intensity of the load. To obtain the bending moment, the ordinates of the moment polygon should be multiplied by the pole distance of the force polygon from which the moment polygon originated; the panel lengths are $=d_0$.

To obtain the actual deflection for a unit load, say 1 ton, the ordinate should be reduced by the ratio $\frac{Hd_0p}{EI_0}$.

Now, $H=0.47$, $d_0=8$ m. (meters), $p=275$ m., E (for steel) $=$ 22,000,000 tons per sq. m., and $I_0=2.78$; consequently the ratio $=\frac{0.47\times8\times275}{22,000,000\times2.78}=0.0000173$.

For example, at 5 the vertical deflection measured by the scale of the drawing is 6.5 m., or 6,500 mm.$\times$0.0000173=0.112 mm. is the deflection caused at 5 by a load of 1 ton placed at 5; and when the left half of the bridge is loaded with a load of 24 tons at each panel point, the vertical deflection at 5 is equal to the sum of the ordinates from 1 to 10 between the two polygons, viz., 43.5 m., or

$$43,500\times24\times0.0000173=18.06 \text{ mm.}$$

For the same form of loading the horizontal displacement of the point 5 towards B will be the sum of the differences between the two polygonal lines $A'C'$ and $A'C'''$ in Fig. $22E'$, or

$$37,000\times24\times0.0000173=15.36 \text{ mm.}$$

(*b*) Deflections Caused by Secondary Stresses.—To the above values the value of the constant C should be added. From equations $(115_a{}^A)$,

$$\Delta y=\frac{C_1}{EI_0}=\frac{I_0Hy_,}{EI_0F_0}=\frac{Hy_,}{EF_0},$$

$$\Delta x=\frac{C_2}{EI^0}=-\frac{I_0Hx_,}{EI_0F_0}=-\frac{Hx_,}{EF_0},$$

and the deflections caused by the secondary stresses are proportional to the ordinates of the axis of the arch. As an example, assume a load of 1 ton at panel center 5, when

$$H=0.47,$$

$$E=22,000,000 \text{ (tons per sq. m.)},$$

and $$F_0=0.235; \text{ then}$$

$$\text{deflection}=\frac{0.47y_,}{0.235\times22,000,000}=0.000000091y_,;$$

$$x=36 \text{ m. and } y_,=30.5 \text{ m.},$$

or $$\Delta y=0.003276 \text{ mm.}$$

and $$\Delta x=-0.002775 \text{ mm.}$$

The deflections caused by the secondary stresses are very small, —about 3% of the deflections caused by the impressed load—and can usually be neglected.

21. Deflections Caused by Horizontal Forces.—These deflections are also given by the differences of the coordinates of two moment polygons, and equation (116[A]) applies when the value of $\mathfrak{M}'$ is substituted for that of $\mathfrak{M}$.

According to equation (76), Chap. VIII,

$$\mathfrak{M}'=y-x\frac{q}{l}\Big]_{x=0}^{x=u} \quad \text{and} \quad \mathfrak{M}'=(l-x)\frac{q}{l}\Big]_{x=u}^{x=l}.$$

Substituting these values in (116[A]) gives for the first part of the equation:

$$\frac{\mathfrak{M}'}{H_{,}}\frac{I_0}{I_{,}}+c=\sum_0^u \frac{y-x\frac{q}{l}}{H_{,}}\frac{I_0}{I_{,}}+\sum_u^l \frac{(l-x)\frac{q}{l}}{H_{,}}\frac{I_0}{I_{,}}+c.$$

The second term of this equation (116[A]) is again $=y\frac{I_0}{I_{,}}$ and is the same horizontal-thrust curve ACB of Fig. 22E which has been reproduced in Fig. 22h.

In Fig. 22I the arch axis ACB has been reproduced and it is desired to find the deflections caused by a horizontal force Q acting at the panel center 5 (where maximum value of $x=u$).

The values of $x\frac{q}{l}$ are measured by the ordinates between the axis AB and the line AD, and those of $-yx\frac{q}{l}$ by the ordinates of the arch axis measured from the line AD.

The values of $(l-x)\frac{q}{l}$ are simply the ordinates measured from the line AB to the line $D''B$. The multiplication of these ordinates by the ratio $\frac{I_0}{I_{,}}$ is accomplished as before, viz., the point f is reproduced from Fig. 22a in Fig. 22I, etc., and the lines ED' and $D''B$ define the ordinates of these products.

The horizontal-thrust curve was produced by an equation of which the denominator was equal to Q of Fig. 22E' (see earlier paragraphs).

The denominator of the first term of equation (116[A]) is $H_{,}$, and to draw the two polygons so that they will correspond, the pole distance of the latter should be reduced to $p'=p\frac{H_{,}}{Q}$. This has been done in Fig. 22j.

The ordinates 1–1′, 2–2′, 3–3′, etc., of Fig. 22*I* are plotted as forces 1, 2, 3, etc., in Fig. 22*i*. For the sake of clearness the scale of this figure is reduced to one-half that of Fig. 22*I*.

With the pole distance p' (see also Fig. 22*j*) the moment polygon $AC'B$ has been drawn in Fig. 22*h*, and the differences of the ordinates indicate the horizontal displacements caused by the horizontal force Q acting at 5; for example, the panel center 3 will move the distance Dd toward B, and the point 5′ will move the distance Ff toward B.

Again, from the laws of reciprocal action, a horizontal force applied at 5′ will move the point 5 the distance fF toward A, and a force applied at 7 will move the point 5 the distance Gg toward B.

Unit of Measurement.—The load unit is equal to $H_{,}=\frac{21.8}{57.5}=0.38Q$, and the ratio for the reduction of the deflections to the scale of the drawing is $\frac{H_{,}d_0p}{EI_0}$.

Now, $H_{,}=0.38$, $d=8$ m., $p=275$ m., $E=22{,}000{,}000$ (tons per sq. m.), and $I_0=2.78$.

$$\therefore\ k\Delta x=0.0000137\Delta x,$$

and when $Q=1$ ton and $k=7{,}200$ mm., the displacement at 5 toward B will be $7{,}200\times0.0000137=0.099$ mm.

Fig. 22*h* shows that horizontal forces acting on one-half of the span cause maximum horizontal deflections.

(*a*) Temperature Stresses Caused by a Temperature Change of 1° C.—From equation (110) of the Appendix,

$$H_t=\pm273\frac{I_0B\cos a}{d_0\Sigma_0 y_m v_m+\dfrac{I_0B\cos a}{F_0}}.$$

The denominator of this equation is equal to the line $A'B''$ of Fig. 22*E'* multiplied by the pole distance p and the panel length d_0, and

$$H_t=\pm273\,\frac{2.78\times0.525\times185}{8\times275\times57.5}=0.525\text{ ton.}$$

(*b*) Deflections Caused by a Change in Temperature.—From equation (120), Chap. VIII,

$$EI_0\Delta y=H_tm_x+2\left(Ewt-\frac{H_t}{F_0}\right)I_0y,$$

where m_x is the moment caused by the loads $y\frac{I_0}{I_t}$ on a beam of the length l. The values of $y\frac{I_0}{I_t}$ are the ordinates of the line DE in Fig. 22d, and the values of m_x are the ordinates of the horizontal-thrust curve ACB of Fig. 22E. For the crown of the arch, $m_x=Ff\times p\times d_0$, $k=Ff$ (Fig. 22E) $=38.5$, $p=275$, $d_0=8$, $t=30°$ C., $Ewt=8{,}190$, $H_t=0.525$, $F_0=0.235$, $I_0=2.78$, $y=42.65$, and $E=22{,}000{,}000$;

$$\Delta y=\frac{H_t m_x}{EI_0}+2\left(8{,}190-\frac{H_t}{F_0}\right)\frac{y}{E}$$

$$=\frac{(2{,}200k+1{,}505.5y)t}{22{,}000{,}000\times 2.78}$$

$$=\frac{[(2{,}200\times 38.5)+(1{,}505.5\times 42.65)]30}{22{,}000{,}000\times 2.78}=0.073 \text{ meter.}$$

The crown, therefore, will rise or sink for a difference in temperature of 30° C.,

$$\Delta y=73 \text{ mm.}$$

Equation (93), which neglects the secondary stresses, gives

$$H_t=-\frac{15}{8}\times\frac{273\times 2.78}{42.65^2}=0.795 \text{ ton.}$$

Special equation (110) (see previous article) gives

$$H_t=0.525,$$

and it is thus seen that in the crescent-shaped arch the temperature stresses are only two-thirds of those in an arch rib in which the moment of inertia increases from the crown to the hinges as the secant which the axis makes with the horizontal.

Special equation (100) of Chap. VIII, for the crescent-shaped arch, gives

$$H_t=\tfrac{1}{2}Ewtk^2F.$$

In the arch of Fig. 22, k averages about $\frac{1}{4}$ and $F=0.228$ (see Fig. 22b), or

$$H_t=\frac{273}{32}\times 0.228=1.95 \text{ tons.}$$

This shows that the equation should only be used when the configuration of the arch satisfies the conditions on which the equation is based, viz., $h=ky$ and $F=F_0 \sec a$.

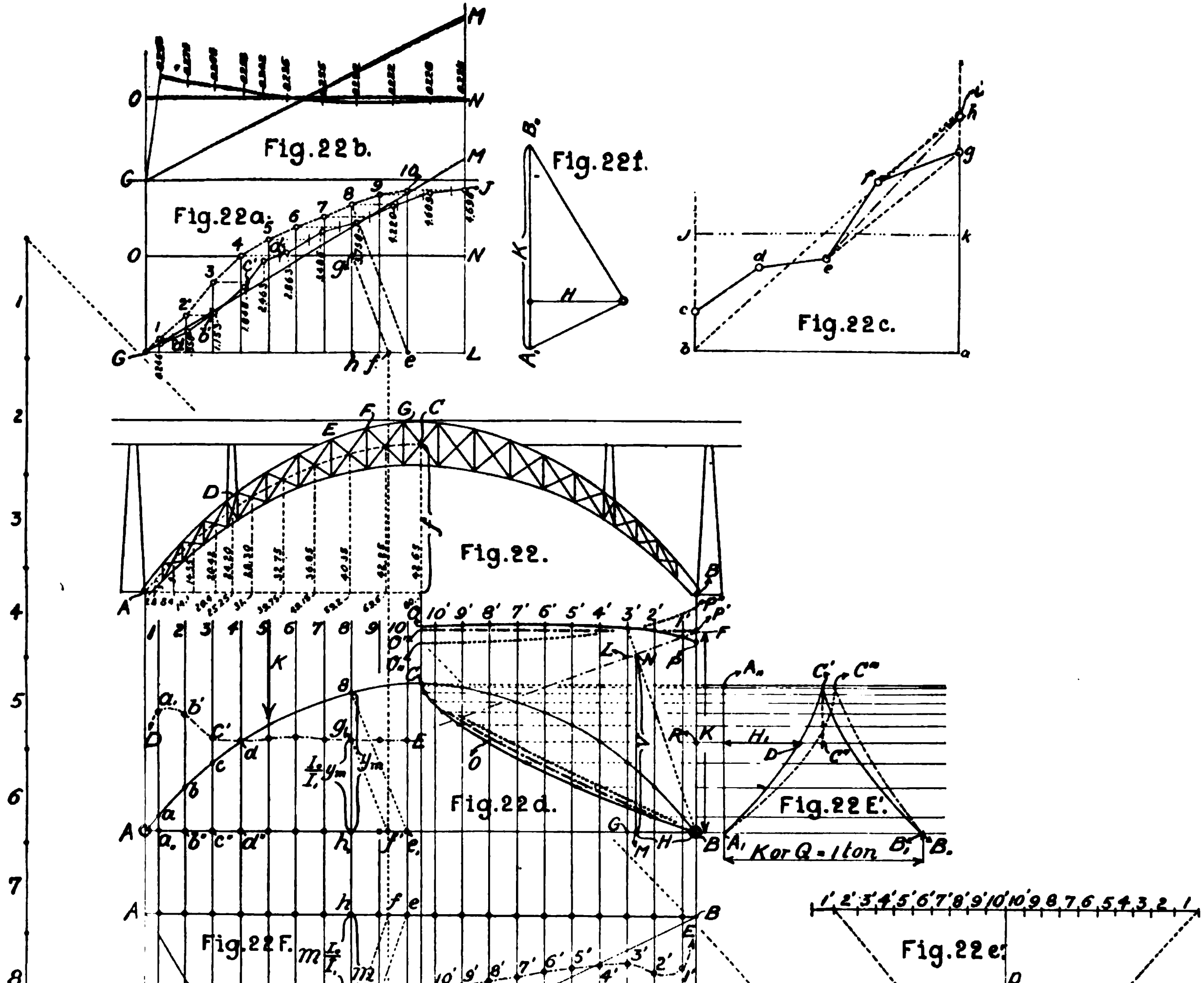
Fig. 22b.
Fig. 22a.
Fig. 221.
Fig. 22c.
Fig. 22.
Fig. 22d.
Fig. 22E.
K or Q = 1 ton
Fig. 22F.
Fig. 22e.

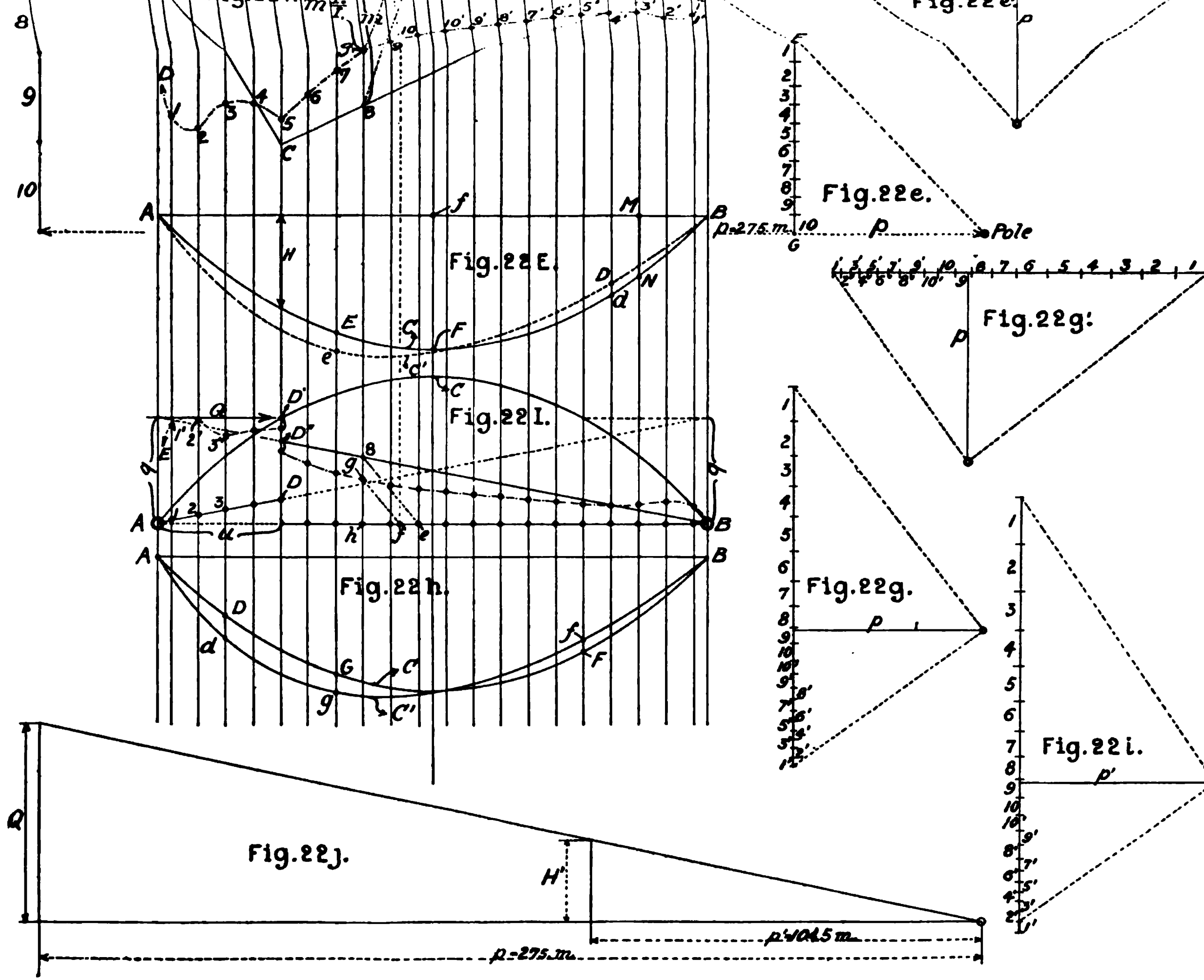

[To face page 98.

To apply equation (100) in this case the value of k should be substituted in equation (99), which will result in equation (93) when $\frac{1}{2}h^2F=I_0$.

To compute the temperature stresses in a crescent-shaped bridge-truss, it is better to use two-thirds of the value obtained from equation (93) for the preliminary computation, and then for the final computation to use equation (120).

In the preliminary computation of the secondary stresses in the crescent-shaped arch, equation (101) of Chap. VIII may be used.

(*c*) Stresses and Deflections Caused by Yielding of the Abutments.—To obtain the stresses caused by a sliding or yielding of the abutments which causes an increase in the span: Equation (110*b*) of the Appendix gives

$$H=\frac{-E\Delta lI_0}{\int_0^b\frac{I_0}{I}y^2ds+\frac{I_0B\cos a}{F_0}}.$$

In this equation the denominator is equal to the line $A_{\prime}B_{\prime\prime}$ of Fig. 22E' and is equal to Qpd_0.

$$(Q=57.5,\quad p=275,\quad d_0=8,\quad I_0=2.78.)$$

Assume that abutment slides 0.05 m.; then

$$H=\frac{-22,000,000\times0.05\times2.78}{57.5\times275\times8}=24.15 \text{ tons}.$$

To obtain the deflection of the crown caused by the shifting of the abutments: Equation (121) of the Appendix gives

$$\Delta y=-\frac{\Delta l}{\int_0^b\frac{I_0}{I}y^2ds+\frac{I_0B\cos a}{F_0}}\left(m_x-2\frac{I_0}{F_0}y\right).$$

In this equation the denominator is again the length of the line $A_{\prime}B_{\prime\prime}$ of F g. 22E', $=Qd_0p$, and m_x is again the ordinate of the horizontal-thrust curve at the center of the span, $=k$;

$$\therefore\ m_x=kpd_0. \qquad p=275, \qquad d_0=8,$$

$$\Delta l=0.05, \qquad A'B''=57.5, \qquad m_x=38.5\times275\times8, \qquad I_0=2.78,$$

$$F_0=0.235, \qquad y=f=42.65;$$

$$\therefore\ \Delta y=-\frac{0.05}{57.5\times275\times8}\left(38.5\times275\times8-2\frac{2.78}{0.235}42.65\right)$$

$$=0.033 \text{ meter}.$$

CHAPTER IV.

HINGELESS ARCHES.

1. Introductory.—As compared with the other types of arches, the hingeless arch is the most rigid, and often the most economical as regards cost of construction. It has been built in metal, stone, and reinforced concrete, and with few exceptions it can be safely stated that the stone arch is built as a hingeless arch.

The advantages which the stone arch possesses over every other form of bridge are its nominal cost of maintenance and its durability; many examples existing of arches now in use which were built more than 1,800 years ago.

Combine with these advantages its ability to stretch over wide spaces with a single span, and that it can often compete successfully with the steel arch as regards the first cost of construction, and the question presents itself forcibly, why is its adoption limited, even for bridges of moderate size?

The uncertainty which exists in determining its stresses gives the answer to this question.

It is generally admitted that the analysis of the stresses according to the elastic theory is the only reliable one, but few have the time, the training, or the patience to grapple with its intricacies. In the following articles the author has not only unravelled these, but he also presents the elastic analysis of the stresses in the hingeless arch as the clearest and simplest of all methods. Moreover, this is done without sacrificing anything on the part of accuracy and without making assumptions which would cast doubts upon the results obtained.

Before entering into a discussion of the method, however, an introductory explanation is advisable for the purpose of preparing the reader for a clear understanding of the subject.

In Chapter I the meanings and uses of the intersection locus and the tangent curves have been defined; the Appendix deals with the analysis of the elastic theory as applied to arches, and the following articles are devoted to its practical application.

The ordinates of the intersection locus and of the tangent curves are dependent on (I) the curvature of the axis of the arch, and (II) on the form of the arch rib at the various planes of section.

I. *The Curvature of the Arch Axis.*—This is not arbitrarily determined. A relatively small change in the curve will aflect the stresses in the arch very materially, from which it fol ows that for an arch of given span, rise, and form of loading there must be a curve the adoption of which will result in minimum stresses, and therefore in maximum strength and economy.

A change in the curvature of the arch axis can be relatively large before it causes an appreciable change in the intersection locus or the tangent curves, provided the area enclosed by the arch axis and its chord does not alter. This is demonstrated later in the chapter and also in the Appendix.

II. *The Form of the Arch Rib at the Various Planes of Section* varies according to the stresses. The steel arch rib is usually of uniform depth, and consists of a web plate with flange angles and flange plates; and changes in the section are made by increasing or decreasing the size or number of the flange plates, or both. An alteration thus made in the section of the arch rib produces a change in its moment of inertia. The relative change in the moment of inertia of such an arch rib is small as compared with that of a solid arch. Any change in the section of the rib increases or decreases its depth, and comparatively small changes in depth influence the moment of inertia materially. For instance, a solid rib whose depths at three planes of section show increases of 10%, 20%, and 30% respectively, will have corresponding increases in the moment of inertia of 33%, 73%, and 120%.

In the computation of the Douro Bridge (Chapter II, Article 18) it was shown that the moment of inertia in a two-hinged arch must change considerably to influence the intersection locus. This is also true for the hingeless arch.

In the two-hinged arch all components pass through the hinges; in the hingeless arch the components are tangents to curves, and a change in the moment of inertia influences these curves.

Special attention is given to this subject in Art. 5 *et seq.*; it suffices here to say that the "character" of the variation in the moment of inertia is also a factor to be considered. This means that a large increase in the depth of the arch rib near the abutments will not influence the tangent curves materially, provided the remainder of the arch rib has no large changes in depth. For example, in a flat arch the moment of inertia may increase from the crown towards the abutments in the same ratio as does the secant of the angle which the arch axis makes with the horizontal. This ratio of increase may extend over a distance equal to seven-tenths of the span, and for the remaining length the increase may be more rapid. In such a case the tangent curve is only influenced near the abutments by this variation. But those are the regions where a change in the tangent curve does not materially affect the positions of the components or the stresses in the arch.

Flat arches closely satisfy the above conditions, and this, taken

in connection with the characteristic of the intersection locus and tangent curves described under II, leads to the conclusion that for flat arches the intersection locus and tangent curves may be plotted from a standard diagram.

When once these locus and tangent lines are known, the computation of the stresses in the arch is simple.

This, however, would confine the application of the elastic theory to special cases. The manner in which the standard diagram has been made general in its application is specially dealt with in Art. 7, which treats of the Correction of the Intersection Locus and Tangent Curves.

The author has divided the subject of hingeless arches into three parts:

The first deals with the application of the elastic theory to a special case, viz., the stresses in a flat arch of 105 ft. span and 11.7 ft. rise.

The second deals with the application of the elastic theory in its broadest sense—and without special conditions—to the computation of stresses in the hingeless arch, and is exemplified by a discussion of the Syra Valley Bridge, which is a masonry arch of 300 ft. span and 55 ft. rise.

The third is a comparison between the first and the second cases, from which the correction of the standard diagram is derived. Deflections and their influence on erection are also treated in this part.

In computing the stresses in a hingeless arch by the use of the standard diagram, as analyzed in Chap. IX of the Appendix, the arch axis is assumed to be a parabola.

The axis of a well-designed stone arch is never a parabola, its rise in proportion to the span being less. There is, however, a relation between the two curves, viz.: when the area enclosed by the arch axis and its chord is equal to the area enclosed by the parabola and its chord, when the difference in the ordinates of the two curves is relatively small, and when the two curves are so placed that their chords coincide, they will have the same intersection locus and tangent curves. This parabola is always referred to as the equivalent parabola.

The stresses in the arch are caused by vertical and horizontal forces.

The vertical forces are the dead load and the live load.

The horizontal forces are caused by changes in temperature and the conjugate pressure of the spandrel filling. The latter can be neglected in flat arches.

In the designing of masonry arches the first steps in the computation are the determination of the curvature of the arch axis, and the dimensions of the arch rib. These two factors determine the dead load, which in turn fixes the position of the line of pressure in relation to the axis of the arch; and the form of the arch in which

these two lines most closey approach each other is the best that can be designed.

Live ioads and temperature changes exert stresses; these, however, vary, and cause either an increase or a decrease in the stresses, as the case may be; as the curvature of the axis can only be defined for one form of loading, and the dead load is large as compared with the live load, it can be stated as a rule that "the dead load defines the curvature of the arch axis."

The dead load is also defined by the dimensions of the arch rib, and the rule just given may be extended to state that "the dimensions of the arch rib also define the curvature of the arch axis."

The dimensions of the arch rib, however, are also controlled by the live load and temperature changes, and under their influence no part of the arch should be subjected to excessive stresses.

Though all these factors affect either directly or indirectly the curvature of the arch axis, there is a difference in the magnitude of their influence.

Relatively large changes in the dimensions of the arch rib exert great influence on the stresses in the arch, but, as compared with the distribution of the dead load, these changes are comparatively small—in fact, in most instances, too small to influence the line of pressure or the curvature. This fact facilitates considerably the determination of the curvature of the arch axis.

Another factor which should be considered is the conjugate pressure of the spandrel filling in arches with a large rise. How the curvature of the arch axis is defined by this pressure is for the present neglected; it will be considered in the article dealing with the "Influence of Horizontal Forces on the Arch."

The first step in the computation of stresses is then to find the line of pressure caused by the dead load alone, and to determine from this line that curvature of the arch axis which approaches the nearest to the line of pressure. (See The Law of Winkler, in Appendix.)

The intensities of the secondary stresses depend largely on the dimensions of the arch rib. In a flat arch these stresses should not be neglected; to include them, however, in the computation of the curve of the arch axis is difficult and inconvenient. Up to this point the only assumptions made concerning the dimensions of the arch rib have been for the purpose of determining the dead load. An error in these assumptions can be considerable before it materially influences the line of pressure in the arch.

It is not so with the secondary stress, as the moment of inertia is one of the factors which determines its intensity, and, as previously mentioned, though a slight change in the depth of the arch rib may not appreciably change the dead load, it will change the moment of inertia.

For this reason the secondary stress is treated as a decrease in temperature.

When the arch axis has been determined, very close assumptions can be made for the dimensions of the arch rib.

From this the secondary stress can be computed, and then those posi-

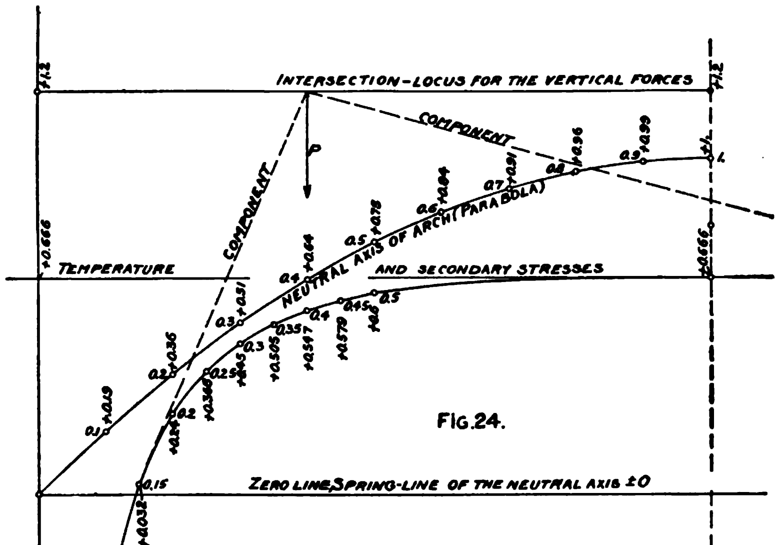

FIG. 24.

tions of the live load are to be determined which, in combination with secondary and temperature stresses, will produce maximum and minimum stresses in the arch rib.

Before illustrating the application of the foregoing method, a brief digression will be made in the following paragraphs for the purpose of demonstrating the distinct features of the computation.

(*a*) In Fig. 24 the standard intersection locus and tangent curves are shown for a parabolic arch with a rise equal to 1 and a half-span equal to 1. (See equations (152) and (153) of Appendix.) To obtain the intersection locus and tangent curves for any other arch whose axis is a parabola, multiply the vertical ordinates of the diagram by the rise of the arch axis, and the horizontal ordinates by one-half the span of the arch.

For a flat arch whose axis is not a parabola, first find the area enclosed by the arch axis and its chord; from this compute the height of a parabola having the same area (the equivalent parabola), and this height multiplied by the vertical ordinates of the diagram will give the ordinates of the intersection locus and the tangent curves.

The line of action of the temperature and secondary stresses in this case is to be found in the following manner:

The area enclosed between the arch axis and its chord is reduced

to a parallelogram whose length equals the span; its height is then the distance above the chord of the arch axis where these forces act (for the parabola this distance is equal to two-thirds of the rise of the axis).

Any corrections to these curves should be made according to the method of Art. 7 (*d*) and Figs. 38 and 38*a*.

The graphical methods of determining the area of any plane figure are shown and described in Art. 18 of the previous chapter and Fig. 22*c*.

(*b*) The first step in the computation of stresses is to assume a curve for the arch axis and the dimensions of the arch rib; from these the dead load is computed.

The experience of the designer is the most important factor in making these assumptions, for there are no rules or equations to guide him.

Various empirical equations have been developed for the determination of the depth of the arch rib at the crown, and though the results obtained may be sufficiently accurate for small arches, they are not so for large spans, and at best yield only dimensions upon which assumptions may be based for preliminary designs.

For this reason those equations which are simplest in form and yield at the same time close results, recommend themselves.

There are fifteen or more of these equations which may be found in pocket-books, etc., to which the reader is referred.

For small arches with circular or elliptic intrados the following rule gives satisfactory dimensions:

Find the radius of a circular arc which most closely coincides with the intrados; add to this radius one-half of the span and take the square root of the sum. Divide this result by 4 and add 0.2 ft.

The dimension thus obtained is for good masonry; for inferior masonry, rubble or brick, the depth thus obtained should be multiplied by from $1\frac{1}{8}$ to $1\frac{1}{3}$ (Trautwine).

The empirical equation which the author uses in his practice is very simple in form. It was developed by Schwartz and gives satisfactory dimensions upon which to base preliminary estimates, even for large arches.

For arches with a rise of less than one-third of the span,

$$d = 3.333n + \frac{1}{1,008} \cdot \frac{W}{s} \frac{l}{f};^{*}$$

for arches with a rise of more than one-third of the span,

$$d = 3.333n + \frac{1}{336} \frac{W}{f}.^{*}$$

* These equations are correct for arches with spans not exceeding 100 ft.; for longer spans the value of d obtained from these equations should be reduced 2% for each additional 11 ft. of span.

d = depth of arch at the crown in feet;
W = weight in lbs. of one-half of the arch, including paving and a fill of less than 3.5 ft. in depth at the crown;
s = stress in the arch in lbs. per square inch;
l = length of span in feet;
f = rise of the arch axis in feet;
n = a coefficient which is usually assumed for bridges = 0.2.*

The first equation is applied to the arch shown in Fig. 25. The maximum stress allowed in the arch is 600 lbs. per square inch, and assuming that there will be no tensile stresses in the arch, and the minimum stress does not drop below zero, the average stress in the arch is assumed to be, for the preliminary computation,

$$600:2=300 \text{ lbs. per sq. in.}$$

The rise of the axis = 11.7 ft.
The span = 105 ft.
The total dead load of one-half the span = 56,700 lbs. for an arch ring 1 ft. wide.

$$d=3.333\times0.2+\frac{1}{1,008}\times\frac{56,700}{300}\times\frac{105}{11.7}=2.35 \text{ ft.},$$

which is the depth for the arch rib at the crown to be assumed for a good quality of concrete or stone.

This figure can be increased for an inferior quality of material, or it may be decreased 15% for a reinforced-concrete arch.

The additions or deductions to be made cannot be expressed by any equation; experience combined with good judgment will decide these.

For the semicircular arch the rise of the arch can be substituted for f, which is then measured from the springing line to the intrados.

When the dead loads have been computed for each panel, a preliminary force polygon, like Fig. 27, may be drawn, I. II, etc., being the panel loads, and the point a being assumed as a trial pole.

With this pole a trial polygon AI, I–II, etc., may be drawn, as in Fig. 26. This will enable the designer to check the accuracy of his assumptions, and corrections can then be made accordingly. The experienced designer can dispense with this process and instantly commence his computations.

2. **Computation of Stresses: Vertical Loads.**—In Fig. 25 is shown a reinforced-concrete arch highway bridge of 105 ft. span and 16.5 ft. rise. The loads are as follows:

* There are many more equations, among which those developed by Low and by Tolkmitt give close results. These forms, however, are not as simple as the one given above, and none enters into the curvature of the arch axis as a factor; still, this is of great importance in the distribution of stresses in the arch, as this chapter will show.

Live load, 100 lbs. per sq. ft.

For a 16-ton road-roller an equivalent concentrated load of 3,000 lbs. per foot width of the arch is assumed.

Concrete, 150 lbs. per cu. ft.

Earth-fill, 120 lbs. per cu. ft.

Pavement, 150 lbs. per cu. ft. (1 ft. thick).

All calculations are for an arch rib 1 ft. wide.

In Fig. 25 the earth-fill has been reduced to an equivalent weight of concrete, and the total dead load for one-half of the span is represented by the area *abcd*.

The half-arch is divided into eight panels of equal length. The line *ef* is a line midway between *ab* and *cd*, and on this line the centers of gravity are located.

The distance $gk=ij$, and $jl=gh$; the points k and l are united by a straight line, and at its intersection with mn the center of gravity is located. This is a well-known construction for determining the center of gravity of a trapezoid. Multiplying kh by one-half the height of the trapezoid and by 150 lbs. gives the weight of this panel of the arch for a width of 1 ft.

The rise of the axis of the arch is 11.7 ft., and the axis is assumed to be a parabola. The intrados of the arch is composed of three parabolas, one with its main axis vertical at d and the other two with their main axes horizontal at the springing line c.

This combination gives a pleasing elliptical curve to the arch.

In Fig. 26 the arch is drawn with its locus LM and its tangent curves $J'K'$ and JK for a rise of 11.7 ft.; the points of application for the live and dead loads are at I, II, . . . XVI.

(*a*) The dead loads are resolved into their components and these are added in Fig. 27, in the same manner as described for the three-hinged braced arch in Chapter I. The broken line $abc \ldots p$ represents the left-hand components, aq the horizontal thrust, and pq the vertical reaction at A (Fig. 26).

It may not be superfluous to point out that though the components are tangents to the curve JK, Fig. 26, yet the resultant of two or more components is not tangent to this curve.

To find the resultant, for example, of 1, 2, and 3: first find the resultant of 1 and 2 in Fig. 26 by bringing 1 and 2 to an intersection at r, and drawing through this point the line ac parallel with a line uniting a and c in Fig. 27; then intersect component 3 with ac in Fig. 26 and draw a line through the intersection point s parallel to ad in Fig. 27, etc. These resultants may be drawn at the same time with the broken line of Fig. 27.

This method may sometimes be useful for making a preliminary computation with a full load, but as it does not give the resultant of the components of a partial load, it is not general in its character.

When the location of the resultant of all the components from 1 to 16 is computed, the starting point A in Fig. 26 of an equilibrium polygon is found, which polygon is the reciprocal of a

force polygon with a pole distance equal to the horizontal thrust aq, Fig. 27, viz.: ap parallel to AI, Fig. 26; a–I–II, Fig. 27, parallel to I–II, Fig. 26, etc.

(b) General Method for Finding the Location of the Resultant of the Components.—A pole P is chosen arbitrarily in Fig. 27, and a reciprocal polygon is drawn in Fig. 26 between the components 1 to 16, viz., Pa, Fig. 26, parallel to Pa, Fig. 27; Pb, Fig. 26, parallel to Pb, Fig. 27, etc.

The intersection of the end rays Pa and Pp in Fig. 26 produces a point through which passes the resultant of all the components from 1 to 16, and a line is drawn through this point parallel to ap of Fig. 27. The resultant thus found is the same as the one found by the former method.

This method is general in its application, and in dealing with maximum and minimum stresses its use will be further described.

(c) Analytical Computation.—If it is desired to treat the arch analytically, the point of intersection A in Fig. 26 may be found by computing the ordinates c_0, c_1, and c_2 from the equations (152) and (153) of the Appendix; the horizontal thrust for each of the forces I, II, etc., may then be measured from Fig. 27 or may be computed (see Fig. 23).

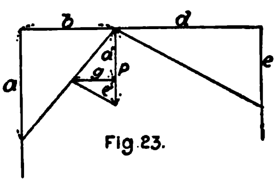

Fig. 23.

The values of a, b, d, and e are given; $b+d$ = length of span, and a and e are obtained from the equations for c_1 and c_2; $e'+a'$ = the force P, and g is the horizontal thrust caused by P.

$$a' : a = g : b,$$

and

$$e' : e = g : d; \quad \text{also} \quad e' = P - a'.$$

$$\therefore \; P - a' : e = g : d,$$

or

$$a' = P - \frac{eg}{d},$$

and this substituted in the first equation gives

$$g = \frac{Pbd}{be + ad} = \text{horizontal thrust of } P.$$

An arbitrary point is now assumed, the most convenient one being L in Fig. 26, and the horizontal thrust multiplied by its distance from L is computed for each force I, II, etc.; these products are added and the total is divided by the sum of all the horizontal thrusts of the forces from I to XVI, the resulting quotient being the distance from L at which the total horizontal force is applied, viz., the point A; from this as a starting point the polygon may be

drawn or computed. For a complete analysis see Appendix; for an analytically computed example see "Syra Valley Bridge," in the latter part of this chapter.

If the analytical method is to be applied throughout, Fig. 27 gives all the data necessary. The location being known of the points p and q and of all the intermediate points of the forces from I to VIII on the line pq in relation to the pole a, if the same methods which are applied in computing a survey are followed, the intersection points (of Fig. 26) on the vertical forces from I to VIII will be determined.

From the foregoing explanation it will be clear that *the line of pressure in the arch is not an arbitrary line* passing through the middle third of the arch, or which is drawn according to any other arbitrary assumption, but is a true line of pressure defined by the static law of forces and the elastic law governing the material.

For the analytical computation of the starting point A in Fig. 26, the horizontal thrusts of the forces I, II, etc., are preferably used, because they are parallel forces. These parallel forces can also be employed in the graphical method, but their use involves two sources of inaccuracy, viz.: the horizontal thrusts of all the forces from V to XVI are located closely together on the drawing, and the horizontal thrusts of the forces I and II are located outside of the drawing; the first of these will produce an inaccurate reciprocal polygon, and the second makes its starting point and end rays indeterminate.

When the left-hand components are used, as shown in Fig. 26, the resultant component 1 . . . 16 can be found with great accuracy.

In using the reciprocal polygon in the following computations, no intersection of its lines, such as Pa and Pp, should be obtained by prolonging these lines in Fig. 26, except for a point of location; and Fig. 27 should always be referred to for the direction of these lines.

(*d*) LIVE LOADS (Figs. 28 and 29).—In Fig. 29 the components 1 to 16 and the reactions 1′ to 8′ of the live load are added, as explained in Chapter II. To obtain their magnitude a larger unit of forces should be taken than is used for the dead load. (A good ratio to use is a unit for the live load which is five times as large as that for the dead load.) With the pole P' the reciprocal polygon of the live-load components is drawn, as previously explained, and with the pole P'' the reciprocal polygon of the live-load reactions may be constructed; in most cases, however, this is not necessary. (The letters and numerals in Figs. 28 and 29 correspond.)

Maximum and Minimum Stresses.—The distribution of the stresses in the arch rib when the position and magnitude of the resultant component are known, has been already partially treated, and Chapter V is specially devoted to this subject. In Fig. 26 the lines of pressure in the arch (from the dead load) are shown as rays of a reciprocal polygon, viz., AI, I–II, II–III, etc.

Now, at the sections A and I, the center of pressure is at the greatest distance (eccentricity) below the axis of the arch, and at

D the maximum eccentricity is above it; these are the weakest sections, and any forces which tend to displace the center of pressure farther down at A and I and farther up at D, will increase this weakness.

Section at A (Fig. 26).—Here f indicates the upper third of the arch rib and g the lower third; any force passing below f will increase the pressure in the arch at h, and any force passing below g will exert tension at i.

In Fig. 30 a tangent has been drawn through the point f to the curve JK, which tangent intersects the intersection locus LM at the point Af. All the components to the left of this point pass below f and will increase the compression at h, and the points I to VII are loaded. The point Ag is the separation point for the point g at the section A, etc.

Road-Roller.—With the road-roller placed at III in Fig. 28, its component will pass the farthest below either f or g, and the magnitude of the component will be the largest. (In order to avoid confusion, the tangent is not drawn in Fig. 28.)

Maximum Compression.—I to VII Loaded with Live Load.—In Fig. 29 the resultant of the components 1 to 7 is ah; in the reciprocal polygon Fig. 28 the rays $P'a$ and $P'h$ intersect at q', and a line is drawn through this point parallel to ah in Fig. 29. In Fig. 28 this line is drawn to an intersection with the component of the dead load AI.

In the same manner the resultant for the loads at I . . . VI has been obtained by drawing a line through the point q'' in Fig. 28 parallel to the line ag in Fig. 29.

From Fig. 26 the resultant AI of the dead-load components 1 to 16 has been transferred to Fig. 28a, and also the live-load resultant of the components from 1 to 7; the magnitude and location of the following forces are then known:

The dead-load resultant, AI;

The live-load resultant (of 1, 2, 3, 4, 5, 6, and 7);

The road-roller.

In Fig. 27 from the point p is drawn a line ps parallel to the line ah in Fig. 29. In Fig. 27 from the point s is drawn a line rs parallel to the component 3 in Fig. 28a (representing the road-roller component), and the line connecting p with r in Fig. 27 is equal to the resultant of the live load and the road-roller combined. In Fig. 28a the resultants of the live load and the road-roller intersect at p, and this point of intersection happens to be also a point of intersection of the dead-load resultant AI.

In Fig. 27 the dead-load resultant is equal to ap, and a line connecting the point a with the point r is equal to the resultant of the live load, the road-roller, and the dead load; and a line ps in Fig. 28a drawn parallel to ar gives the location and direction of this resultant. This line ps has been left out of the drawing to avoid confusion.

(*e*) Temperature and Secondary Stresses.—In an earlier article it was explained how the compression in the arch tends to shorten it and consequently has the same effect as a decrease in temperature.

The horizontal thrust caused by temperature changes acts in a horizontal line at two-thirds of the rise of the axis [for analysis see Appendix, equations (164*a*) and 164*b*)], and its magnitude is expressed by the equation

$$H_t = \frac{45EItw}{4f^2}.$$

The secondary stress

$$H_s = -\frac{45nI}{4f^2}.$$

In these equations

E = modulus of elasticity (for concrete 1:2:4, and the stresses caused in this arch, E = 2,000,000, approx.);

n = stress per square inch above erection stress (usually the stress caused by live load, temperature, and secondary stress);

t = degrees F. above or below normal (in this case assumed as 20° on account of the great mass of material in the structure);

w = coefficient of expansion and contraction for concrete $= \frac{1}{150,000}$;

I = average moment of inertia of a unit width of arch (12 ins.) expressed in inches;

f = rise of the neutral axis in inches.

In this case the secondary stress exerts a horizontal thrust of 700 lbs., and the temperature a thrust of 3,000 lbs.

(*f*) All the forces have been redrawn in Fig. 28*a*.

The line *ps* is (as previously determined) the resultant of all the loads and intersects *NO* at *s* (*NO* is the location of the temperature thrust). In Fig. 27 the horizontal thrust caused by the secondary stress is represented by the line *at*, a decrease in temperature by the line *tu*, and an increase in temperature by the line *tv*. The line joining *r* and *v* gives the stress in the hottest weather, and the line joining *r* and *u* gives the stress in the coldest weather; and drawing in Fig. 28*a*, through the point of intersection *s*, a line parallel to *ru* or *rv* of Fig. 27 gives the location of these stresses. In Fig. 28*a* these two forces are indicated by the same letters—*rv* and *ru*.

Minimum Stress in Upper Fibers of the Arch.—In Fig. 28 the line through q'' is again found as the resultant of the live load (for the loads from I to VI), and it intersects the road-roller component at R' in Fig. 28*b*. In Fig. 29 *ag* is the resultant of the live-load components 1 to 6, and is transferred to Fig. 27 as ps'; here it is combined with the road-roller component $r's'$, giving the resultant pr', and in Fig. 28*b* the line $R'p'$ is drawn parallel to pr' in Fig. 27. This line in-

tersects the dead-load resultant AI at p', etc. All the forces are shown in Fig. 28*b*, the final results being the forces $r'v$ and $r'u$, both obtained in the same manner as described for Fig. 28*a*. If in Fig. 27 the resultant of all the loads is combined with the horizontal thrust caused by secondary stress and highest temperature, $r'v$ will be the total stress; the figure shows, however, that $r'v$ will practically coincide with rv and will be less in magnitude by the distance $r'r$; also, in Figs. 28*a* and 28*b*, this line will closely coincide with rv and cause less stress in the extreme fibers than rv; and therefore it will not cause maximum compression.

In the coldest weather the stress will be equal to $r'u$ (Fig. 27), and drawing a line parallel to $r'u$ through s' in Fig. 28*b* gives $r'u$. The section A will receive the greatest tensile stress per square inch from $r'u$, and the greatest compressive stress per square inch from ru, as the following figures will show.

Before finding the stress per square inch, the forces should be resolved into axial pressure and shear, since they are inclined considerably downward toward the plane of section; this has been done in Fig. 27, and (for section A)

ru = 107,200 lbs. compression and 25,600 lbs. shear.
$r'u$ = 105,600 " " " 25,700 " "
rv = 112,900 " " " 23,300 " "

(*g*) Distribution of the Stress Over the Cross-Section.—(See also Chapter V.)—In the following illustration the arch rib is assumed to be of concrete mixed in the proportions 1:2:4.

Depth of arch rib = 56 ins. . . . . =	4.66 ft.
The axis of the arch rib is distant from the upper side of rib (4.66 ÷ 2)	2.33 "
rv is distant from the upper side of the rib . .	2.66 "
ru " " " " " " " " " . .	3.10 "
$r'u$ " " " " " " " " " . .	3.12 "
Sectional area of arch rib = 56×12 . . . . =	672 sq. ins.

If the force acts in the axis of the arch the stress per sq. in. will be equal to the force divided by the area.

	rv	ru	$r'u$
Intensity of the force, in lbs.	112,900	107,200	105,600
Compression per sq. in., in lbs.	168	159.5	157
Eccentricity of the force, in ft.	0.33	0.77	0.79
" expressed in terms of the depth of arch rib as a unit (0.33 ÷ 4.66, etc.)	0.071	0.165	0.17
Unit stress in lower fibers (see Chap. V, Art 3) (6×0.071)+1 . . . . =	−1.426	−1.99	−2.02
Unit stress in upper fibers (−2+1.426) . . . . =	−0.574	−0.01	+0.03
Max. compression in lower fibers, in lbs. per sq. in. (168×1.426, 159.5×1.99, and 157×2.02) . . =	−239	−318	−311
Max. stress in upper fibers, in lbs. per sq. in. (168×0.574, etc.) . . . . =	− 97	− 1	+ 3

These figures show that the increase in the eccentricity of the force caused by temperature changes is an important factor in the computation.

If the maximum shear for concrete is assumed as 50 lbs. per sq. in., then the concrete can safely resist a shear of 33,600 lbs. and the maximum shear at this section will be 25,700 lbs.; the dimensions of the arch rib are therefore sufficient to resist the shear and are well inside the safe limit. The arch rib could be reduced in depth at this point, but such a procedure would detract from its esthetic appearance.

(f') SECTION D, FIG. 30.—All the forces to the left of the point Df will cause maximum tension in the lower fibers, and all the forces to the left of the point Dg will cause maximum compression in the upper fibers of the arch. The eccentricity of the dead-load resultant III–IV in Fig. 26 is above the neutral axis of the arch, and the magnitude of the live load is only a small fraction of that of the dead load; for this reason no form of loading could cause the eccentricity of the resultant of all the forces to shift below the neutral axis.

The computation for determining the maximum tension is not shown in the diagrams, as the resultants of all the forces in the two forms of loading are nearly alike in value, and the computation lines would only confuse. The force VII comes very close to the neutral line Dg in Fig. 30, and the computation will show that, whenever this is the case, it makes no difference in the maximum stress whether this load is included in the computation or left out of it; the two following forms of loading are used in the computation:

I, II . . . VI loaded, and
I, II . . . VII loaded.

I *to* VI *loaded.* (See Fig. 28.)—The reactions $1'$, $2'$, $3'$ and the components 4, 5, 6 are in the section.

In Fig. 29 the resultant of the components 4, 5, 6 is a line joining the points d and g. At d the ray to the pole P' is dP', and at g it is $P'g$. Drawing lines parallel to these rays in Fig. 28 produces the intersection point Q, which is also the point of intersection of the resultant of the three components; and drawing through this point a line parallel to the line dg in Fig. 29 gives the location and direction of this resultant.

For the reactions $1'$, $2'$, $3'$ the same construction may be followed, but Fig. 28 will show that all the reaction lines from I to VIII are drawn as tangents to the curve $K'J'$, and the tangent points of all these forces differ very little; and no error is made by drawing the resultant of these forces as a tangent to the curve $K'J'$. Fig. 29 gives the resultant of these three reactions, and drawing in Fig. 28 a line tangent to the curve $K'J'$ and parallel to $1'$, $2'$, $3'$ of Fig. 29, gives the location and direction of this resultant.

This line intersects the resultant of the components at T. In Fig. 29 the reactions are added to the components, viz., the line

ge' is added to the line *dg*, and the line *e'd* gives the magnitude and direction of the resultant of these forces; and drawing in Fig. 28 a line through *T* parallel to *e'd* of Fig. 29 gives the location and direction of this force.

The point *T'* in Fig. 28 is found in the same manner to be the intersection point of the resultant when the points I, II, ... VII are loaded.

Road-Roller.—When the road-roller is placed at either I, II, or III, the reaction is in the section, and the comparative values of these reactions can be judged from Fig. 29, in which 1' is very small and 3' the largest, while their distances from the core point *f* differ but slightly; when the road-roller is placed at III it will give the largest value of these three positions. If the road-roller is shifted still farther to the right, its component will be in the section, and if it is placed at either IV or V, the comparative value of each component can be judged from Fig. 29; when placed at V, the magnitude of the component is the largest. But, as Fig. 29 shows, the difference between components 4 and 5 is relatively small, and, as Fig. 28 shows, the distance from the component 4 to the core point *f* is a great deal larger than the distance from *f* to component 5; consequently, of the two positions of the road-roller, that at IV will give the larger value.* The two following positions have to be investigated:

Road-roller at III and the reaction in the section;

Road-roller at IV and the component in the section.

The relative intensity of 3' to 4 is as 4:9.5.

The relative distances from 3' and 4 to the point *f* are as 6.3:2.7, and the road-roller placed at III will cause the greatest stresses in the extreme fibers of the arch.

Though the moments of both forces with respect to the point *f* are nearly alike, the reaction deflects upward from the neutral axis at the section, the component deflects downward, and the final resultant is drawn from an intersection point to the right of section *D*.

When the road-roller is placed at III, its reaction (see Fig. 28*c*) intersects the live-load resultant at V.

The dead-load,† the temperature, and the secondary-stress resultants have been transferred from Fig. 27 to Fig. 27*c*, viz.: *ap''* is the dead-load resultant, *vt* an increase in temperature, *tu* a decrease in temperature, and *at* the secondary stress.

At the point *p''* is added the live-load resultant *p''s'''*, and at the point *s'''* is added the road-roller reaction *s'''r'''*; and the line connecting *p''* with *r'''* is the resultant of these two forces, and drawing in Fig. 28*c* a line *SV* through the point *V* and parallel to *p''r'''* gives its location and direction. This resultant intersects the temperature and secondary thrusts *NO* at *S* in Fig. 28*c*.

Rise (or Fall) in Temperature.—In Fig. 27*c* the final resultant of

* The reader can draw pencil lines on the diagram. No lines are drawn, as they would only make the figure confusing.

† The dead load is resolved last in order to avoid parallel forces.

all the forces will be the greatest at the highest temperature, viz., the line joining the points v and r'''; the eccentricity of the dead-load resultant is above the neutral axis, and Fig. 27*c* shows that the line $r'''v$ tends to increase this eccentricity; and the line connecting u with r''' is not only shorter than $r'''v$, but will also tend to lessen the eccentricity, and maximum stress is caused during the highest temperature.*

In Fig. 28*c* the temperature is combined with the force SV, viz., the line SW'; the resultant of these combined forces intersects the dead-load force at W', which is the point where the resultant of all the forces intersects, and a line should be drawn through this point parallel to the line vr''' of Fig. 27*c*.

The point W is obtained in the same manner, and the magnitude and direction of the resultant are given in Fig. 27*c*, viz., the line vr''.

(g') Stresses in the Arch at Section D.—The results of the three forms of loading are as follows:

a. I to V loaded; total force, 94,200 lbs.; eccentricity above the axis, 0.7 ft., or in units, $\frac{0.7}{2.5}=0.28$.

b. I to VI loaded; total force, 95,400 lbs.; eccentricity above the axis, 0.69 ft., or in units, $\frac{0.69}{2.5}=0.276$.

c. I to VII loaded; total force, 96,900 lbs.; eccentricity above the axis, 0.67 ft., or in units, $\frac{0.67}{2.5}=0.268$.

The height of the arch rib is 2.5 ft. (30 ins.), its width 1 ft. (12 ins.), and its sectional area = 360 sq. ins.

If there were no eccentricity, the pressure per square inch would be (section D):

$$\begin{aligned} a.&—\ 94{,}200 \text{ lbs.} \div 360 = 262 \text{ lbs.} \\ b.&—\ 95{,}400 \text{ ''} \div 360 = 265 \text{ ''} \\ c.&—\ 96{,}900 \text{ ''} \div 360 = 269 \text{ ''} \end{aligned}$$

The stress (in units) is divided as follows:

$$\begin{aligned} a &= (0.28\ \times 6)+1 = -2.68 \text{ units minus } 2 = +0.68 \text{ unit} \\ b &= (0.276\times 6)+1 = -2.656 \text{ '' '' } 2 = +0.656 \text{ ''} \\ c &= (0.268\times 6)+1 = -2.608 \text{ '' '' } 2 = +0.608 \text{ ''} \end{aligned}$$

The stresses per square inch in the extreme fibers are:

a.	Upper fibers:	$2.68\ \times 262 = -704$ lbs.	Lower fibers:	$0.68\ \times 262 = +180$ lbs.
b.	" "	$2.656\times 265 = -704$ "	" "	$0.656\times 265 = +174$ "
c.	" "	$2.608\times 269 = -703$ "	" "	$0.608\times 269 = +165$ "

An arch with such stresses is dangerously weak and should therefore be reinforced; more is said on this subject in Chap. V.

* The intersection point from which the final force is drawn is W', which is located at the right of the section.

(f'') AND (g'')—SECTION AT I.—In Fig. 30 f indicates the upper third and g the lower third. The reactions $1'$, $2'$, . . . $8'$ and the components 9, 10, 11, . . . 16 are in the section. The dead-load pressure VIII–IX in Fig. 28 passes below the axis of the arch (see Fig. 30); all forces passing below f cause compression in the lower fibers, and all forces passing below g cause tension in the upper fibers of the arch rib.

Maximum compression is caused, as previously explained, by the reactions $1'$, $2'$, $3'$, $4'$, $5'$, and $6'$, and the components 11, 12, . . . 16; the road-roller is placed at XIII.*

The resultants are obtained as before, and are drawn in Figs. 27*d* and 28*d*; the dead-load stress is also drawn in these figures. The road-roller component is combined with the live loads, and the resultant of these forces intersects the dead-load resultant at V′. The magnitude and direction of the resultant of the live load, the road-roller, and the dead load are those of the line ar^{IV} in Fig. 27*d*, and drawing a line parallel to ar^{IV} through V′ in Fig. 28*d* gives the location, direction, and magnitude of the resultant of these forces, all as formerly described. V″ is the point of location of the resultant of all forces that will cause maximum tension in the top of the arch rib.

These forces are combined with the secondary stress and the highest temperature stress NO by the moment method, resulting in vr^{IV} and vr^{V} in Fig. 27*d*. All the numerical values are inserted in Fig. 28*d*, and no further explanation is needed. vr^{IV} causes a compression of 691 lbs. per sq. in. in the bottom fibers, and a tension of 81 lbs. per sq. in. in the top fibers.

These figures indicate that the dimensions of the arch rib of a stone, a brick, or a concrete arch should be increased.

The foregoing completely outlines the method for determining the maximum stresses in the hingeless arch rib which are caused by vertical forces; the following additional notes thereon, however, may not be out of place. (See Influence of Change of Form.)

Maximum and Minimum Stresses.—The determination of the maximum and minimum stresses in the arch rib differs in this respect from methods thus far in vogue: that the eccentricity of the dead-load pressure in the arch rib above or below the neutral axis is the starting point of the investigation.

This results from the fact that the stresses caused by the live load are very small as compared with those caused by the dead load, and are, for this reason, able to cause only a relatively small increase in the intensity of the pressure; they are, however, able to increase

* The road-roller can shift its position over a considerable distance without materially influencing the stresses in the arch, and a close investigation for the purpose of ascertaining the position which causes maximum stresses is therefore unnecessary.

the eccentricity of the point of application of the total load to a greater degree, and increased eccentricity is equivalent to increased stress in the extreme fibers of the arch.

One of two forms of loading will produce a maximum stress; but which of the two will yield the larger can only be found by trial, because the resultant of all the forces shifts up and down according to the manner of loading. This graphical method presents a survey of all the work performed, indicating instantly to the eye the causes of maximum stresses, and the locations of the weakest points.

It also shows that the application of the elastic theory to the computation of stresses in the hingeless stone arch is simple and offers much less difficulty than any other method. This is one of the purposes of the present work; because, notwithstanding its accuracy and the able analyses in which Winkler, Müller-Breslau, Mohr, Melan, and others have presented it, the elastic theory finds only a limited application on account of its intricacy.

Various methods for finding the stresses in arches are extensively employed, which are more or less of an experimental character.

The one in which the reciprocal polygon is so balanced that its rays are confined to the middle third of the arch rib is most favored. In this method one-half the span is loaded with live load, temperature and other stresses being generally neglected. This is known as the "one-third method."

The application of this method to the arch in the preceding example would indicate that the dimensions given to the arch rib were sufficient for concrete; the computation by the correct method, however, proves the arch to be weak.

The one-third method really makes an assumption and then proceeds to shape the computation to prove the assumption correct.

Though it may be true that the many factors which influence the erection of the arch will modify its stresses, it is, nevertheless, a rational method, employed in all engineering constructions, to first ascertain the true stresses exerted in a structure, and then make such allowances as are dictated by a regard for safety.

It is not the object of this work to condemn any method; on the contrary, for large arches the author has recommended at the beginning of this article the application of the one-third method for the preliminary determination of an approximately correct arch rib; and after that his method is to be applied for the purposes of determining the maximum stresses and of making such changes in the arch rib as may be indicated.

In making graphical computations of this nature a wooden straight-edge, at least 30 inches long, should be used, the sides of which are parallel and true; also one large triangle (about an 18-inch) and several smaller ones,—all absolutely true.

Do not use a steel straight-edge or a parallel ruler—the one is too heavy, and the other too unreliable to produce accurate work.

3. Horizontal Forces Acting in a Longitudinal Direction.—These may be caused by the wind pressure on a roof or by the spandrel filling on a bridge.

As previously explained, the intensity of either of these forces is rather indefinite. This is especially true of the conjugate pressure of the spandrel filling, as its intensity may vary from zero to a maximum caused by hard-packed damp fill. To make the computation of stresses possible, some assumption regarding probable earth pressure should be made, the usual one being the average between two forms of earth pressure. This assumption seems reasonable and is made the basis of the following computations.

One form is determined by considering the pressure of loose earth against the vertical projection of the extrados.*

The other form is determined from the abutting pressure of damp earth packed against the same area.

Rankine gives for the pressure of loose earth:

$$p=qh\,\frac{1-\sin a}{1+\sin a}; \quad . \quad . \quad . \quad . \quad . \quad . \quad . \quad . \quad (a)$$

and for the abutting pressure of packed earth:

$$p'=qh\,\frac{1+\sin a}{1-\sin a}. \quad . \quad . \quad . \quad . \quad . \quad . \quad . \quad . \quad (b)$$

In these equations, p = the pressure per square foot of vertical projection; h = the depth in feet of the center of the pressed vertical surface below the top of the fill; a = the angle of the natural slope of the earth with the horizontal (usually assumed as 30°; sin a = 0.5); q = the weight per cubic foot of earth = 120 lbs.

In Fig. 25 the pavement was assumed as 1 ft. thick and weighing 150 lbs. per cubic foot.† This should be reduced to the weight of earth, or 1 ft. is increased to $1\times\frac{150}{120}=1.25$ ft.

The same panel division made in Fig. 25 has been adhered to in Fig. 32, and aa' equals the vertical projection of the surface ab which is subjected to the earth pressure I′; its point of application is the point a'', and the height of the earth causing the pressure is equal to $a''a'''$. For the surface bc the vertical projection equals bb', the depth of the resultant earth pressure equals $b''b'''$, and the pressure equals II′, etc. The numerical values have been inserted in the figure, viz., $aa'=1.6$ ft., $a''a'''=11.25$ ft., etc. All com-

* Some engineers use the first form only; which of the two methods should be followed depends largely on conditions and the character of the filling material.

† Only for arches supporting a high bank or for arches with a large rise should the earth pressure be computed. In flat arches, such as the one used in the illustration, earth pressures are neglected, the computations being made only to show the method used.

119

tc.,

.bs.

ing

.II'
)9

the
5),
ent
sed
hat
to
ich

ich
/er,

her
ırly
'om

rib
31;
de-
om-
less

the
fer-
ted

ntal

3.
These
filling
As
is ratl
of the
mum
of str
sure s
forms
made
Or
earth
Tl
damp
Ra

and f

In
proje
surfa
the e
q=th
In
150 l
earth
Tl
in Fi
which
is the
is equ
bb', t
press
in th

* S
follow
† C
should
in the
only t

putations are made for an arch 1 ft. wide, and 1.6 ft., 2.25 ft., etc., are then the areas of pressure in square feet.

The average pressure per square foot is:

$$\frac{p+p'}{2}=\left(\frac{1}{3}+3\right)\frac{qh}{2}=\frac{5}{3}qh.$$

Now, $q=120$ lbs. and $\frac{p+p'}{2}=200h$, which is the pressure in lbs. per square foot of vertical projection of the pressed area. Calling this area F, then $Q=200hF$, and $F=1.6$ sq. ft., 2.25 sq. ft., etc.

Proper substitutions will give the following pressures in lbs.:

At	I′	II′	III′	IV′	V′	VI′	VII′	VIII′
	3,600	4,140	2,800	1,628	912	504	267	99

(*a*) The Standard Diagram and Its Use.—In computing the stresses in the arch caused by horizontal forces, equations (154), (155), and (156) of the Appendix * define the intersection locus and tangent curves of the standard diagram of Fig. 31. This diagram is based on the assumption that the axis of the arch is a parabola, and that the moment of inertia of the arch rib increases from the crown to the abutments in the same ratio as the secant of the angle which the axis makes with the horizontal.

Any other curvature of the arch axis produces a diagram which will differ from that shown in Fig. 31; this difference, however, is small and can be neglected. (See also Art. 6 of this chapter.)

Though the intrados of an arch may be elliptical, or of any other similar curvature, the axis of the arch is the line to be particularly considered, its curvature defining the loci, and its deviation from the parabola being relatively small, even in arches of large rise.

A considerable change in the moment of inertia of the arch rib will produce a diagram which will differ still more from that of Fig. 31; but, for the reasons given at the beginning of the article, this departure may be ignored and Fig. 31 be generally applied to the computation of the stresses caused by horizontal forces in a hingeless arch.

The course to be pursued in the computation is practically the same as that followed in the treatment of the dead load; such differences as are necessary to insure greater accuracy are specially pointed out in the following paragraphs.

---

* See also Appendix for the analysis of the stresses caused by horizontal forces in a hingeless arch.

Use of the Standard Diagram (Fig. 31).

Components of the Horizontal Forces.—In Fig. 31 the neutral axis of a hingeless parabolic arch rib ACB is shown. The horizontal forces (as Q) are assumed to act from right to left. The intersection locus is the line CF, and the tangent curve for the left-hand components is the line DE; the right-hand components all gather at the point E'.*

The rise of the neutral axis and one-half the length of span are each equal to unity; to obtain the curves for an arch of any rise or span, multiply the vertical ordinates of diagram by the rise of the neutral axis of the arch, and the horizontal ordinates by one-half the span of the arch. It will, however, rarely be necessary to do this, except in dealing with the wind pressure on a roof (where the pressure is exerted either on one side or the other side of the roof, but never on both sides at the same time).

The computer should draw for himself, once for all, on a large scale, the diagram shown in Fig. 31, using for the vertical ordinates a scale about twice as large as that for the horizontal ordinates.

To resolve (for example) the force Q into its components, the force line is prolonged to an intersection a' with the intersection locus; the right-hand component $a'a''$ is drawn to the intersection point E', and the left-hand component aa' is drawn tangent to the curve DE. If the force Q acts from left to right, the operation is reversed.

In Fig. 32 the forces I′, II′, etc., are the horizontal pressures caused by the earth fill against the arch ring, and, the arch being symmetrical, these forces are symmetrical with respect to the center line of the arch.

If in Fig. 31 the arch ACB were a free body subjected to two equal and opposite forces, Q, acting horizontally, these two forces would tend to bend the arch and bring the points A and B closer together, until this bending created (internal) forces in the *material* of the arch and formed a system of forces in equilibrium with the forces Q. The arch as a body would not move or change its position, all vertical forces caused by symmetrical forces Q would be in equilibrium and their resultant would be equal to zero.

Horizontal forces only remain, and the resultant of these must be a horizontal force. The arch is not a free body but is held rigidly at A and B, and the tendency of these points to come closer together is resisted by the abutments; from which it follows that *the resultant horizontal force must be in equilibrium with the resultant of the bending stresses created in the arch, and with the reactions at the abutments.*

---

* The intersection points of all the right-hand components lie so closely together on a curve tangent to DE that no appreciable error is involved in assuming them all to meet at E'.

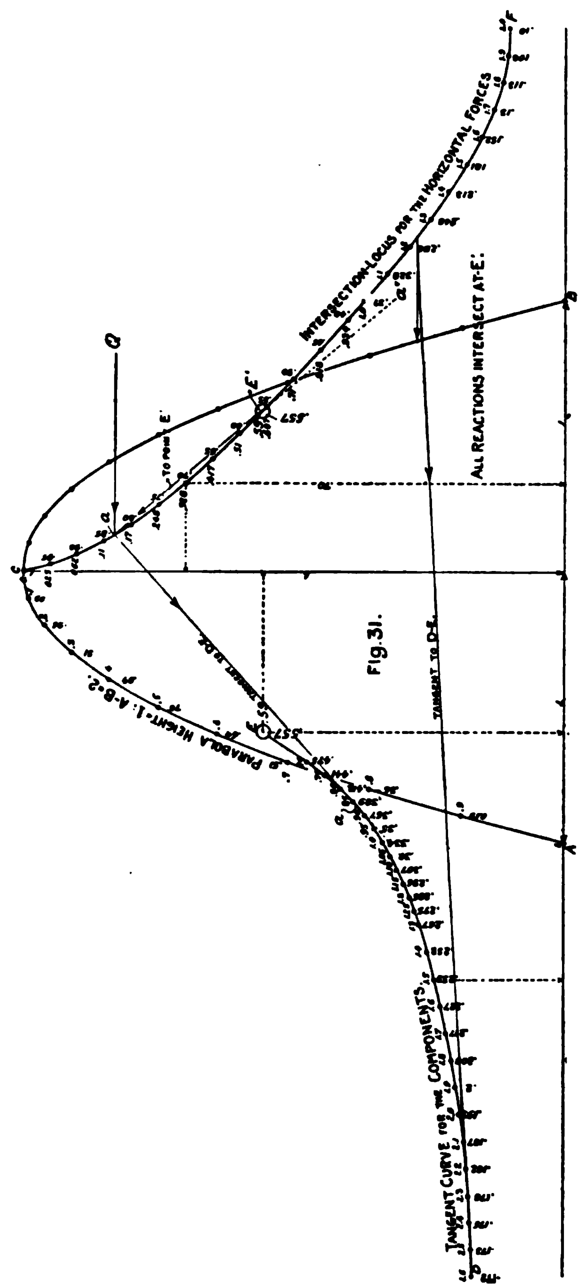
INTERSECTION-LOCUS FOR THE HORIZONTAL FORCES
ALL REACTIONS INTERSECT AT E.
TANGENT CURVE FOR THE COMPONENTS
TANGENT TO D-E
Q
E'

Fig. 31.

If more than one pair of symmetrical forces act on the arch, all these forces will have a horizontal resultant, and the location of this resultant above the horizontal axis AB will bear a certain ratio to the rise of the arch; and, so long as all vertical distances of the horizontal forces from the axis AB, the ordinates of the neutral axis, the loci, and the tangent curves are increased or diminished in the same proportion, the ratio will not change.

If the loci and tangent lines in Fig. 32 were plotted to correspond to a rise of 11.7 ft. and a span of 105 ft., the components of the horizontal forces would make a very small angle with the horizontal; and to determine with any degree of accuracy the intersection point of the two components into which each horizontal force is resolved, would be impossible. This would render the computation ineffectual. The ratio mentioned above, however, will obviate this difficulty.

The ordinates of all the horizontal forces in Fig. 32 are measured and plotted on the line xx of Fig. 33. The points C and C' are joined by a straight line, and lines are drawn parallel to CC' through the points I′, II′, etc., the points of intersection of these lines with the line CG being the ordinates for the proportional location of the horizontal forces.

Fig. 33 is a duplicate of Fig. 31, in which the intersection points I, II, etc., of the horizontal forces with the intersection locus only are indicated. The point E is the gathering point of all the left-hand components of the horizontal forces which act on the left side of the arch, and the curve $E'D'$ is the tangent curve for the right-hand components of these same forces. The curve ED is the tangent curve for the left-hand components of the horizontal forces acting on the right side of the arch, and the point E' is the gathering point for the right-hand components.

(*b*) Computation of the Resultant of the Left-Hand Components.—To obtain the relative magnitudes and directions of the components of the horizontal force XV, its intensity is plotted from the intersection point b (which the horizontal force makes with the intersection locus) to the scale of forces; the line ac is drawn parallel to bD, which is tangent to the curve DE, and the line cb is drawn from the point b to the gathering point E'. The line ac is then equal to the relative magnitude of the right-hand component, and the line cb is equal to the left-hand component of this horizontal force. A perpendicular dropped from the point c divides the horizontal force into the left-hand horizontal thrust ad, and the right-hand horizontal thrust db; and the line cd is equal to the vertical reactions at the supports, these reactions being equal and opposite in direction.*

* The computation shows that so long as the ratio of the vertical ordinate of the point b to the rise CG does not change, the horizontal thrusts ad and db do not change, no matter what the rise of the arch may be. In dealing with

The magnitude of the left-hand component of the horizontal force II is equal to the magnitude of the right-hand component of the horizontal force XV. In the following computation only the left-hand components of the forces are needed. A line from II to the gathering point E gives the direction of the left-hand component of II, and cb gives its magnitude; for this reason the two components ac and cb are numbered 15 and 2.

In a similar manner the left-hand components of all the other horizontal forces are obtained and added together in Fig. 33*a*. In performing the addition notice should be taken of the direction in which the components act (the left-hand components of the forces I to VIII act from left to right, and those of the forces IX to XVI from right to left).

The resultant of all these components is the horizontal line HJ, and this resultant is held in equilibrium by the stresses in the arch.*

(*c*) LOCATION OF THE RESULTANT.—Assuming an arbitrary pole P and drawing in Fig. 33 a reciprocal polygon for the components from 1 to 16 will determine the intersection point L of the end rays PJ and PH; this is the point through which the resultant passes.

Fig. 33*a* gives the magnitude of the resultant as 7,880 lbs., and Fig. 33 gives its distance from the axis xx as $0.238\times$the rise $C_{,}G$, or 2.79 ft. for a rise of 11.7 ft.†

(*d*) RESULTANT OF THE EARTH PRESSURE AND THE ABUTMENT REACTION OF THE DEAD LOAD.—Fig. 26 gives the line AI as the location and direction of the abutment reaction of the dead-load components from 1 to 16, and this line has been transferred to Fig. 32; Fig. 27 gives the direction and magnitude of this resultant. The portion enclosed by the triangle apq of Fig. 27 has been reproduced in Fig. 32*a*.

In this latter figure the resultant of the earth pressure is plotted in its proper direction dp, and the line joining a and d gives the magnitude and direction of the resultant of both forces (or the reaction at the left-hand abutment). In Fig. 32 the two resultants intersect

---

wind pressure the actual magnitude of the components ac' and $c'b$ should be obtained. For this purpose the true intersection locus and tangent curves should be plotted to scale in Fig. 32 and the actual components drawn in this figure. If now the lines ac' and bc' are drawn in Fig. 33 parallel to these actual components, Fig. 32 will give their direction and location and Fig. 33 their magnitude,—which can now be measured with great accuracy.

* Assume the forces IX to XVI in Fig. 33 to represent the concentrated pressures at the panel points of the arch caused by the wind acting on the right side; then a straight line joining H and K, measured to the scale of forces, will be equal in magnitude and direction to the reaction at the left abutment. In the same manner a straight line joining J and K will give the direction and magnitude of the reaction at the right abutment on the exaggerated vertical scale employed; a reduction to the true scale should be then made.

† To obtain the components a piece of tracing-cloth is placed over the standard diagram (like Fig. 31), and upon this all the computations are made. Figs. 33 and 33*a* were drawn in this manner and will serve as a guide.

at E, and this is also the point of intersection of the total reaction. A line AE drawn through this point and parallel to the line ad in Fig. 32a gives the starting line of the reciprocal polygon in the arch of Fig. 32. In Fig. 32a the forces I, II, etc., are drawn parallel to the forces I, II, etc., in Fig. 32, and the polygon AC is drawn as previously described.

(*e*) Effect of Earth Pressure on the Arch.—From the very nature of its construction the force AI in Fig. 32 has increased in eccentricity and diminished in magnitude.

Fig. 32a shows that the resultant arch pressure in section II–III of Fig. 32 has not changed in location or magnitude, and also that the force III–IV has not changed its eccentricity but has increased its magnitude—not sufficiently, however, to appreciably affect the stresses previously obtained.

At the crown of the arch it is different; here the eccentricity has increased, and the magnitude of the force has increased by the distance qq', and for this point a new set of stress values will be obtained which are larger than those previously computed.

A comparison between Figs. 26 and 32 shows that the addition of the earth pressure has had the effect of increasing the curvature of the line of pressure in the arch from A to III, and has caused a decrease in the curvature from III to C, the two curves coinciding between II and III. This is due to the fact that in both figures the force II–III results from the same ray in the force polygon [viz., a–(II–III) of Fig. 32a], and if the line of pressure in the arch be transferred from Fig. 26 to Fig. 32 it will clearly show the effect of the earth pressure. The difference between the two lines, however, is too small to be clearly shown in the figure, and they are consequently omitted.

4. Influence of Change of Form on the Arch.*—In Figs. 26 and 32 the line of pressure AC is shown, and its rays AI, III–IV, and VIII–IX deviate considerably from the axis of the arch rib and cause very high stresses in the extreme fibers. The axis of the arch is a parabola, and the amount of the deviation in Fig. 26 is reproduced in Fig. 34, AB being the parabolic axis and $A'B'$ the line of pressure caused by the dead load. If the form of the arch could be changed so that the neutral axis and the line of pressure would coincide, and at the same time the area enclosed between the new neutral axis and the line AC were equal to the area enclosed by the parabola AB and the line AC, the intensity of the forces would not change materially, but the eccentricity of the line of pressure caused by the dead-load forces would become zero. But this, as Fig. 34

* In the Appendix will be found the analysis of the elastic theory as applied to hingeless arches, and various deductions therefrom are specially described in the following articles. (See Art. 7 of this chapter.)

This article shows the application of the author's method to the hingeless masonry arch; it is scarcely necessary to mention that it is equally applicable to the two- or the three-hinged arch of either steel or masonry.

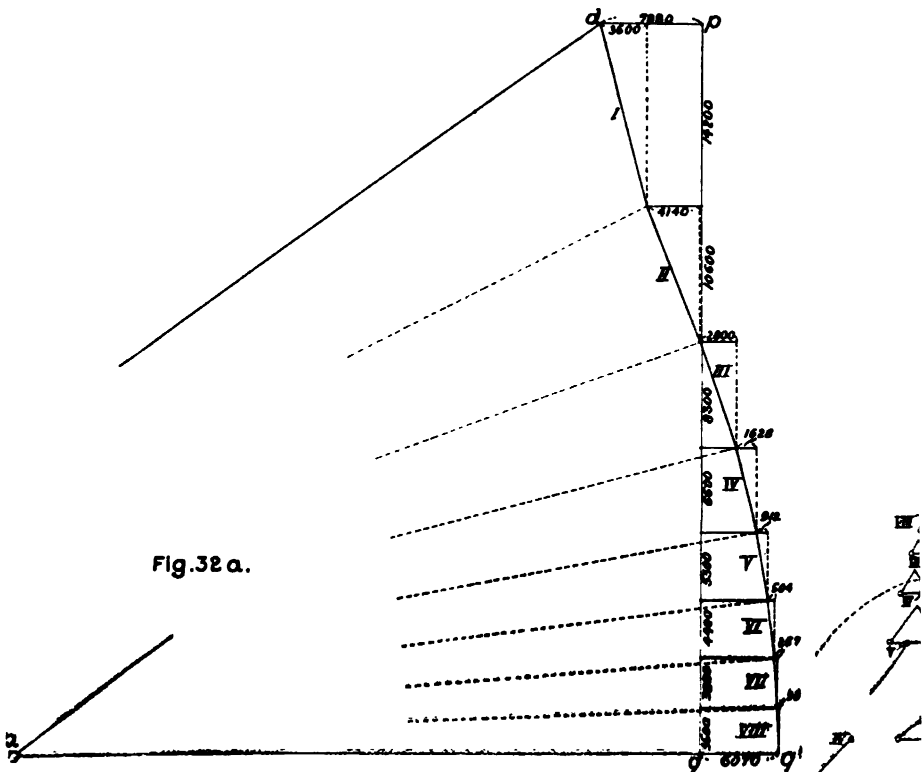

Fig.32 a.

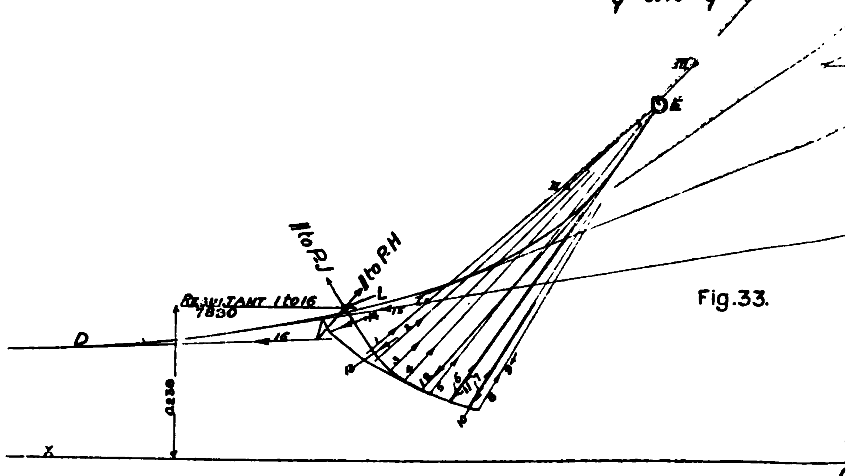

Fig.33.

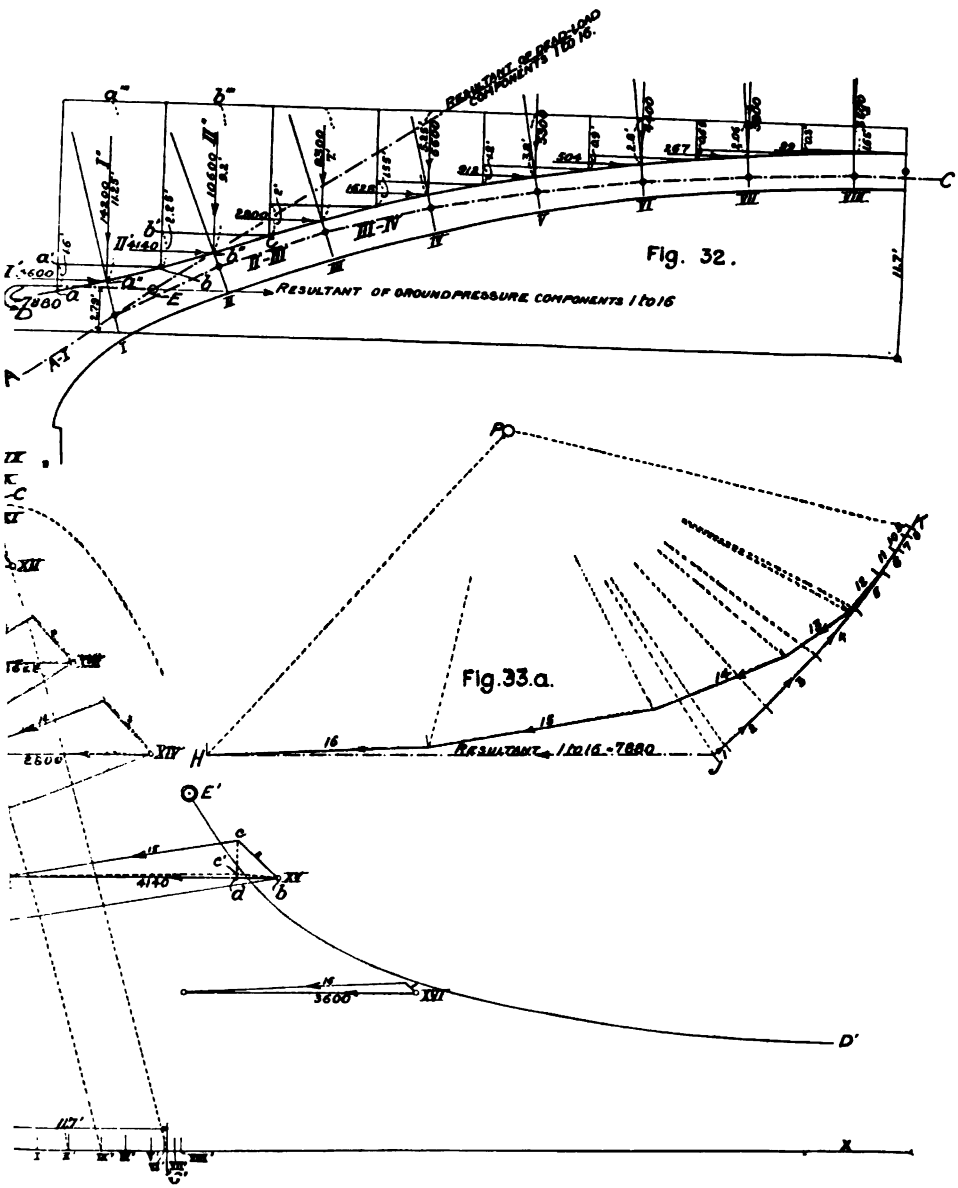

[To face page 124.

shows, is impossible. Previous computations, however, have shown that the maximum stresses in the extreme fibers of the arch rib are:

	Lbs. per sq. in.	
At section A:	-318	Lower
	$+\ 3$	Upper
" " D:	-704	"
	$+180$	Lower
" " I:	-691	"
	$+\ 81$	Upper

(*a*) At A the stress could be higher, but at D and I the stresses are too high and should be reduced. The next best change in form

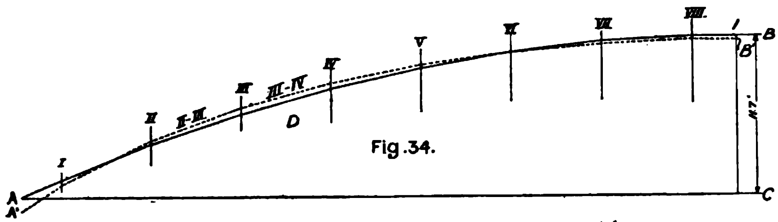

Fig.34.

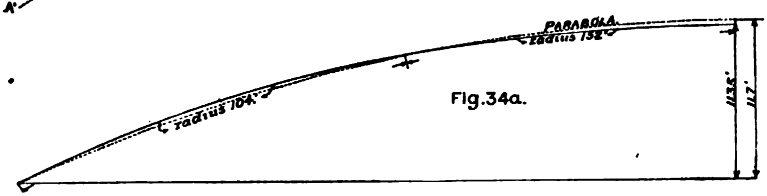

Fig.34a.

would therefore be to have the neutral axis coincide with the line of pressure at the point B' and at the force III–IV.

The area enclosed by this assumed neutral axis and the line AC should again be equal to the area enclosed by the parabola AB and the line AC. This result is not possible; but a line can be drawn which very nearly coincides with the given points and satisfies the second condition. This line will intersect the parabola at A, and the line of pressure at II, and thence pass below the line of pressure at the remaining points, the greatest eccentricity occurring near the point V.*

This neutral axis has been drawn in Fig. 34*a*, its rise is 11.35 ft., and it consists of two circular curves—with radii of 152 ft. and 104 ft., respectively. The equivalent parabola has been drawn as a dotted line.

The effect of this change on the stresses in the extreme fibers of the arch at the section I is as follows:—

The maximum stresses at the crown were 691 lbs. compression

* Railroad curves are very useful for drawing such lines.

per sq. in. in the lower fibers and 81 lbs. tension per sq. in. in the upper fibers.

These stresses change to 508 lbs. compression per sq. in. in the lower fibers and 102 lbs. compression per sq. in. in the upper fibers.

The height of the arch rib is 27 ins.*

These figures show clearly the effect of a change in curvature of the arch axis on the stresses in the arch; not only that, but they show the difference between the methods now used and the proposed method, viz., *instead of adapting the forces to the arch,* as is done in the one-third or any other method, *the arch is designed to suit the forces.*

This is a sound principle that should govern the design of any structure.

After the change in form has been settled on, a new computation of stresses can be made; but in most cases this is not necessary, when the change does not materially influence the distribution of the dead load.

To modify the arch axis of Fig. 32 so that it will approach as closely as possible to the line of pressure AC is not as difficult as the correction of Fig. 26. This latter has been left for the reader to determine, and it will give him an opportunity to test his comprehension of the method.

SYRA VALLEY BRIDGE.

5. Determination of the Intersection Locus and the Tangent Curves for the Hingeless Arch.—GENERAL METHOD.—In the foregoing articles the horizontal thrust is computed from an intersection locus and tangent curves which are drawn for a hingeless parabolic arch rib whose moment of inertia increases from the crown to the supports in the same ratio as the secant of the angle which the arch axis makes with the horizontal.

To illustrate the *general method,* the treatment of the hingeless arch which is given in the Appendix is here analytically and graphically applied to the masonry arch over the Syra Valley, near Plauen, Saxony. This is a rubble-masonry arch with a span of 300 ft. and a rise of 60 ft. The arch rib is 6 ft. deep at the crown and 13.33 ft. at the abutments. With the above-mentioned ratio applied to this arch rib its depth should be only 6.54 ft. at the abutments. The following computations will show that the tangent curves are strongly influenced by the wide variations in the moments of inertia of this arch rib.

It will also be seen that the computation of the intersection locus and tangent curves is laborious and complicated, and further that the form and dimensions of the arch must be assumed before any

* If the height of the arch rib were 24 ins., the stresses would be 602 lbs. compression per sq. in. in the lower fibers and 86 lbs. compression per sq. in. in the upper fibers.

computation is possible. The computation may show that the assumptions are greatly in error and that all the labor expended is, in consequence, useless. Add to this the intricate calculations necessary to obtain the intersection locus and the tangent curves, and it is not astonishing that the application of the elastic theory to the computation of stresses in hingeless masonry arches has found little favor with the profession. And yet the fact is admitted that it is the only theory whose use results in accurate and reliable dimensions.

If the intersection locus and the tangent curves are known at the beginning of the computation, the application of the elastic theory, according to the author's method, is no more laborious or intricate than any other method now in vogue for proportioning the arch. Preceding articles have shown this.

The factors which determine the ordinates of the locus and the tangent curves are:

1st. The curve of the arch axis.

2d. The variation in the moment of inertia.

If a simple correction be made to the diagrams shown in Figs. 24 and 31 so that these two variables are included as factors which define the ordinates of the lines mentioned, the application of the elastic theory changes from the most intricate and laborious to the simplest and clearest method for the computation of the stresses in arches.

How the author has arrived at this solution will be demonstrated in the following paragraphs. It hardly needs to be added that these paragraphs are also applicable to a metal arch.

(*a*) Computation of the Average Moments of Inertia.—Fig. 35 shows a longitudinal section of the Syra Valley Bridge, and the line ABC is its axis. For the analytical, as well as the graphical, method the arch of this figure is divided into twenty equal panels, the lines I, II, etc., representing the centers of these panels.

In Fig. 35*a* the area $AA'C'C$ represents the arch rib developed, AC being the length of the semiaxis, the points I, II, etc., in Fig. 35 corresponding with those in Fig. 35*a*.

To find the moment of inertia of the arch rib at the points I to X, the computation may be made analytically; the graphical method, however, is short and simple.

The moment of inertia of an arch ring 1 ft. wide is

$$\frac{13.33^3 \times 1}{12} = 197.5 \text{ ft.}^4 \text{ at } A,$$

and

$$\frac{6^3 \times 1}{12} = 18 \text{ ft.}^4 \text{ at } C.$$

Now assume the moment of inertia at A equal to unity; then the moment of inertia at $C=$

$$18:197.5 = 0.0913,$$

and the depth CC' of the arch rib expressed in units is

$$CC' = \sqrt[3]{0.0913} = 0.451.$$

The depth of the arch at $A = \sqrt[3]{1} = 1$, and the point D can be found by construction or from the two similar triangles $AA'D$ and $CC'D$, the ordinates measured from AD to the line $A'D$ representing the depth of the arch rib at I, II, etc., expressed in the unit AA'.

To find the square of the height CC', a line $C'A''$ is drawn parallel to AD, and the line $A''D$ is drawn to an intersection with CC', giving the point C''.

From similar triangles,

$$\frac{CD}{AD} = \frac{C'C}{A'A}; \quad C'C = A''A, \quad \text{and}$$

$$\frac{CD}{AD} = \frac{C''C}{A''A} = \frac{C''C}{C'C}; \quad \text{or}$$

$$\frac{C'C}{A'A} = \frac{C''C}{C'C}. \quad \text{Now} \quad A'A = 1,$$

$$\therefore \frac{\overline{C'C}^2}{1} = C''C.$$

In the same manner it is proved that

$$\overline{C'C}^3 = C'''C.$$

The same construction can be applied to the points I, II, etc., successively. The points so found are joined by the line $A'C'''$, and the ordinates of this line measured from the line AC represent the moments of inertia expressed in the unit $A'A$.

In Fig. 22*b* (Chap. III, Art. 18) was illustrated the method of obtaining the average moment of inertia. This same construction has been applied to Fig. 35*a*, and the ordinate measured from the axis AD to the line EF is equal to the average moment of inertia (I_0), expressed in the unit $A'A$.

For the purposes of the computations which immediately follow, the moments of inertia have been transferred to the panel lines I, II, III, corresponding to those of Fig. 35, and are indicated by small black circles.

When the analytical method is applied, a table like VII should be arranged (see end of chapter). The first line gives the values of the ordinates of the arch axis at the panel points I, II, etc.

The second line gives the values of the angle which each plane of section makes with the vertical at the panel points. The third line gives the angle of the curve for each panel, and the fourth the length of the curve in each panel.

In the fifth line is given the depth of the arch rib at each panel point, and in the sixth the moment of inertia at each panel point. (The average moment of inertia $=90.7$ ft.^{4})

(*b*) Graphical Computation of the Horizontal Thrust H.—*Vertical Forces.*—In the Appendix the following equations define the locus and tangent curves for vertical forces:

$$H=\frac{\int_{-\frac{l}{2}}^{+\frac{l}{2}}\frac{\mathfrak{M}}{I_{\prime}}y\,dx}{\int_{-\frac{l}{2}}^{+\frac{l}{2}}\frac{y^2dx}{I_{\prime}}+\frac{l}{F_0}}; \quad \ldots \ldots \quad (128A)$$

$$X_1=\frac{\int_{-\frac{l}{2}}^{+\frac{l}{2}}\frac{\mathfrak{M}}{I_{\prime}}x\,dx}{\int_{-\frac{l}{2}}^{+\frac{l}{2}}\frac{x^2dx}{I_{\prime}}}; \quad \ldots \ldots \quad (129A)$$

$$X_2=\frac{\int_{-\frac{l}{2}}^{+\frac{l}{2}}\frac{\mathfrak{M}}{I_{\prime}}dx+\frac{HB}{F_0r}}{\int_{-\frac{l}{2}}^{+\frac{l}{2}}\frac{dx}{I_{\prime}}}. \quad \ldots \ldots \quad (130A)$$

Also,

$$v_m=\frac{d_m}{6d_0}\frac{I_0}{I_{\prime}}(2y_m+y_{m-1})+\frac{d_{m+1}}{6d_0}\frac{I_0}{I'_{m+1}}(2y_m+y_{m+1}), \quad (131A)$$

$$v'_m=\frac{d_m}{6d_0}\frac{I_0}{I'_m}(2x_m+x_{m-1})+\frac{d_{m+1}}{6d_0}\frac{I_0}{I'_{m+1}}(2x_m+x_{m+1}), \quad (132A)$$

$$v''_m=\frac{1}{2}\frac{d_m}{d_0}\frac{I_0}{I'_m}+\frac{1}{2}\frac{d_{m+1}}{d_0}\frac{I_0}{I'_{m+1}}. \quad \ldots \ldots \quad (133A)$$

Substituting these latter values in (128*A*), (129*A*), and (130*A*) gives

$$H=\frac{\Sigma_0^l \mathfrak{M}_m v_m}{\Sigma_0^l y_m v_m+\frac{I_0 l}{F_0 d_0}}, \quad . \quad . \quad . \quad . \quad . \quad . \quad . \quad . \quad (135A)$$

$$X_1=\frac{\Sigma_0^l \mathfrak{M}_m v'_m}{\Sigma_0^l x_m v'_m}, \quad . \quad . \quad . \quad . \quad . \quad . \quad . \quad . \quad . \quad . \quad (136A)$$

$$X_2=\frac{\Sigma_0^l \mathfrak{M}_m v''_m+H\frac{I_0 B}{F_0 d_0 r}}{\Sigma_0^l v''_m}. \quad . \quad . \quad . \quad . \quad . \quad . \quad (137A)$$

Further, for the location of the axis *DD*,

$$y_2=\frac{\int \frac{I_0}{I_I} y' dx}{\int \frac{I_0}{I_I} dx}=\frac{\Sigma_0^l y'_m v''_m}{\Sigma_0^l v''_m}. \quad . \quad . \quad . \quad . \quad (138A)$$

Again,

$$\Sigma_0^l \mathfrak{M}_m v_m=\frac{l-g}{l}\Sigma_0^g x'_m v_m+\frac{g}{l}\Sigma_g^l (l-x'_m) v_m, \text{ etc.}$$

In Fig. 35 $d_m=d_0$, etc., all panel lengths being equal.

In the present example the following modifications of equations (131*A*), (132*A*), and (133*A*) will give sufficiently accurate results:

$$v_m=\frac{I_0}{I_I} y_m, \quad . \quad . \quad . \quad . \quad . \quad . \quad . \quad . \quad (131B)$$

$$v'_m=\frac{I_0}{I_I} x_m, \quad . \quad . \quad . \quad . \quad . \quad . \quad . \quad . \quad (132B)$$

$$v''_m=\frac{I_0}{I_I}. \quad . \quad . \quad . \quad . \quad . \quad . \quad . \quad . \quad . \quad (133B)$$

The first value to be computed is $\frac{I_0}{I_I}$ (see Fig. 35*a*). For instance, to obtain the value of $\frac{I_0}{I_I}$ at the panel center X, a panel length *be*

may be made the unit, and the line ad be drawn parallel to the line ce. From similar triangles,

$$bd = be\frac{ab}{bc}.$$

Now, be is the unit, $ab = I_0$, and $bc = I_{\prime}$;

$$\therefore\ bd = \frac{I_0}{I_{\prime}}.$$

The point d has been transferred to d' on the panel center X.

In the same manner the remaining values of $\frac{I_0}{I_{\prime}}$ have been computed, and the upper points on the ordinates are connected by the line $d'f$, the ordinates of which, measured from AD, represent the values of $\frac{I_0}{I_{\prime}}$ at the panel points when one panel length is the unit of measurement.

The values of $\frac{I_0}{I_{\prime}}$ have been inserted in the seventh line of Table VII.

The next value to be computed is that of y_2, or the distance of the axis DD from the axis AB (Fig. 35). From equation (138A),

$$y_2 = \frac{\Sigma_0^l y'_m v''_m}{\Sigma_0^l v''_m},$$

and from equation (133B),

$$v''_m = \frac{I_0}{I_{\prime}}.$$

If the moment of inertia is assumed to be a constant, it will disappear from the equation; and when numerator and denominator are multiplied by d_0, the numerator of equation (138A) will simply represent the sum of all the areas $= \Sigma y' d_0 =$ area ACB, and the denominator will represent the span $AB = \Sigma d_0 = l$, or, the value of the fraction will represent the height of a parallelogram which has the same area as the figure ACB.

In the above equation the variation of the moment of inertia appears as a factor in the fraction.

In either case the values of v''_m can be considered as horizontal forces acting in the axis of the arch, and the value of the numerator is equal to the moment of these horizontal forces with reference to the line AB.

The values of $\frac{I_0}{I_{\prime}}$ are given in Fig. 35*a* by the ordinates of the line $d'f$; these ordinates have been plotted as the forces of a force polygon in Fig. 35*b*, and, with a pole distance$=\frac{1}{2}\Sigma v''_m$, the reciprocal polygon AB has been drawn in Fig. 35*B*. The intersection of the first polygon segment between 0 and I with the vertical BD gives the point E. This is the point through which the resultant of all the horizontal forces passes, the line ED is then the height of the equivalent parallelogram, and the point E is the location of the axis DD of Fig. 35. It should be observed that in Fig. 35*b* the pole distance $AP=\frac{1}{2}\Sigma v''_m=AP'$, and the line PP' forms an angle of 45° with the line AP'. Now, in Fig. 35*B*, $AD=$one-half of the moment of all the forces v''_m, EA is parallel to PP' of Fig. 35*b*, and in Fig. 35*B* the line $ED=AD$; or

$$\Sigma_0^l\, y'_m v''_m = 2\times ED\times \tfrac{1}{2}\Sigma v''_m = \overline{ED}\Sigma v''_m,$$

or

$$y_2=\frac{\Sigma y'_m v''_m}{\Sigma v''_m}=\frac{\overline{ED}\Sigma v''_m}{\Sigma v''_m}=\overline{ED}=45.865 \text{ ft.}$$

The values of y can now be obtained by simple subtraction, and these values have been inserted in line 8 of Table VII—negative in sign when the ordinate is below the axis DD, and positive when above.

The value of v_m can be computed analytically or graphically, as follows: The point d is transferred from Fig. 35*a* to the axis DD of Fig. 35, and the line ad is drawn parallel to the line ce; from similar triangles,

$$ab=cb\frac{bd}{be}.$$

Now, $cb=y$, $bd=\frac{I_0}{I_{\prime}}$, and $be=1$;

$$\therefore\ ab=y\frac{I_0}{I_{\prime}}=v_m.$$

The values for v_m have been found in a similar manner for all the panel points, and lie on the line af in Fig. 35. These values have been inserted on the ninth line of Table VII.

The computation can here be checked, viz.: the sum of the ordinates of the line af above the line DD should be equal to the sum of the ordinates below the line DD.

The next value to be computed is that of equation (135*A*):

$$H=\frac{\Sigma_0^l\, \mathfrak{M}_m v_m}{\Sigma_0^l y_m v_m+\frac{I_0 l}{F_0 d_0}}.$$

In this equation $\Sigma_0^l \mathfrak{M}_m v_m$ is, as stated before (Art. 18 (*b*), Chap. III), the bending moment caused by the vertical forces v_m at a point x_i; $\Sigma y_m v_m$ is the maximum bending moment with relation to the axis AB caused by the horizontal forces v_m;

$$\frac{I_0 l}{F_0 d_0} = \text{a constant} = \frac{90.7 \times 300}{9.66 \times 15} = 188.$$

Computation of $\mathfrak{M}_m v_m$.—The ordinates of the line af of Fig. 35 measured from the axis DD have been plotted as vertical forces in the force polygon Fig. 35*c'*. Of these forces, 7, 8, 9, and 10 are positive, and 1, 2, 3, 4, 5, and 6 are negative, and the sum of the positive forces is equal to the sum of the negative forces (all of which is shown in Fig. 35*c'*). Now, with an arbitrary pole distance p, which is here chosen as equal to 80 ft., the reciprocal polygon ACB of Fig. 35C' has been drawn, and, for the load K placed at IV, the value of

$$\Sigma \mathfrak{M}_m v_m = \text{line } ab \times p.$$

Computation of $\Sigma y_m v_m$.—In Fig. 35*c* the forces v_m have been plotted as the horizontal forces of a force polygon with the pole distance p ($=p$ in Fig. 35$c' = 80$ ft.), and the reciprocal polygon ACB of Fig. 35C being drawn,

$$\Sigma y_m v_m = \text{line } AB \times p.$$

The constant was found on a preceding page to be equal to 188, and in order to plot the same it should be divided by the pole distance, or

$$188 \div 80 = 2.35,$$

which is equal to the distance $B_{\prime}B_{\prime\prime}$ and

$$\Sigma y_m v_m + \frac{I_0 l}{F_0 d_0} = \text{the line } A'B'.$$

For the panel point IV,

$$H = \frac{\Sigma_0^l \mathfrak{M}_m v_m}{\Sigma_0^l y_m v_m + \frac{I_0 l}{F_0 d_0}} = \frac{\text{line } ab \text{ of Fig. } 35C'}{\text{line } A'B' \text{ of Fig. } 35C}.$$

The horizontal thrust is given in a similar manner on the load line for any position of the load K, as the ordinates of the curve ACB of Fig. 35C', and these ordinates are to be divided by the constant value $A'B'$ of Fig. 35C.

(*c*) Analytical Computation of H.—Following this method the denominator of equation (135A) is found to be equal to 4,974 +188=5,162.

On line 13, Table VII, are given the values of $\mathfrak{M}_m v_m$ at the respective panel points, and on line 14 the values of H.

For example, a load of twenty tons placed at panel point VIII of Fig. 35 causes a horizontal thrust

$$H=20\times 1.1654=23.308 \text{ tons.}$$

(*d*) Computation of X_1.—The value of equation (136A) should now be found.

$$X_1=\frac{\Sigma_0^l \mathfrak{M}_m v'_m}{\Sigma_0^l x_m v'_m}.$$

From equation (132B),

$$v'_m=\frac{I_0}{I_1}x_m \text{ (see Appendix);}$$

x_m is measured from the center of the span, and its various values are represented in Fig. 35 by the ordinates of the line EF measured from the axis AB; EF forms an angle of 45° with the axis AB. These ordinates are reduced in the same manner as previously described, in the ratio $\frac{I_0}{I_1}$, resulting in the line GH.

The ordinates of this line GH have been plotted as vertical forces in the force polygon of Fig. 35d', and in Fig. 35D' the reciprocal polygon ABC has been drawn with the pole distance p'.

In the force polygon of Fig. 35d' the first ray AP should make an angle of 45° with the line AB; and to obtain a horizontal closing line AB in the reciprocal polygon ACB of Fig. 35D', a trial pole should be chosen in Fig. 35d'. From this force polygon a trial polygon can be drawn in Fig. 35D', and from this the true pole can be found in Fig. 35d'; the polygon ABC of Fig. 35D' can then be drawn, its end segment BD forming an angle of 45° with the line AB, and AD being equal to $\frac{1}{2}l$; or if the whole polygon be drawn, the length of the line which is intercepted by the end segments of the reciprocal polygon on the center line will be equal to $2\times AD=l$. The reason for this construction will be seen from the following:

For a load placed at IV′,

$$\Sigma\mathfrak{M}_m v'_m=\text{line } a'b'\times p_{\prime},$$

$$\Sigma x_m v'_m \ =2\times\text{line } AD\times p_{\prime}.$$

Now, $2 \times AD = l$; consequently

$$X_1 = \frac{a'b' \times p_l}{l \times p_l} = \frac{a'b'}{l}.$$

(e) Computation of X_2.—The value of X_2 remains to be solved:

$$X_2 = \frac{\Sigma_0^l \mathfrak{M}_m v''_m + H\dfrac{I_0 B}{F_0 d_0 r}}{\Sigma_0^l v''_m}.$$

From equation (133B) the values of $v''_m = \dfrac{I_0}{I_1}$ = the ordinates of the line fd' of Fig. 35a. These ordinates have been plotted as vertical forces of a force polygon in Fig. 35e', and with a pole distance $= \frac{1}{2}\Sigma v''$ the reciprocal polygon $A'C'$ of Fig. 35E' has been drawn. When a load is placed at IV, $\mathfrak{M}_m v''_m$ = line $a''b'' \times$ pole distance $\frac{1}{2}\Sigma v''$, and $\Sigma_0^l v''_m = 2 \times \frac{1}{2}\Sigma v'' = \Sigma v''$.

In the expression $H\dfrac{I_0 B}{F_0 d_0 r}$,

$$H = \frac{\text{line } ab \text{ of Fig. } 35C'}{\text{line } A'B' \text{ of Fig. } 35C} \quad \text{and} \quad \frac{I_0 B}{F_0 d_0 r} = \text{a constant};$$

or

$$H\frac{I_0 B}{F_0 d_0 r} = 0.3298 \times \frac{90.7 \times 325.56}{9.66 \times 15 \times 234.36}$$

$$= 0.3298 \times 0.869 = 0.2865,$$

and

$$X_2 = \frac{\text{line } a''b'' \times \frac{1}{2}\Sigma v'' + 0.287}{\Sigma v''} \quad \text{(see Fig. } 35E')$$

$$= \frac{\text{line } a''b''}{2} + \frac{0.287}{\Sigma v''}.$$

But $\Sigma v''$ is the sum of all the ordinates of the line fd' of Fig. 35$a = 2 \times 17.12 = 34.24$, consequently

$$X_2 = \frac{\text{line } a''b''}{2} + 0.00837.$$

This addition caused by the secondary stress is so small that it is negligible, and the equation may therefore be written

$$X_2 = \frac{\text{line } a''b''}{2}.$$

From equations (125) of the Appendix,

$$X_1 = H\frac{c_2 - c_1}{l}, \quad \text{and} \quad X_2 = He_0. \quad . \quad . \quad . \quad (125A)$$

For the load placed at IV, Figs. 35C and 35C' give, as before,

$$H = \frac{ab}{A'B'} = \frac{21.37}{64.79} = 0.3298;$$

$$X_2 = He_0 = \frac{\text{line } a''b'' \text{ of Fig. } 35E'}{2},$$

or

$$e_0 = \frac{a''b''}{2H}.$$

To obtain the value of e_0, a reduction should be made:

As previously found, $H = \dfrac{ab \text{ of Fig. } 35C'}{A'B' \text{ of Fig. } 35C}$,

or

$$2H = \frac{ab}{\frac{1}{2}A'B'} = \frac{ab}{\frac{1}{2}K}.$$

In Fig. 35C' the line DD has been drawn parallel to AB and at a distance therefrom $= \frac{1}{2}A'B' = \frac{1}{2}K$. One panel length is again assumed as the unit, and, from similar triangles, $cd = ae\dfrac{ce}{ab}$;

$$ae = 1, \quad ce = \tfrac{1}{2}K,$$

$$\therefore \ cd = \frac{\frac{1}{2}K}{ab} = \frac{1}{2H}.$$

Similarly, by transferring the point d from Fig. 35C' to d'' in Fig. 35E' on the prolongation of the line $e''b''$,

$$c''e'' = c''d''\frac{a''b''}{a''e''}.$$

Now, $c''d'' = cd$ of Fig. 35$C' = \dfrac{1}{2H}$, $a''e'' = 1$;

$$\therefore \ c''e'' = \frac{a''b''}{2H} = e_0.$$

In Fig. XX of the Appendix it will be seen that the distance from the axis Dx to the closing line of the moment polygon at the

center of the span is equal to e_0. In Fig. 35E' the axis DD has been drawn and also the axis ACB of the arch in its proper position with respect to this axis.

From Fig. 35D',

$$X_1 = \frac{a'b'}{l} = H\frac{c_2 - c_1}{l},$$

and

$$\frac{a'b'}{H} = c_2 - c_1;$$

also

$$\frac{a'b'}{2H} = \frac{c_2 - c_1}{2},$$

and $\frac{c_2 - c_1}{2}$ gives the ordinates of the closing line of the moment polygon above and below the axis $EE_{\prime}$ in Fig. 35E'.

The reduction $\frac{a'b'}{2H}$ has been made in the same manner as was explained for X_1 and the line $a'c' = \frac{c_2 - c_1}{2}$ in Fig. 35D'.

In Fig. 35E' the ordinates of the curve GG' give the values e_0 for the successive positions of the load K.

In Fig. 35D' the ordinates of the line AI give the values of $\frac{c_1 - c_2}{2}$ for the successive positions of the load K.

(*f*) Construction of the Moment Polygon (see Fig. 35E').—The direction and location of the closing line of the moment polygon are already determined, and the pole distance H is known; and to obtain the final result the moment polygon should be drawn.

Equation (139) of the Appendix gives

$$V_{\prime} = \mathfrak{V}_{\prime} + X. \quad . \quad . \quad . \quad . \quad . \quad . \quad . \quad (139a)$$

$\mathfrak{V}_{\prime}$ is the reaction caused by a load on a simple beam, and

$$X_1 = H\frac{c_2 - c_1}{l},$$

and

$$V_{\prime} = \mathfrak{V}_{\prime} + H\frac{c_2 - c_1}{l}.$$

The load $K = A'B'$ (Fig. 35C); the line $D'D'$ is drawn in Fig. 35C' parallel to AB at the distance K from same, and also the line

BD'; then the line $af = \mathfrak{V}_{,}$. Through the point f a line $fg_{,}$ is drawn parallel to the line FF' of Fig. 35E'. In Fig. 35C' the point b is transferred to g and $ga = g_{,}i = H$ when ah represents K.

The point g is transferred to $g_{,}$ on the line $g_{,}f$, and this point is then the pole of the force polygon in which $ai = V_1$ and $ih = V_2$.

In Fig. 35E' the lines FJ and $F'J$ are drawn parallel to the line ag' and $g'h$ of Fig. 35C'; the point J in Fig. 35E' is a point of the intersection locus, and the lines JF and JF' are the components of the force K and are tangents to the tangent curves.

By changing the position of the load successively from I to II . . . I′, the intersection locus LL' and the tangent curve MM' are obtained.

In the same figure the line ll' is the intersection locus and the line mm' the tangent curve for an equivalent arch whose axis is a parabola and whose moment of inertia varies as the secant of the angle which the arch axis makes with the horizontal.

The equivalent arch is a parabola whose area is equal to the area ACB included between the arch axis and the horizontal AB. The rise of this parabolic axis is 55.68 ft.

(b'). Analytical Solution of (b). (Secondary stress included.) —To obtain, for example, H_4 (see line 9, Table VII):

$$\begin{aligned}
&-15.561\times1\times15\\
&-18.366\times2\times15\\
&-20.553\times3\times15 = -113.952\times15 = 1709.28 = \mathfrak{M}_4 v_4.
\end{aligned}$$

$$\begin{aligned}
&-20.553\times6\\
&-18.366\times16.58\\
&-15.561\times25.53\\
&-12.033\times33.05\\
&-\ \ 7.633\times39.30\\
&-\ \ 2.178\times44.37 = -1{,}619.394 \quad \text{(See lines 1 and 9, Table VII.)}
\end{aligned}$$

$$\begin{aligned}
&+\ \ 4.593\times48.35\\
&+13.081\times51.29\\
&+23.154\times53.22\\
&+35.497\times54.18 = +4{,}106.35
\end{aligned}$$

$$+2{,}487 \quad \times2 = 4{,}974 = \Sigma y'_m v_m.$$

$$\frac{I_0 l}{F_0 d_0} = \frac{90.7\times300}{9.66\times15} = \frac{188}{5{,}162} = \Sigma y'_m v_m + \frac{I_0 l}{F_0 d_0}.$$

$$H = \frac{1{,}709.28}{5{,}162} = 0.3311.$$

By using the graphical method the value 0.3298 is obtained, or a difference of but 0.0013; both methods therefore give practically the same results.

(d'). Analytical Solution of (d). (Secondary stress included.) —To obtain, for instance, X'_4:

First, $\Sigma x_m v'_m$ should be obtained (see line 11, Table VII):

$$2\times\Sigma\left\{\begin{array}{l} 32.018\times\ \ 7.5 \\ 70.832\times\ 22.5 \\ 90.471\times\ 37.5 \\ 97.030\times\ 52.5 \\ 98.268\times\ 67.5 \\ 95.922\times\ 82.5 \\ 91.552\times\ 97.5 \\ 86.084\times 112.5 \\ 79.962\times 127.5 \\ 73.469\times 142.5 \end{array}\right\} = 8{,}553.104\times 2\times\tfrac{15}{2} = 128{,}296.5 = \Sigma x_m v'_m.$$

Second, the reaction should be computed:

$$8{,}553.104\times\tfrac{15}{2}\times\tfrac{1}{150} = 427.665;$$

$$15\times\Sigma\left\{\begin{array}{l} \ \ \ 427.665\times 3.5 \\ -\ 86.084\times 1 \\ -\ 79.962\times 2 \\ -\ 73.469\times 3 \end{array}\right\} = 15{,}455.61 = \mathfrak{M}_4 v'_4;$$

$$\frac{15{,}455.61}{128{,}296.5} = 0.12047 = X_1;$$

$$X_1 = H\frac{c_2-c_1}{l},\quad\text{or}\quad \frac{c_2-c_1}{2} = \frac{X_1 l}{2H} = \frac{0.12047\times 300}{2\times 0.3298} = 54.79.$$

To obtain, for instance, X_2 for position IV:
First obtain $\Sigma v''_m$ (see line 7, Table VII):

$$\begin{array}{r} 0.51557 \\ 0.60170 \\ 0.76519 \\ 0.93900 \\ 1.16270 \\ 1.45580 \\ 1.84820 \\ 2.41250 \\ 3.14810 \\ 4.26910 \\ \hline \end{array}$$

$$17.11786\times 2 = 34.236 = \Sigma v''_m;$$

$$15\times\Sigma\left\{\begin{array}{l} +17.118\ \ \times 3.5 \\ -\ 0.7652\times 1 \\ -\ 0.6017\times 2 \\ -\ 0.5156\times 3 \end{array}\right\} = 845.97 = \mathfrak{M}_4 v''_4;$$

$$H\frac{I_0B}{F_0d_0r}=0.3298\times\frac{90.7\times 325.56}{9.66\times 15\times 234.36}=0.287;$$

$$X_2=He_0,\quad e_0=\frac{X_2}{H},$$

and

$$e_0=\frac{845.97+0.287}{34.236\times 0.3298}=75.229.$$

To obtain the ordinates of the components at the verticals:

$$\begin{aligned} e_0 &= 75.229 \\ y_2 &= 45.865 \\ \hline y_2-e_0 &= -29.364 \\ \frac{c_2-c_1}{2} &= 54.79 \\ \hline c_1 &= -84.154 \\ c_2 &= +25.426. \end{aligned}$$

To obtain the ordinate of the intersection locus at IV:

$$\begin{aligned} V_1 &= \mathfrak{D}_1+X_1; \\ \mathfrak{D}_1 &= \frac{16.5}{20}\times 1=0.825\left(=\frac{247.5}{300}\times 1\right); \\ X_1 &= \phantom{\frac{16.5}{20}\times 1=\,}0.12 \\ \hline V_1 &= 0.945 \end{aligned}$$

z_0+y_2 = ordinate of the intersection locus.

Vertical ordinate of the intersection locus measured from the point of intersection of the component with the left vertical (a vertical projection of the line JF, Fig. 35E'),

$$x_1\frac{V_1}{H}=52.5\times\frac{0.945}{0.3298}=150.43,$$

or the ordinate of the intersection locus =

$$+150.43-84.154=66.276.$$

6. Horizontal Forces.—Before taking up the subject of the correction of the intersection locus and the tangent curves, a few remarks will be made concerning the horizontal forces acting on the arch.

In the analysis given in the Appendix [see equations (135^a), (136^a), (137^a), (140), etc.], the values of H, X_1, and X_2 are defined for a horizontal force.

After the detailed explanation of the effect of horizontal forces on the two-hinged arch (see Art. 19, Chap. III), and that of the influence of vertical forces on a hingeless arch in the foregoing paragraphs, a brief consideration of the effect of the horizontal forces on a hingeless arch should be sufficient.

In Fig. 35*d* a force polygon has been drawn of the forces v'', which are assumed to act horizontally. This figure is a duplicate, on a smaller scale, of the force polygon of Fig. 35*d'*, and the reciprocal polygon of Fig. 35*D* has been drawn therefrom.

If a horizontal force, as Q, be applied to the arch, as in Fig. 35, Fig. 35*B* will give the value of X_2, Fig. 35*C* the value of H_h, and Fig. 35*D* the value of X_1. By observing the same conditions and making the same reductions as explained in the Appendix, and as described for the vertical forces, the intersection locus and tangent curves for the horizontal forces can be obtained.

For the reasons hitherto stated the author recommends the application of the intersection locus and the tangent curves shown in Fig. 31 for the computation of the stresses caused by horizontal forces. The maximum error in the stresses thus found will not exceed 6 per cent., and this is insignificant in comparison with the error which is possible and probable in the assumptions made regarding the intensity of the forces.

A rigid analytical treatment is therefore an unnecessary refinement, and in the following paragraphs horizontal forces will not be further considered.

7. Correction of the Intersection Locus and the Tangent Curves.—The intersection locus and the tangent curves of Fig. 35*E'* contain the following factors:

1. The influence of the secondary stress.
2. The variation in the moment of inertia.
3. The curvature of the arch axis as compared with the parabola.

The influence of these three factors will be successively eliminated from the locus and tangent curves, and the corresponding changes which take place in these lines will be shown.

With a combination of the analytical and graphical methods these changes can be clearly set forth.

(*a*) Elimination of the Secondary Stress.—Referring to equations (135*A*), (136*A*), and (137*A*), the factors $\frac{I_0 l}{F_0 d_0}$ and $H\frac{I_0 B}{F_0 d_0 r}$ represent the influence of the secondary stress.

In Fig. 35*C*, $B_{\prime}B_{\prime\prime}$ represents the value $\frac{I_0 l}{F_0 d_0}$, and when this factor is neglected, the ordinates of the line ACB of Fig. 35*C'* divided by the line AB will give the values of H; these values are inserted in line 14, Table VIII.

(It should be observed that H has increased—compare with line 14, Table VII.)

In equation (136A) no factor representing the secondary stress appears, and $X_1=\dfrac{\Sigma_0^l \mathfrak{M}_m v'_m}{\Sigma_0^l x_m v'_m}$; $a'b'$ of Fig. 35D' remains the same, and line 17, Table VIII, is not changed.

From equation (125A), however,

$$X_1=H\frac{c_2-c_1}{l}, \quad \text{or} \quad \frac{c_2-c_1}{2}=\frac{X_1 l}{2H}.$$

In this equation H has increased, and the value of $\dfrac{c_2-c_1}{2}$ must therefore diminish. This is shown by line 15, Table VIII.

In equation (137A) appears the term $H\dfrac{I_0B}{F_0d_0r}$, which expresses the secondary stress. If this term is to be dropped from the equation, the latter will read:

$$X_2=\frac{\Sigma_0^l \mathfrak{M}_m v''_m}{\Sigma_0^l v''_m}.$$

In the graphical computation of X_2 (Fig. 35E') the secondary stress has been neglected. On line 16, Table VII, however, the secondary stress is included. From equation (125A), $X_2=He_0$,

$$\therefore\ e_0=\frac{\Sigma_0^l \mathfrak{M}_m v''_m}{H\Sigma_0^l v''_m}.$$

In this equation the numerator has decreased and the denominator increased, and the value of e_0 must therefore decrease, as shown on line 16, Table VIII.

The value of $V_1(=\mathfrak{D}_1+X_1)$ is not affected by the secondary stress.

(*b*) Elimination of the Variable Moment of Inertia.—As the Appendix shows, under the heading of special equations, when the moment of inertia becomes a constant, $v_m=y_m$, $v'_m=x_m$, and $v''_m=1$; and equation (138) becomes

$$y_2=\frac{\Sigma_0^l y'_m v''_m}{\Sigma_0^l v''_m}=\frac{\Sigma y'_m}{20}=\frac{743.74}{20}=37.187.$$

It should be observed that y_2 is the height of a parallelogram with a length equal to l and an area equal to that enclosed by the arch axis and the line AB. This area$=$11,135 sq. ft., and the span $=$300 ft.;

$$\therefore\ y_2=\frac{11,135}{300}=37.12.$$

There is a slight discrepancy between these two values, which, if equations (131), (132), and (133) of the Appendix had been applied, would not have appeared. In this case, however, it is so slight that it will not materially influence the results of the computation.

This discrepancy is common to all the values subsequently obtained for equations (135), (136), and (137); it also exists in the earlier computations, and for this reason its effect is neutralized.

With this new value for y_2 another table is arranged in which the angles a and b, the panel length of the arch axis, and the ratio $\frac{I_0}{I_1}$ disappear; also the factors F, F_0, and v'_m. Also, $\Sigma - y = \Sigma + y$.

When the secondary stress is neglected, equations (135), (136), and (137) become:

$$H = \frac{\Sigma \mathfrak{M}_m v_m}{\Sigma y'_m v_m}; \qquad v_m = y_m.$$

$$X_1 = \frac{\Sigma \mathfrak{M}_m v'_m}{\Sigma x_m v'_m}; \qquad v'_m = x_m.$$

$$X_2 = \frac{\Sigma_0^l \mathfrak{M}_m v''_m}{\Sigma_0^l v''_m}; \quad v''_m = 1.$$

$$\Sigma y'_m v_m = 2 \times \Sigma \left\{ \begin{array}{l} -31.187 \times \ 6 \\ -20.607 \times 16.58 \\ -11.657 \times 25.53 \\ - \ \ 4.137 \times 33.05 \\ \\ + \ \ 2.113 \times 39.30 \\ + \ \ 7.183 \times 44.37 \\ +11.163 \times 48.35 \\ +14.103 \times 51.29 \\ +16.033 \times 53.22 \\ +16.993 \times 54.18 \end{array} \right\} = 4{,}951.3.$$

For the load at IV,

$$\mathfrak{M}_m v_m = \Sigma \left\{ \begin{array}{l} 11.657 \times 1 \times 15 \\ 20.607 \times 2 \times 15 \\ 31.187 \times 3 \times 15 \end{array} \right\} = 2{,}196.48,$$

and $$H = \frac{2{,}196.48}{4{,}951.3} = 0.44362.$$

See also the deductions made in Art. 1 (*e*), Chap. IX, of Appendix, viz.:

$$X_1 = K \frac{g(l-g)}{l} \frac{(l-2g)}{l^2} = 2X_2 \frac{l-2g}{l^2};$$

$$X_2 = K \frac{g(l-g)}{2l}.$$

Again,

$$X_1 = H\frac{c_2 - c_1}{l}, \quad \text{and} \quad X_2 = He_0;$$

further,

$$z_0 = 8\frac{H}{K}\frac{e_0^2}{l}, \quad \text{and}$$

$$z_1 = 2\frac{l-g}{l}e_0.$$

When g is expressed as a function of l, equal to kl, and $k=1$, these equations change into

$$X_2 = \frac{l}{2}k(1-k), \quad \text{and}$$

$$X_1 = 2X_2\frac{1-2k}{l}.$$

When the load is successively placed at I, II, etc., $k=\frac{1}{40}, \frac{3}{40}, \frac{5}{40}$, etc. For the load at IV, $k=\frac{7}{40}$, and

$$e_0 = \frac{l}{2}\frac{k(1-k)}{H} = \frac{150 \times 7 \times 33}{40 \times 40 \times 0.4436} = 48.817.$$

When $k=1$,

$$z_0 = 8H\frac{e_0^2}{l};$$

for the load at IV,

$$z_0 = 8 \times 0.4436 \times \frac{48.817^2}{300} = 28.192,$$

and the ordinate of the intersection locus is

$$y_2 + z_0 = 37.187 + 28.192 = 65.379.$$

In the equation $z_1 = 2\frac{l-g}{l}e_0$, kl can be substituted for the value g, which gives

$$z_1 = 2(1-k)e_0;$$

and for the load at IV,

$$z_1 = 2 \times \frac{33}{40} \times -48.817 = -80.548,$$

and $c_1 = -z_1 + y_2 = -80.548 + 37.187 = -43.36,$

$$z_2 = -2e_0 + z_1 \qquad = -17.086,$$

$$c_2 = -z_2 + y_2 \qquad = +20.1.$$

All these values are inserted in Table IX.

(*c*) CONSTRUCTION OF THE INTERSECTION LOCUS AND THE TANGENT CURVES, AND PRELIMINARY DIMENSIONS.—The Syra Valley Bridge is again taken as an example. Assume the arch axis to be the arc of a circle,* its span 300 ft., and its rise 54.3 ft.

A table of ordinates of the arch axis is now arranged, similar to line *a* of Table X (reduced to a rise = 1).

The equivalent parabola has a rise of 55.781 ft., and its ordinates are tabulated similar to line *b* of Table X (reduced to a rise $= \frac{55.781}{54.3} = 1.026$).

Preliminary Dimensions.—Such an arch should be built with the least possible material consistent with stability and durability, and by trial an arch is found which, including masonry, filling, and paving, weighs 522 tons for a ring 1 ft. wide. Fig. 35 shows this arch.

To obtain the depth of the arch rib at the crown, an average stress (= 320 lbs. per sq. in.) is assumed; in this case the maximum stress should not exceed 640 lbs. per sq. in. Then

$$h = 3.333q + \frac{W}{n}\frac{l}{f} \times 0.62; \dagger$$

in which $q = 0.2$ = a coefficient of the equation;

$W = 522,000$ lbs.;

$l = 300$ ft.·

$n = 320$ lbs. per sq. in.;

$f = 54.3$ ft.;

$\therefore\ h = 6$ ft. (rounded off).

The angle which the arch axis makes with the horizontal at the abutment = 39° 48′ 2″. The approximate depth of the arch rib at the abutment is $h \sec^3 a = 13.23$.

For the Syra Valley Bridge, depth = 13.33 ft.

---

* The arch axis has been assumed to be part of a circle. The Syra Valley Bridge is used only as an example for the purpose of illustrating the application of the equations of the Appendix, and to show the different steps required for designing such an arch. The use of the circular arc facilitated the work for the author [see Art. 9 (*a*)]. In the actual design the ordinates of the arch axis in panels 1 to 6 are shorter than those of a circular arch, and in the remaining panels they are longer.

† 300 ft. − 100 ft. = 200 ft.; 200 ÷ 11 = 19; 100% − (19×2%) = 62%.

Now I_0 must be approximated:

$$13.33^3=2,369 \ldots\ldots\ldots\ldots\ldots\ldots \quad 2,369\div12=197.42$$
$$6^3=\ \ 216 \ldots\ldots\ldots\ldots\ldots\ldots \quad 216\div12=\ 18$$
$$2,153\div3=718;\ \times1.2=\ \ 862;\div12=\ 71.83$$
$$71.83+18=89.83\sim90.$$

In the above computation the area representing the moment of inertia of the arch rib is considered as defined by a common parabola. The ordinates which represent this moment of inertia, however, form an area which is defined by a cubic parabola, including a constant factor equal to the moment of inertia at the crown. For an approximation, however, the above assumption is sufficiently close.

The added 20% represents a factor, part of which results from the constant, *i.e.*, the moment of inertia at the center of the span. The ordinates which measure the moment of inertia should be erected on an axis which is equal to the length of the curve, but in the foregoing approximation they have been considered as ordinates erected on an axis which is equal to one-half the span; the discrepancy caused by this contraction is covered by the remaining part of the factor. The curve has the same ratio to its horizontal projection as that which the secant bears to the horizontal at all points of the curve. At the center of the span this ratio=1, and it increases towards the supports. The approximation employed is only for the purpose of obtaining the intersection locus and the tangent curves, and it should be remembered that the variation in the moment of inertia must be large in order to influence these lines,. for which reason any greater refinement in the computation is unnecessary.

The foregoing computation for obtaining the depth of the arch rib at the crown is applicable to an arch of any rise, including the semicircular arch. The dimensions of the semicircular arch rib at the abutments, however, if so determined, would be infinitely large, and the foregoing approximation is therefore not applicable. It can, however, be safely used where the rise does not exceed one-third of the span, and its application in the designing of large arches furnishes the computer with initial data which will closely correspond with the final results. As a concrete illustration of this the Syra Valley Bridge has been cited.

It is not likely, however, that a 300-ft. arch will ever be built with a rise exceeding 100 ft., and for large arches the foregoing approximations are therefore general in their application. For small arches assumptions may be made by the experienced designer which will yield sufficiently accurate results.

The correction of the intersection locus and tangent curves can now be made, and the procedure is divided into two parts:

(1) The correction of the intersection locus and tangent curves of the parabolic arch so that they will correspond to the curvature of the true arch axis;

(2) The alteration of the thus corrected intersection locus and tangent curves so that they will correspond to the variation in the moment of inertia of the arch rib.

(*d*) Correction of the Intersection Locus and Tangent Curves of the Standard Diagram to Correspond with the True Curvature of Any Arch.—The height of a parallelogram on AB having an area equal to that included between the arch axis and the line AB is equal to 37.187 ft.

A parabola of the same area on AB will have a rise $=37.187\times\frac{3}{2}=$ 55.781 ft., and to make a comparison possible, when the coordinates of the circular arch are reduced to correspond to a rise of arch $=1$, the similarly reduced ordinates of the parabola should be increased in the ratio

$$\frac{55.781}{54.3}=1.026.$$

The ordinate of the intersection locus of the parabola is then $1.026\times1.2=1.231$.

The reduced arch axis is shown in Fig. 38 by the heavy line ACB, and the equivalent parabola by the dotted line $AC'B'$.

The intersection locus for the equivalent parabola is the dotted line DE, and the tangent curve is the dotted line FG. These lines are plotted from Fig. 24, all the vertical ordinates of same being multiplied by 1.026 (Line IV, Table X).

An intersection locus and a tangent curve are drawn for the Syra Valley Bridge, assuming that the moment of inertia increases in the same ratio as the secant of the angle which the axis makes with the horizontal. (See ordinates of Table X, line III.)

The intersection locus is the line $D_{,}E_{,}$, and the tangent curve is the line $F'G'$.

Fig. 38 clearly shows the difference between the two loci and between the two tangent curves.

It should be observed that, on account of the exaggerated vertical scale employed, this difference appears to be considerable; on the true scale it would almost completely disappear.

To make the correction to the intersection locus, draw a line parallel to the line DE and at a distance bb' below DE, which distance is equal to BB'. If the crown B' of the equivalent parabola is located below the crown B of the arch axis, the distance bb' should be plotted upward from the line DE.

The figure shows that the locus thus obtained deviates only from the true locus line at the panel points I and I′ and is therefore practically correct.

To make the correction to the tangent curve, draw the parabola so that it is tangent to the curve AB at the points A and B, the points A to correspond in both curves; this parabola is indicated by the dash-and-dot line $AC''B$.

The most convenient method for obtaining this line is to draw the parabola on tracing-cloth and shift it into position over the work.

The differences between the lines ACB and $AC''B$ are divided by 1.2, and these quotients are plotted from the tangent curve FG, e.g., $ef \div 1.2 = e'f'$.* Observe that these differences are measured and plotted in a radial direction, and not as vertical ordinates.

The points thus obtained are joined, and the line so produced is the tangent curve $G'F'$.

(*e*) Correction of the Standard Diagram to Correspond with the Variation in the Moment of Inertia of the Arch Rib.—The maximum moment of inertia was found to be 197.42 ft.^{4}, the minimum 18 ft.^{4}, and the average or $I_0 = 90.7$ ft.^{4}

Now, I_0 can be expressed as a ratio in comparison with the rise of the arch, and this ratio, which is empirical, $= 0.2f_,$; I_0 can also be expressed in the rise of the equivalent parabola, or $I_0 = 0.2f_, \times 1.026 = 0.205f_,$.

The value $0.2f_,$ is a factor obtained from the application of the analysis of the hingeless arch to large existing structures of that class.

In the foregoing example $f_, = 1.026f$, and $I_0 = 0.205f_, = 90.7$ ft.^{4}.

The maximum and minimum moments of inertia should now be expressed in terms of the rise of the arch, or

$$I_A = 197.42 = \frac{197.42}{90.7} \times 0.205 = 0.45f_, \qquad \text{and}$$

$$I_C = 18 \quad = \frac{18}{90.7} \times 0.205 = 0.041f_,.$$

To construct the cubic parabolic area which represents the moment of inertia of the arch rib at the panel points, $I_A = 0.45f_,$ should be reduced to unity so that $\sqrt[3]{1} = 1$; then the ordinate representing I_C should be reduced by the ratio $\dfrac{0.041}{0.45}$.

Or, when $I_A = 1$,

$$I_C = \frac{0.041}{0.45} \times 1 = 0.0912,$$

and the height of the arch rib at the crown (taking the depth of the arch rib at the abutments as a unit) will be $\sqrt[3]{0.0912} = 0.45$.

* In most cases it is sufficiently accurate to plot the differences between the lines without making the division; for example, $ef = e'f'$, etc.

Now in Fig. 38*a* I_A has been measured off $=0.45=DF$, and to measure the depth of the arch rib at the crown to the same scale, $0.45\times0.45=0.2025$,* which, when measured from the axis EF, will give the point B; and a straight line passing through the points D and B will intersect the axis EF at the point E, in which point the needle† is placed for the construction of the cubic parabola CD.

The construction of the cubic parabola has been shown in Chapter IV (Douro Bridge), and a few words should suffice here to explain the operation. The points 1, 2, 3, etc., are transferred to the line AD by drawing lines parallel to EF, the needle is placed at E, and these points are transferred again to the panel lines, etc. This construction has been shown for point 7; it is first transferred to $7'$, from there to $7''$, thence to $7'''$, and finally to $7''''$.

The points are then joined, resulting in the cubic parabola DC, which has its vertical axis at E.

The work can be checked at this point, as the ordinate of the point C measured from the axis EF should be equal to 0.C41.

The point C is transferred to A and a common parabola AB is then drawn, which has its vertical axis at B, while the line BD is a tangent to this parabola at the crown B. The construction is the same as described in an earlier paragraph, viz., the point 3 is transferred to $3'$ (line 3–$3'$ parallel to DE) and $3'$ to $3''$ (line $3'$–$3''$ intersects at B), the needle being placed at the point B.

The ordinates between these two parabolas give the difference in the ordinates between the two tangent curves F_1G_1 and F_2G_2; for example, $gh=g'h'$ and $ij=i'j'$.

The tangent curve thus obtained is correct to about the point where it intersects II, and for all practical purposes it is correct throughout; it will closely coincide with the actual tangent curve from the points G_2 to F_2, which is plotted from the ordinates of Table X.

The correction of the intersection locus is obtained as follows: A straight line is drawn through the point of intersection a (Fig. 38*a*) of the two parabolas AB and CD and the point E. This line produces the point H, and a common parabola is drawn through the points a and H; its crown is located at H, and the tangent to the crown is a horizontal line parallel to the axis EF.

To draw a parabola which satisfies these conditions a vertical axis JJ is erected through the point a, and the intersection points of the panel lines with the axis aH are transferred to the line JJ; the needle is placed at the point H, and the intersection points on JJ

---

* It is merely by chance that the two values happen each to be equal to 0.45; it should be remembered that one expresses the moment of inertia of the arch rib at the abutment when the rise of the arch axis equals unity, and the other the depth of the arch rib at the crown when the depth of the arch rib at the abutment equals unity.

† The most convenient method for constructing either the common or the cubic parabola is to place a needle at the point E to reproduce the intersections on the ordinates.

are transferred back to the panel lines; the line HI drawn through the points thus obtained is the desired parabola. The construction has been shown for the point $2'$, which is transferred to JJ by drawing a line $2'2''$ parallel to EF, and the point $2''$ is transferred to the point $2'''$ by prolonging a line which passes through the points $2''$ and H.

This parabola is usually very flat, and for this reason it does not differ materially from a circular arc; and the problem resolves itself then into finding the third point I. The point o is transferred to o' and this point is transferred back to I, and through the points H–a–I a circular arc is drawn (with a railroad curve).

To obtain the intersection locus, the vertical ordinates between the two lines CD and HI are plotted from the line $d_,e_,$ in Fig. 38, viz., $k'l'=kl$, etc.

This construction produces the line D_3E_3.

The line D_2E_2F is the true intersection locus, and the error is clearly shown in the figure. Though its influence on the final result is very small, it may sometimes be desirable to eliminate this error from the intersection locus. The distance d_1D_2 is 0.6 of the distance d_1D_3. and the point D_2 can thus be located; and from this point a curve is drawn which is tangent to the line D_3F at the point e.

Any error in the intersection locus and the tangent curves to the left of II and to the right of II′ is very inconsiderable, and does not affect the result of the computation by one part in ten thousand.

The point K in Fig. 38 is the point of action of the horizontal thrust caused by temperature changes and by the secondary stress.

The corrections have all been plotted to the exaggerated vertical scale employed, and the reduction to the true scale is a simple process which needs no further explanation.

In designing large arches this reduction is not necessary. The first object of the computation is to find the point of intersection of the line of pressure with the vertical passing through the abutment. The simplest, quickest, and most accurate way is to combine the graphical and the analytical methods; using the graphical method to find the intersection of the components with the vertical through A, and the intensity of the horizontal thrust for each single load; and the analytical method to find the point of application of the resultant of the horizontal thrusts caused by the single loads. From this point in the computation either the graphical method formerly described or the analytical method described in the following article may be employed to find the line of pressure.

That the diagram of Fig. 38 can be used to find the horizontal thrusts, hardly needs an explanation. To illustrate its simplicity the following figures are given:

The rise of the arch axis (equivalent parabola) = 55.78 ft.,

One-half the span . . . . = 150 ft.,

and $$\frac{150}{55.78}=2.6 \text{ (approx.)}.$$

In Fig. 38 the rise of the equivalent parabola $=1.026$,
One-half the span " " " " $=1$,

and $$\frac{1}{1.026}=0.975.$$

And to measure the intensity of the horizontal thrust by the scale of forces, the actual panel loads should be multiplied by $(2.6\times0.975=)$ 2.54.

For example, to measure the horizontal thrust caused by a load of 1 ton placed at the panel point IV, a force of 2.54 tons should be plotted on the panel line IV and resolved into its components; and the horizontal thrust thus obtained will be the true horizontal thrust, notwithstanding the vertical distortion of the diagram.

This method yields results of great accuracy, which would be impossible to obtain were the true vertical scale used.

It is also advisable in the designing of large arches to make all preliminary computations for an equivalent parabolic arch axis with a rise and half-span each equal to unity, making the necessary corrections to the intersection locus and tangent curves. When the line of pressure has been computed, an arch axis is then found which most closely approaches to the line of pressure, as previously described in this chapter.

This method enables the designer to do his work accurately and quickly for large arches, and especially for masonry and reinforced-concrete arches.

The preliminary dimensions for a reinforced-concrete arch of, say, 800 ft. span, are obtained in a short time, and are sufficiently accurate to base final computations upon; the method explained in Figs. 35 to 35E should then be followed.

For arches with spans not exceeding 150 ft. the graphical method previously described gives sufficiently accurate results, and the experience of the designer will decide the corrections to be made to the intersection locus and tangent curves.

(*f*) Application of the Corrected Standard Diagram.—The diagram of Fig. 38 can not only be used for the computation of the stresses in the arch from which it was derived, but various arches may also be computed with it, provided that the rises are between one-fifth and one-sixth of their respective spans.

For this purpose the standard diagram is drawn for an equivalent parabola whose rise $=1$ and whose half-span $=1$.

Assume the rise of the desired arch to be approximately one-sixth of the span. To obtain the true horizontal thrust, all panel loads should be multiplied by 3. The resolution of forces is made and the horizontal thrust of each panel load is measured with the scale of forces. The intersection of the components with the verticals passing through the abutments is found (in Fig. 35E' the distances DF and DF'). These points are joined by the line FF' and the distance e_0 can be measured, which distance is then expressed in the

rise of the parabola as unity. Then the point of intersection with the vertical through A of the resultant of all the horizontal thrusts is computed analytically. This point will be located by an ordinate measured from the axis DD, which ordinate is expressed in the rise of the parabola as unity.

The line of pressure may then be computed, preferably analytically, and the ordinates thus obtained are plotted. The resultant horizontal thrust caused by the secondary stress is then computed.*

In Fig. 38, from the correction of the tangent curve, its point of application K is known. From this the location and intensity of two horizontal forces are known, which forces act in opposite directions, viz., the point of application of the line of pressure at the crown, and the point of application of the secondary-stress thrust. The intensity of the resultant of these two forces is the difference between them, and its point of application can be found by the moment method. It is located above the line of pressure first obtained.

From this point (where the resultant of these two forces intersects the vertical at the crown of the arch) a new line of pressure is computed, with a horizontal thrust which is equal to the difference between the horizontal thrust caused by the panel loads and the one caused by the secondary stress.

This new line of pressure will be located partly above and partly below the line of pressure first obtained.

The curvature of the arch axis may now be corrected, as previously described, and the former computations should be repeated when the difference between the arch axis thus found and the equivalent parabola is considerable.†

In this connection attention should be called to the fact that a large difference between the parabola and the arch axis cannot be corrected by changing the arch axis; such a difference indicates that the dimensions which were initially assumed for the arch rib are wrong.

When, finally, a good curve has been obtained for the arch axis, it may be found that its rise differs considerably from the one originally assumed. Suppose it is too high: this will not necessitate the repetition of all the former work. When the elevation of the crown of the arch is immaterial, all the vertical ordinates are to be reduced in the ratio which the rise of the true equivalent parabola divided by the half-span bears to unity, or one unit of rise as used in

---

* In large arches this stress should never be neglected; though the force be small, it can greatly influence the eccentricity of the line of pressure.

† No specific rule can be prescribed in regard to the necessity for recomputation; the designer's experience must guide him. The author would state in a general way that an increase or decrease of 5% in the rise will necessitate a recomputation; and if this gives a still larger deviation, the dimensions of the arch rib should be corrected.

the standard diagram divided by one unit which represents the half-span.

If the elevation of the crown is fixed, a reduction should be made. Assume the arch axis to be 5% too high; then the reduction mentioned in the former paragraph should be multiplied by the ratio $100 \div 105$, and the horizontal thrust by the ratio $105 \div 100$.

When the rise of the arch axis is to be increased 5%, the inverse ratios are to be used.

The location and intensity of the forces which form the line of pressure are now known, and the next step in the computation is to find the stresses caused by a maximum and minimum change in temperature.

The operation is similar to that for finding the influence of the secondary stress. It will give two more lines of pressure, one for the highest and one for the lowest temperature.

In the case of large reinforced-concrete or masonry arches, the live loads have been included in the panel loads with which the computations have thus far been made.

If otherwise, the three lines of pressure are combined with that form of loading which will give the maximum stresses. The *modus operandi* for computing these stresses has been fully explained in previous articles of this chapter, and an example for the analytical computation of the line of pressure is given in Art. 8 *et seq.*

(*g*) When Corrections (*d*) and (*e*) Should be Made.—It is impossible to formulate any general rule in this connection, as the matter must be left largely to the experience of the designer. A few observations, however, may not be without value.

Variation Resulting from the Difference between the Arch Axis and a Parabola.—The object of the computation should not be lost sight of. It is not the solution of a mathematical problem; on the contrary, mathematics is only the means to an end, viz., a well-designed arch; and as applied to the Syra Valley Bridge, if the correction made for the difference in curvature between the arch axis and the parabola should be neglected, it would not materially affect the result.

Influence of the Variation in the Moment of Inertia of the Arch Axis.—The nearer the variation in the moment of inertia approaches to a constant, or the nearer the magnitude of I_1 approaches to that of I_0, the nearer the lines AB and DC in Fig. 38*a* will approach to the axis GB. The greatest differences between I_1 and I_0 occur at the center and near the supports, and though these differences influence the tangent curves very materially, it should be observed, for example, that the extreme right component, viz., the one drawn from I′ in Fig. 38, is a tangent to the tangent curve at the point F_2.

The extreme left component at I can be drawn as a vertical line, and where the variations are maximum, their influence on the stresses in the arch becomes practically zero; the variations of greatest in-

fluence on the stresses are found between panels 2 and 8 (Fig. 38*a*).

In the masonry arch there exists a uniformity in the change of the depth of the arch rib. The moment of inertia is the cube of the depth, and relatively small changes in this dimension result in large changes in the moment of inertia; for this reason, in designing large masonry arches, the influence of the variation in the moment of inertia should always be investigated.

In the steel arch the depth of the arch rib is often uniform, and an increase in the section of the rib is made by the addition of flange plates; here a correction of the intersection locus and tangent curves may be an unnecessary refinement.

If any doubt should exist in the mind of the designer, he should make the corrections as described; the more so, as they do not involve laborious computations, being easily obtained by the use of a slide-rule and a little skill.

It should be remembered that the final operation in the designing of large arches is to compute the deflections caused by dead and live loads. In order to obtain these, a final computation is made in which all the data are given, and this final computation should be partly analytical and partly graphical, using the equations employed for the computations of Figs. 35, etc. This final computation will serve as a check upon the preceding work, and will disclose any discrepancies contained therein.

8. Analytical Computation of the Line of Pressure.—The line of pressure has been determined graphically in the former articles, it is desirable, however, to check this computation by analytical methods.

A table should be arranged, similar to Table XI, giving the dead loads K of each panel.

The arch being symmetrical (see Fig. 35E'), the dead load of panel IV is equal to the dead load of panel IV′.

The horizontal thrust for the load placed at IV acts at F, and for the load at IV′ acts at F'. The distance EF = the distance $E'F'$, and, if the starting point of the line of pressure on the vertical at the support A is to be found as an ordinate from the axis DD, the horizontal thrust multiplied by the distance DF, plus the horizontal thrust multiplied by the distance DF', is equal to the horizontal thrust multiplied by twice the distance e_0. This distance e_0 can be found with great accuracy from the distorted diagram of Fig. 38, it being expressed in the rise of the equivalent parabola as unity. See also Art. 7 (*f*) in this connection.

The sum of the moments of the horizontal thrust for all the panel loads is

$$\Sigma kH2e_0.$$

In the following table the values of K are the panel loads computed from the arch in Fig. 35.

TABLE XI.

Panels.	H'.*		K.			H.		e_0.†		Ton-feet.
[1]	0	×	59.18	× 2	=	0 ;	×	∞	=	0
[2]	0.0594	×	46.41	× 2	=	5.52;	×	185.63	=	1,025
[3]	0.172	×	37.33	× 2	=	12.84;	×	105.15	=	1,352
[4]	0.3298	×	23.82	× 2	=	15.72;	×	75.229	=	1,184
[5]	0.5223	×	20.92	× 2	=	21.82;	×	59.603	=	1,300
[6]	0.7369	×	18.31	× 2	=	26.94;	×	50.146	=	1,347
[7]	0.9578	×	16.31	× 2	=	31.24;	×	43.995	=	1,375
[8]	1.1654	×	14.52	× 2	=	33.86;	×	39.907	=	1,352
[9]	1.3351	×	13.05	× 2	=	33.90;	×	37.371	=	1,265
[10]	1.4379	×	11.19	× 2	=	32.10;	×	35.962	=	1,153
			261.04 tons			213.94 tons				11,353 ton-feet.

$\therefore z_1 = 11{,}353 : 213.94 = 53.1$ ft.
$y_2 = 45.87$

$c_1 = -\ 7.23$ ft.

* See Table VII, Line 14. † See Table VII, Line 16.

The reciprocal polygon therefore commences 7.23 ft. below the point A.

The intersections should now be found on the panel lines I, II, etc.

The weight of one-half the arch = 261.04 tons, and the total horizontal thrust caused by the dead load = 213.94 tons.

The ordinate of the line of pressure on

[1] $= \dfrac{261.04}{213.94} \times 7.5$ ft. $= 9.2$ ft.; -7.23 ft. . . . . $= +\ 1.97$ ft.
the ordinate of the arch axis $= y'$ . . . . $=\ \ 6$ "

and the line of pressure passes below the axis . . . . $-\ 4.03$ "

[2] $261.04 - 59.18 = 201.86$; $\dfrac{201.86}{213.94} \times 15 = 14.16$; $+1.97$ . . $= +16.13$ "
the ordinate of the arch axis $= y'$ . . . . $=\ 16.58$ "

and the line of pressure passes below the axis . . . . $-\ 0.45$ "

[3] $201.86 - 46.41 = 155.45$; $\dfrac{155.45}{213.94} \times 15 = 10.9$; $+16.13$ . . $= +27.03$ "
y' . . . . $=\ 25.53$ "

and the line of pressure passes above the axis . . . . $+\ 1.5$ "
etc.

The intensity of the force from

A to [1] $= \sqrt{261.04^2 + 213.94^2} = 337$ tons
[1] to [2] $= \sqrt{201.86^2 + 213.94^2} = 294$ "
[2] to [3] $= \sqrt{155.45^2 + 213.94^2} = 265$ " , etc.

In an arch of these dimensions the live load is but a small fraction of the dead load. Were the arch designed for a highway bridge, a live load of 100 lbs. per sq. ft. would give but 1,500 lbs., or 0.75 ton per panel.

The method of dealing with live loads has already been discussed graphically, and it may be applied to this arch; the analytical treatment follows the procedure set forth in the preceding paragraphs.

NOTE.—The foregoing computations were made with a slide-rule, and may not, in consequence, be correct in the decimal places; this, however, is of small importance for a masonry arch of the dimensions given. (Secondary stresses are included in the computations.)

(*a*) TEMPERATURE STRESSES.—From equation (162) of the Appendix,

$$H_t = \frac{EI_0 wtl}{d_0\left(\Sigma_0^l y'_m v_m + \dfrac{I_0 l}{F_0 d_0}\right)}. \quad . \quad . \quad . \quad . \quad (162A)$$

From Fig. 35*C*,

$$d_0\left(\Sigma_0^l y_m v_m + \frac{I_0 l}{F_0 d_0}\right) = 5,162 \times 15 = 77,430.$$

Now E in ton-feet $= 140,000$ (masonry);
$t =$ about $15°$ F. above or below normal.

In establishing this temperature, the mass of the structure should be considered. Extreme cold or extreme heat cannot penetrate far into the mass of the arch, while the intrados is never exposed to the sun's rays or the cold winter winds, and the extrados in an arch of these dimensions is so well protected that practically it experiences no temperature changes.

$$l = 300 \text{ ft.};$$
$$w = 0.000004 \text{ for } 1° \text{ F.};$$
$$Ew = 0.56;$$
$$\therefore H_t = \frac{90.7 \times 0.56 \times 15 \times 300}{77,430} = 2.96 \text{ tons.}$$

This force acts on the axis DD which is parallel to AB (see Fig. 35*E'*) and 45.865 ft. distant therefrom.

The ordinates of the line of pressure between I and II are +1.97 ft. and +16.13 ft. on I and II, respectively;

$$45.87 - 1.97 = 43.9 \text{ ft.}$$
$$45.87 - 16.13 = 29.74 \text{ "}$$

The difference between the ordinates on I and II is 14.16 ft., as previously obtained, or

$$\frac{43.90}{14.16}\times 15 = 46.4 \text{ ft.}$$

The horizontal thrust from dead load and maximum temperature is $213.94 + 2.96 = 216.90$ tons, and $\frac{201.86}{216.90}\times 46.4$ ft. $= 43.2$ ft., which is the ordinate of the point of intersection of the line of pressure on the panel line I, and which ordinate is measured from the axis DD, Fig. 35; or, when measured from the axis AB, the ordinate is

$45.87 - 43.2 =$ . . . . 2.67 ft.
$y' =$ . . . . 6 "

and the line of pressure passes below the axis 3.33 "

And though the intensity of the force has not been materially changed by the change in temperature, the point of application of this force has shifted $(2.67 - 1.97 =)0.7$ ft. towards the arch axis.

If the extreme low temperature had been used in the computation, the point of application of the force would have been shifted away from the arch axis, which would have caused an increase in the stresses of the extreme fibers.

The denominator of equation (162A) contains in its value the curvature of the arch axis, the variation of the moment of inertia, and the secondary stress. The last two factors are unknown to the designer when he commences the computation of his arch. To enable him to use an approximation in which these unknown quantities disappear, the first term of equation (165) of the Appendix is useful, viz.:

$$H_t = \frac{6EI_0wt}{z_0f}.$$

This equation is for a parabolic arch axis and $z_0 = \frac{8}{15}f$, so that

$$H_t = \frac{45EI_0wt}{4f^2},$$

and substituting $Ew = 0.56$,

$$H_t = \frac{45\times 90.7\times 0.56\times 15}{4\times(54.3)^2} = 2.91 \text{ tons.}$$

This value is sufficiently close to 2.96 tons for all practical purposes.

The point of application of this force is on the axis DD, which axis is found from the correction of the tangent curves to be 45.87 ft. above the line AB.

(*b*) Effect of a Yielding of the Abutments.—The stress in the arch due to this cause can be treated as a temperature change, and equation (162) or (165) gives the intensity of the horizontal thrust, viz.:

$$H_s = \frac{EI_0\Delta l}{d_0\left(\Sigma_0^l y_m v_m + \frac{I_0 l}{F_0 d_0}\right)}.$$

Assume that the abutments yield, increasing the span 0.1 ft.; then

$$H_s = \frac{140{,}000 \times 90.7 \times 0.1}{77{,}430} = 17.05 \text{ tons,}$$

and acts along the line DD.

This horizontal thrust acts in the same manner as a decrease in temperature on the stresses in the arch, and, though the increase in the intensity of the force is small, it is shown on a preceding page that a horizontal thrust of 2.96 tons resulting from a decrease in temperature causes an increase of eccentricity of 0.7 ft. in the line of pressure; and the yielding of 0.1 ft. of the abutment will increase this eccentricity 3.6 ft., and consequently more than double the stresses in the extreme fibers of the arch rib.

This demonstration shows how necessary it is for the strength of the arch that the abutments should be rigidly fixed.

Effect of a Change in the Curvature of the Arch Axis.—All the equations which determine the intersection locus and the tangent curves of the hingeless arch are defined mainly by the variation in the moment of inertia and the area enclosed by the arch axis and the line AB. For convenience this line AB will be called the "chord of the arc," and the area enclosed is then the area of a segment.

A change in the form or curvature of the arch may be made and, provided the area of the segment does not alter, the intersection locus and the tangent curves will not change appreciably. This was demonstrated in Art. 7 of the present chapter, and unless the change in the curvature of the axis is very marked, the change in the locus and tangent curves can be ignored.

From this it follows that "a change in the curvature of the arch axis does not influence the *position* or the *magnitude* of the line of pressure, so long as the area of the segment remains unchanged."

This principle affords a convenient method of improving the form of the arch and reducing the stresses therein, by simply changing its curvature. The application of this method was described in Art. 4 of the present chapter.

9. Deflections of the Hingeless Arch and Their Influence on the Erection.—A knowledge of the deflections of the arch is of great importance, not only for the determination of its displacements under the live load, but more particularly on account of its change of form when the centers are lowered.

The arch is erected resting on falsework, and in that position it is practically without stress or weight. When the falsework is removed the dead load exerts itself and causes stresses. These stresses bring about a change of form in the arch, and, unless the designer is sure that these stresses and the change of form which they cause correspond to those found by computation, much of the labor expended has been wasted.

In the following paragraphs the Syra Valley Bridge is again used as an example, though the process is applicable in the same manner to a hingeless steel arch.

An arch should be erected on falsework which is so arranged that any change in form of the latter during erection can be remedied by wedges, but preferably by set-screws or some other mechanical means. An unyielding falsework or centering should be built, if conditions permit, and the lagging should be of uniform thickness so that the finished falsework presents a smooth and even surface.

A good, practical rule for the erection of arches under 150-ft. span, on an unyielding falsework, is that the centers for such a falsework should be framed for a rise of arch greater than the final rise by an amount equal to one eight-hundredth part of the span. The time between the finishing of the arch and the striking of the centers should be regulated by the nature of the material of which the arch is built, varying from 30 days for good concrete to 60 days for rubble masonry in cement mortar.

Great care should be taken to lower the centers uniformly, preference being given to mechanical devices for the support of the centering which will effect a gradual and even movement.

Any tendency of the centering to rise at the crown when the haunches are loaded, should be counteracted by loading the crown, this load to be varied, according to necessity, so that no changes will take place in the form of the centering except those caused by direct stress; these changes are to be corrected by raising the supports of the centering.

The concrete or masonry should be laid in transverse sections of the full width of the arch, and between timber forms whose planes are normal to its axis. The lengths of the sections should be such that the center section, or a pair of intermediate or end sections, can be completed in one day.

Ordinarily, work should be started at the center section, and carried thence towards the ends. This, however, is not an inflexible rule, and it may be changed to suit the design and the conditions.

For an arch of 300 ft. span the increase in rise should be more definitely determined than is possible by using the rule given on the

preceding page, viz.: The increase in rise should be equal to the deflection of the arch when its centering is lowered, or to the deflection caused by the dead load.

From equation (171) of the Appendix,

$$\frac{o}{H}=\left(m\frac{I_0}{I_1}+c\right); \quad . \quad . \quad . \quad . \quad . \quad . \quad . \quad (171^A)$$

from equation (166),

$$o=M\frac{I_0}{I_1}+\frac{I_0}{r\cos a}\left(\frac{P}{F}-Ewt\right); \quad . \quad . \quad . \quad . \quad . \quad (166^A)$$

also, from Equations (167) and (168),

$$-EI_0\Delta y=M_{o_v}+C_1; \quad . \quad . \quad . \quad . \quad . \quad (167^A)$$

$$EI_0\Delta x=M_{o_h}+C_2. \quad . \quad . \quad . \quad . \quad . \quad (168^A)$$

The influence of the secondary stress on the deflection is so small that $\frac{I_0}{r\cos a}\frac{P}{F}$ in equation (166^A) may be neglected. The deflection caused by changes in temperature is computed separately, and equations (171^A) and (166^A) are written:

$$\frac{o}{H}=m\frac{I_0}{I_1}; \quad . \quad . \quad . \quad . \quad . \quad . \quad . \quad (171^B)$$

$$o=M\frac{I_0}{I_1}. \quad . \quad . \quad . \quad . \quad . \quad . \quad . \quad (166^B)$$

It is desired to obtain the vertical deflections of the arch for a load placed at IV, Fig. 35E'.

The components for a load at IV are the lines FJ and $F'J$. The moment M at any point of the arch axis is equal to the vertical ordinate from the component to the arch axis multiplied by the horizontal thrust. If this ordinate is called y_3,

$$M=y_3H \quad \text{and} \quad o=\frac{I_0}{I_1}y_3H.$$

The reduction $\frac{I_0}{I_1}$ has been repeatedly described and can be performed graphically or analytically; the author, however, recommends the analytical method for computing the deflections. The ordinates of the dotted line $J'L$, measured to the components FJF_1, are equal to $\frac{I_0}{I_1}y_3$, and the sum of all these ordinates should be equal

to zero. This is in accordance with Winkler's law, and gives a means of checking the computation.

The computation of $m\frac{I_0}{I_1}$ can be made graphically, with sufficient accuracy and a great saving in time and labor; and for the purpose of obtaining the additional rise for the centering, the graphical method gives all the ordinates direct.

The ordinates of the line $J'L$ are plotted as vertical forces in a force polygon (see Fig. 36), *e.g.*, force $1=J_{,}J_{,,,}$ etc.; the positive ordinates are plotted downward and the negative ordinates upward, or *vice versa*. Fig. 36 shows this clearly: forces 1, 2, and 3 are plotted downward, 4, 5, 6, 7, 8, and 9 upward, 10, 10′, 9′, 8′, 7′, 6′, and 5′ downward, and 4′, 3′, 2′, and 1′ upward; and the figure shows that the force polygon is a closed polygon.

An arbitrary pole distance (here 100 ft.) is now chosen, and the reciprocal polygon $ABCDE$ is drawn in Fig. 36*a*, the line AE being the closing line of the polygon.

The ordinate 4–4′ multiplied by the pole distance of 100 ft. gives the value of $m\frac{I_0}{I_1}$ when the load is placed at IV, and $Hm\frac{I_0}{I_1}=M_{o_v}$. The above ordinates are the averages of the several panels, and

$$\Delta y=\frac{Hm\frac{I_0}{I_1}d_0}{EI_0}.$$

Now H (from Table VII or Figs. 35C and 35C') $=0.3298$ ton when $K=1$ ton; $m\frac{I_0}{I_1}=21.2$ ft.$\times 100=2{,}120$ ft.; E in ton-feet $=140{,}000$; $I_0=90.7$, and $d_0=15$ ft.

When these values are substituted in the above equation the deflection is obtained in feet, or, when multiplied by 12,

$$\Delta y=\frac{\overset{\text{Inches}}{12}\times\overset{H}{0.3298}\times\overset{m\frac{I_0}{I_1}}{2{,}120}\times\overset{d_0}{15}}{140{,}000\times 90.7}=0.00992 \text{ in.}$$

Fig. 36*a* shows further that the point C corresponds with the point C'' of Fig. 35E'. This is the point where no deflection takes place. To the left of this point the arch sinks, and to the right it rises; C is therefore the point of contraflexure.

To obtain the deflection caused by a vertical load placed at the crown, Figs. 36*b* and 36*B* show that it is only necessary to construct one-half of each polygon, as they are symmetrical with respect to the center line.

To obtain the deflection for a load of one ton: the horizontal thrust is 1.4379 tons, and

$$\Delta y=\frac{12\times15\times1.4379\times5.2\times100}{140,000\times90.7}=0.01062 \text{ in.}$$

(ab measured with the scale of the drawing $=5.2$ ft.; pole distance $=100$ ft.)

The point C in Fig. 36B is again the point of contraflexure, and a load placed between the points A and C will cause a rise of the crown, etc.

To obtain the horizontal displacement of the arch, Figs. 36 or 36b should be drawn as force polygons, with the forces acting horizontally, and the corresponding reciprocal polygons should be drawn on the horizontal lines I, II, etc., which were used for the construction of Figs. 35B, 35C, and 35D.

(a) INCREASE IN THE RISE TO BE GIVEN TO THE CENTERING.—While the computation of this value is practically identical with the one described in preceding paragraphs, yet in order to relieve the designer of all uncertainty, the work will be repeated.

In Art. 8 was described the analytical method for computing the eccentricity of the line of pressure with respect to the axis of the arch. The ordinates are as follows:

I	II	III	IV	V	VI	VII	VIII	IX	X
−4.03	−0.45	+1.50	+2.26	+2.62	+2.69	+2.43	+1.41	+2.105	+3.23*

These values multiplied by $\frac{I_0}{I_1}$ (from Table VII) give respectively:

−2.08	−0.27	+1.15	+2.12	+3.05	+3.92	+4.49	+3.50	+6.62	+13.75

In this case it is advisable to add the value of the constant

$$C=\frac{I_0}{F_0 r\cos a}=\frac{90.7}{9.66\times234.36\times0.7683}=+0.0522,$$

and the forces for the force polygon are then

--2.03	−0.22	+1.20	+2.17	+3.10	+3.97	+4.54	+3.55	+6.67	+13.8

A pole distance is now computed, as follows:

Pole distance $=\frac{1}{n}\,\frac{EI_0}{Hd_0\times12\text{ (inches)}}$, and, assuming $n=10$, H (from Art. 8) $=213.94$ tons, $E=140,000$ (ton-feet), $I_0=90.7$, and $d_0=15$ ft., the pole distance $=33$ ft.

* These values show that the line of pressure passes 3.23 ft. above the axis of the arch at the crown. By changing the curvature of the axis, as described in Art. 8 of this chapter, it will increase in rise, and it will be seen now that the circular arch axis was only assumed by the author for the purpose of illustrating the application of corrections.

Plotting the forces and the pole distance to the same scale and drawing the reciprocal polygon, the ordinates of the polygon will be equal to ten times the deflections at the panel points in inches, caused by the dead load, when these ordinates are measured with the scale of the force polygon. When this scale $= \frac{1}{10}$, the ordinates of Fig. 37*a* are equal to the deflection in inches.

Fig. 37 is the force polygon and Fig. 37*a* the reciprocal polygon. The increase in the rise to be given to the centers has been inserted in each panel, and the deflection at the crown $= 3.98$ ins.

When the proper correction is made to the curvature of the arch axis, and the conjugate pressure of the earth fill behind the vertical wall is considered in the computation, the deflections shown in the diagram decrease considerably.

The foregoing figures show, in connection with the erection of a large arch, how necessary it is to compute the deflections at the panel points caused by the dead load.

For an arch of these dimensions no empirical equation can be given that is general in its application, as the above figures conclusively prove that the curvature of the axis is an important factor.

According to the practical rule stated previously in this chapter, the increase in rise to be given to the centers at the crown of the arch under consideration is 2.25 ins.; and after the centers are lowered, the axis of the arch will be found to be too low. (See Art. 10, Shrinkage of Masonry.)

10. Deflection of the Hingeless Arch Caused by Temperature Changes, Shrinkage of Masonry, and Yielding of Abutments.—Each of these causes may be assumed to affect the arch in the same manner as would a change in temperature, and for this reason they are treated together.

A change in temperature of 15° F. causes a horizontal thrust of 2.96 tons; and an increase in the span of 0.1 ft., due to yielding of the abutments, causes a horizontal thrust of 17.05 tons [see Art. 8 (*a*)].

Shrinkage of the Masonry.—Information on this subject is very meager. In a masonry arch the shrinkage finds its origin in the mortar joints, and rubble masonry contracts more than dimension-stone masonry. Some investigations have been made on the subject, from which it appears that the shrinkage is largely caused by the cement in the mortar which binds together the stone blocks in the masonry, or the broken stone in the concrete.

Coefficients of Shrinkage:

Cement	0.0014 to 0.0034
1 cement: 3 sand	0.0008 to 0.0015
1 cement: 5 sand	0.0008 to 0.0014

In the arch under consideration there are 110 half-inch joints, or total length of joints $= 4.58$ ft.

Assuming a 1:3 mortar to be used, the average shrinkage coeffi-

cient is taken as 0.0012, and the total shrinkage in the length of the arch is $4.58 \times 0.0012 = 0.0055$ ft.

The total length of the arch axis is 325.5 ft., and the coefficient of contraction is 0.000016 ($= 0.0055 \div 325.5$).

The coefficient of contraction for 1° F. is 0.000004, and the shrinkage of the masonry will consequently have the same effect on the arch as a drop in temperature of 4°, decreasing the horizontal thrust by $\frac{4}{15} \times 2.96 = 0.79$ ton.

From equation (173) of the Appendix,

$$EI_0 \Delta y = H_t m_x + 2\left(Ewt - \frac{H_t}{F_0}\right) I_0 y.$$

H_t, as obtained before for a change of temperature of 1° F., $= 0.197$ ton$\left(= \frac{2.96}{15}\right)$. Calling this horizontal thrust h_t, then $H_t = th_t$.

For the shrinkage of the masonry ($H = 0.79$ ton), m_x is the ordinate of the horizontal thrust curve at the point of the arch axis to be investigated (see Fig. 35C'). At the crown, $m_x = CE \times p \times d_0$; $k = CE = 92.5$, $p = 80$, $d_0 = 15$, and $m_x = 1{,}200k$. $H_t = 0.197$. $Ewt = 140{,}000 \times 0.000004 = 0.56$ (foot-ton) for 1° F.;

$$I_0 = 90.7,$$

$$F_0 = 9.66,$$

and

$$\Delta y = \left[\frac{h_t m_x}{EI_0} + \frac{2\left(Ew - \frac{h_t}{F_0}\right) y_1}{E}\right] t$$

$$= \left[\frac{0.197 \times 1{,}200k}{140{,}000 \times 90.7} + \frac{2\left(0.56 - \frac{0.197}{9.66}\right) y_1}{140{,}000}\right] t.$$

Δy will be expressed in feet, and to obtain the deflection in inches the above value should be multiplied by 12, which gives

$$\Delta y = (0.0002232k + 0.000000924 y_1) t.$$

For the deflection at the crown $k = 92.5$, $y_1 = 54.3$, and with a temperature difference of 15°

$$\Delta y = (0.0206 + 0.00004) 15 = 0.369 \text{ in.}$$

The second term represents the deflection caused by the secondary stress and is equal to but 0.06 in. It may therefore be neglected and the equation written

$$\Delta y = \frac{H_t m_x}{EI_0} t.$$

The shrinkage in the masonry will then cause a deflection of

$$\tfrac{4}{15}\times 0.369=0.098 \text{ in.}$$

In shaping the falsework an additional rise of 0.1 in. should be given to it; and in computing the stresses in the arch, the horizontal thrust caused by shrinkage is to be considered as an initial stress. This value is small, and no grave error is committed by neglecting it completely.

To obtain the deflection caused by the yielding of the abutments equation (173) of the Appendix gives

$$\Delta y=-\frac{\Delta l}{W}\left(m_x-2\frac{I_0}{F_0}y_1\right),$$

and

$$W=\int_0^l \frac{I_0}{I_1}y^2ds+\frac{I_0}{F_0}\frac{l}{d_0}.$$

In these equations m_x is again the ordinate of the horizontal-thrust curve (Fig. 35C') at the point x_1, and W the line $A'B'$ of Fig. 35C.

$W=pd_0\overline{A'B'}=80\times 15\times 64.8=77{,}760$; $I_0=90.7$; $F_0=9.66$; y_1 at the crown of the arch $=54.3$; consequently m_x is again equal to $kpd_0=1{,}200k$, and

$$\Delta y=-\Delta l\frac{1{,}200k-18.82y_1}{77{,}760}.$$

At the crown $k=92.5$, and $y_1=54.3$; assuming $\Delta l=0.1$ ft.,

$$\Delta y=0.1\frac{111{,}000-1{,}022}{77{,}760}=0.1415 \text{ ft.}=1.7 \text{ ins.}$$

This completes the calculations required for the hingeless masonry arch. As a useful exercise for the student desiring to test his understanding of this chapter, the author would suggest that he first find the curve of the Syra Valley arch from the ordinates given in Art. 9 (*a*). for which the stresses in the arch at the crown become a minimum for dead load only;

Second, that he find the curve for which the stresses in the arch are most advantageously distributed, when the arch sustains the dead-load stress and the initial stress caused by shrinkage and an increase in temperature of 10° F.;

Third, that he determine the stresses in the arch caused by a yielding of the abutments which increases the span by ½-in.;

Fourth, and as a final exercise, that he compute the conjugate pressure of the spandrel filling against the vertical wall of Fig. 35 (using equation (*a*), Art. 3, of the present chapter), and also find the line of pressure in the arch, employing the graphical method, and checking results by an analytical computation.

TABLE
SYRA VALLEY
SECONDARY STRESS—VARIABLE

	Panel Points.	1	2	3	4
1	$I_0=234.36 \quad f=54.3 \quad y_1$	6	16.58	25.53	33.05
2	$90^\circ-\alpha$	52° 32′ 51″	57° 2′ 13″	61° 18′ 32″	65° 24′ 46″
3	β	4° 35′ 34″	4° 22′ 51″	4° 11′ 17″	4° 2′ 13″
4	s	18.784	17.985	17.129	16.442
5	$F_0=9.66 \quad h=F$	12.8276	12.0173	11.2457	10.5050
6	$I_0=90.7 \quad I_1=$	175.9	144.6	119.4	96.6
7	$\Sigma v''m=34.236. \quad \frac{I_0}{I_1}=v''m$	0.51557	0.6017	0.76519	0.9390
8	$y_2=45.865, \quad y_1-y_2=y$	−39.865	−29.285	−20.335	−12.815
9	$y\frac{I_0}{I_1}=vm$	−20.553	−18.366	−15.561	−12.033
10	xm	142.5	127.5	112.5	97.5
11	$\Sigma xmv'm=128{,}296.5 \quad xm\frac{I_0}{I_1}=v'm$	73.469	79.962	86.084	91.552
12	$\Sigma y'mvm=4{,}974. \quad y'mvm$	−123.32	−304.51	−397.25	−397.70
13	$\mathfrak{M}_m vm$	0	308.295	891.48	1709.28
14	$\Sigma y'mvm+\frac{I_0 l}{F_0 d_0}=\frac{m}{K}=H$	0	0.0594	0.172	0.3298
15	$X_1=H\frac{c_2-c_1}{l}$ or $\frac{X_1 l}{2H}=\frac{c_2-c_1}{2}$	....	167.47	85.88	54.79
16	$\frac{X^2}{H}=e_0$	....	185.63	105.15	75.229
17	X_1	....	0.0664	0.0985	0.1205
18	$\mathfrak{V}_1$	0.975	0.925	0.875	0.825
19	$\mathfrak{V}_1+X_1=V_1$	....	0.9914	0.9735	0.9455
20	$z_0+e_0+\frac{c_2-c_1}{2}=-\frac{V_1}{H}\times x_1$	....	374.99	212.24	150.43
21	$+y_2-e_0-\frac{c_2-c_1}{2}=c_1$	....	−307.24	−145.17	−84.15
22	$+y_2-e_0+\frac{c_2-c_1}{2}=c_2$	....	+27.70	+26.59	+25.43
23	Ordinates of locus $=y_2+z_0$	....	67.75	67.07	66.28

TABLE
SYRA VALLEY
VARIABLE MOMENT OF
(NO SECONDARY

Panel Points.		1	2	3	4
H	(14)	....	0 063	0.1792	0.3437
X_1	(17)	....	0.0664	0.0985	0.1205
$\frac{c_2-c_1}{2}$	(15)	....	160.72	82.416	52.585
e_0	(16)	....	177.86	100.62	71.904
V_1	(18)	....	0.9914	0.9735	0.9455
$z_0+e_0+\frac{c_2-c_1}{2}=\frac{V_1}{H}x_1$	(20)	....	359.89	203.69	144.45
$+y_2-e_0-\frac{c_2-c_1}{2}=c_1$	(21)	....	−292.72	−137.17	−78.62
$+y_2-e_0+\frac{c_2-c_1}{2}=c_2$	(22)	....	+28.73	+27.66	+26.55
Ordinates of locus $=y_2+z_0$	(23)	....	+67.18	66.52	65 83

VII.

BRIDGE.

MOMENT OF INERTIA—CURVATURE.

5	6	7	8	9	10		
39.30	44.37	48.35	51.29	53.22	54.18		1
69° 23′ 11″	73° 15′ 31″	77° 3′ 13″	80° 47′ 29″	84° 29′ 26″	88° 9′ 3″		2
3° 55′ 23″	3° 50′ 1″	3° 45′ 59″	3° 43′ 12″	3° 40′ 48″	3° 40′ 41″		3
16.046	15.679	15.404	15.215	15.051	15.043		4
9.7821	9.0758	8.3818	7.6964	7.0184	6.3407		5
78.0	62.3	49.07	37.6	28.81	21.1		6
1.1627	1.4558	1.8482	2.4125	3.1481	4.2691		7
−6.565	−1.495	+2.485	+5.425	+7.335	+8.315		8
−7.633	−2.178	+4.593	+13.081	+23.154	+35.497		9
82.5	67.5	52.5	37.5	22.5	7.5		10
95.922	98.268	97.03	90.471	70.832	32.018		11
−299.98	−96.63	+279.56	+671.29	+1232.30	+1923.30	$\frac{I_0 l}{F_0 d_0} = 188$	12
2706.98	3819.17	4964.03	6039.99	6919.74	7452.18		13
0.5223	0.7369	0.9578	1.1654	1.3351	1.4379		14
37.84	26.84	18.86	12.57	7.23	2.37		15
59.603	50.146	43.995	39.907	37.371	35.962		16
0.1318	0.1319	0.1204	0.0977	0.0643	0.0227		17
0.775	0.725	0.675	0.625	0.575	0.525		18
0.9068	0.8569	0.7954	0.7227	0.6393	0.5477		19
117.19	95.935	80.97	69.765	61.051	54.28		20
−51.58	−31.12	−16.99	−6.61	+1.26	+7.53		21
+24.10	+22.56	+20.73	+18.53	+15.72	+12.27		22
65.61	64.82	63.98	63.16	62.31	61.81		23

VIII.

BRIDGE.

INERTIA AND CURVATURE.

STRESS.)

5	6	7	8	9	10
0.5442	0.7678	0.9980	1.2140	1.3910	14.980
0.1318	0.1319	0.1204	0.0977	0.0643	0.0227
36.316	25.756	18.101	12.065	6.938	2.276
56.912	47.832	41.929	38.005	35.656	34.221
0.9068	0.8569	0.7954	0.7227	0.6393	0.5477
112.47	92.07	77.708	66.954	58.592	52 093
−47.36	−27.72	−14.17	−4.21	+3.29	+9.37
+25.27	+23.79	+22.04	+19.93	+17.17	+13.92
65.11	64.35	63.54	62.75	61.88	61.46

TABLE

SYRA VALLEY

CURVATURE ONLY (NO VARIABLE MOMENT

Panel Points		1	2	3	4
$f=54.3$	y_1	6	16.58	25.53	33.05
$y_2=37.187$, $y_1-y_2=y$		−31.187	−20.607	−11.657	−4.137
$\Sigma y'mvm=4{,}951.3$	$H=$	0	0.0945	0.2514	0.4436
	e_0	....	110.14	65.739	48.817
	z_0	....	30.564	28.552	28.192
Ordinates of intersection locus		....	67.751	65.739	65.379
	s_1	....	203.759	115.043	80.548
	c_1	....	−106.57	−77.856	−43.36
	s_2	....	16.521	16.435	17.086
	c_2	....	20.67	20.752	20.10

TABLE

SYRA VALLEY

ORDINATES OF THE INTERSECTION LOCUS.

Panel Points			1	2	3	4
$y_2=0.844$		I		1.246	1.232	1.218
$y_2=0.844$		II		1.234	1.224	1.212
$y_2=0.683$		III		1.206	1.204	1.202
$y_2=0.683$	(Parabola)	IV			1.231	
ORDINATES OF c_1.						
		c_1 I		−5.66	−2.675	−1.55
		c_1 II		−5.39	−2 525	−1.451
		c_1 III		−3.070	−1.433	−0.798
		c_1 IV	−10.260	−2.965	−1.502	−0.865
ORDINATES OF c_2.						
With inertia, with secondary		c_2 I		+0.511	+0.49	+0.471
" " without secondary		c_2 II		+0.529	+0.510	+0.488
Without inertia, without secondary		c_2 III		+0.300	+0.385	+0.371
(Parabola)		c_2 IV	+0.403	+0.300	+0.376	+0.360
ORDINATES OF THE ARCH-AXIS RISE=1 (AND OF THE PARABOLA RISE=1.026).						
Arch axis	y_1	a	0.1105	0.305	0.470	0.608
Parabola	y_1	b	0.1	0.2845	0.448	0.593
			0.0075	0.2775	0.4375	0.5775

I. Including secondary stress, variable moment of inertia, and curvature.
II. Including variable moment of inertia and curvature.

IX.

BRIDGE.

OF INERTIA; NO SECONDARY STRESS).

5	6	7	8	9	10
39.30	44.37	48.35	51.29	53.22	54.18
+2.113	+7.183	+11.163	+14.103	+16.033	+16.993
0.6484	0.8467	1.0233	1.1664	1.2666	1.3182
40.36	35.322	32.156	30.142	28.941	28.377
28.138	28.17	28.217	28.257	28.29	28.306
65.325	65.357	65.404	65.444	65.477	65.493
62.558	51.217	43.41	37.678	33.293	29.796
−25.371	−14.03	−6.22	−0.49	+3.89	+7.39
18.162	19.427	20.902	22.606	24.589	26.958
19.03	17.76	16.29	14.58	12.6	70.23

X.

BRIDGE.

5	6	7	8	9	10	
Ordinates of the Intersection Locus.						
1.207	1.192	1.178	1.161	1.146	1.138	
1.198	1.183	1.167	1.153	1.141	1.131	
1.201	1.201	1.202	1.203	1.204	1.205	
Ordinates of c_1.						
−0.951	−0.573	−0.313	−0.1217	+0.0205	+0.139	
−0.872	−0.511	−0.261	−0.078	+0.053	+0.166	
−0.468	−0.258	−0.115	−0.008	+0.083	+0.145	
−0.572	−0.334	−0.166	−0.043	+0.040	+0.108	for 1.026
Ordinates of c_2.						
+0.444	+0.415	+0.382	+0.341	+0.29	+0.226	
+0.462	+0.431	+0.394	+0.350	+0.298	+0.237	
+0.351	+0.327	+0.300	+0.270	+0.236	+0.196	
+0.341	+0.318	+0.290	+0.256	+0.215	+0.166	for 1.026
Ordinates of the Arch-axis Rise = 1 (and of the Parabola Rise = 1.026).						
0.725	0.817	0.891	0.945	0.981	0.998	$f=1$
0.715	0.818	0.9	0.961	1.002	1.022	$f'=1.026$
0.6975	0.7975	0.8775	0.9375	0.9775	0.9975	1

III. Curvature only.
IV. Ordinates for the equivalent parabola.

CHAPTER V.

STRESSES IN ARCH SECTIONS—DISTRIBUTION OF STRESSES OVER AN IRREGULAR AREA UNDER NORMAL LOAD.

1. Stresses in a Bar Subjected to Compression and Bending.—(See also Chapter VII, Article 1.)—If a bar is acted on by exterior forces and their resultant reactions, and a normal section is taken through this bar, all forces to the left of the section can be reduced to two in number, viz. (see Fig. 39): one acting at right angles to the plane of the section and called axial force, the other acting at right angles to the axis of the bar and called the cross-bending force. The second is usually provided for by lateral stiffening, and is not shown in the figure.

The center of gravity of the section is the origin of a coordinate system, in which the axis XX coincides with the tangent to the axis of the bar. A second cross-section is located at an infinitely small distance from the first section.

The axial force is assumed to act at a point outside the center of gravity of the section, and will therefore produce an angular as well as a longitudinal displacement of the two neighboring sections.

The dimensions of the section of the bar being small as compared to its length, it is allowable to assume that the dimensions of the neighboring cross-sections do not change during these displacements. It is further assumed that the material of the bar is homogeneous throughout.

On these assumptions the following deductions are based:

In Chapter VIII (Appendix) an analysis is given which leads to the following equations:

$$-n=\frac{P_x}{F}+\frac{M_x}{Fr}+\frac{M_x rv}{J(r+v)}, \quad \ldots \ldots \quad (7)$$

$$-n=\frac{P_x}{F}+\frac{M_x v}{I}. \quad \ldots \ldots \ldots \ldots \quad (7a)$$

In these equations

n = stress per unit area;
P_x = axial force;

F = area of the section of the arch rib;
M_x = bending moment;
r = radius of curvature of the axis of the arch rib at the section;
i = radius of gyration;
v = vertical ordinate of an element of area of the section;
$J = \int \frac{kv^2}{k+v} df$ [see equations (9) and (9a) of Appendix];
I = moment of inertia of the section.

The shearing forces are neglected and the main stresses on the arch rib coincide with the normal stresses, and the above equations express the division of these stresses over the section of the arch rib. In these equations the only variable quantities are n and v, the value of n increasing with the value of v. The maximum and minimum values for v are $+v_1$ and $-v_2$ (see Fig. 40), and these values substituted in the equations give

$$n_1 = -\frac{P_x}{F} - \frac{M_x}{Fr} - \frac{M_x r v_1}{J(r+v_1)}, \quad n_2 = -\frac{P_x}{F} - \frac{M_x}{Fr} + \frac{M_x r v_2}{J(r-v_2)}; \quad (1)$$

and

$$n_1 = -\frac{P_x}{F} - \frac{M_x v_1}{I}, \qquad n_2 = -\frac{P_x}{F} + \frac{M_x v_2}{I}. \quad . \quad . \quad . \quad . \quad (1a)$$

Equations (1a) apply when the radius of curvature of the arch is very large as compared with the depth of the arch rib. This relation obtains in nearly all problems having to do with the design of rib arches, and the equations may therefore be used without involving appreciable errors.

If, in a further analysis of equations (1a), in place of M_x its value $P_x p_x$ [see equation (2), Appendix] be substituted,

$$n_1 = -\frac{P_x}{F}\left(1 + \frac{F p_x v_1}{I}\right), \quad n_2 = -\frac{P_x}{F}\left(1 - \frac{F p_x v_2}{I}\right). \quad . \quad . \quad (1b)$$

These equations show that the distribution of the stresses over the area of the section is particularly dependent on the distance p_x, that is (see Fig. 2), the distance from the point G to the point (x, y) of the arch axis, the point G being the point of intersection of the plane of section with the force R_1, which is the resultant of all the exterior forces.

In equations (1b) the value i^2F can be substituted for I; then

$$n = -\frac{P_x}{F}\left(1 + \frac{p_x v}{i^2}\right), \quad . \quad . \quad . \quad . \quad . \quad . \quad . \quad . \quad (2)$$

and the normal stresses are distributed over the section as follows:

$$\overset{v=v_1}{n_1=-\frac{P_x}{F}\left(1+\frac{p_x v_1}{i^2}\right)},\quad \overset{v=0}{n_0=-\frac{P_x}{F}},\quad \overset{v=-v_2}{n_2=-\frac{P_x}{F}\left(1-\frac{p_x v_2}{i^2}\right)}. \qquad (3)$$

These equations show that n_1 and n_2 are stresses of the same kind when $1+\frac{p_x v_1}{i^2}>0$ and $1-\frac{p_x v_2}{i^2}>0$, or $1+\frac{p_x v_1}{i^2}<0$ and $1-\frac{p_x v_2}{i^2}<0$. Only the first condition can be satisfied, the second being impossible. The first condition gives

$$p_{x_i} > -\frac{i^2}{v_1}, \text{ and at the same time } < \frac{i^2}{v_2}. \quad . \quad . \quad . \quad . \qquad (4)$$

Equation (4) shows that an arch-rib section has two points, N_1 and N_2, at the distances j_1 and j_2 from the axis of the arch (see Fig.

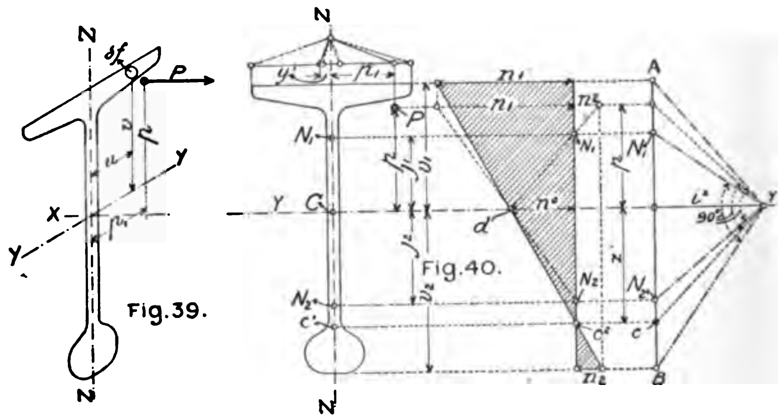

40) which divide the section so that the normal stresses over it are of one kind when the force P passes between these two points.

$$j_1=\frac{i^2}{v_2} \quad \text{and} \quad j_2=-\frac{i^2}{v_1}. \quad . \quad . \quad . \quad . \quad . \quad . \quad . \qquad (5)$$

When the force passes through the point N_2 the stress n_1 will be zero, and when the force passes through the point N_1 the stress n_2 will be zero. N_2 can be called the zero point for the stress n_1 in the upper fibers, and N_1 the zero point for the stress n_2 in the lower fibers of the section.

(*a*) Core, Core Points, and Core Lines.—The points N_1 and N_2 indicate the limits between which the force P can shift and cause normal stresses of but one kind in the section. In this book these

points are called the "core points" of the section, the lines joining these points in the consecutive sections of an arch rib are called the "core lines," and the space between these two points at any section is called the "core" of the section.

Graphical Construction of the Core Points.—The core and the core points are important factors in the computation of stresses in arches, and when their location is known the maximum stresses in the section can be easily determined.

In equations (5) the quantities i and v are functions of the section of the arch rib, from which it follows that j_1 and j_2 are functions which depend only on the form of the section, being independent of the force P and its point of application with regard to the section.

The points N_1 and N_2 can be easily found by construction (see Fig. 40). Equations (5) may be written

$$j_2:i=i:v_1 \quad \text{and} \quad j_1:i=i:v_2.$$

In these equations i is the radius of gyration of the section and is measured from an axis AB to the scale of the drawing on a line which passes through the center of gravity of the section. From the point thus obtained a right-angled triangle is drawn so that one of its sides intersects the axis at A or B; its other side then intersects the axis at N_2 or N_1. The construction is shown in the figure and requires no further explanation.

(*b*) Computation.—The introduction of the quantities j_1 and j_2 into equation (3) gives

$$\left.\begin{aligned} n_1&=-\frac{P_x}{F}\left(\frac{j_2+p_x}{j_2}\right)=-\frac{P_x(j_2+p_x)}{I}v_1=-\frac{M_{N_2}v_1}{I},\\ n_2&=-\frac{P_x}{F}\left(\frac{j_1-p_x}{j_1}\right)=-\frac{P_x(j_1-p_x)}{I}v_2=+\frac{M_{N_1}v_2}{I}.\end{aligned}\right\} \quad . \quad . \quad . \quad (6)$$

M_{N_2} and M_{N_1} represent the moments of the exterior forces with the core points N_2 and N_1 as fulcrums.

Equations (6) can also be written in the form

$$n_1=-\frac{P_x}{F}\left(1+\frac{p_x}{j_2}\right), \qquad n_2=-\frac{P_x}{F}\left(1-\frac{p_x}{j_1}\right), \quad . \quad . \quad (6a)$$

from which the stresses in the extreme fibers can be found by the graphical method as ordinates which are measured on a line coinciding with the force P.

$$\frac{P_x}{F}=\text{a constant}=n_0=\text{force } P_x \div \text{total area of section.}$$

This value of n_0 is plotted in Fig. 40 on a line which passes through the center of gravity of the section. The line joining N_2 and d, pro-

longed to an intersection with the force P, determines the ordinate n_1 on this force, and the line joining d and N_1, prolonged to an intersection with the force P, determines the ordinate n_2.

To find the point in the section where the stress n equals 0 (which can be called the zero point of the section), the value of n in equation (2) is placed equal to zero, which gives

$$i^2 = -p_x v.$$

This shows that the zero point is not only a function of the form of the section, but also of the distance p_x.

This equation indicates that p_x and v are again the two parts of a hypothenuse, as already explained; the construction lines are all shown in Fig. 40, and further comment is unnecessary.

In this figure the force P does not act in the vertical axis ZZ of the beam, but at a distance p_1 therefrom.

To obtain the distribution of the stresses over the section, the computations described in the former paragraphs should be made independently for the axes YY and ZZ, and to obtain the total stress at any point of the section, the stress obtained with respect to the axis YY for this point should be added to that obtained with respect to the axis ZZ for the same point.

2. **Example.—Distribution of the Stresses in an Arch Rib of Any Arbitrary Section** (see Fig. 40).—The arch rib assumed is a 9-in. Pencoyd deck-beam (No. 63); weight per foot = 24.68 lbs.; sectional area = 7.26 sq. ins.; radius of gyration with respect to the Y-axis = 3.44 ins.; distance from neutral axis to the top of beam = 4 ins.

Distance of core point N_1 from neutral axis $= 3.44^2 \div 5 = 2.37$ ins.
" " " " N_2 " " " $= 3.44^2 \div 4 = 2.96$ ins.

(*a*) *Dead Load.*—The dead load causes a pressure of 8,000 lbs., and its center of application is located 1 in. above the neutral axis.

The maximum stress in the upper fibers of the beam $= \dfrac{2.96+1}{2.96}$ $= -1.335$ units compression, and in the lower fibers $= 2 - 1.335 = 0.665$ units compression.

If the load were applied at the center, the stress per square inch would be $8{,}000 \div 7.26 = 1{,}103$ lbs., and

Compression in upper fibers $= 1.335 \times 1{,}103 = 1{,}470$ lbs.
" " lower " $= 0.665 \times 1{,}103 = 736$ "

(*b*) *Live Load.*—From one form of live load a pressure of 20,000 lbs. is caused, and its center of application is located 8 ins. above the neutral axis.

Extreme fiber stress in units:

Upper fibers, $\dfrac{2.96+8}{2.96} = 3.71$ units compression.

Lower fibers, $3.71 - 2 = 1.71$ " tension.

Uniformly distributed stress per sq. in. $=20{,}000 \div 7.26 = 2{,}760$ lbs., and extreme fiber stress

in upper fibers $=2{,}760 \times 3.71 = 10{,}230$ lbs. per sq. in. compression;
in lower fibers $=2{,}760 \times 1.71 = 4{,}710$ " " " " tension.

Another form of live load causes a pressure of 19,000 lbs., and its center of application is located 9 ins. below the neutral axis.

Extreme fiber stress in units:

$$\text{Lower fibers, } \frac{2.37+9}{2.37} = 4.78 \text{ units compression;}$$

$$\text{Upper fibers, } 4.78-2=2.78 \text{ " tension.}$$

Uniformly distributed stress per sq. in. $=19{,}000 \div 7.26 = 2{,}620$ lbs. Extreme fiber stress

in lower fibers $=2{,}620 \times 4.78 = 12{,}520$ lbs. per sq. in. compression;
in upper fibers $=2{,}620 \times 2.78 = 7{,}280$ " " " " tension.

The stresses in the upper fibers vary from an initial stress of 1,470 lbs. compression to $(10{,}230+1{,}470=)$ 11,700 lbs. compression, and reverse to $(7{,}280-1{,}470=)$ 5,810 lbs. tension.

In the lower fibers the stresses vary from an initial stress of 736 lbs. compression to $(12{,}520+736=)$ 13,256 lbs. compression, and reverse to $(4{,}710-736=)$ 3,974 lbs. tension.

It should be noted that while the first form of live load produces a greater axial force, the second produces the greater stresses on account of the greater eccentricity of the force.

Therefore, *to find the maximum stresses in an arch, the maximum axial force and the maximum eccentricity of a force must both be investigated.*

3. Distribution of the Stresses in a Solid Arch Rib.—

$$\text{The moment of inertia of a solid rib} = \frac{bh^3}{12} = I.$$

$$\text{The area of a solid rib} = bh = F.$$

$$\text{The square of the radius of gyration } i^2 = \frac{I}{F},$$

or

$$i^2 = \frac{bh^3}{12} \times \frac{1}{bh} = \frac{h^2}{12}.$$

From equation (5) of this chapter and Fig. 40, the distance from the core point to the center of gravity C is

$$j' = \frac{i^2}{v_2},$$

and the section is symmetrical, or

$$j_1 = j_2 \quad \text{and} \quad v_2 = \tfrac{1}{2}h.$$

Also,
$$j' = \frac{h^2 \times 2}{12h} = \tfrac{1}{6}h,$$

which means that the core points are located at one-sixth of the depth of the section above or below the axis.

This is shown in Fig. 41, in which the core points N^1 and N^2 are indicated. The depth EF of the arch rib is taken as the unit of measurement for the point of application of the force; for example, when the force acts at B, its eccentricity is 0.1 of the depth. This

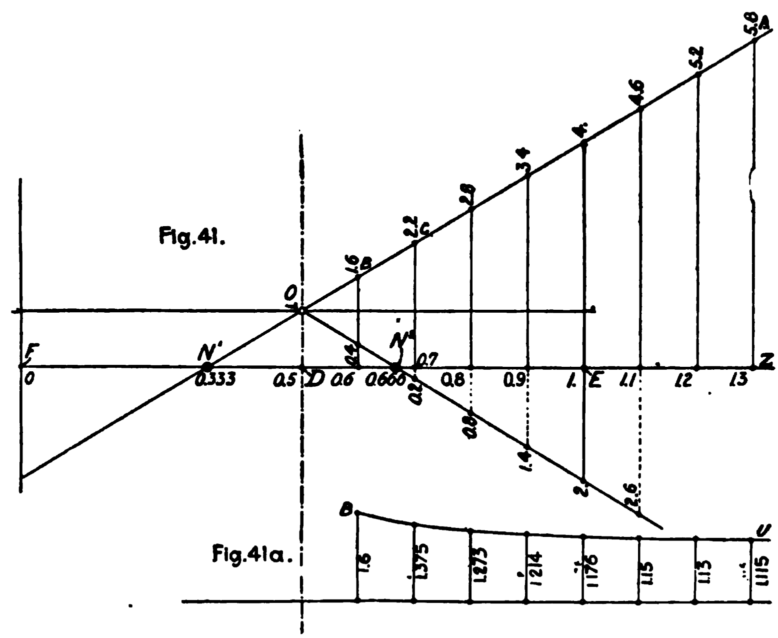

Fig. 41.

Fig. 41a.

figure is convenient for the purpose of reading the stresses of the extreme fibers in units. Its construction follows from the explanation of Fig. 40, viz.: the distance OD = the stress per square inch when the force acts at the center of the section. In this figure the line OD represents the unit stress. Again, the lines ON^1 and ON^2 are drawn, and, as hitherto explained, these lines intercept ordinates on the load lines which are equal to the stresses in the extreme fibers.

(*a*) Ratio of Change in the Maximum and Minimum Stresses as Compared with a Change in the Eccentricity of the Force.—Let the load be assumed to act at B. Then eccentricity = 0.1, the

stress at $E=1.6$ units compression, and the stress at $F=2-1.6=0.4$ unit compression.

If the load acts at C, eccentricity $=0.2$, stress at $E=2.2$ units compression, and stress at $F=2.2-2=0.2$ unit tension, etc.

It should be noted that the sum of the maximum and the minimum fiber stresses is always equal to twice the unit stress. This must be so when it is remembered that the area representing the distribution of stress over the section is a trapezoid, and that the force causing the stress always passes through its center of gravity.

It should be further noted that for every 0.1 of eccentricity of the force the maximum and minimum stresses vary 0.6 unit, which constant of change facilitates the computation of the stresses.

For example, let the force act at a distance above the center of gravity of the section equal to 0.2365 unit. The unit stresses in the extreme fibers are then

$$0.2365 \times 6+1=2.419 \text{ compression,}$$

and

$$=0.419 \text{ tension.}$$

(*b*) Effect of Eccentricity of the Force as Compared with that of its Magnitude.—The ordinates of the line OA measured from the axis ZZ represent the maximum unit pressures per sq. in. in the extreme fibers for a unit force whose point of application shifts parallel to the neutral axis between O and A.

When the force acts at O the unit pressure at the extreme fibers $=1$ unit; at B (where eccentricity $=0.1$) the pressure is 1.6 units; at C 2.2 units, etc.

When the force shifts from O to B the pressure in the extreme fibers rises from 1 to 1.6 units, which is an increase of 0.6 unit, and in order to obtain the same increased pressure without shifting the force, the force itself should be increased in the same ratio (1.6:1).

If the force is shifted from B to C, the maximum pressure per square inch increases from 1.6 to 2.2 units, and in order to obtain the same increased pressure without shifting the force, the latter should be increased in the ratio $2.2:1.6=1.375$, etc.

The respective values thus obtained are plotted and represented by the line BU in Fig. 41*a*.

Shifting the live load on an arch may therefore cause either an increase in the force or an increase in the eccentricity of the force, and the problem ordinarily to be solved in dimensioning arch ribs is to determine which of these yields the maximum stresses.

The foregoing paragraphs have demonstrated how the stresses are distributed over a section when the intensity and the position of the force with relation to the axis of the section are known.

The many examples given have shown how the position and intensity of the force with relation to the axis of an arch are found, and the following article deals specially with the distribution of the stresses over a section made up of two materials, viz., concrete and steel.

4. Stresses in a Reinforced-Concrete Arch Section.—When concrete and steel act together in a beam, the stresses in these two materials are divided in the same ratio as that of their respective moduli of elasticity. For instance, the modulus of elasticity of good concrete (1:2:5) may be assumed as 2,000,000, and that of steel as 30,000,000; the ratio then between these two moduli is 1:15, and a force of 1 pound will cause the same elongation or contraction in a bar of concrete that 15 pounds will cause in a bar of steel of the same dimensions.

The relation between the contraction of concrete and the stress which causes it is the subject of continuous investigation; the data available, however, are meager and diverse.

Fig. 42 represents one of the many tests made by Professor Bach on concrete three months old. In this figure the abscissas represent 1,000,000 times the contraction of the concrete, and the ordinates

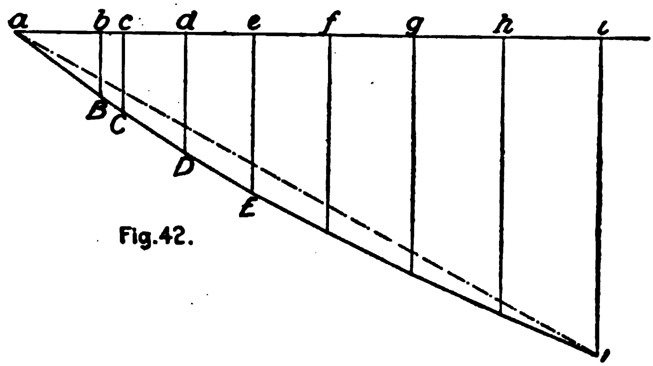

Fig. 42.

represent the corresponding stress in the concrete. For example, when the concrete contracts 0.0000306 of its length ($=ab$), the stress in the concrete is 114 lbs. per sq. in. $=bB$; when the concrete contracts 0.0000853 of its length ($=ae$), the stress is 284 lbs. per sq. in. $=eE$, etc. The area enclosed by the figure aiI represents the area of stress in the concrete, and the line aI is a curved line; to compute the stress in a concrete section the deviation of the line aI from a straight line should be considered. This could be done with great accuracy if the line aI were not subject to change; every bar of concrete tested, however, will produce a different line aI.

The differences between the results obtained can be assigned to the following causes:

1. The age of and the moisture in the concrete.
2. The composition of the concrete.
3. The mode of manufacture.

These three factors are sufficient to produce an infinite number of results. The stress in a well-designed arch rib is compressive, and for this reason the line of Fig. 42 should be considered as com-

mencing at the point B; and this line BI deviates so slightly from a straight line that in the following examples it is assumed to be a straight line. This is a small error on the safe side, and is negligible when considered in connection with 1, 2, and 3.

Many works have been written dealing specially with concrete and reinforced concrete, to which the author refers, the foregoing being only for the purpose of introduction to the examples which follow.

(*a*) EXAMPLE: STRESSES IN THE SECTION OF A CONCRETE ARCH.—The stresses at the section I of Fig. 28*d* will be considered.

The total axial force is 98,900 lbs., its distance from the top of the arch is 1.6 ft. = 19.2 ins., and the depth of the arch rib is 27 ins.

Area of section 1 ft. wide $= 12 \times 27 = 324$ sq. ins.

If the force were applied at the center of the section the unit stress per sq. in. would be $98{,}900 \div 324 = 305.25$ lbs.

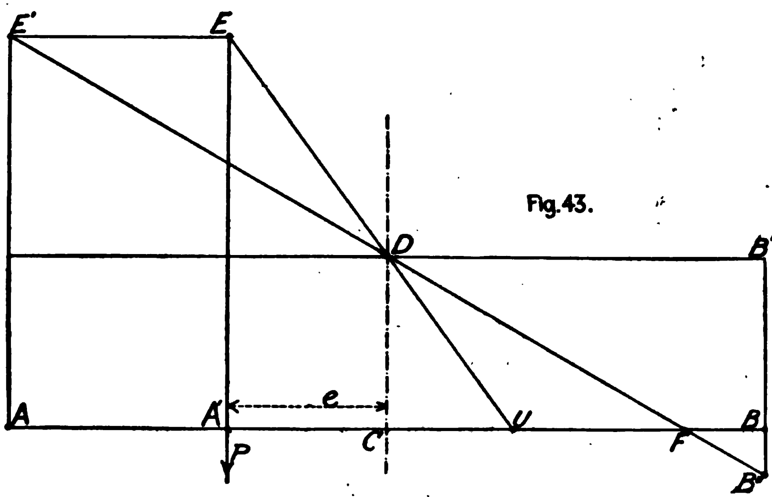

Fig. 43.

In Fig. 43 the line AB is equal to 27 ins., and the eccentricity e of the force $= 19.2 - 13.5 = 5.7$ ins.

The upper core point is indicated by the letter U, and the distance $CU = \frac{1}{6}AB$.

The distance $BB' =$ unit stress $= 305.25$ lbs. per sq. in.

As explained in this chapter, the line EU, which passes through the core point U and the unit-stress point D on the neutral axis of the arch rib, intersects the load line at E and cuts off the distance EA'; this distance, when measured with the scale of forces, gives the stress in the extreme fibers at $A = 691$ lbs. compression.

Transferring the point E to E' and drawing the line $E'DB''$, the intersection of this line with BB' cuts off the distance BB'' ($= 81$ lbs. tension), and the force P passes through the center of gravity of the trapezoid $AE'FB''B$, and there is no stress at the point F.

Fig. 43 shows that the stresses in the arch are too high and that steel bars should be introduced.

The introduction of steel changes the location of the neutral axis of the arch and also that of its core points. These changes are very small and need not be considered, ordinarily, in practice. The error resulting from this procedure results in an excess of steel section, and is therefore on the safe side.

The designer who wishes to consider this change can do so by assuming the steel replaced by a bar of concrete of the same strength; the concrete then will have a sectional area 15 times that of the steel.

The center of gravity of this added concrete is assumed to coincide with that of the steel, and for this altered section the moment of inertia and the radius of gyration are found.

From these the distances of the two core points from the neutral axis are determined, and the remainder of the computation is then performed in the same manner as the one which follows, or, preferably, according to the equation in (*e*) of the present article.

In the following sections

q = pressure per square inch of the axial force acting at the center of gravity of the section;

s = that portion of the pressure q which is resisted by the concrete;

$s_{,}$ and $s_{,,}$ = maximum and minimum stresses per square inch in a section of the arch rib;

e = distance between the axial force and the center of gravity of the section;

b = distance between the center of gravity of the steel and the axial force;

a = distance between the center of gravity of the area of pressure of the concrete and the axial force;

f = distance between each core point and the center of gravity of the section;

C = the resultant of all the interior normal stresses in the concrete;

I = the resultant of all the interior normal stresses in the steel.

(*b*) First Proposition: There Shall Be no Tensile Stresses in the Arch Rib, and the steel is to be imbedded as near to A as is consistent with good construction (see Fig. 44). The line AB is the depth of the arch rib, P is the axial force, and e is its eccentricity. The place where the steel is imbedded in the concrete is indicated by the letter F, and its distance from the force P is equal to b. The distance of the center of gravity of the area of pressure for the concrete from the force P equals a, and the line C represents the resultant force in the concrete, which line must pass through the lower core point D''' of the arch rib.

Now, from conditions of equilibrium,

$$bP = (a+b)C, \quad \text{or} \quad \frac{C}{P} = \frac{b}{a+b}.$$

From the two similar triangles $D'''FG'$ and DFG,

$$\frac{b}{a+b}=\frac{s}{q}, \quad s=\frac{qb}{a+b},$$

and $GD=s$. The maximum stress in the concrete $s'=2s$, and drawing the line $A'''K$ to an intersection with the concrete resultant CK gives the point K, which must also be the point of intersection of a line which passes through G'' and the core point U. The line joining

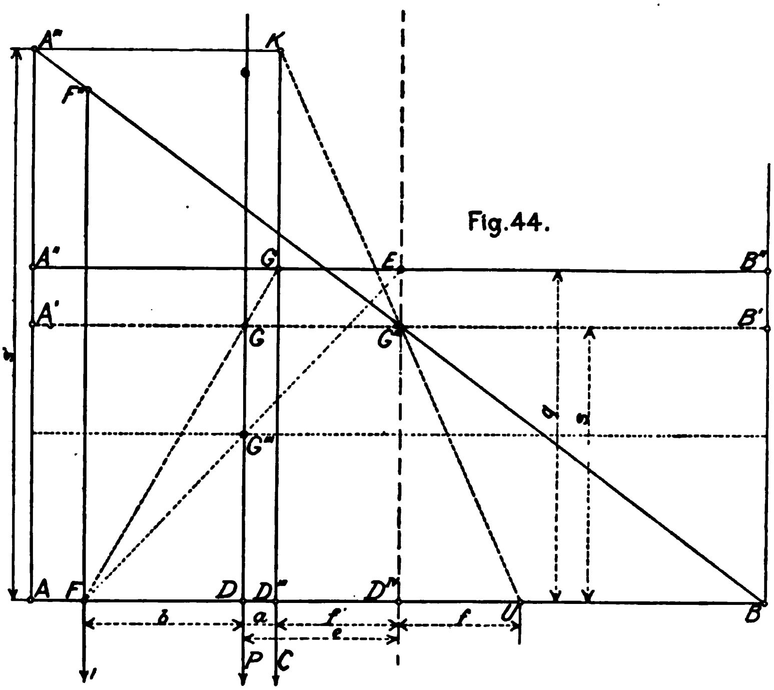

Fig.44.

A''' and B must intersect the neutral axis of the arch at G'', the two last-mentioned lines serving as a check on the computation.

The area $AA'''B$ represents the distribution of the pressure in the concrete; the line FF'' represents the pressure in the concrete where the steel is imbedded, and $15FF''$ the pressure per square inch in the steel; the area $A'A''B'B''$ represents the deficiency in the strength of the concrete which must be made up by the steel.

Analytical Computation.—The known quantities are as follows:

$AB=27$ ins.;
Sectional area of the arch rib $=27\times 12=324$ sq. ins.;
$P=98{,}900$ lbs.;
$q=P\div 324=305.25$ lbs. per sq. in.;

$e = 5.7$ ins.;
$b = 13.5 - 2 - 5.7 = 5.8$ ins.;
$f = \frac{1}{6}AB = 4.5$ ins.;
$a = e - f = 5.7 - 4.5 = 1.2$ ins.;
$s = \frac{qb}{a+b} = \frac{305.25 \times 5.8}{1.2 + 5.8} = 252.92$ lbs. per sq. in.;
$s_1 = 2s = 2 \times 252.92$ lbs. $= 505.84$ lbs. per sq. in., or the maximum pressure in the concrete;
$q - s = 305.25 - 252.92 = 52.33$ lbs.

The area $A'A''B'B''$ represents the deficiency in the strength of the concrete, and is the amount of stress to be sustained by the steel.

Stress at F, or $FF'' = \frac{505.84 \times 25}{27} = 468$ lbs.

Stress in the steel $= 15 \times FF'' = 15 \times 468 = 7{,}020$ lbs. per sq. in.

Stress to be sustained by the steel for an arch ring 1 ft. wide $= 12 \times 27 \times 52.33 = 16{,}955$ lbs. $=$ area $A'A''B'B''$.

$16{,}955 \div 7{,}020 = 2.45$ sq. ins., or the required steel section.

A $1\frac{1}{4}$-in. round bar has a sectional area of 1.227 sq. ins., and steel bars of this size placed 2 ins. above the intrados of the arch and spaced 6 ins. apart will satisfy this condition.

Other sections of the arch should be investigated, and the largest section of bar required is the one to be used throughout.

It is possible to obtain an equal pressure per square inch in the concrete over its whole area, and the center of pressure then coincides with the neutral axis of the arch; and the line FE divides q into two parts, the point through which the division line passes being the point G'''.

The figure shows that a large amount of steel is required to satisfy this assumption, and that it results in a very low compression per square inch for the steel. This is not economical, but it indicates that a surplus of steel placed at F tends to reduce the stress in the concrete. If this surplus were placed near B it would be of little use, the stress in the steel never exceeding 15 times the stress in the concrete and being very small at this point.

(c) Second Proposition: Maximum Economy Must Be Had in the Use of Steel.—This is effected when the greatest permissible compression is allowed in the concrete, and the steel is imbedded as near to A as is consistent with good construction (see Fig. 45). The line AB again represents the depth of the arch rib (27 ins.), P (98,900 lbs.) is the axial force, and $e = 5.7$ ins. is its eccentricity. The largest permissible compression in the concrete $= s' = 600$ lbs. per sq. in., and q again equals $98{,}900 \div (12 \times 27) = 305.25$ lbs. per sq. in.

Now, I is again the steel resultant and C the concrete resultant, and from conditions of equilibrium $I + C = P$.

The steel cannot be placed closer to the edge than 2 ins. $= h_{\prime}$, and the value of b is known, viz., $13.5 - h_{\prime} - e = 13.5 - 2 - 5.7 = 5.8$ ins.;

f is the distance of the upper core point U from the neutral axis of the arch, and is again equal to $\frac{1}{6}\times$depth of the rib; g=distance of force P from upper core point U.

Sufficient data are now known to find a. From the similar triangles $D'''FG'$ and DFG,

$$\frac{DG}{D'''G'}=\frac{FD}{FD'''};$$

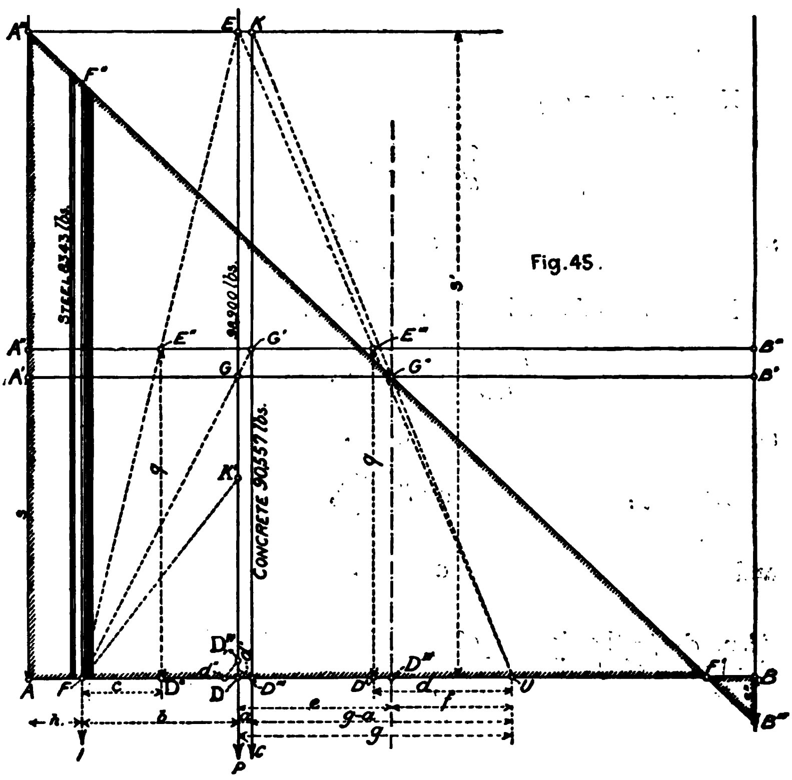

Fig. 45.

also, from conditions of equilibrium, $bP=(a+b)C$, and

$$\frac{\text{Concrete}}{\text{Concrete}+\text{steel}}=\frac{C}{P}=\frac{b}{a+b}=\frac{s}{q},$$

and $$s=\frac{bq}{a+b}.$$

From the two equal triangles $KD'''U$ and $G''D^{\text{IV}}U$,

$$\frac{G''D^{\text{IV}}}{KD'''}=\frac{D^{\text{IV}}U}{D'''U}, \quad \text{or} \quad \frac{s}{s'}=\frac{f}{g-a},$$

and
$$s=\frac{fs'}{g-a}.$$

From this it follows that

$$\frac{bq}{a+b}=\frac{fs'}{g-a}, \quad \text{or} \quad a=b\frac{gq-fs'}{fs'+qb}.$$

Now q can be expressed in terms of s', viz.,

$$\frac{q}{s'}=i, \quad \text{or} \quad q=is',$$

and
$$a=b\frac{ig-f}{f+ib}.$$

From the similar triangles EDU and $E'''D'U$,

$$\frac{E'''D'}{ED}=\frac{D'U}{DU}, \quad \text{or} \quad \frac{q}{s'}=\frac{d}{g}=i,$$

and
$$ig=d.$$

Similarly,
$$c=ib=\frac{q}{s'}b,$$

and
$$a=\frac{d-f}{f+c}.$$

Also, $d-f=$ the length of the line $D'D^{\text{IV}}=DD_{,}^{\text{IV}}=d'$, and $f+c=$ the length of the line DK'.

Join F and K' and draw the line $D_{,}^{\text{IV}}d''$ parallel to FK' through the point $D_{,}^{\text{IV}}$; this gives the line $d''D$, which is equal to a (see similar triangles DFK' and $d''D_{,}^{\text{IV}}D$). Measuring the distance a to the right of D gives the point D''' through which the concrete resultant passes, and if the vertical line $D'''K$ be drawn, it will intersect $A''B''$ at G'.

A straight line is now drawn through the points G' and F, intersecting the axial force P at G, through which point the line $A'B'$ is drawn parallel to $A''B''$. This line divides the area $ABB''A''$ into two parts, viz.: $A'A''B''B'$, which represents the deficiency in the strength of the concrete—to be provided for by the steel, and the area $AA'BB'$, which is equal to the share of the pressure to be borne by the concrete

A straight line drawn through the points U and G'' intersects the line KD''' at K, and the line $KD'''=AA'''=s'$. Drawing a line through the points A''' and G'' to an intersection with the line BB' determines the point B''', and the area $BF'B'''$ represents the tensile stress in the concrete.

The line FF'' represents the pressure in the concrete where the steel is imbedded, and fifteen times the length of this line represents the compression in the steel.

The area $A'A''B'B''$ divided by $(15\times FF'')$ will give the area of the steel in square inches for an arch ring *one* inch wide. (For an arch ring one foot wide multiply area by 12.)

It will be seen that the computation checks itself, because the line joining U and G'', prolonged, must intersect the maximum stress line for the concrete at K.

Analytical Computation.—The known quantities are

$AB=27$ ins.;
Sectional area of arch rib $=324$ sq. ins.;
$P=98{,}900$ lbs.;
$q=P\div 324=305.25$ lbs. per sq. in.;
$h'=2$ ins.;
$e=5.7$ ins.;
$b=13.5-5.7-2=5.8$ ins.;
$f=\frac{1}{6}AB=4.5$ ins.;
$g=e+f=5.7+4.5=10.2$ ins.;
$s'=$ maximum permissible stress in concrete $=600$ lbs. per sq. in.;

$$\frac{q}{s'}=i=\frac{305.25}{600}=0.5083;$$

$$a=b\frac{ig-f}{f+ib}=5.8\frac{(0.5083\times 10.2)-4.5}{4.5+(0.5083\times 5.8)}=0.533 \text{ in.};$$

$$s=\frac{bq}{a+b}=\frac{5.8\times 305.25}{6.333}=279.5 \text{ lbs. per sq. in.}$$

Eccentricity of $C=e-a=5.7-0.533=5.167$ ins.
Maximum compression per square inch in concrete

$$=\left[\left(\frac{5.167}{27}\times 6\right)+1\right]279.5=-600 \text{ lbs. (check).}$$

Maximum tension per square inch in concrete

$$=0.148\times 279.5=+41 \text{ lbs.}$$

Stress in steel:

Stress in concrete at $F=\left(\frac{600+41}{27}\times 25\right)-41=553$ lbs.

Stress in steel per square inch $=15\times 553=8{,}295$ lbs.

Total deficiency of the concrete $=(305.25-279.5)\times 27=695.25$ lbs. for an arch ring 1 in. wide.

For an arch 1 ft. wide, deficiency $=12\times 695.25=8{,}343$ lbs.

Area of steel required for an arch ring 1 ft. wide $=8{,}343\div 8{,}295=$ 1.006 sq. ins.

Two $\frac{13}{16}$-in. round bars have a sectional area of $(2\times 0.5185=)$ 1.036 sq. ins., and these spaced 6 ins. apart (2 ins. from the intrados of the arch) will give the most economical distribution of the material.

It should be remembered that other sections of the arch are to be investigated, and that the section requiring the largest area for the steel determines the size of bars to be used.

The tension of 41 lbs. per sq. in. in the concrete, however, is objectionable. The new positions of the neutral axis and the true core points should now be determined, and a computation with these will show that the tensile stresses have disappeared.

It is also desirable to insert small bars in the arch rib near *B*. Though these bars may seem theoretically superfluous, in practice they are useful to provide for any extra stress in the arch that may be caused by contraction, and to prevent cracks in the concrete.

Whenever a computation shows tension in the concrete, another one should be performed according to the exact method; * if necessary, corrections should be made either in the section of the arch rib, or in the curvature of the arch axis.

It should be well understood that there are no tensile stresses in a well-designed arch. As to the use of steel in arches to make up for the deficiency in the strength of the arch rib, the most economical distribution will be obtained by inserting the steel on the compression side of the arch. The author would recommend as a rule that the most economical distribution of the material be first ascertained, and then that such additions of steel be made as the judgment of the designer, the conditions of the locality, and the foundations may dictate.

In case any steel is used at *B*, either two $\frac{1}{2}$-in. rods should be inserted for every foot of width of the arch ring, or a strong wire construction should be employed. The $\frac{13}{16}$-in. bar used has a circumference of 2.55 ins., and one bar resists a compression of 4,180 lbs.

(*d*) Adhesion of the Concrete to the Steel.—Tests made at Columbia University, May 9 and July 8, 1903, furnish a variety of values for the adhesion between the bar and the concrete. The tests made on bars three months after they were imbedded in the concrete are as follows:

Rusted bars............	642	lbs. per square inch (block split).
Clean bars.............	431	" " " " " "
Painted bars (red lead)..	128	" " " "
" " (oil).......	23	" " " "

* Use equation in (*e*) of this article.

The first two values should have been undoubtedly higher, as the blocks split before the bars were pulled out.

Assuming 100 lbs. as the adhesion of a clean bar to the concrete, the $\frac{11}{8}$-in. bar would require a length imbedded in the concrete

$$=\frac{4{,}180}{100\times 2.55}=19 \text{ ins.}$$

These figures show that the use of twisted or specially designed rods is of no practical value in the construction of the concrete-steel arch. In designing such an arch, the following two points require special attention:

1. The arch should be so designed that the line of pressure of the dead load will approach as near as possible to the neutral axis of the arch. (See Art. 4, Chap. IV, on the effect of a change of form.)

2. The steel should be placed in the most effective manner. In any arch where these two injunctions are observed, maximum strength and economy will be obtained.

Settling of the abutments will influence the stresses in the arch, but a judicious use of steel, combined with a thorough knowledge of the effect which a change in form has on the stresses in the arch, will furnish the means of overcoming the injurious effects of such subsidence.

(*e*) Stresses in a Reinforced-Concrete Arch Rib.—The following particulars are assumed to be known:

The dimensions of the arch rib,
The intensity and the point of application of the axial force, and
The location and sectional area of the steel bars.

Let O = area of steel for an arch ring 1 in. wide;
I = resultant of all the forces acting in the steel;
s' = maximum stress in concrete;
C = resultant of all the forces acting in the concrete;
s'' = minimum stress in concrete;
s''' = stress in concrete where the steel is imbedded;
q = average stress per square inch $=\frac{P}{A}$;
P = axial force;
A = sectional area of arch rib 1 ft. wide;
b = distance from the force P to the center of gravity of the steel;
s = average stress in concrete;
e = distance from the force P to the center of gravity of the section;
l = depth of arch rib;
$h_{,}$ = distance from the center of the steel to the outside of the rib.

To solve this problem the distance a should be found. (See Fig. 45.)

$$s'''=\frac{s'-s}{\frac{1}{2}l}(\tfrac{1}{2}l-h_{,})+s=\frac{(\frac{1}{2}l-h_{,})s'+h_{,}s}{\frac{1}{2}l}=\frac{is'+h_{,}s}{\frac{1}{2}l};\quad \tfrac{1}{2}l-h_{,}=i;$$

$$I=15Os'''=15O\frac{is'+h_{,}s}{\frac{1}{2}l};$$

$$q-s=\frac{I}{l}=\frac{30O}{l^2}(is'+h_{,}s)=M(is'+h_{,}s);\quad \frac{30O}{l^2}=M.$$

In a previous article it was found that

$$s=\frac{bq}{a+b},\quad s'=s\frac{g-a}{f}=\frac{bq}{a+b}\,\frac{g-a}{f};$$

consequently $$q-s=q-\frac{bq}{a+b}=M\left(i\frac{bq}{a+b}\cdot\frac{g-a}{f}+h_{,}\frac{bq}{a+b}\right),$$

and $$1-\frac{b}{a+b}=M\left(i\frac{b}{a+b}\,\frac{g-a}{f}+h_{,}\frac{b}{a+b}\right).$$

From this $$a(f+Mbi)=Mb(ig+h_{,}f),$$

$$a=Mb\frac{ig+h_{,}f}{f+Mbi}.$$

Substituting in this equation the values for M and i gives

$$a=\frac{30O}{l^2}b\frac{(\frac{1}{2}l-h_{,})g+h_{,}f}{f+\frac{30O}{l^2}b(\frac{1}{2}l-h_{,})}.$$

Substituting this value of a in the equation for s' gives the maximum stress per square inch in the concrete.

This equation, as previously referred to, should be used when a second computation is necessary, in which case the exact location of the neutral axis and the core points are to be used.

(*f*) Example [Application of (*e*)].—It is required to find the moment of inertia and the core points of the concrete-steel section just considered.

Area of the arch rib $=12\times27\quad=A=324$ sq. ins.
Added concrete $\quad=14\times\ 1.04=B=\ \ 15$ " " (for steel bars).

Total $=339$ " "

Distance from center of gravity of A to face $=13.5$ ins.
" " " " " " B " " $=25$ "

$$\begin{aligned}\text{Moment} = 13.5\times 324 &= 4{,}374\\ 25\ \times\ 15 &= \ \ 375\\ \hline &\ \ 4{,}749\end{aligned}$$

Distance from center of gravity of total section to face $=4{,}749\div 339=14$ ins.

To obtain the moment of inertia the section is divided into three parts. The area A is divided into the part A' above the neutral axis, and the part A'' below the neutral axis; the area B is computed by itself.

The height of the part $A'=27-14=13$ ins., the distance from its center of gravity to the neutral axis is 6.5 ins., and its moment of inertia

$$=(13\times 12\times 6.5^2)+\frac{13^3\times 12}{12}=\ 8{,}788.$$

The moment of inertia of A''

$$=(14\times 12\times 7^2)\ +\frac{14^3\times 12}{12}=10{,}976.$$

The distance from the center of gravity of the part B to the center of gravity of the whole section $=25-14=11$ ins., its area $=15$ sq. ins., and its moment of inertia $=15\times 11^2=1{,}815$.

The moment of inertia of the whole section is equal to the sum of these values $=21{,}579$.

The total area as before $=339$ sq. ins.

The square of the radius of gyration $=21{,}579\div 339=63.65$, and the core points are situated at the following distances from the axis:

$$f=63.65\div 13=4.89 \text{ ins.}$$
$$f'=63.65\div 14=4.55\ \text{"}$$

Now, the steel area for an arch ring 1 in. wide $=$

$$O=\frac{1.04}{12}=0.087. \qquad e=5.2 \text{ ins.},$$

$$l=27 \text{ ins.},\qquad b=5.8 \text{ ins.},\qquad h_{,}+b=7.8 \text{ ins.},$$

$$h_{,}=\ 2 \text{ ins.},\qquad g=4.89+13-7.8=10.09 \text{ ins.};$$

$$a=\frac{30\times 0.087}{27^2}\times 5.8\times\frac{(11.5\times 10.09)+(2\times 4.89)}{4.89+\frac{30\times 0.087}{27^2}\times 5.8\times 11.5}$$

$$=0.509.$$

(When this value of a becomes equal to zero, there will be no tension in the concrete.)

Now, $$q = 98{,}900 \div 339 = 290 \text{ lbs. per sq. in.},$$

and $$s' = \frac{5.8 \times 290}{6.309} \times \frac{10.09 - 0.509}{4.89} = 523 \text{ lbs.},$$

$$s = \frac{5.8 \times 290}{6.309} = 266 \text{ lbs.},$$

$$s'' = (2 \times 266) - 523 = 9 \text{ lbs. tension.}$$

The designer who demurs even to this amount of tension can overcome same by increasing the rod diameter a small fraction of an inch; the author does not deem it objectionable.

Notation for Articles 5, 7, and 8.

A = sectional area of the beam;

$a = \frac{u}{H}$;

$c = \frac{M}{dH^2}$;

d = width of a beam subject to bending;

E = modulus of elasticity;

E_c = " " " of concrete;

E_0 = " " " " metal;

F = stress in the metal;

f_t = tensile stress in the metal;

H = depth of a beam subjected to bending;

I = moment of inertia;

j = ratio of distance between extreme fiber and neutral axis of a beam to its depth;

K = single load;

k = any ratio;

l = length of beam;

M = bending moment or moment of resistance;

$m = \frac{E_0}{E_c}$;

n = ratio of metal section to beam section $= \frac{O}{A}$;

O = sectional area of the metal reinforcing bars;

P = pressure or force;

p = uniformly distributed load;

q = pressure per unit area $= \frac{P}{A}$;

r = radius of gyration;
S = shear;
s' = maximum compressive stress in the concrete of beam;
u = distance from the neutral axis of a beam to the surface subjected to the greatest compression;
v = distance from the center of gravity of the tensile reinforcements to the neutral axis of the beam;
$\left.\begin{matrix} x \\ y \end{matrix}\right\}$ = coordinates;
z = distance from the center of gravity of the tensile reinforcements to that surface of the beam which is subjected to maximum compression.

5. Column Formulas for Masonry and Reinforced Concrete.—In these materials a distinction is made between stresses resulting from direct compression and those due to compression and bending. Prevailing practice, which is based on experiments, dictates that stresses resulting from direct compression or tension should not be as great as those resulting from bending.

In piers and abutments no bending stresses should exist, and all that was said in Arts. 1, 2, etc., of this chapter applies to them. In addition, unknown internal stresses which result from settling, together with the uneven shrinkage of the materials of construction, warrant the use of a high factor of safety. For piers and abutments this factor should be 10 or more, and in arches it varies from 4 to 10, according to conditions.

(a) REINFORCED CONCRETE. DIRECT COMPRESSION.—The longitudinal reinforcements of the column are of small sectional area as compared with that of the column itself.

In this case a transverse section of the column is displaced parallel to itself by a load P.

$$P = qA + FO. \quad . \quad . \quad . \quad . \quad . \quad . \quad . \quad . \quad . \quad (1)$$

Now, $\dfrac{s'}{E_c} = \dfrac{F}{E_0}$, or $F = s'\dfrac{E_0}{E_c}$, and $m = \dfrac{E_0}{E_c}$;

$$\therefore \; F = ms',$$

and

$$P = s'(A + mO). \quad . \quad . \quad . \quad . \quad . \quad . \quad . \quad . \quad . \quad (2)$$

Equation (2) can be used to investigate a structure already designed.

From (2),

$$mO = \frac{P}{s'} - A. \quad . \quad . \quad . \quad . \quad . \quad . \quad . \quad . \quad . \quad (3)$$

Assume $\frac{O}{A}=n$ to be known;

$$q=\frac{P}{A},$$

and if m is assumed $=\frac{E_0}{E_c}=10,$

$$q=s'(1+10n), \quad . \quad . \quad . \quad . \quad . \quad . \quad . \quad . \quad . \quad (4)$$

and $$O=nA.$$

This, with a permissible stress in the concrete of 400 lbs. per sq. in., gives the following:

nA	q
0	400 lbs. per sq. in.
0.005	420 " " " "
0.01	440 " " " "
0.02	480 " " " "
0.03	520 " " " "
0.04	560 " " " "
0.05	600 " " " "
etc.,	

each additional per cent. of steel increasing the value of q by 40 lbs.

In the construction of reinforced-concrete columns a length of column exceeding 20 diameters is seldom used. In case such a column is required, it should be designed to resist flexure, and any of the well-known column formulas may be applied.

For example, Euler's formula states that

$$P=\pi^2\frac{IE}{(kL)^2}.$$

For a rectangular reinforced-concrete column,

$$I=\frac{bd^3}{12}+mOy^2,$$

where y=distance from center of steel to axial plane of column.

Assuming $$\frac{E_0}{E_c}=10,$$

$$P=\pi^2E_c\frac{\frac{bd^3}{12}+10Oy^2}{(kL)^2}.$$

k is a factor which depends on the conditions obtaining at the ends of the column, viz.:

(a) Both ends rounded, $k=1$;

(b) Both ends fixed, $k=0.5$;

(c) One end fixed, the other rounded, $k=\sqrt{0.5}$;

(d) " " " " " free, $k=2$.

Assuming a factor of safety of 4 gives

(a) $$P=2.48\frac{E_c}{L^2}\left(\frac{bd^3}{12}+10Oy^2\right);$$

(b) $$P=9.87\frac{E_c}{L^2}\left(\frac{bd^3}{12}+10Oy^2\right);$$

(c) $$P=4.94\frac{E_c}{L^2}\left(\frac{bd^3}{12}+10Oy^2\right);$$

(d) $$P=0.62\frac{E_c}{L^2}\left(\frac{bd^3}{12}+10Oy^2\right).$$

In these formulas the area of the reinforcement is not deducted from the area of the column in obtaining the moment of inertia of the concrete.

Generally this error is small, but in columns with a large sectional area of reinforcement the deduction should be made.

Accordingly,

$$P=q(A-O)+FO,$$

and the former equations change to

$$P=s'[A+(m-1)O],$$

$$F=ms',$$

and $$(m-1)O=\frac{P}{q}-A.$$

Now $n=\frac{O}{A}$, and $\frac{E_0}{E_c}=m$ is again assumed $=10$;

$$q=s'(1+9n),$$

and $$O=nA.$$

These last equations give the following values when $s' = 400$ lbs. per sq. in.:

n	q
2.5%	490
3%	508
4%	544
5%	580
6%	616
7%	652
8%	688
9%	724
10%	760

Euler's formula also changes to

$$P = \pi^2 E_c \frac{I + (m-1)I_s}{(kL)^2}.$$

I_s, or the moment of inertia of the steel, is equal to y^2mO. This means that the steel is replaced by an equivalent mass of concrete, and that its moment of inertia is taken around the axial plane of the column, the moment of inertia around its own axis being neglected. This was done in the example in Art. 4 (*f*) of this chapter.

When a column is very long it should be investigated for bending, and when $r = \sqrt{\frac{I}{A}}$, Euler's formula changes to

$$q = \pi^2 \frac{r^2 E}{L^2}.$$

In concrete E varies according to the nature and intensity of the stress. When a column bends under a load, the successive changes of stress can be described as follows:

The load first exerts a uniform compressive stress. If it be increased this stress increases up to a point where the column commences to bend. Any increase in the load now will induce a tensile stress in the extreme fibers on the convex side, thus reducing the compression on that side; on the concave side, however, the compressive stress increases. For very low stresses the same modulus of elasticity may be used for both tension and compression; but for the stresses which are generally assumed, these moduli differ.

If the ratio of the smaller to the larger modulus of elasticity be indicated by j, the distance from the neutral axis to the extreme fibers having the lesser modulus by x, and the depth of the section equal to unity, then, the two components of the couple being equal,

$$jx^2 = (1-x)^2, \quad \text{or} \quad x = \frac{1}{1+\sqrt{j}}.$$

The components pass through the centers of gravity of the areas representing the distribution of the stresses over the section, which areas are assumed to be defined by straight lines. The areas repre-

senting the additional compression on the concave side and the tension on the convex side are triangles, and the distance between their centers of gravity is $\frac{2}{3}$ of unity, or the distance between the two forces of the couple is $\frac{2}{3}$ of the total depth 1, and is independent of the value of x. Hence

$$jx^2 = \frac{1}{\left(1+\frac{1}{\sqrt{j}}\right)^2}.$$

Euler's formula may now be written

$$\frac{l}{L} = \frac{1}{\pi}\sqrt{\frac{f}{E}},$$

and the following table may be made out:

When	$j=1$	0.5	0.25	0.09
	$x=0.5$	0.586	0.667	0.77
and	$jx^2=0.25$	0.172	0.111	0.053

and the moments are proportional to

	E	$0.688E$	$0.444E$	$0.21E$.

In using Euler's formulas these values must therefore be substituted for E.

(*e*) Hooped Columns.—The hooped column is of recent origin, and experimenters differ in their results. The following rule for computing such columns is based on those parts of the various experiments where some agreement exists.

(See the experiments of Considère, Dunn, etc., and the deductions made from them. See also the experiments made at the Watertown Arsenal, described in *Engineering News*, July 9, 1906, which also gives some valuable information on coefficients of elasticity, etc.)

In dimensioning the hooped column, consider the area of the column as composed of

(1) The sectional area of the concrete inside the hooping.
(2) The sectional area of the longitudinal bars.
(3) 2.4×the sectional area of the hooping wire.

Allow 650 lbs. per sq. in. pressure in the concrete.

Assume $\frac{E_0}{E_c}$ = from 15 to 10.

Allow a tension of from 8,000 lbs. for iron to 10,000 lbs. for steel in the reinforcement, and consider same to consist of the area (2) plus the area (3).

(The above-mentioned experimenters recommend stresses in the concrete of from 1,500 to 2,000 lbs. per sq. in., but until more knowledge exists as to the effect of repetition stresses on such columns, the author is of the opinion that the value which he assigns is preferable.)

Space the hooping wire (the pitch of the spiral) from $\frac{d}{8}$ to $\frac{d}{10}$, d being the diameter of the spiral.

Make the total area of the longitudinal rods from 1 to 0.8 per cent. of the area enclosed by the spiral winding, and the diameter of the spiral wire about 2% of the diameter of the spiral. Any desired addition may be made to the sectional area of the longitudinal reinforcements, the foregoing figures being given as minima.

The strength of the column should be computed according to the methods described in (a) of the present article.

6. Column Formulas for Steel and Wood.—In the following standard American formulas the letters indicating the factors are those which are in general use, and differ from those given in the Appendix.

f = elastic limit of the material,
= 34,000 lbs. per square inch for wrought iron,
= 42,000 " " " " " steel;
E = modulus of elasticity,
= 27,000,000 for wrought iron (inch-pounds),
= 29,000,000 " steel (inch-pounds);
l = length of column in inches;
r = radius of gyration in inches $=\sqrt{\frac{I}{A}}$;
p = load in lbs. per sq. in.;
π = length of semicircular arc when radius equals 1 = 3.1416;
d = least lateral dimension of a wooden column.

(In bridge building, columns in which $\frac{l}{r}>150$ should not be used.)

FORMULAS FOR THE ULTIMATE STRENGTH OF COLUMNS.

Gordon's Formulas:

Pivoted ends . . . . $p=\dfrac{f}{1+a\left(\dfrac{l}{r}\right)^2}$;

Fixed ends . . . . $p=\dfrac{f}{1+\dfrac{a}{4}\left(\dfrac{l}{r}\right)^2}$;

One end fixed, the other pivoted . . . . $p=\dfrac{f}{1+\dfrac{4}{9}a\left(\dfrac{l}{r}\right)^2}$.

Euler's Formulas:

Pivoted ends . . . . $p=\dfrac{\pi^2E}{\left(\dfrac{l}{r}\right)^2}$;

Fixed ends . . . . $p=\dfrac{4\pi^2E}{\left(\dfrac{l}{r}\right)^2}$;

One end fixed, the other pivoted . . . . $p=\dfrac{\frac{9}{4}\pi^2E}{\left(\dfrac{l}{r}\right)^2}$.

Johnson's Formulas:

		When	
Pin Ends,	Wrought Iron,	$\frac{l}{r} \leqq 170,$	$p = 34{,}000 - 0.67\left(\frac{l}{r}\right)^2.$
		$\frac{l}{r} \geqq 170,$	$p = \frac{432{,}000{,}000}{\left(\frac{l}{r}\right)^2}.$
	Mild Steel,	$\frac{l}{r} \leqq 150,$	$p = 42{,}000 - 0.97\left(\frac{l}{r}\right)^2.$
		$\frac{l}{r} \geqq 150,$	$p = \frac{456{,}000{,}000}{\left(\frac{l}{r}\right)^2}.$
Round Ends, Cast Iron,		$\frac{l}{r} \leqq 70,$	$p = 60{,}000 - \frac{25}{4}\left(\frac{l}{r}\right)^2.$
		$\frac{l}{r} \geqq 70,$	$p = \frac{144{,}000{,}000}{\left(\frac{l}{r}\right)^2}.$
Flat Ends,	Wrought Iron,	$\frac{l}{r} \leqq 210,$	$p = 34{,}000 - 0.43\left(\frac{l}{r}\right)^2.$
		$\frac{l}{r} \geqq 210,$	$p = \frac{675{,}000{,}000}{\left(\frac{l}{r}\right)^2}.$
	Mild Steel,	$\frac{l}{r} \leqq 190,$	$p = 42{,}000 - 0.62\left(\frac{l}{r}\right)^2.$
		$\frac{l}{r} \geqq 190,$	$p = \frac{712{,}000{,}000}{\left(\frac{l}{r}\right)^2}.$
	Cast Iron,	$\frac{l}{r} \leqq 120,$	$p = 60{,}000 - \frac{9}{4}\left(\frac{l}{r}\right)^2.$
		$\frac{l}{r} \geqq 120,$	$p = \frac{400{,}000{,}000}{\left(\frac{l}{r}\right)^2}.$
	White Pine,	$\frac{l}{d} \leqq 60,$	$p = 2{,}500 - 0.6\left(\frac{l}{d}\right)^2.$
	Short-Leaf Yellow Pine,	$\frac{l}{d} \leqq 60,$	$p = 3{,}300 - 0.7\left(\frac{l}{d}\right)^2.$
	Long-Leaf Yellow Pine,	$\frac{l}{d} \leqq 60,$	$p = 4{,}000 - 0.8\left(\frac{l}{d}\right)^2.$
	White Oak,	$\frac{l}{d} \leqq 60,$	$p = 3{,}500 - 0.8\left(\frac{l}{d}\right)^2.$

Note.—The foregoing formulas do not include any factor of safety.

(*a*) FORMULAS TO BE USED IN DIMENSIONING.—*Johnson's Formulas* (factor of safety = 4):

PIN ENDS,
- Wrought Iron, $p = 8{,}500 - 0.17\left(\frac{l}{r}\right)^2.$
- Mild Steel, $p = 10{,}500 - 0.24\left(\frac{l}{r}\right)^2.$

FLAT ENDS,
- Wrought Iron, $p = 8{,}500 - 0.11\left(\frac{l}{r}\right)^2.$
- Mild Steel, $p = 10{,}500 - 0.16\left(\frac{l}{r}\right)^2.$

TOP CHORDS,

WROUGHT IRON.
- Live-load stresses, $p = 8{,}000 - 30\frac{l}{r}.$
- Dead-load stresses, $p = 16{,}000 - 60\frac{l}{r}.$

MEDIUM STEEL.
- Live-load stresses, $p = 10{,}000 - 40\frac{l}{r}.$
- Dead-load stresses, $p = 18{,}000 - 70\frac{l}{r}.$

POSTS,

WROUGHT IRON.
- Live-load stresses, $p = 7{,}000 - 40\frac{l}{r}.$
- Dead-load stresses, $p = 14{,}000 - 80\frac{l}{r}.$
- Wind stresses, $p = 10{,}000 - 60\frac{l}{r}.$

MEDIUM STEEL.
- Live-load stresses, $p = 9{,}000 - 50\frac{l}{r}.$
- Dead-load stresses, $p = 18{,}000 - 100\frac{l}{r}.$
- Wind stresses, $p = 12{,}000 - 70\frac{l}{r}.$

Assumed initial stress p for lateral struts

$$= 9{,}000 - 50\frac{l}{r} \text{ (for wrought iron)}$$

$$= 10{,}000 - 60\frac{l}{r} \text{ (for medium steel).}$$

(*b*) Tension Members (Mild Steel):

Eye-bars	$p=18{,}000$
Shapes	$p=16{,}000$
Flanges (floor-beams and stringers)	$p=14{,}000$
Hip Verticals (eyes)	$p=16{,}000$
" " (shapes)	$p=14{,}000$
Adjustable Rods (steel)	$p=16{,}000$
" " (iron)	$p=13{,}000$
Lateral Rods	$p=18{,}000$
" Shapes	$p=16{,}000$

(*c*) Shear (Mild Steel):

Webs	$p=10{,}000$
Pins and Rivets	$p=12{,}000$

(*d*) Bending Stresses:

Rolled Sections (mild steel)	$p=16{,}000$
Timber Beams	$p=2{,}000$

(*e*) Rollers:

Static Load (in lbs. per linear inch)	$=600d$
Moving Load (in lbs. per linear inch)	$=200d$

(d = diameter of roller.)

(*f*) Impact $=I$; L = length of span.

For Railroad Bridges . . . . $I=\dfrac{400}{L+500}$.

" Highway Bridges . . . . $I=\dfrac{100}{L+150}$.

(*g*) Reversing Stresses.—Add to the greater area $\frac{4}{5}$ of the lesser area. For maximum stresses due to wind, dead, and live loads, the strain in the material may be 15% higher. In *bridges* reversal of stresses caused by wind loads may be neglected.

(*h*) Modifications for Spans over 400 Ft. Long.—For spans of 400 ft. and over the foregoing figures may be higher. Also, a harder quality of steel may be used for the main girders.

When an allowance is made for impact, the distinction between live- and dead-load stresses is not necessary, and the stresses given for the dead load are to be used in dimensioning.

7. Bending Moments and Shearing Forces in Beams.—In the following equations

M = bending moment;
K = concentrated load at center of span;
p = distributed load;
l = length of span;
S = shearing force.

The inferiors $_C$ and $_A$ indicate that values are to be taken at the center ($_C$) or near the support ($_A$).

(*a*) Beam Freely Supported:

$$M_C = \frac{Kl}{4} \quad . \quad . \quad . \quad . \quad (1) \qquad S = \frac{K}{2} \quad . \quad . \quad . \quad . \quad . \quad (1')$$

$$= \frac{pl^2}{8} \quad . \quad . \quad . \quad . \quad . \quad (2) \qquad = \frac{pl}{2} \quad . \quad . \quad . \quad . \quad . \quad (2')$$

(*b*) Beam Fixed at Both Ends:

$$M_C = +\frac{pl^2}{24} \quad . \quad . \quad . \quad (3) \qquad M_C = +\frac{Kl}{8} \quad . \quad . \quad . \quad . \quad (3')$$

$$M_A = -\frac{pl^2}{12} \quad . \quad . \quad . \quad (4) \qquad M_A = -\frac{Kl}{8} \quad . \quad . \quad . \quad . \quad (4')$$

$$S = \frac{pl}{2} \quad . \quad . \quad . \quad . \quad . \quad (5) \qquad S = \frac{K}{2} \quad . \quad . \quad . \quad . \quad . \quad (5')$$

The ends, however, are never so securely built-in that they can be considered as fixed, and the average therefore lies between (*a*) and (*b*), depending on conditions. A reinforced-concrete beam is neither uniform in section nor in strength.

Many constructors use

$$M_C = +\frac{pl^2}{10}.$$

This gives a bending moment at the support

$$= M_A = -\left(\tfrac{1}{8} - \tfrac{1}{10}\right)pl^2 = -\tfrac{1}{40}pl^2.$$

Also,

$$M_C = +\frac{Kl}{6}, \quad \text{or} \quad M_A = -\frac{Kl}{12}.$$

These values, however, are often found insufficient, and it is better to employ the following: *

$$M_C = +\frac{pl^2}{12} \quad . \quad . \quad . \quad . \quad (6) \qquad M_C = +\frac{3Kl}{16} \quad . \quad . \quad . \quad . \quad (6')$$

$$M_A = -\frac{pl^2}{24} \quad . \quad . \quad . \quad . \quad (7) \qquad M_A = -\frac{Kl}{16} \quad . \quad . \quad . \quad . \quad . \quad (7')$$

(*c*) Beam Fixed at One End and Freely Supported at the Other.—In such a beam the point of contraflexure is distant from the fixed end

(I) $0.267l$ for a uniformly distributed load, and

(II) $0.33l$ for a concentrated load at the center.

* These averages have been derived from experience.

The maximum bending moment for (I) is at $0.367l$ from the free end, or

$$M_{\max.} = +\frac{9}{128}pl^2, \quad . \quad . \quad . \quad (8) \qquad M_A = -\frac{pl^2}{8}, \quad . \quad . \quad . \quad . \quad . \quad (9)$$

and for (II)

$$M_{\max.} = +\frac{5}{32}Kl, \quad . \quad . \quad . \quad (10) \qquad M_A = -\frac{3}{16}Kl. \quad . \quad . \quad . \quad (11)$$

Shearing Values:

At the fixed end, $S_{\max.} = \frac{5}{8}pl = \frac{11}{16}K.$ . . . . (12)

At the free end, $S \quad = \frac{3}{8}pl = \frac{5}{16}K.$ . . . . (13)

Assuming again mean averages gives:

		Uniform Load.	Concentrated Load at Center.	
	$M_{\max.}$	$= +0.097pl^2$	$= +0.203Kl.$ . . .	(14)
	M_A	$= -\frac{1}{16}pl^2$	$= -\frac{3}{32}Kl.$	(15)
At fixed end,	$S_{\max.}$	$= \frac{9}{16}pl$	$= \frac{19}{32}K.$	(16)
At free end,	S	$= \frac{7}{16}pl$	$= \frac{13}{32}K.$	(17)

(*d*) Slabs.—When l = shorter span and l_1 = longer span, the bending moments as obtained for beams must be multiplied by $\frac{l_1^4}{l_1^4+l^4}$ when l is the span, and by $\frac{l^4}{l_1^4+l^4}$ when l_1 is the span.

The shortest span will give the largest bending moment, or, if

l_1 is infinitely large, $\frac{l_1^4}{l_1^4+l^4} = 1;$
$l_1 = l,$ " $= 0.5;$
$l_1 = 2l,$ " $= 0.94.$

Reinforced-concrete slabs should be investigated as beams in both directions, and parallel reinforcing bars should also be provided in the direction of their longer dimensions.

The coefficients for the longer sides will be as follows:

When l_1 is infinitely large, $\frac{l^4}{l^4+l_1^4} = 0;$
" $l_1 = l,$ " $= 0.5;$
" $l_1 = 2l,$ " $= 0.06.$

M_A and $S_{max.}$ are at the fixed end of the beam. Applying these coefficients to (6) and (7) gives

Shorter Span (l).	Longer Span (l_1).
$M_C=+\frac{pl^2}{12}\times\frac{l_1^4}{l_1^4+l^4}$	$M_C=+\frac{pl_1^2}{12}\times\frac{l^4}{l^4+l_1^4}$
$M_A=-\frac{pl^2}{24}\times\frac{l_1^4}{l_1^4+l^4}$	$M_A=-\frac{pl_1^2}{24}\times\frac{l^4}{l^4+l_1^4}$

For square slabs

$$M_C=+\frac{1}{24}pl^2 \qquad\qquad M_A=-\frac{1}{48}pl^2$$

For slabs freely supported, the bending moments at the center are

Shorter Span (l).	Longer Span (l_1).
$M_C=\frac{pl^2}{8}\times\frac{l_1^4}{l_1^4+l^4}$	$M_C=\frac{pl_1^2}{8}\times\frac{l^4}{l^4+l_1^4}$

In the foregoing equations M expresses the bending moment in a beam caused by the exterior forces, and in the equations of Art. 8 M expresses the moment of resistance in a beam; these two moments form a system which is in equilibrium, and they are therefore indicated by the same letter.

8. Longitudinal Stresses in a Reinforced Beam Subjected to Bending.—The general treatment is the same as that of Shäffer, Landsberg, Marsh, and Considère. The beam will be considered as having a rectangular section. No tensile stresses are to be resisted by the concrete, but solely by the reinforcing bars, which are to be placed near the face of the beam where tensile stresses develop. (Single system of reinforcement.)

It is further assumed that the sectional area of these bars is small as compared with that of the beam.

Compressive and tensile resistances in a beam are equal (see Fig. 45a), and the compressive area is assumed to be a parabola, with its main axis coinciding with the plane of section. When $AA''=s'$ the above law gives

$$\frac{2}{3}s'ud=Of_t. \quad . \quad . \quad . \quad . \quad . \quad . \quad . \quad . \quad . \quad (1)$$

The plane of section is not distorted after bending takes place, or

$$\frac{AA'}{AD}=\frac{CC'}{CD}.$$

Also, $$AA':CC'=\frac{s'}{E_c}:\frac{f_t}{E_0},$$

or $$\frac{s'}{uE_c}=\frac{f_t}{vE_0}. \qquad (2)$$

But $m=\frac{E_0}{E_c}$; consequently, substituting in (2),

$$f_t=s'm\frac{v}{u}. \qquad (3)$$

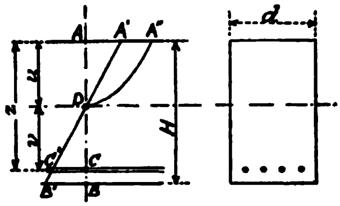

Fig. 45 a.

The total moment of resistance is equal to the moment of resistance of the concrete in compression plus that of the steel in tension, and, as the distance from the center of gravity of the parabola to the neutral axis $=\frac{5}{8}u$,

$$M=\left(\frac{5}{8}u\times\frac{2}{3}s'ud\right)+vf_tO,$$

or $$M=\frac{5}{12}s'u^2d+vf_tO; \qquad (4)$$

and substituting (3) in (1) and (4) gives

$$\frac{2}{3}u^2d-mOv=0, \qquad (5)$$

and $$M=\frac{s'}{u}\left(\frac{5}{12}u^3d+mOv^2\right). \qquad (6)$$

Now $v=z-u$, and this, when substituted in (5), gives

$$\frac{2}{3}u^2d-mO(z-u)=0,$$

or $$u=-\frac{3}{4}\frac{mO}{d}+\sqrt{\frac{9m^2O^2}{16d^2}+\frac{3mOz}{2d}}, \qquad (7)$$

and (6) may be written

$$M=\frac{s'ud(8z-3u)}{12}. \qquad (8)$$

These equations can be used to investigate a structure, the values of z, O, d, and m being obtained from the plans; with these values u may be found from (7), and this substituted in (8) gives s'. f_t may then be found from (3).

These equations can also be used to find the dimensions of a beam by trial, but for this purpose the following ones are better adapted:

$$O=nHd; \quad u=aH; \quad M=cdH^2.$$

m is assumed $=10$.

In practice it has been found that a sufficient covering of concrete over the bars is obtained when the ratio z to H is as follows:

$$\text{For slabs,} \quad z=\frac{5}{6}H, \quad \text{and} \quad h'=\frac{1}{6}H;$$

$$\text{For beams,} \quad z=\frac{9}{10}H, \quad \text{and} \quad h'=\frac{1}{10}H.$$

When these values of O, u, and M are substituted in (7), and z is made equal to $\frac{5}{6}H$, it changes to

$$u=\frac{15}{2}nH\left(-1+\sqrt{1+\frac{2}{9n}}\right),$$

and

$$a=\frac{u}{H}=\frac{15}{2}n\left(-1+\sqrt{1+\frac{2}{9n}}\right); \quad . \quad . \quad . \quad . \quad . \quad (9)$$

also,

$$v=\frac{H}{6}(5-6a). \quad . \quad . \quad . \quad . \quad . \quad . \quad . \quad . \quad . \quad . \quad (10)$$

Substituting these values in equation (8) gives

$$c=s'a\frac{20-9a}{36}, \quad . \quad . \quad . \quad . \quad . \quad . \quad . \quad . \quad (11)$$

and equation (3) gives

$$s'=\frac{3f_ta}{5(5-6a)}; \quad . \quad . \quad . \quad . \quad . \quad . \quad . \quad . \quad (12)$$

and this value substituted in (11) gives

$$c=f_ta^2\frac{20-9a}{60(5-6a)}. \quad . \quad . \quad . \quad . \quad . \quad . \quad (13)$$

Substituting $\frac{9}{10}H$ for z in (9) and (10) gives

$$u=\frac{15}{2}nH\left(-1+\sqrt{1+\frac{6}{25n}}\right).$$

$$a=\frac{u}{H}=\frac{15}{2}n\left(-1+\sqrt{1+\frac{6}{25n}}\right). \quad . \quad . \quad . \quad . \quad (9^a)$$

$$v=\frac{H}{10}(9-10a). \quad . \quad . \quad . \quad . \quad . \quad . \quad . \quad . \quad . \quad . \quad (10^a)$$

Further,
$$c=s'a\frac{12-5a}{20}. \quad (11^a)$$

$$s'=\frac{f_t a}{9-10a}. \quad (12^a)$$

$$c=f_t a^2\frac{12-5a}{20(9-10a)}. \quad (13^a)$$

In a beam subjected to bending many experiments have shown that the concrete elongates from $\frac{1}{1,000}$ to $\frac{2}{1,000}$ before cracks appear. This would occur if the stress in the steel were $\frac{29,000,000}{1,000}=29,000$ lbs., and, assuming that the bond between the steel and the concrete is not broken, the tensile side of the beam needs no investigation. This is not true for beams with a very large ratio of metal to concrete, but in a beam designed with a view to combining strength and economy, such a ratio is avoided.

To design the most economical beam it is necessary to find the relations between n, a, and c. Equation (1) gives, when $O=ndH$ and $u=aH$ are substituted therein,

$$n=\frac{2}{3}\frac{s'}{f_t}a.$$

From (12) or (12^a):

For Slabs.	For Beams.	
$a=\frac{25s'}{30s'+3f_t}$;	$a=\frac{9s'}{10s'+f_t}$.	(14)
$n=\frac{50(s')^2}{9f_t(10s'+f_t)}$;	$n=\frac{6(s')^2}{f_t(10s'+f_t)}$.	(15)

Equations (15) give the ratio between the concrete and steel in terms of the maximum stresses of these materials. Equations (14) define the location of the neutral axis in terms of the maximum stresses in the two materials, and (11) and (13) express the relation between the bending moment and the dimensions of the beam.

In designing reinforced-concrete beams or columns, the quality of the concrete is an important factor, and should be determined before making the computations.

The maximum compressive stress to be allowed in the concrete should not exceed 400 lbs. per square inch, and should be reduced according to the quality (except for hooped columns, where the stresses may be higher—see Article 5, *ante*).

Shearing stresses should not be greater than 50 lbs. per square inch.

TABLE XI.

STRENGTH OF MATERIALS IN TENSION.

(Stresses at the point of rupture in lbs. per sq. in.)

CAST IRON (13,600 to 29,000)	16,500
WROUGHT IRON ($E=25,000,000$ to $27,000,000$):	
Round or square bars (1-in. to 2-in.)	50,000 to 54,000
Test-pieces cut from large bars ($\frac{1}{2}$-in. square)	50,000 to 53,000
Large bars (sectional area about 7 sq. ins.)	46,000 to 47,000
Plates and structural shapes	48,000 to 51,000
Plates over 36 ins. wide	46,000 to 50,000
Wire	70,000 to 100,000
Wire rope	90,000
STEEL (according to hardness)	65,000 to 120,000
($E=27,000,000$ to $30,000,000$.)	
TIMBER (seasoned):	
White oak, American	10,000 to 18,000
" " European	10,000 to 19,800
Pine (white, red, and pitch)	10,000
Long-leaf yellow pine	12,600 to 19,200
ARTIFICIAL STONE:	
Brick laid in cement mortar	280 to 300
Concrete	0 to 300
Lime mortar	0 to 50

TABLE XII.

ULTIMATE RESISTANCE OF MATERIALS TO COMPRESSION.

	Lbs. per Sq. In.
Cast iron	82,000 to 145,000
Wrought iron	36,000 to 40,000
White pine, American	5,400
Long-leaf yellow pine	8,500
White oak, American	8,000
" " British	10,000
" " Dantzic	7,700
Brick, soft (in lime mortar)	550 to 800
Strong brick	1,100
Fire-brick	1,700
Granite	5,000 to 18,000
Limestone	4,000 to 16,000
Sandstone (ordinary)	2,500 to 10,000
Concrete: Portland cement, 1; sand, 3. 2 years old	2,600
" " " 1; " 2; stone, 4: 2 " "	3,000
" " " 1; " 3; " 6: 2 " "	2,700
" Rosendale " 1; " 3; " 4; gravel, 2	1,000
" Portland " 1; " 1; cinders, 3	1,000

(E for 1:2:5 concrete $=2,000,000$, approx.)
(E for 1:1:3 cinder concrete $=500,000$, approx.)

CHAPTER VI.

STRESSES CAUSED BY LATERAL WIND PRESSURE.

As the points of support for an arch are the lowest points of the structure, any lateral forces tend to topple it over, and to keep it in a stable position lateral bracing is therefore necessary.

The roadway is usually located above the arch and supported by columns, which arrangement affords an effective method for lateral stiffening.

Wind pressure is the force which will tend to disturb the upright position of the arch, and to provide for this force two methods may be employed to transfer it to the abutments.

(The horizontal framework which transfers the action of wind pressure to the abutments will be called "wind girders" in the following articles.)

The first method, which is also the simplest for computation, is the one where the wind girder is located under the floor of the bridge; the bridge floor (buckle-plate construction) itself may also form the wind girder. In this case the wind pressure is transferred from the arch to the wind girders by means of vertical lateral bracing, and the ends of the wind girders transfer the reactions caused by these forces to the supports of the arch by means of a framework.

The second method employs two wind girders, one located under the bridge floor—as described under the first method—and the other in the cylindrical surface of the arch; the computation of the stresses in the latter is rather complicated.

According to the nature of the structure and the condition of the locality, other methods may present themselves. These, however, can be considered as special cases, and a discussion of the two methods enumerated will be sufficient to indicate how others may be applied.

1. First Method: The Wind Girder under the Floor Resists all the Wind Pressure.—In Fig. 46 AB and $A'B'$ represent two arch ribs, and the wind girder is represented by CD, $C'D'$. The wind girder is assumed to be symmetrical with respect to the center, and the diagonals resist tension only. When the wind blows on the opposite side of the bridge, another system of diagonals (which has been omitted from the drawing) is stressed.

The wind pressure is assumed to be concentrated at the panel points *of the arch* and at the panel points *of the wind girder*. The panel loads at the wind girder are directly transmitted to the points C' and D', and thence to the supports A, A' and B, B'; the stresses in the members are computed according to the methods used for all framed girders supported at the ends.

The panel loads on the arch are transferred through the lateral diagonals to the wind girder; for example, the force W is transmitted through the diagonal ac to the point c, and produces at b a downward vertical force P, at c an upward vertical force $P'=P$, and also a horizontal force $W'=W$. The vertical forces P and P' cause the reactions V and V', and the horizontal thrusts H and H', respectively, at the left and right supports.

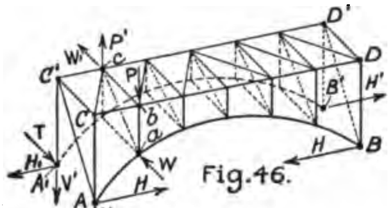

Fig. 46.

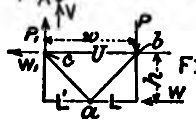

Fig. 46a.

The force W' acts as a horizontal load on the wind girder, and its intensity is added to that of the direct panel loads of the wind girder, producing the horizontal reaction T at A'.

When the length of the vertical ab is small as compared with the distance CC' between the two arches AB and $A'B'$, a system of lateral bracing, as shown in Fig. 46*a*, may be used.

The intensity of the wind pressure W at the panel points is computed in the usual way. From the figure, $W'=W$. To obtain the intensity of P and P', assume b or c to be the fulcrum; then

$$hW=P'w=-Pw,$$

or

$$P'=-P=\frac{hW}{w}$$

(upward and downward directions are respectively indicated by $+$ and $-$).

The values thus found for P are vertical forces acting on the arch, and the computation of the stresses which they cause in the arch rib can be performed according to the methods described in Chapters II and III.

The stress in L is compression, and is equal to W. The stress in U, caused by W, is tension, and is equal to W. To the stress U should be added the stress caused by the direct panel wind pressure at b.

The computation of the wind stresses is simple and does not require further explanation. There is, however, one point which deserves attention.

The end frame $AA'C'$ will be subject to temperature stresses,

as no provision can be made for lateral expansion and contraction at the supports A and A'.

To determine these stresses, compute the maximum change in length in the member CC' caused by an extreme temperature change. The sectional area of $A'C'$ and of AC are known. Apply a horizontal force equal to 1 in the direction of CC' at the point C', and compute the stress this force causes in the members $A'C'$ and AC'. Compute from these stresses the change in length of these members, and from this change the horizontal displacement of the point C' caused by a force$=1$.

The total expansion or contraction of the member CC' has already been computed, and the stresses in $A'C'$ and AC' are as much larger than those caused by the unit horizontal force as the actual displacement is larger than the displacement caused by the unit force. (See Arts. 7 *et seq.*, Chap. III.)

2. Second Method: Two Wind Girders—One Located under the Floor System and the Other in the Cylindrical Surface of the Arch. —The first girder is computed according to the method described in the preceding article, and only the computation of the stresses in the second girder will here be discussed.

In Fig. 47 this wind girder is shown with panel loads$=W$; ΣW is the sum of all these panel loads, and the distance a of its point of application from the line AB can be readily determined.

The vertical reaction V at the point A can then be found, viz.:

$$\frac{a \times \Sigma W}{2w} = V = -V''.$$

The value of W' is equal to the horizontal reactions caused by the loads W, or $W' = \frac{\Sigma W}{2}$. There is no horizontal reaction at A'. The value of H has to be found in an indirect manner.

In Fig. 47*a* one panel has been shown on a larger scale, and the force Q (which is in the section) represents the sum of all the interior forces at the panel.* For the panel 1–2 of Fig. 47, for example,

$$Q = \tfrac{1}{2}\Sigma W - W_1.$$

Now, from Fig. 47*a*, it follows that

$$Q = D_m \cos a \cos c,$$

$$\cos a = \frac{w}{e}, \quad \cos c = \frac{e}{d};$$

$$\therefore \; Q = D_m \frac{w}{d}, \quad \text{or} \quad D_m = Q\frac{d}{w}.$$

---

* This is equivalent to the shear in a simple girder.

Further, $$V_m = D_m \sin c = Q\frac{y'}{w},$$

$$L_m = D_m \cos c \sin a = Q\frac{x'}{w},$$

and $$Q_m = Q.$$

The forces are now all defined, and are indicated in Fig. 47*b*; the value of H can be computed according to Chapter III or IV.

To compute the wind stresses in the cylindrical wind girder, the method is as follows:

(*a*) Compute the stresses in the chords of the wind girder, conceiving same to lie in a plane (see horizontal projection in Fig. 47*c*).

(*b*) Compute the stresses in the diagonals in their actual position,

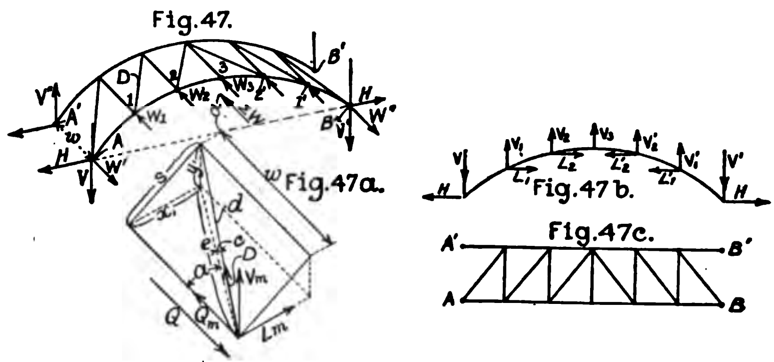

that is, in the cylindrical surface; and from these compute the vertical and horizontal forces at the panel points.

(*c*) Compute from *a* and *b* the stresses in the chords of the wind girder according to Chapter III or IV.

To obtain the stresses in the chords, combine the stresses described under (*a*) and (*c*) with those of the live load, the dead load, and the temperature, to give maximum and minimum stresses.

The stresses in the wind verticals and the diagonals are obtained from (*c*).

The additional stress in the arch rib, which is caused by lateral wind pressure, should be computed for long spans only; for short spans this stress can be neglected.

In the previous paragraphs only simple systems of bracing have been illustrated Double systems should be separated into two simple ones, each resisting one-half of the wind pressure, and the stresses in the members which are common to both systems should be added.

3. **Forces Acting on the Arch.**—Arches are used for bridges and roofs, and the forces acting on an arch are

(1) The dead load;
(2) The live load;
(3) Wind pressure and snow load;
(4) Temperature stresses.

In the foregoing chapters the intensity of each of these forces was assumed to be known; this article will deal with the determination of the intensities of these forces in the order above enumerated.

(*a*) THE DEAD LOAD.—The dead load may be considered as embracing all those forces whose actions on the arch are constant and cause permanent stresses.

Thus, in the case of a highway bridge or a roof, the weight of the structure, including the weight of the roadway or the roof covering, does not change, and this weight causes permanent stresses in the arch. To compute these stresses the character and distribution of the load over the structure must be known, and some assumptions must be made to render the computation possible.

As regards the stone or concrete arch, the experience of the designer must very largely serve as guidance. Such aids, however, as may facilitate his work, are given in Chapter IV [Arts. 1 and 6 (*c*)].

For the steel arch some such empirical formula as the following may be used to calculate the dead load, but in this case also experience must guide the designer in its proper application:

$$d=\frac{d_1\left(0.1429\frac{1}{n}+1.78n\right)+p\left(0.309+0.169\frac{1}{n}+1.77n+0.9n^2\right)+504+(16.2+0.0513l)nl+2.052l}{\frac{1,333}{l}+3-0.1429\frac{1}{n}-0.762n},$$

where d = weight of arch rib with lateral and wind bracing,
d_1 = weight of roadway,
p = live load,
} in lbs. per running foot of bridge;

l = span in feet;

$n=\frac{f}{l}=\frac{\text{rise}}{\text{span}}$.

The roadway of the bridge includes the floor-beams, the stringers, and everything supported by the stringers, such as the ties and rails on a railway bridge, or the floor, deck, and paving of a highway bridge.

In designing a steel arch, its form is approximately decided on, also the mode of supporting the bridge deck. This, ordinarily, indicates the spacing of the floor-beams, and the purpose for which the bridge is built defines the spacing of the stringers and the nature of the deck.

With these data the value of d_1 may be determined, and substituted in the formula.

The formula is written for a stress of 8,000 lbs. per sq. in. in the gross sections of the bridge members. For long-span bridges this stress may be higher, and the distribution of the material can be accomplished with greater economy (the construction factor is less).

(The formula gives values which are from 10 to 15 % too large for very long spans.)

To cover every case with an empirical expression is impossible, but for spans up to 250 ft. the above formula is practically correct; for a span of 500 ft. its result should be reduced by 15%. For any span between these lengths the value should be reduced in proportion, or about 0.6% for each additional 10 ft. of span beyond 250 ft.

(*b*) The Live Load.—The purpose of this book does not permit of any discussion of this subject.

In general it may be said that for highway bridges a uniformly distributed load plus one concentrated load (that of a road-roller) will suffice for all cases.

The author uses in his practice over and above the distributed load a concentrated load of 3,000 lbs. for an arch ring 1 foot wide, or a load of 20,000 lbs. covering a width of roadway of 9 feet.

For railroad bridges, wheel loads may be used in the computation. Such a form of loading makes the computation unnecessarily laborious, and the method of substituting for these loads equivalent uniform loads gives equally as good results and lightens the work.

The impact which may be caused by the live load is a rather indefinite quantity, and its effect on the arch is, to a large extent, influenced by the depth of the arch rib. The deeper the arch rib the more rigid the bridge. This rigidity, however, is offset by the temperature stresses, because the deeper the arch rib, the higher the temperature stresses will be. The designer has therefore to select from between these two, and experience and good judgment are here necessary.

Many pocket-books give a variety of tables for the live load, and the author refers to them for more information on this subject.

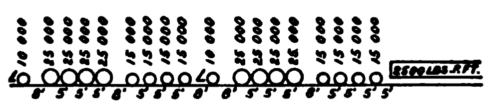

Fig. 48.

Fig. 48 shows two locomotives weighing 340,000 lbs. and covering a length of track of 105 ft. For a bridge which is longer than 105 ft., the additional length is covered with 2,500 lbs. per ft. per track.

This is the standard loading in the United States; for a heavier loading the values are multiplied by 1.2, 1.4, 1.6, etc. From this figure a table can be made of equivalent uniform loads which will cause approximately the same bending moments as the wheel load.

TABLE XIII.

STANDARD SYSTEM OF EQUIVALENT LOADS (PER FOOT PER TRACK) FOR RAILROAD BRIDGES.

Span in Feet.	Load in Pounds.	Span in Feet.	Load in Pounds.	Span in Feet.	Load in Pounds.
10	8,000	21	5,030	55	3,790
11	7,270	22	4,950	60	3,700
12	6,570	23	4,880	65	3,620
13	6,000	24	4,820	70	3,550
14	5,670	25	4,770	75	3,490
15	5,550	30	4,520	80	3,440
16	5,450	35	4,310	85	3,400
17	5,330	40	4,130	90	3,370
18	5,300	45	4,000	95	3,350
19	5,210	50	3,890	100	3,340
20	5,110				

To obtain the equivalent load for any heavier type of loading, multiply the above values by the ratio of the weight of the locomotives and tenders to those of Fig. 48.

(Tables XIV, XV, and XVI, which follow, are taken from Dr. J. A. L. Waddell's "De Pontibus," by permission of the author.)

Table XVI gives coefficients of impact, the first column indicating the span of the bridge, the second column giving the impact coefficients for railroad bridges (which should also be used for electric railways), and the third column the same coefficients for highway bridges.

To obtain the load per square foot to be used in the computation for a span of 50 ft., the use of the tables is as follows:

For a city bridge carrying the heaviest traffic (Class A), the load is 112.5 lbs. per sq. ft., the impact coefficient is 1.5, and the load per sq. ft. to be used is $1.5 \times 112.5 = 169$ lbs.

For a country bridge, the load is 75 lbs. per sq. ft., the impact coefficient 1.5, and the load to be used is 113 lbs. per sq. ft.

For an electric railway bridge (Class 1), the load is 830 lbs., the coefficient is 1.7273, and the load to be used is 1,434 lbs. per sq. ft., etc.

(*c*) WIND AND SNOW LOADS.—Values for wind pressure have been determined by experiments, and the maximum pressure (except in a tornado) on a surface which is normal to the direction of the wind is 45 lbs. per square foot for small surfaces, and 30 lbs. per square foot for large surfaces.

Hutton found from his investigations that the intensity of the normal component of the wind pressure on a roof may be expressed by the empirical equation

$$u' = u \sin a^{1.84 \cos a - 1},$$

where u' = the intensity of the normal component per sq. ft.;

u = the pressure on a vertical surface per sq. ft.;

a = the angle of inclination of the roof surface to the horizontal.

Table XIV.

HIGHWAY BRIDGES. LIVE LOAD PER SQUARE FOOT.

SPAN	CLASS A	CLASS B	CLASS C	SPAN	CLASS A	CLASS B	CLASS C	SPAN	CLASS A	CLASS B	CLASS C
0	120.0	100.0	80.0	125	102.0	84.8	68.0	250	86.9	72.0	57.9
5	119.2	99.4	79.5	130	101.3	84.2	67.5	255	86.4	71.6	57.5
10	118.4	98.8	79.0	135	100.7	83.7	67.1	260	85.9	71.2	57.2
15	117.6	98.1	78.5	140	100.0	83.2	66.7	270	84.9	70.4	56.5
20	116.9	97.4	78.0	145	99.4	82.6	66.2	280	83.9	69.6	55.8
25	116.2	96.8	77.5	150	98.8	82.0	65.8	290	82.9	68.8	55.1
30	115.4	96.2	77.0	155	98.2	81.5	65.4	300	81.9	68.0	54.4
35	114.6	95.6	76.5	160	97.5	81.0	65.0	325	79.5	66.2	52.9
40	113.9	95.0	76.0	165	96.9	80.5	64.5	350	77.2	64.5	51.5
45	113.2	94.4	75.5	170	96.2	80.0	64.1	375	75.1	62.9	50.1
50	112.5	93.8	75.0	175	95.6	79.4	63.7	400	73.1	61.4	48.8
55	111.7	93.1	74.5	180	95.0	78.9	63.3	425	71.3	59.9	47.5
60	111.0	92.5	74.0	185	94.4	78.3	62.9	450	69.6	58.5	46.3
65	110.3	91.9	73.5	190	93.8	77.8	62.5	475	68.1	57.1	45.2
70	109.6	91.3	73.1	195	93.2	77.3	62.1	500	66.8	55.8	44.2
75	108.9	90.7	72.6	200	92.6	76.8	61.7	525	65.6	54.6	43.4
80	108.2	90.1	72.1	205	92.0	76.3	61.3	550	64.5	53.6	42.7
85	107.5	89.5	71.6	210	91.4	75.8	60.9	575	63.5	52.8	42.1
90	106.8	88.9	71.2	215	90.8	75.3	60.5	600	62.6	52.1	41.6
95	106.1	88.3	70.8	220	90.2	74.8	60.1	625	61.9	51.5	41.2
100	105.4	87.7	70.3	225	89.6	74.3	59.7	650	61.3	51.0	40.9
105	104.8	87.1	69.9	230	89.1	73.9	59.4	675	60.8	50.6	40.6
110	104.1	86.6	69.4	235	88.5	73.4	59.0	700	60.4	50.3	40.4
115	103.4	86.0	69.0	240	88.0	73.0	58.6	725	60.2	50.1	40.2
120	102.7	85.4	68.5	245	87.4	72.5	58.2	750	60.0	50.0	40.0

Table XV.

HIGHWAY BRIDGES—ELECTRIC RAILWAY. LOADS PER LINEAR FOOT OF TRACK.

(Loads cover a width of ten feet.)

Span	Class I	Class II	Class III	Class IV	Span	Class I	Class II	Class III	Class IV	Span	Class I	Class II	Class III	Class IV
10	2400	3200	4000	3360	35	1110	1505	1875	1815	110	425	525	690	1150
11	2280	3050	3800	3200	36	1085	1475	1835	1790	115	410	505	665	1125
12	2170	2920	3640	3070	37	1060	1445	1795	1770	120	400	485	640	1100
13	2070	2800	3510	2960	38	1040	1415	1755	1750	125		470	620	1080
14	1990	2690	3395	2860	39	1020	1390	1720	1730	130		455	600	1060
15	1915	2590	3285	2775	40	1000	1365	1685	1710	135		445	580	1040
16	1850	2490	3180	2700	42	960	1315	1620	1675	140		435	560	1020
17	1785	2405	3080	2630	44	925	1270	1565	1645	145		425	540	1000
18	1725	2325	2985	2560	46	890	1225	1515	1620	150		415	525	985
19	1670	2245	2890	2495	48	860	1180	1465	1600	155		410	510	970
20	1615	2175	2800	2430	50	830	1140	1415	1580	160		405	495	955
21	1565	2110	2715	2370	52	800	1100	1365	1560	170		400	480	920
22	1520	2050	2630	2310	54	775	1060	1320	1540	180			465	885
23	1480	1995	2550	2255	56	755	1025	1280	1520	190			450	855
24	1440	1945	2475	2200	58	735	990	1240	1500	200			435	825
25	1400	1895	2400	2150	60	715	955	1200	1480	210			420	795
26	1365	1850	2330	2105	65	665	875	1125	1440	220			410	765
27	1330	1805	2265	2060	70	620	815	1050	1400	230			405	740
28	1300	1760	2205	2020	75	580	765	980	1360	240			400	715
29	1270	1720	2150	1985	80	550	720	930	1325	250				690
30	1240	1680	2100	1950	85	525	680	880	1290	260				665
31	1210	1640	2050	1920	90	500	645	835	1255	270				640
32	1185	1605	2005	1890	95	475	610	790	1225	280				615
33	1160	1570	1960	1865	100	455	580	750	1200	290				595
34	1135	1535	1915	1840	105	440	550	720	1175	300				585

TABLE XVI.

IMPACT COEFFICIENTS.

SPAN	R.R.	HWY.	SPAN	R.R.	HWY.	SPAN	R.R.	HWY.	SPAN	R.R.	HWY.
1	.7984	.6623	37	.7449	.5348	73	.6981	.4484	145	.6202	.3389
2	.7968	.6579	38	.7435	.5319	74	.6968	.4464	150	.6154	.3333
3	.7952	.6536	39	.7421	.5291	75	.6957	.4444	155	.6107	.3279
4	.7936	.6494	40	.7407	.5263	76	.6944	.4425	160	.6061	.3226
5	.7921	.6452	41	.7394	.5236	77	.6932	.4405	165	.6015	.3175
6	.7905	.6410	42	.7380	.5208	78	.6920	.4386	170	.5970	.3125
7	.7889	.6369	43	.7367	.5181	79	.6908	.4367	175	.5926	.3077
8	.7874	.6329	44	.7353	.5155	80	.6897	.4348	180	.5882	.3030
9	.7858	.6289	45	.7339	.5128	81	.6885	.4329	185	.5839	.2985
10	.7843	.6250	46	.7326	.5102	82	.6873	.4310	190	.5797	.2941
11	.7828	.6211	47	.7313	.5076	83	.6861	.4292	195	.5755	.2899
12	.7812	.6173	48	.7299	.5051	84	.6849	.4274	200	.5714	.2857
13	.7797	.6134	49	.7286	.5025	85	.6838	.4255	210	.5634	.2778
14	.7782	.6098	50	.7273	.5000	86	.6826	.4237	220	.5556	.2703
15	.7767	.6061	51	.7260	.4975	87	.6814	.4219	230	.5480	.2632
16	.7752	.6024	52	.7247	.4951	88	.6803	.4202	240	.5405	.2564
17	.7737	.5988	53	.7233	.4926	89	.6791	.4184	250	.5333	.2500
18	.7722	.5952	54	.7220	.4902	90	.6780	.4167	260	.5263	.2439
19	.7707	.5917	55	.7207	.4878	91	.6768	.4149	270	.5195	.2381
20	.7692	.5882	56	.7194	.4854	92	.6757	.4131	280	.5128	.2326
21	.7678	.5848	57	.7181	.4831	93	.6745	.4115	290	.5063	.2273
22	.7663	.5814	58	.7169	.4808	94	.6734	.4098	300	.5000	.2222
23	.7648	.5780	59	.7156	.4785	95	.6723	.4082	325	.4848	.2105
24	.7634	.5747	60	.7143	.4762	96	.6711	.4065	350	.4706	.2000
25	.7619	.5714	61	.7130	.4739	97	.6700	.4049	375	.4571	.1905
26	.7605	.5682	62	.7117	.4717	98	.6689	.4032	400	.4444	.1818
27	.7590	.5650	63	.7105	.4695	99	.6678	.4016	450	.4211	.1667
28	.7576	.5618	64	.7092	.4673	100	.6667	.4000	500	.4000	.1539
29	.7561	.5586	65	.7080	.4651	105	.6612	.3922	550	.3810	.1429
30	.7547	.5556	66	.7067	.4630	110	.6557	.3846	600	.3636	.1333
31	.7533	.5525	67	.7055	.4608	115	.6504	.3774	650	.3478	.1250
32	.7519	.5495	68	.7042	.4587	120	.6452	.3704	700	.3333	.1176
33	.7505	.5465	69	.7030	.4566	125	.6400	.3636	750	.3200	.1111
34	.7491	.5435	70	.7018	.4546	130	.6349	.3571	800	.3077	.1053
35	.7477	.5405	71	.7005	.4525	135	.6299	.3509	850	.2963	.1000
36	.7463	.5376	72	.6993	.4505	140	.6250	.3448	900	.2857	.0952

This equation gives the following values for a pressure of 1 lb. per sq. ft. of vertical surface:

$a=$	5°	10°	15°	20°	25°	30°	35°	40°	45°	50°	55°	60°
u'(lbs.)=	0.13	0.24	0.35	0.46	0.56	0.66	0.75	0.84	0.90	0.95	0.99	1.00

When a is larger than 60°, u' is assumed to be 1 lb. per sq. ft.

The direction of the wind is also often assumed to make an angle of 15° with the horizontal, which would mean that the pressure of the wind is exerted on a normal surface which is inclined 15° to the vertical. The vertical pressure on a roof is then equal to the wind pressure multiplied by the sine of 15° and acts on the horizontal projection of the roof surface. The horizontal pressure is equal to the wind pressure multiplied by the cosine of 15° and acts on the vertical projection of the roof surface.

The last method is simpler in its application and gives good results; it has been used in Chapter III, Article 17.

The intensity of the wind pressure is regulated by the location of the structure. In New York City, for example, 35 lbs. per sq. ft. is generally adopted as covering every condition.

For railroad bridges the wind loads include a pressure of 300 lbs. per lin. ft. on a train, and the center of this pressure acts at a height of 8 ft. above the rail. This wind load may be treated in the computation as a moving load.

For the anchorage of the bridge the assumption is made that the whole structure is loaded with a train of empty cars which weigh 1,000 lbs. per foot per track.

For highway bridges the wind load includes a pressure of 250 lbs. per lin. ft. on a train of wagons, and the center of this pressure acts at a height of 6 ft. above the pavements. This wind load may also be treated as a moving load.

The area exposed to the wind in a bridge includes the area of the windward girder plus 0.7 of the area of the leeward girder or girders.

According to the locality, the snow load is estimated from 10 to 30 lbs. per sq. ft. of horizontal projection, and it is assumed that no snow will remain on a surface which inclines 45°. (See Chapter III, Article 17.)

(*d*) Temperature Stresses.—These are caused by changes in temperature. To what extent the structure is influenced by these changes depends on its location and on the nature of the structure.

On steel arches their effect is very considerable; in addition to this the structure absorbs heat, so that the temperature of the steelwork often rises 25° F. above that of the surrounding air. For this reason the extreme changes in temperature for such a structure are assumed to be from 60° to 75° F. above or below the normal temperature, which should be assumed as 50° F.

On stone or concrete arches their effect is relatively small, depending largely on the amount of material covering the arch. Rarely will

the temperature exceed 25° F. above or below the normal in a masonry arch.

It will naturally suggest itself that the influence of a change in temperature does not make itself felt in an equal degree and at the same time in all parts of the structure. This is applicable to the steel arch as well as to the one of stone. To make the computation of stresses possible a maximum change is assumed, and all intermediate conditions are covered by it.

The coefficient of expansion for steel is 0.000007, and for stone or concrete $\frac{1}{150,000}$, for 1° F. Both coefficients are practically equivalent, and the same value is assumed in the case of the reinforced-concrete arch, which facilitates the computation of its stresses.

4. Determination of the Type of Arch.—This article deals with the determination of the type of arch for a bridge.

For roof trusses the selection of the type of arch is largely dependent on the character of the building, and so many conditions govern its selection that it is impossible to lay down broad rules.

In general, the roof arch is of the two- or the three-hinged type. The two-hinged type is preferable for its greater rigidity, since the displacement caused by expansion and contraction is distributed over its whole length. In the three-hinged type all this displacement is confined to the crown hinge, and in flat roofs it may be considerable, necessitating constant care and watching against leakage.

The use of tie-rods to fix the abutment hinges in position should be avoided, if possible, in all cases where these rods are out of reach for easy inspection.

The type of arch for a bridge must be one of the following three:

(*a*) The three-hinged arch;
(*b*) The two-hinged arch;
(*c*) The hingeless or fixed arch;

and for the one decided upon it must be determined whether it should be built as an arch rib or as an arched framework.

To enable an intelligent selection to be made the comparative advantages of each system will now be discussed.

(*a*) The Three-Hinged Arch.—The stresses in the three-hinged arch are statically defined and are easily computed. This advantage, however, should not carry any weight, as the foregoing examples have shown that with the author's method the two-hinged arch offers no greater difficulty, and computation of the stresses in the hingeless arch is only a little more laborious. Changes in temperature cause no stresses in the three-hinged arch, and, with a proper supervision of the erection, no unknown stresses can develop in it. Yielding of the abutments, unless excessive, does not create appreciable stresses in the arch. These advantages have given the three-hinged arch a preference, but the disadvantages attached to this type nevertheless are well worthy of consideration. In the first place, the wind bracing is interrupted at the point where it should resist the

greatest stresses. Second, the vertical movement of the crown caused by temperature changes is about one-third larger than in either the two-hinged or the hingeless arch, and this ratio increases for the deflections caused by the live load, particularly under the influence of single heavy loads. Its horizontal displacement also is larger, and when the roadway is required to be water-tight, this type of arch cannot be considered.

(b) THE TWO-HINGED ARCH.—The computation of the stresses in this arch, as mentioned under (a), can be performed with the same precision as that of the three-hinged arch and without more labor. Its vertical movement caused by live loads and temperature changes is less than that in the three-hinged arch.

On account of the temperature stresses developed in the arch, more material would apparently be required for its construction. In this connection, however, the fact should not be lost sight of that a maximum live-load stress, together with the dead-load stress and a maximum temperature stress, requires a combination of circumstances which will rarely, if ever, occur during the lifetime of the bridge. For this reason it is good practice to allow here a higher stress in the material, and steel may be stressed with at least 1,200 lbs. per square inch more, while for reinforced concrete and good stone masonry the stress may be increased by 100 lbs. per square inch. (In the examples given the author has used for reinforced concrete a maximum of 600 lbs. per square inch.)

When this permissible increased stress in the material is considered, and in addition the greater relative cost of construction for the crown hinge, and the increased quantity of metal required in the wind bracing of the three-hinged arch, it can be safely stated that the two types of arches are on an equality as regards their costs of construction.

(c) THE HINGELESS ARCH.—This is the most rigid type of all, and in this regard it exhibits an advantage over the two-hinged arch.

The examples which have been given show that the computation of its stresses requires more labor, and also that a slight yielding of the abutments very materially influences the stresses in the arch. In most cases this latter can be prevented; but where unavoidable, the hingeless arch must be left out of consideration.

On account of the intricacy which has hitherto characterized the application of the elastic theory, and the uncertainty regarding the stresses in the arch as obtained by any other method, this type of arch has been neglected to such an extent as almost to amount to prejudice.

Extensive experiments for the Kaiser Wilhelm Bridge at Müngsten, however, have shown that the hingeless arch not only requires less material for its construction than does the two-hinged type, but that the distribution of the metal is such that its cost of erection is less. With this economical showing and the employment of the simple and dependable method of computation outlined by the author, it

would seem that no valid objection could now be made to the use of the hingeless arch.

(*d*) ARCH RIB.—All masonry or concrete arches are built of solid ribs. In the construction of the steel arch, however, a selection can be made of either the rib or the frame; and the rib may be solid, or it may be composed of chords and web members.

The rib arch gives a more pleasing and esthetic effect than the framed arch. As regards the material required for construction, there is no substantial difference between the two; the rib, however, shows a slight disadvantage in this respect.

(*e*) THE ARCHED FRAMEWORK.—Though its esthetic effect is not so pleasing, the arched framework possesses great advantages in erection, especially in places where falsework would be expensive or impossible. This subject was extensively discussed in Chapter III (Art. 7).

5. Comparison of Stresses and Deflections in the Three Types.—(*a*) YIELDING OF THE ABUTMENTS (STRESSES CAUSED BY).—*Three-Hinged Arch.*—From equation (28) of the Appendix,

$$\Delta f = -\frac{l}{4f}\Delta l,$$

where Δl represents the increase in the span caused by the yielding of the abutments.

Let $\quad \dfrac{l}{f}=12, \quad$ and $\quad \Delta l = 1$ in.;

then $\quad \Delta f = -3$ ins.

For a uniform load p, $\quad H=\dfrac{pl^2}{8f},$

and
$$\Delta H = \frac{p(l+\Delta l)^2}{8(f+\Delta f)} - \frac{pl^2}{8f},$$

or
$$\frac{\Delta H}{H} = \frac{f\Delta l(2l+\Delta l) - l^2\Delta f}{l^2(f+\Delta f)},$$

and again $\Delta f = -3$ ins., $\Delta l = 1$ in. Taking $l = 2{,}000$ ins., $f = \dfrac{2{,}000}{12}$, and substituting these values together with those above for Δf and Δl gives

$$\frac{\Delta H}{H} = 0.0193.$$

Two-Hinged Arch.—From equation (121) of the Appendix, for a parabolic arch rib with an approximately constant section,

$$\Delta f = -\frac{25}{128}\frac{l}{f}\Delta l \frac{1-\frac{96}{5}\frac{I}{Fl^2}}{1+\frac{15}{8}\frac{I}{Ff^2}},$$

and substituting $I = \frac{h^2}{4}F$ gives (when F = area of the arch rib)

$$\Delta f = -\frac{25}{128}\frac{l}{f}\frac{\left(1-\frac{48h^2}{10l^2}\right)}{\left(1+\frac{15h^2}{32f^2}\right)}\Delta l;$$

and assuming that

$$\frac{h}{f} = \quad \frac{1}{3} \quad \frac{1}{4} \quad \frac{1}{5} \quad \frac{1}{10}, \text{ and that } \frac{f}{l} = \frac{1}{12},$$

gives $$\frac{h}{l} = \quad \frac{1}{36} \quad \frac{1}{48} \quad \frac{1}{60} \quad \frac{1}{120}; \text{ also, if } \Delta l = 1 \text{ in.},$$

$$\Delta f = -2.22 \quad -2.272 \quad -2.297 \quad -2.332.$$

(For a three-hinged arch $\Delta f = 3$ ins.)

These figures show not only the comparative deflections of the two types of arches, but also the influence of the depth of the arch rib upon the deflections in the two-hinged arch.

When, in Equation (110^a) of the Appendix, $\frac{\Delta l}{l}$ is substituted for Ewt, the horizontal thrust then changes to

$$\Delta H = -\frac{15EI}{8f^2\left(1+\frac{15}{8}\frac{I}{Ff^2}\right)}\frac{\Delta l}{l} = -\frac{15EFh^2}{32f^2+15h^2}\frac{\Delta l}{l},$$

and if, again,

$$l = 2{,}000 \text{ ins.}, \quad \Delta l = 1 \text{ in.}, \quad \text{and} \quad E = 29{,}000{,}000,$$

when $$\frac{f}{h} = \quad 3 \quad 4 \quad 5 \quad 10$$

$$\frac{\Delta H}{F} = 717 \quad 413 \quad 267 \quad 68 \text{ lbs. per sq. in.}$$

The stresses developed at the crown of the arch by the yielding of the abutments

$$=n=-\frac{\Delta H}{F}\left(1\mp\frac{2f}{h}\right).$$

If the values of $\frac{\Delta H}{F}$ which are given above are used and

$\frac{f}{h}$ (as before) =	3	4	5	10	
$n_u=$	$-3,585$	$-2,891$	$-2,403$	$-1,292$	lbs. per sq. in.
$n_l=$	5,019	3,717	2,937	1,428	" " " "

(The inferiors u and l indicate upper and lower chords, respectively.)

These values show the injurious effects of a yielding of the abutments on a two-hinged arch, and that these stresses increase with the depth of the arch rib.

The effect of a yielding of the abutments on a hingeless arch is greater and has been specially dealt with in Chapter IV, Article 8.

(*b*) Deflections Caused by Changes in Temperature.—From the analysis given in the Appendix it follows that the effect of a change in temperature on the stresses in the arch rib increases with its depth, in the two-hinged and the hingeless arches. In the three-hinged arch this change develops no stresses.

The crescent-shaped two-hinged arch, however, is an exception, its temperature stresses being comparatively low.

To compute the temperature stresses the analysis in the Appendix on this subject gives all the necessary information.

To facilitate its application the equations have been written in a simple form, viz.:

Two-Hinged Arch with Parallel Chords:

$$n_t=\pm Ewt\frac{15}{32}\frac{h}{f}\,\frac{2\mp\frac{h}{f}}{1+\frac{15}{32}\left(\frac{h}{f}\right)^2},$$

and if $E=29,000,000$, and $w=0.000007$ for steel ($Ew=203$), the stress caused by a change of 1° F. is

$$n_t=\pm 3,045\frac{2\frac{f}{h}\mp 1}{32\left(\frac{f}{h}\right)^2+15}.$$

Two-Hinged Crescent-Shaped Arch:

$$n_t = 101.5 \frac{2\frac{f}{h} \mp 1}{2\left(\frac{f}{h}\right)^2 + \frac{1}{2}}.$$

Hingeless Arch.—When n_c is the stress at the crown and n_a the stress at the abutments caused by a temperature change of 1° F., and when in the numerator the upper sign is that of the stress in the upper chord and the lower sign that of the stress in the lower chord,

$$n_c = \pm \frac{15}{8} Ew \frac{1 \mp \frac{3}{2}\frac{h}{f}}{1 + \frac{45}{16}\frac{h^2}{f^2}};$$

and when $Ew = 203$,

$$n_c = \pm 380.6 \frac{\frac{f}{h} \mp \frac{3}{2}}{\frac{f^2}{h^2} + \frac{45}{16}}.$$

$$n_a = \mp \frac{15}{4} Ew \frac{\left(1 \pm \frac{3}{4}\frac{h}{f}\right)\frac{h}{f}}{1 + \frac{45}{16}\frac{h^2}{f^2}};$$

and when $Ew = 203$,

$$n_a = \mp 761.2 \frac{\frac{f}{h} \pm \frac{3}{4}}{\frac{f^2}{h^2} + \frac{45}{16}}.$$

To compare the relative stresses in the two types a table has been made for various values of $\frac{f}{h}$, and a temperature change of 1° F. gives for the hingeless arch the stresses in the bottom chord at the crown, and those in the top chord at the abutments; for the two-hinged arch the stresses in the bottom chord at the crown; and for the crescent-shaped arch the chord stresses (which are constant over the full lengths of the chords).

The actual stresses may be obtained by multiplying the figures by $\mp t$.

$\frac{f}{h}=$	0	1	2	3	4	5	10	∞
HINGELESS ARCH:								
Abutments: top chord	203	349	308	241	191	157	79.4	0
Crown: bottom chord	203	250	195.5	145	110.5	88.5	42.5	0
TWO-HINGED ARCH, bottom chord at crown:								
Parallel chords.......	203	194	106.5	70.5	51.6	40.8	19.6	0
Crescent-shaped......	203	121	59.7	38.4	27.8	22.1	10.6	0

(Stresses in lbs. per sq. in.)

The vertical movement at the crown caused by changes in temperature can be computed from equations (28), (120), and (173) of the Appendix. For flat arches with practically constant sectional areas, the following approximate equations may be developed:

Three-hinged arch: $$\Delta f=\frac{l}{4f}wtl\left(1+\frac{8}{3}\frac{f^2}{l^2}\right)$$

Two-hinged arch: $$\Delta f=\left(\frac{25}{128}\frac{l}{f}+2\frac{f}{l}\right)\frac{wtl}{1+\frac{15}{32}\frac{h^2}{f^2}}$$

Hingeless arch: $$\Delta f=\left(\frac{15}{64}\frac{l}{f}+2\frac{f}{l}\right)\frac{wtl}{1+\frac{45}{16}\frac{h^2}{f^2}}$$

For a ratio of $\frac{l}{f}=10$, a temperature change of 180° F., and $w=0.00126$,

when $\frac{f}{h}=$	1	2	3	4	5	10	∞	
Δf (hingeless arch) =	$\frac{1}{1{,}210}$	$\frac{1}{540}$	$\frac{1}{416}$	$\frac{1}{373}$	$\frac{1}{352}$	$\frac{1}{326}$	$\frac{1}{317}$	$\times l$
Δf (two-hinged arch) =	$\frac{1}{550}$	$\frac{1}{418}$	$\frac{1}{394}$	$\frac{1}{386}$	$\frac{1}{382}$	$\frac{1}{379}$	$\frac{1}{374}$	$\times l$
Δf (three-hinged arch) =	$\frac{1}{314}$			constant				$\times l$

For $\frac{f}{h}=\infty$ the three types of arches should give equal values; the differences result from the assumptions which are made in the above approximate equations.

This table shows that there is not so great a difference between the two-hinged and the hingeless arches as there is between the two- and three-hinged arches, and, though the stresses caused by temperature changes are greater in the hingeless arch than in the two-hinged arch, the deflections are nearly the same, for all practical purposes.

To show the comparative effects caused by changes in the ratio $\frac{l}{f}$, the following table is made out for $\frac{f}{h}=3$:

	$\frac{l}{f}=$ 8	9	10	11	12	
Hingeless arch,	$\Delta f=\frac{1}{498}$	$\frac{1}{454}$	$\frac{1}{416}$	$\frac{1}{383}$	$\frac{1}{355}$	$\times\, l$
Two-hinged arch,	$\Delta f=\frac{1}{468}$	$\frac{1}{428}$	$\frac{1}{394}$	$\frac{1}{364}$	$\frac{1}{338}$	$\times\, l$
Three-hinged arch,	$\Delta f=\frac{1}{386}$	$\frac{1}{347}$	$\frac{1}{314}$	$\frac{1}{287}$	$\frac{1}{264}$	$\times\, l$

This table shows the relative temperature deflections in the three types of arches even more strikingly than the former one.

(c) Vertical Deflection of the Crown Caused by the Live Load.—The following equations may be deduced from equations (57), (113^a), (167), and (168) of the Appendix.

For a fully-loaded bridge with a uniformly distributed load:

Three-hinged arch: $$\Delta f=\frac{1}{32}\frac{pl^2}{EF}\frac{l^2}{f^2}\left(1+\frac{8}{3}\frac{f^2}{l^2}\right)$$

Two-hinged arch: $$\Delta f=\frac{1}{8}\frac{pl^2}{EF}\left(\frac{25}{128}\frac{l}{f}+2\frac{f}{l}\right)\frac{l}{f\left(1+\frac{15}{32}\frac{h^2}{f^2}\right)}$$

Hingeless arch: $$\Delta f=\frac{1}{8}\frac{pl^2}{EF}\left(\frac{15}{64}\frac{l}{f}+2\frac{f}{l}\right)\frac{l}{f\left(1+\frac{45}{16}\frac{h^2}{f^2}\right)}$$

Comparing these equations with those which give the deflections caused by a change in temperature shows that the relative deflections correspond.

The greatest deflection of the crown is approximately obtained by loading either the middle third or the first and last thirds of the span.

From the above equations the following expressions may be deduced for the deflection of the crown, it being assumed that the middle third of the span is loaded:

Three-hinged arch: $$\Delta f=\frac{1}{1{,}944}\frac{pl^2}{EF}\frac{5{,}400+148\frac{l^2}{h^2}+2{,}025\frac{l^2}{f^2}}{60}$$

Two-hinged arch: $$\Delta f=\frac{1}{1{,}944}\frac{pl^2}{EF}\frac{92{,}928+320\frac{l^2}{h^2}+9{,}225\frac{l^2}{fh}}{384+180\frac{h^2}{f^2}}$$

Hingeless arch: $$\Delta f=\frac{1}{1{,}944}\frac{pl^2}{EF}\frac{18{,}048+32\frac{l^2}{h^2}+2{,}205\frac{l^2}{f^2}}{64+180\frac{h^2}{f^2}}$$

For $\frac{l}{f}=10$ these equations give the following values:

When $\frac{f}{h}=$	1	10
Hingeless arch:	$\Delta f=0.51\frac{pl^2}{EF}$	$4.36\frac{pl^2}{EF}$
Two-hinged arch:	$\Delta f=0.963\frac{pl^2}{EF}$	$5.62\frac{pl^2}{EF}$
Three-hinged arch:	$\Delta f=1.91\frac{pl^2}{EF}$	$14.46\frac{pl^2}{EF}$

These values show the large deflection of the three-hinged arch, as compared with the other two types.

The deflection of the crown caused by a single load at the center of the arch shows this disadvantage of the three-hinged arch still more.

The equations are as follows:

Three-hinged arch: $$\Delta f=\frac{Kl}{48EF}\frac{40+15\frac{l^2}{f^2}+2\frac{l^2}{h^2}}{5}$$

Two-hinged arch: $$\Delta f=\frac{Kl}{48EF}\frac{600+60\frac{l^2}{f^2}+3\frac{l^2}{h^2}}{32+15\frac{h^2}{f^2}}$$

Hingeless arch: $$\Delta f=\frac{Kl}{48EF}\frac{360+45\frac{l^2}{f^2}+\frac{l^2}{h^2}}{16+45\frac{h^2}{f^2}}$$

(*d*) HORIZONTAL DISPLACEMENT OF THE CROWN CAUSED BY THE LIVE LOAD.—This displacement may be computed from equations (40) or (56) of the Appendix, for the three-hinged arch.

For the two- and three-hinged arches these displacements are the same. For the hingeless arch the shifting of the crown caused by a single vertical load

$$=\Delta x_c=\frac{Kfl^2}{48EI}\left(\frac{g}{l}\right)^2\left(1-2\frac{g}{l}\right)\left(3-4\frac{g}{l}\right),$$

and the maximum shifting of the crown (when g = distance from a single load to the abutment, g' = length of uniform load measured from the abutment) is as follows:

Two- and three-hinged arches................
- single load, $g=\frac{1}{2}l$, $\Delta x_c=\frac{5}{384}\frac{fl}{h^2}\frac{Kl}{EF}$;
- uniform load, $g'=\frac{1}{2}l$, $\Delta x_c=\frac{1}{240}\frac{fl}{h^2}\frac{pl^2}{EF}$.

Hingeless arch..........
- single load, $g=0.289l$, $\Delta x_c=\frac{1}{186}\frac{fl}{h^2}\frac{Kl}{EF}$;
- uniform load, $g'=\frac{1}{2}l$, $\Delta x_c=\frac{1}{640}\frac{fl}{h^2}\frac{pl^2}{EF}$.

These equations show the great advantage of the hingeless arch over the other two types.

(*e*) ANGULAR DISPLACEMENTS AT THE HINGES.—These are directly obtained from the equations on page 248 of the Appendix.

For the two-hinged arch the angular deflection caused by a single load is, according to equation (112) of Appendix (see also foot-note on page 284),

$$\Delta a=\frac{2}{3}\frac{K}{EF}\frac{g}{l}\left(1-\frac{g}{l}\right)\frac{120\left(1+\frac{g}{l}-\frac{g^2}{l^2}\right)+15\left(2-\frac{g}{l}\right)\frac{l^2}{f^2}+8\left(3-9\frac{g}{l}+5\frac{g^2}{l^2}\right)\frac{l^2}{h^2}}{32+15\frac{h^2}{f^2}},$$

and that from a change in temperature

$$=\Delta a=20wt\frac{l}{f}\,\frac{1+9\frac{h^2}{l^2}+\frac{32}{5}\frac{f^2}{l^2}}{32+15\frac{h^2}{f^2}}.$$

6. The Abutments.—The abutment resists all vertical loads, the horizontal thrust of the arch, and often also the horizontal thrust of the earth-fill. These horizontal thrusts act in opposite directions, and the resulting thrust must be less than that caused by either force.

In computing the stability of the abutment, the thrust caused by the fill is not usually considered, except as an addition to the factor of safety, because the bridge must be secure before the filling is placed behind the abutments.

The abutment must in the first place be secure against overturning, and consequently it should be able to withstand the action of the arch when the earth pressure behind the abutment is neglected; and it should also withstand the action of the earth pressure when the counteraction of the arch is neglected. This, however, is given only as a general rule—special conditions will dictate their own rules.

In addition, the abutment should be secure against sliding, which is liable to occur, particularly in flat arches. The forces acting in the abutments often require that the joints in the masonry be laid at an angle with the horizontal. The friction angle can be assumed as 22°, and this requires that the line of pressure shall not exceed an angle of 22° with the perpendicular to the joints in the masonry.

A good method of construction for large stone arches is to continue the abutment as a part of the arch to the foundation bottom, increasing the dimensions of the arch rib gradually so that the pressure on the foundation remains well within the limit of safety. This construction will make the center line of pressure also the center line of the abutment, and all joints are then at right angles to this line. (See Fig. 35,—Syra Valley Bridge.) A very good example of this construction is presented in the stone bridge over the Petrusse Valley, in Luxemburg.

It is impossible to lay down general rules, as each case should be investigated for itself.

In computing the stresses in the abutments the graphical method is preferable, as all the important elements in the design can be clearly shown, while it is difficult to handle them analytically in anything like as effective a manner. Special attention should be devoted to the manner in which the stresses are distributed over the foundation, as it is usually there that any yielding of the abutments originates, and the liberal use of material in that part of the structure is of great advantage. (Art. 8, Chapter IV, shows the injurious effect of a yielding of the abutments in a large arch.)

To compute the continuation of the line of pressure of the arch in the abutments, they should be divided into panels, in the same manner as is the arch; and the weight and the center of gravity of each of these panels should be found, and force diagrams constructed in the same manner as was described for the stone arch. Those parts of the abutment that can be considered as inactive in the distribution of the stress should be left out of the computation; though they form part of the main body, their homogeneity with it may be disturbed.

The plane of the foundation should preferably be at right angles to the line of pressure.

To determine the thickness of the abutments for small arches, and

in the preliminary design of arches of moderate span, Trautwine's formula gives good results:

$$t=0.2r+0.1f+2,$$

where t = thickness of abutment;
r = radius of curvature;
f = rise of the arch (all dimensions in feet).

This in connection with his equation for the depth of the arch rib at the crown (on page 105) gives good dimensions for arches of spans under 50 ft. For longer spans and good material and workmanship, the dimensions for the abutments, as obtained from this formula, are too large. This is, however, a defect which is inherent in all empirical formulas, and results from the very nature of the structure. The author's formula for the dimension of the arch at the springing line, which is also the dimension of the abutment (see page 145), is not free from this objection, as there explained.

7. **The Intermediate Piers.**—These piers are generally subjected to large stresses, and the greatest care should be used in their design. Apart from their own weight and that of the arches resting on them, they resist the horizontal thrust of the arches for various conditions of loading.

The stresses in the masonry should be investigated in every part, and this, in connection with the condition of the foundation bottom, should determine its dimensions. Special care should be taken that the line of pressure in the pier is always located in the middle third (the core) of the pier, so that all stresses are compressive. Often the use of reinforced concrete may be advantageous, and the computation of the stresses in the pier should be made in the same manner as for those in the stone arch rib, as analyzed in the Appendix and in Chapter V, Arts. 2, etc.

The safe stresses in a pier cannot be assumed as high as those in the arch, particularly when the pier stands in water. The strength of wet masonry, and especially of wet concrete, is less than that of dry concrete. This fact is well known; but experiments to determine their relative strengths have been few in number, and there are no reliable data on the subject. The author uses in his practice for good concrete (1:2:5) a compressive stress not to exceed 300 lbs. per sq. in., or, in round figures, 22 tons per sq. ft. For good stone masonry he uses the same stress and makes reductions according to the quality of the work. (No tensile stresses are to be allowed.)

For 1:2:4 concrete, deposited under water, he confines the maximum stress to 20 tons per sq. ft.

In dimensioning the piers the first condition to be investigated is the maximum pressure which results from the greatest load that may have to be supported by the piers. This occurs when the two adjoining spans are fully loaded. In many cases these spans are equal, and the resultant force of all the loads acting on the pier is

then vertical and coincident with the center line of the pier; and there is no horizontal thrust acting in the pier.

The next condition to be investigated is the maximum horizontal thrust which may act on the pier (overturning of the pier). For this purpose one span is loaded so as to make the horizontal thrust a maximum at the same time that the distance between its point of application and the bottom of the pier is the greatest. (The maximum turning moment is then to be found.) The other span is loaded so as to make the turning moment a minimum.

This condition of loading gives a resultant force which is not vertical and does not coincide with the center of the pier. With this resultant the stability of the pier and its stresses are investigated, first at the highest, and then at the lowest, water-level, and the pier is to be designed for the condition producing the maximum stresses.

In Chapter IV is described and illustrated the procedure for finding the maximum overturning moments, and Chapter V gives the method for determining the stresses in the pier. Any discussion of the stresses in the pier which did not also consider those in the arch would be unsatisfactory and misleading (in many cases), and the author therefore refers to these chapters for such particulars.

The water is assumed to penetrate under the foundation of the pier, when the latter is to be investigated for overturning. To obtain the pressure on the foundation this point must be definitely settled; because when the water cannot penetrate under the pier, the water-level is immaterial in computing the weight of the pier, which is then determined by the specific gravity of the masonry. The pressure on the foundation is considerably greater in this case.

It is generally safe to assume that the water does penetrate underneath the foundation, and in this case the pressure thereon is less than if otherwise.

The overturning moments caused in a pier become large when the two adjoining spans differ in length. Usually in the shorter span the rise of the arch decreases in the same ratio as the span.

If the horizontal thrusts of the two adjoining spans are the same, the rise of the arch should decrease in the same ratio as the squares of the spans. (This is approximately true—see analysis in the Appendix.)

In designing a succession of arches, however, esthetic considerations dictate that the springing lines of all the arches must be in the same horizontal plane, that the center span be the longest, and that the adjoining spans to the right and left of the center decrease in length.

It is generally conceded that five spans give the best esthetic effect. The lengths of these spans should decrease from the center to the shore in about the proportions 102, 98, and 96; and their rises decrease as 9.75:9:7. The intermediate piers in such a structure will be subjected to bending moments, which will increase considerably with the depth of the foundation.

When in connection with such a bridge the water rises to a level where it submerges part of the arches, special care should be exercised in the design of the intermediate piers; because such a succession of arches may be safe at low tide, but dangerously unstable at high tide.

The points here referred to may not properly belong in a work dealing with the application of the elastic theory to arches; but the shape of the arch is the very foundation on which all computations are based, and the points mentioned have been included for the purpose of calling attention to facts of which the theorist may completely lose sight.

8. Dimensions of Existing Arches.—To guide the designer in his preliminary work, tables of existing arches have been added; and for a few the source of information is given, to enable him to look up such details as may be of interest.

To determine the form of loading, especially for bridges, and the allowable stresses in materials, reference should be made to the many standard treatises and pocket-books devoted to these particular subjects, as they hardly come within the province of the present work.

The author refrains from giving any tables on these subjects, because, in stone and masonry arches especially, the character of the material, the location of the arch, the purpose for which it is used, the facilities at the command of the builder, and the experience of the engineer, are all factors which enter into the determination, and which are incapable of numerical expression. For this reason such tables would only lead to error, or, were the values so low as to be safely applicable under all conditions, they would entail an extravagant use of material.

Table XIX gives the material stresses for many existing masonry arches. A study of this table shows a wide variation in the stresses employed; for example, in the Kaiser Wilhelm Bridge (No. 57) the stress in the granite is as high as 750 lbs. per sq. in. Such a stress, in the best of material, in a design where the engineer is absolutely certain of the line of resistance in the arch and the intensity of the force, is safe. If, however, it were entered in a table as the permissible stress in granite, it would, unquestionably, lead to erroneous assumptions.

Also, in the examples of Chapter IV, stresses of 600 lbs. per sq. in. have been used in concrete. This is a very high value, but what was said in a preceding paragraph applies equally here; it is the experience and ability of the engineer which must establish these factors.

The radius of curvature at the crown of the Syra Valley Bridge is 220 ft.; in Table VII the radius of curvature for this arch is given as 234 ft., which shows that the intrados is not a circular arc, as has been assumed in Chapter IV.

Table XVII.

WROUGHT-IRON AND STEEL ARCHES.

No.	Location.	No. of hinges.	Span in feet.	Rise in feet.	Description.
1	Niagara Bridge	2	854	172	Arch rib, parallel chords, height 26.4 ft.; latticed web.
2	Viaur Viaduct, France	3	733	179	Two cantilevers with anchor arms, each 317 feet long.
3	Rhine Bridge, Bonn	2	626.4	75.3	Spandrel-braced; curved upper chord; depth at crown = 16 ft., at abutments = 35 ft. Abutment verticals are anchored together under the roadway.
4	Rhine Bridge, Düsseldorf	2	604.2	92.3	Spandrel-braced; curved upper chord.
5	Luiz I, Douro, Portugal	0	575	148.4	
6	Niagara	2	559	116	Spandrel-braced.
7	Garabit Viaduct	2	550	173	Crescent arch; depth at crown = 33 ft.
8	Douro Bridge, Oporto, Portugal	2	533	194	Crescent arch rib; depth at crown = 20 ft.
9	Pia Maria	2	525	122.4	
10	Grüntnal B'dge, Oestsee Canal	2	522	71.8	Crescent arch.
11	St. Louis, Mississippi River	0	520	47	Arch rib, parallel chords; latticed web.
12	Washington Bridge, New York	2	517	93.2	Arch rib, parallel chords.
13	Wupperthal Bridge, Muengsten	0	500 (clear)	229	Arch rib; depth at crown = 5 ft., at abutments = 13 ft.; latticed web.
14	Zambesi River, Africa	2	500	90	Spandrel-braced.
15	Paderno Viaduct	0	492	123	
16	Minneapolis	3	456	90	Spandrel-braced.
17	Rochester Bridge	2	416	67	Spandrel-braced.
18	Rhine Bridge, Worms	2	387	58 (rise of bottom chord)	Spandrel-braced; height of spandrel at hinges, 41.7 ft.; at crown, 9.5 ft. Abutment verticals are anchored together under the roadway.
19	Pont de Szegedin	......	361	28	
20	Austerlitz Bridge, Paris	3	357	39	Each half is crescent-shaped, resting on brackets 54.7 ft. long; total span = 466 ft.
21	Stony Creek, Can. Pac. Ry.	3	336	80	
22	Pons Palatinus	2	334	455(rad.)	
23	Coblenz, Rhine	2	315	31.5	Arch rib, parallel chords.
24	Pesth	2	305	8	Spandrel-braced.
25	Arcola Bridge, Paris	0	262.5	20.2	
26	Blauw-Krantz	0	229.6	97	Spandrel-braced.
27	Pont Moran de Rhône	2 & 0	221.1	14.6	
28	Verona	2	219	32.8	
29	St. Giustina, South Tyrol	2	196.8	36.7	
30	Pont de Rouen	2 & 0	179.1	14.9	
31	Franz Bridge, Danube River	3	177	....	Spandrel-braced.
32	Garibaldi Bridge, Rome	0	173.7	6.3	Spandrel-braced.
33	Cerveyrette Gorge, France	0	172.2	37.7	
34	Cedar Ave., Baltimore	3	150	38	Spandrel-braced.
35	Albert Bridge, over the Clyde	2	114	....	Latticed spandrels.
36	30th Street Bridge, Phila.	3	64.1	12	

References (by number).—Annales des Ponts et Chaussées: 2 (1898, I, p. 215; II, p. 329)—8 (1878, I, p. 101)—25 (1854, II, p. 246). Deutsche Bauzeitung: 18 (1896, p. 109; 1900, pp. 569 and 585). Engineer (London): 26 (Vol. 59, No. 1522). Engineering News: 5 (1886, II, p. 7)—7 (1885, I, p. 549)—14 (1905, Oct. 5)—20 (1905, Dec. 7)—36 (1870, I, p. 69). Hutton, W. R., "The Washington Bridge over the Harlem River at New York": 12. Railroad Gazette: 6 (1896, Apr. 24). Scientific American: 12 (1886, p. 278)—16 (1886, p. 255). Springer, Julius, "The Wupperthal Bridge," Berlin, 1904: 13. Woodward, C. M., "A History of the St. Louis Bridge," 1881: 11. Zentralblatt für Bauverwaltung: 1 (1898, p. 318; 1899, p. 566)—3 (1898, p. 617)—10 (1891, p. 214; 1894, p. 508)—29 (1890, p. 220). Zeitschrift für Bauwesen: 23 (1864, pp. 395, 529, 625). Zeitschrift des Oesterreichischen Ingenieur- und Architekten-Vereins: 19 (1883, p. 7).

Table XVIII.

WROUGHT-IRON AND STEEL ROOFS.

No.	Location.	Number of hinges.	Span in feet.	Rise in feet.	Remarks.
1	Liberal Arts Building, Columbian Exposition, Chicago	3	368	206.3	
2	Main Building, Lyons Exposition	2	361	108	
3	Trainshed, Philadelphia, Pa	3	300	108.5	
4	Station, Phila., P. & R. Ry.	3	259	88	
5	Jersey City, P. R. R.	3	252.7	89.8	Tie-rods.
6	St. Pancras Ry. Station	0	240	124.8	
7	Trainshed, Cologne	2	209	78.7	
8	Dome of Horticultural Building, Columbian Exposition	0	181.6	91	
9	Drill Hall, 22d Regiment, N. Y.	0	176	62	Tie-rods.
10	" " 12th Regiment, N. Y.		171.3	55.6	"
11	" " 1st Regiment, Chicago	3	155.5	77.5	
12	Dancing Hall, Saltair Beach	3	118.7	54	
13	Machinery Hall, Columbian Exposition, Chicago	3	115.2	93.5	

Table XIX.

DIMENSIONS OF MASONRY ARCHES.

No.	Location.	No. of hinges	Span l in feet.	Rise f in feet.	Rib. Depth in feet at crown.	Rib. Depth in feet at abutments.	Max. compression in lbs.	Materials of construction. Remarks.
1	Bridge over the Syra Valley....	0	300	60	6	13.3	620	Rubble masonry. Radius at crown = 220 ft.
2	" " " Pétrussa Valley.	0	240 (260)	54 (104)	4.8	7.2	....	Span at the foot of the abutments = 260 ft. Rubble masonry, in 3 rings. Crown radius = 183 ft. (Deutsche Bauz., 1902, No. 84).
3	New Bridge over the Adda, at Morbegno (Italy)..........	3	233	33.3	5	7.3	700	Rubble masonry, in 3 rings, with steel hinges. Crown radius = 250 ft.
4	Cabin John Aqueduct, Washington, D. C...............	0	224	58	9.7	20.3	....	In two rings, without bond; crown radius = 140 ft.
5	Pruth Bridge, Jaremcze.........	0	217	59.7	7	10.3	344	Sandstone, in 3 rings. Crown rad. = 128 ft.
6	Prince Regent Bridge, Munich...	3	213	21.3	3.3	4.2	563	Limestone, with 3 steel hinges.
7	Gutach Bridge.................	0	213	53.7	6.7	9.3	440	Rubble masonry, in 3 rings of sandstone; crown radius = 133 ft.
8	Bridge near Gour Noir.........	0	207	53.7	5.7	14	380	Granite ashlar, in 3 rings; crown rad. = 120 ft.
9	Lavaur Bridge.................	0	205	91.7	5.5	9.3	288	Rubble masonry, in 3 rings; crown radius = 104 ft.
10	Grosvenor Bridge over the Dee..	0	203	42.7	4.1	6.1	....	Dimension stone with lead in the joints; crown radius = 142 ft.
11	Mulden Bridge, Gochren, Saxony;	3	200	22.5	3.7	4	450	Granite rubble masonry, granite hinges; greatest depth of rib = 5 ft.
12	Maximilian Joseph Bridge, Munich	3	200	20	3.3	4.2	563	Limestone, with 3 steel hinges.
13	Gour Noir.....................	0	197	52.8	5.6	13		
14	Schwaendenholz Bridge.........	0	190	47.5	6	8.7	432	Rubble masonry, sandstone; crown radius = 119 ft.
15	Hannibal Bridge over the Volturne, at Naples............	0	183	47	6.7	16.7	....	Brick arch; crown rad. = 190 ft. (basket handle).

16	Devil's Bridge, at Barrizzo, over the Sele (Italy)	0	183	45	6.7	11.7	....	Brick arch; crown rad. = 191 ft. (basket handle).
17	Ballochmoyle Bridge, Ayr, Scot.	0	180	90	4.5	6	......	
18	Drac Bridge, at Claix (Isère, Fr.)	0	173	26.8	5	10.3	......	Rubble masonry; crown radius = 153 ft.
19	Neckar Bridge, Neckarhausen	3	170	15.5	2.8	3	498	Concrete, with 3 steel hinges.
20	Donau Bridge, Munderkingen	3	167	16.7	3.3	3.7	475	Concrete, with 3 hinges; crown rad. = 233 ft.
21	Antoinette Bridge	0	167	53	5	7.6	375	Rubble masonry, in rings; crown radius = 103 ft.
22	Nalon Valley Bridge, Segados, Sp.	3	167	15	3.7	3.7	507	Concrete, with 3 hinges.
23	Valley Bridge of Nogent, over the Marne	0	167	83.3	6	15	....	Rubble masonry; crown radius = 83 ft.
24	Pruth Bridge at Jamma	0	160	38	5.7	8.7	314	Sandstone, in rings.
25	Wheeling, W. Va	0	159	28	4.5	6	......	Circular arc.
26	London, Thames River	0	152	37.1	4.9	10	......	Ellipse.
27	Gloucester, England	0	150	35	4.5	......	......	“
28	Elyria, Ohio	0	150	27	3.8	4.5	......	Circular arc.
29	Turin, Italy	0	148	18	4.9	......	......	“ “
30	Putney, Thames River	0	144	19.3	4.2	4.2	......	Two spans of 129 ft. and two of 112 ft.
31	Alma Bridge, Paris	0	141	28	4.9	......	......	Ellipse. Concrete.
32	Pont-y-tu-Prydd, Taff R., Wales	0	140	35	2.6	......	......	
33	Bridge over the Ariege, Castelet	0	137	46.6	4.2	7.5	250	Rubble masonry, in rings.
34	Pruth Bridge, Worochta	0	133	33.3	4.7	7.3	268	Sandstone, in rings.
35	Coulouvrenière Bridge, Geneva	3	133	18.5	3.3	4	250	Concrete.
36	Rebuzo Valley R. R. Bridge, Quillan-Rivesaltes	0	133	66.6	4.3	8.7	183	Semicircle; rubble masonry, in 3 rings.
37	Boucicault Bridge, Saône River	0	133	16.7	3.5	4.1	249	Dimension stone.
38	Valley Bridge, Villefranche, R. R. Prodas-Olette	0	131	56.7	4.7	6.7	250	Depth of arch rib at foundation = 10 ft.
39	Neckar Bridge, Gemmrichheim	3	127	18.3	2.7	3	275	Concrete.
40	Washington, D. C	0	125	39	6	8.5	....	Concrete (Eng. News, Nov. 16, 1905, and April 19, 1906).
41	Murg Bridge, Baiersbronn	3	110	11	2	2.7	636	Dimension stone.
42	Peru, Indiana	0	100	15.3	2	3.5	....	Reinforced concrete, 7 spans (1 = 100, 2 = 95, 2 = 85, 2 = 75 ft.); water rises above the springing line of arches (Eng. News, March 29, 1906).

TABLE XIX—*Continued.*

DIMENSIONS OF MASONRY ARCHES.

No	Location.	No. of hinges.	Span l in feet.	Rise f in feet.	Rib. Depth in feet at crown.	Rib. Depth in feet at abutments.	Max. compression in lbs.	Materials of construction. Remarks.
43	Charrey, Saône River	0	100	12.5	3.8	4.9	152	Ashlar masonry.
44	Oder Bridge, Frankfort	0	100	12.5	2.7	4.3	......	Brick.
45	Enz Bridge, Höfen	3	93	9.3	3.3	5	300	Dimension stone.
46	Wertach Bridge. Nesselwang	0	92	......	2.7		230	Rubble masonry.
47	Elkader, Iowa	......	84	27	3	4	......	Limestone-rubble masonry.
48	Forbach Bridge, Baiersbronn	3	83	10	2	2.7	730	Dimension stone.
49	Crueize Viaduct, R. R. Marvejois-Neussargues	0	83	41.5	4.3	8.7	112	Rubble masonry.
50	Bléré Bridge, Nevers Tours (str.)	0	80	......	3.7	4.5	208	Ashlar masonry.
51	Conemaugh Viaduct, Penna. R. R.	0	80	40	3	3.5	.....	Sandstone, in lime, without sand.
52	Schuylkill Falls	0	80	26	3	3	......	Ashlar masonry.
53	Herkules Bridge, Berlin	0	78	11	2.8	3.5	500	Dimension sandstone.
54	Lein Bridge	3	77	11.7	1.7	2.7	......	Concrete.
55	Westminster Bridge, Thames River	0	76	38	7.6	14	.....	Circular arc.
56	Albany St. Arch, New Brunswick, N. J	0	75	15	2.4	2.4	.....	Masonry.
57	Kaiser Wilhelm Bridge, Berlin	0	74	13.3	2.7	5	750	Dimension granite masonry.
58	Oberbaum Bridge, Berlin	0	73	11.4	2.6	3.4	300	Brick, in cement mortar.
59	Black Rock Tunnel Bridge, P. & R. Ry	......	72	16.5	2.8	2.8	.....	Circular arc.
60	Neckar Bridge, Mühlheim	3	73	7.3	1.5	2	250	Concrete.

APPENDIX.

Notation.

A = left support.
B = right support,
= total length of the arch axis.
C = crown of the arch,
= center of gravity of the section.
D = axis for the ordinates of the arch axis in the hingeless arch.
E = modulus of elasticity of the material.
F = total area of a section of the arch rib.
F_0 = average area of a section of the arch rib.
H = horizontal thrust caused by vertical forces.
H_1 = " " " " horizontal forces.
I = moment of inertia.
I_0 = average moment of inertia.
$J = \int \frac{rv^2}{r+v} df$ [(5) and (5^a)].
K = vertical force.
L = single force acting in an arbitrary direction.
M = bending moment; M_x = bending moment at x.
$\mathfrak{M}$ = bending moment of a simple beam.
N = core point of an arch-rib section.
(N' upper core point, N_2 lower core point.)
$\mathfrak{O}$ = vertical reaction of the forces o [see equation (116)].
P = axial force (segment of an equilibrium polygon).
$\mathfrak{P}$ = uniformly distributed load.
Q = horizontal force.
R = reaction at the supports (R_1 = reaction at A, R_2 = reaction at B).
S = shearing force.
V = vertical reaction (V_1 = reaction at A. V_2 = reaction at B).
$W = \int_0^b \frac{I_0}{I} y^2 ds + \frac{I_0}{F_0} B \cos a$ [see equation ($11C^b$)].
X = ordinates of the closing line of the moment polygon in the hingeless arch; X_1 = end ordinates at A and B, and X_2 = ordinate on the vertical axis at the center of the span.
Y = vertical axis passing through the center of the span in the hingeless arch.
Z = axis.

a = angle which the plane of section makes with the vertical.
a_0 = " " " axis makes with the horizontal at the support.
b = " " " resultant R makes with the tangent at (x, y).
c = lever arm of the force R.
c = ordinate of the closing line of the moment polygon from the axis AB.
d = angle which the load L makes with the horizontal.
d = panel length; d_0 = average panel length.
e = angle which the chord of the arc makes with the horizontal.
e = ordinates of the closing line of the moment polygon from the axis DD.
f = rise of the arch,
= an element of area of the section.
g = distance of the load L from the support A or B.
g' = " " " " L from the support to the point (x, y) of the arch axis.
g' = length of a uniform load measured from the support A.
h = depth of arch rib.
i = radius of gyration.
j = distance between the core points and the gravity axis of section.
$k = \frac{x}{l}$.
l = length of span.
m = reference letter for panel point.
m_x = ordinate of the horizontal-thrust curve multiplied by the pole distance p and the average panel length d_0.
n = normal stress per unit area of the section.
o = the forces for the construction of the deflection curves [see equations (111) and (116)].
p = lever-arm of the force P,
= pole distance of the force polygon.
q = lever-arm of the horizontal force Q.
r = radius of curvature of the arch axis.
s = length of the arch axis between the points (x, y) and (x', y'), or between the points 0 and (x, y).
t = temperature in degrees F.
u = horizontal ordinate of the section of the arch rib,
= abscissa of the point of application of the force Q.
v = vertical ordinate of the section of the arch rib.
w = coefficient of linear expansion of the material for a change of temperature of 1° F.
x = abscissa of a point on the arch axis.
x_0 = " " the intersection locus for horizontal forces.
y = ordinate of a point on the arch axis.
z = " " the intersection locus for vertical forces.
z_1 = ordinate at the left support.
z_2 = " " " right support.
z_0 = " on the load line.

CHAPTER VII.

MATHEMATICAL ANALYSIS OF THE ELASTIC ARCH.

In the analysis undertaken in this chapter the author has mainly followed the theories of Winkler, Mohr, Müller-Breslau, Melan, Shâffer, and others, making such additions and explanations as seem necessary for a proper understanding and an intelligent application of the method to the computation of stresses in the arches treated in previous chapters.

1. **Relation between the Exterior Forces and the Interior Stresses in the Arch.**—Equations (2) of Chapter I define the normal stress and shear. In that chapter it was also shown that for the point (x, y) of the arch the load may be replaced by the force $R_{,}$; this force in turn can be replaced by the two forces $H_{,}$ and $V_{,}$, or the two forces P and S, which forces are applied at the center of gravity of the section, and a pair of forces should be added which cause the moment M_x.

If the moment turns in a clockwise direction around the point (x, y) of the arch, it will be called positive and be indicated by $+$; when the moment turns in the opposite direction, it will be called negative and be indicated by $-$.

(*a*) The examples in the foregoing chapters have shown how to treat the shearing forces in arch ribs; in the following paragraphs the analysis for the determination of the axial stresses will be considered.

In Fig. VIII, n = the normal stress in an element of the section;

df = an element of the section $= du\,dv$;

F = the area of the whole section $= \int df$;

P = the force P of Fig. II, Chapter I;

M_x = the bending moment at the point $(x, y) = Pp$;

r = radius of curvature of the axis of the beam at the point (x, y).

$$\left.\begin{aligned} P_x+\int n df &=0,\\ M_x+\int vndf &=0,\\ \int undf &=0. \end{aligned}\right\} \quad . \quad . \quad . \quad . \quad . \quad . \quad . \quad (1)$$

To analyze the stress it is assumed that the plane of a section is still a plane after the force has bent the beam, and that the axis of the beam remains in the same plane during bending. ds_v is the length before bending of a fiber between two sections of the beam, which sections are infinitely close together, and Δds_v is its change in length caused by the bending of the beam; the length of this fiber then becomes

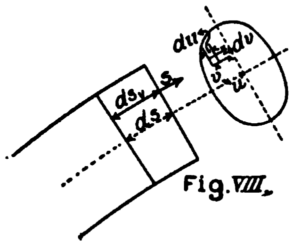

Fig. VIII.

$$ds_v + \Delta ds_v.$$

The angle between the two sections $= -da$, and the bending causes a change in this angle of $-(da + \Delta da)$.

It is assumed that the bending of the beam increases its curvature, which increases the angle $-da$ and makes Δda negative.

Now

$$ds_v = ds - vda \text{ (see Fig. VIII)},$$

and

$$ds_v + \Delta ds_v = ds + \Delta ds - v(da + \Delta da);$$

and deducting the first equation from the second gives

$$\Delta ds_v = \Delta ds - v\Delta da,$$

and the relative change in the length of the fibers will be

$$\frac{\Delta ds_v}{ds_v} = \frac{\Delta ds - v\Delta da}{ds - vda};$$

or, by substituting $ds = -rda$ (r = radius of curvature),

$$\frac{\Delta ds_v}{ds_v} = -\frac{\Delta ds - v\Delta da}{da(r+v)} = \left(-\frac{\Delta ds}{da} + \frac{v\Delta da}{da}\right)\frac{1}{r+v} = \left(\frac{r\Delta ds}{ds} - \frac{rv\Delta da}{ds}\right)\frac{1}{r+v},$$

$$\frac{\Delta ds_v}{ds_v} = \left(\frac{\Delta ds}{ds} - v\frac{\Delta da}{as}\right)\frac{r}{r+v}. \quad \ldots \ldots \quad (2)$$

If the change in length of the fiber is caused by the normal stress n and by a change in temperature t with a coefficient of expansion w,

$$\frac{\Delta ds_v}{ds_v} = \frac{n}{E} + wt,$$

and equation (2) gives

$$n=E\left(\frac{\Delta ds}{ds}-v\frac{\Delta da}{ds}\right)\frac{r}{r+v}-Ewt, \quad . \quad . \quad . \quad . \quad . \quad . \qquad (3)$$

which, when substituted in (1), gives

$$\left.\begin{aligned} P_x&=-E\frac{\Delta ds}{ds}\int\frac{r}{r+v}df+E\frac{\Delta da}{ds}\int\frac{rv}{r+v}df+EwtF,\\ M_x&=-E\frac{\Delta ds}{ds}\int\frac{rv}{r+v}df+E\frac{\Delta da}{ds}\int\frac{rv^2}{r+v}df+Ewt\int vdf. \end{aligned}\right\} \quad . \qquad (4)$$

Now $\int df=F$, and $\int vdf=0$; or all the elements of the section added are equal to the total area of the section, and the moments of the area of the section on each side of the horizontal axis of gravity are equal.

The term $\int\frac{r}{r+v}df$ may be reduced as follows:

$$\int\frac{r}{r+v}df=\int df-\int\frac{vdf}{r+v}=F-\frac{1}{r}\int vdf+\frac{1}{r}\int\frac{v^2df}{r+v}=F+\frac{1}{r^2}\int\frac{rv^2}{r+v}df,$$

and

$$\frac{rv}{r+v}df=\int vdf-\int\frac{v^2df}{r+v}=-\frac{1}{r}\int\frac{rv^2}{r+v}df.$$

For abbreviation

$$\int\frac{rv^2}{r+v}df=J. \quad . \quad . \quad . \quad . \quad . \quad . \quad . \quad . \quad . \quad . \qquad (5)$$

Making these substitutions in (4) gives

$$\frac{P_x}{E}=\left(-\frac{\Delta ds}{ds}+wt\right)F-\left(\frac{\Delta da}{ds}+\frac{1}{r}\frac{\Delta ds}{ds}\right)\frac{J}{r},$$

and

$$\frac{M_x}{E}=\left(\frac{\Delta da}{ds}+\frac{1}{r}\frac{\Delta ds}{ds}\right)J.$$

From these

$$\left.\begin{aligned} -\frac{\Delta ds}{ds}&=\frac{P_x}{EF}+\frac{M_x}{EFr}-wt,\\ \frac{\Delta da}{ds}&=\frac{P_x}{EFr}+\frac{M_x}{EFr^2}-\frac{wt}{r}+\frac{M_x}{EJ}, \end{aligned}\right\} \quad . \quad . \quad . \quad . \quad . \quad . \quad . \quad . \qquad (6)$$

which, when substituted in (3), give

$$-n=\frac{P_x}{F}+\frac{M_x}{Fr}+\frac{M_x rv}{J(r+v)}. \quad \dots \dots \quad (7)$$

$\frac{P_x}{F}$= a constant value, $\frac{M_x}{Fr}$= a constant value, and $\frac{M_x rv}{J(r+v)}$ can be written $\frac{M_x r}{J}\frac{v}{r+v}$, where $\frac{M_x r}{J}$ is a constant, and $\frac{v}{r+v}$ a variable.

The last factor indicates that the values of n, plotted as ordinates from the plane of section, are located in a surface whose curvature is that of a hyperbola having one of its asymptotes parallel to the tangent and passing through the center of curvature of the beam (when $n=-\infty$, or $v=-r$), and the other asymptote parallel to the v axis (when $v=\infty$, which makes $r+v=\infty$) and located at the distance

$$-n=\frac{P_x}{F}+\frac{M_x}{Fr}+\frac{M_x r}{J}. \quad \dots \dots \quad (8)$$

n is equal to zero, when

$$v=-\frac{\frac{P_x r}{F}+\frac{M_x}{F}}{\frac{P_x}{F}+\frac{M_x}{Fr}+\frac{M_x r}{J}}; \quad \dots \dots \quad (9)$$

and when $P_x=0$,

$$v=-\frac{rJ}{J+Fr^2}, \quad \dots \dots \quad (10)$$

and the neutral axis passes through the center of gravity of the section for $P_x=0$ $(v=0)$ only when r becomes ∞, or when the axis of the beam was plane before bending.

The value of J in (5) can be expressed as a progression in the following manner:

$$J=\int\frac{v^2 r}{r+v}df=\int v^2 df-\frac{1}{r}\int v^3\left(1-\frac{v}{r}+\frac{v^2}{r^2}-\frac{v^3}{r^3}\dots\right)df.$$

In this equation $\int v^2 df$ is the moment of inertia I of the section with respect to the u-axis, and if the section is symmetrical with respect to this axis, the factors v^3, v^5, etc., disappear, and

$$J=I+\frac{1}{r^2}\int v^4\left(1+\frac{v^2}{r^2}+\frac{v^4}{r^4}-\dots\right)df. \quad \dots \dots \quad (5^a)$$

When the radius of curvature r is large in comparison with the depth of the beam, the second member of the above equation approaches closely to zero in value, and

$$J=I.*$$

This approximation can be applied to equations (6) and (7), giving the following general equations, which are also applicable to straight bars:

$$-\frac{\Delta ds}{ds}=\frac{P_x}{EF}-wt, \quad \frac{\Delta da}{ds}=\frac{M_x}{EI}, \quad . \quad . \quad . \quad . \quad . \quad . \quad (6^a)$$

$$-n=\frac{P_x}{F}+\frac{M_x v}{I}. \quad . \quad . \quad . \quad . \quad . \quad . \quad . \quad . \quad . \quad . \quad (7^a)$$

---

* The introduction of the moment of inertia into the elastic equations in place of the factor J has been criticized; to show the student the groundlessness of the objection, the equation is applied to the Syra Valley Bridge, as follows: In round figures its radius of curvature $r=240$ ft., and the average height of the arch rib $h=10$ ft.; $\therefore\ \frac{h}{r}=\frac{1}{24}=k$. Expanding equation (5),

$$J=\int\frac{v^2r}{r+v}df=\int\left[v^2-\frac{1}{r}v^3+\frac{1}{r^2}v^4-\frac{1}{r^3}v^5+\frac{1}{r^4}v^6\ldots\right]df.$$

As $df=dudv$,

$$J=\left[\frac{v^3}{3}-\frac{1}{r}\frac{v^4}{4}+\frac{1}{r^2}\frac{v^5}{5}-\frac{1}{r^3}\frac{v^6}{6}+\frac{1}{r^4}\frac{v^7}{7}\ldots\right]u$$

$$=\left[1-\frac{1}{r}\frac{24h}{4\times16}+\frac{1}{r^2}\frac{24h^2}{5\times32}-\frac{1}{r^3}\frac{24h^3}{6\times64}+\frac{1}{r^4}\frac{24h^4}{7\times128}\ldots\right]\frac{h^2}{24};\ A(v=+\tfrac{1}{2}h)$$

$$=\left[1+\frac{1}{r}\frac{24h}{4\times16}+\frac{1}{r^2}\frac{24h^2}{5\times32}+\frac{1}{r^3}\frac{24h^3}{6\times64}+\frac{1}{r^4}\frac{24h^4}{7\times128}\ldots\right]\frac{h^2}{24};\ A(v=-\tfrac{1}{2}h).$$

The sum of these two progressions gives the value of J for the whole section, and $\frac{h^2A}{12}=\frac{uh^3}{12}=I$,

$$J=\left[1+\frac{3}{20}\frac{h^2}{r^2}+\frac{3}{112}\frac{h^4}{r^4}+\frac{3}{192}\frac{h^6}{r^6}\ldots\right]I,$$

or

$$J=I\left[1+\frac{3}{20}k^2+\frac{3}{112}k^4+\frac{3}{192}k^6\ldots\right],$$

and for $k=\frac{1}{24}$,

$$J=[1+0.00026+0.00000008\ldots]I=0.00026008I\ .$$

The manner in which the progressions have been developed shows why one-half of the terms have dropped out from equation (5^a). It also proves that the introduction of the factor J does not make the equations too involved, but only their application more laborious.

Another criticism is in regard to the elimination of all the terms in equations (6^a) and (7^a), in which the factor r appears in the denominator of equations (6) and (7). In reality, in a well-designed bridge, the error thus introduced is even less than the one just discussed relating to the factor J. The reader can easily convince himself of this by using the values obtained from Figs. 26 to 34.

The third equation of (1) should also be true. To test this, substitute in $\int undf=0$ the value of n from (3), which gives

$$E\left(\frac{\Delta ds}{ds}-wt\right)\int udf-E\frac{\Delta da}{ds}\int\frac{ruv}{r+v}df=0.$$

In this expression $\int udf=0$, and $E\frac{\Delta da}{ds}r$ may be eliminated from the equation, leaving

$$\int\frac{uv}{r+v}df=0,$$

which holds true when the section is symmetrical with respect to its vertical axis. When r is large as compared with the depth of the beam, $r+v$ is practically equal to r, and r being a constant, it disappears from the equation, leaving

$$\int uvdf=0.$$

2. **Analysis of the Change of Form of an Arch Rib.**—Let (x, y) and (x_0, y_0) be the coordinates of two points on the axis, and ss_0 the distance between them along the axis.

CHANGE IN THE LENGTH OF THE AXIS OF A BEAM.—To determine the change in the length of the arc ss_0, equation (6_1) should be integrated between the limits s and s_0, which gives

$$\Delta s-s_0=\Delta wt(s-s_0)-\int_{s_0}^{s}\left(\frac{P_x}{EF}+\frac{M_x}{EFr}\right)ds. \quad . \quad . \quad . \quad (11)$$

When r is large,

$$\Delta s-\Delta s_0=wt(s-s_0)-\int_{s_0}^{s}\frac{P_x}{EF}ds. \quad . \quad . \quad . \quad . \quad . \quad . \quad (11^a)$$

Change in the Angle a.—The change in the angle which the plane of section makes with the vertical, or which the tangent to the curve makes with the horizontal at these same points, is obtained by integrating equation (6_2) between the limits set, which gives

$$\Delta a-\Delta a_0=\int_{s_0}^{s}\left(\frac{P_x}{EFr}+\frac{M_x}{EFr^2}+\frac{M_x}{EJ}\right)ds-wt\int_{s_0}^{s}\frac{ds}{r}.$$

In this equation $wt\int_{s_0}^{s}\frac{ds}{r}=wt\frac{s-s_0}{r}$, and $\frac{s}{r}=-a$; and substituting these values in (11) gives

$$\Delta a-\Delta a_0=\int_{s_0}^{s}\frac{M_x}{EJ}ds-\frac{\Delta s-\Delta s_0}{r}. \quad . \quad . \quad . \quad . \quad (12)$$

When r is very large in comparison with the depth of the arch rib,

$$\varDelta a-\varDelta a_0=\int_{s_0}^{s}\frac{M_x}{EI}ds+wt(a-a_0). \quad . \quad . \quad . \quad (12^a)$$

Change in the Radius of Curvature.—r_1 is the radius of curvature of the axis after the beam has been bent, and

$$\frac{1}{r_1}=-\frac{da+\varDelta da}{ds+\varDelta ds};$$

from this it follows that

$$\frac{1}{r_1}-\frac{1}{r}=-\frac{da+\varDelta da}{ds+\varDelta ds}+\frac{da}{ds}{}^{*}=-\frac{\frac{\varDelta da}{ds}+\frac{1}{r}\frac{\varDelta ds}{ds}}{1+\frac{\varDelta ds}{ds}},$$

and when the values of $\frac{\varDelta ds}{ds}$ and $\frac{\varDelta da}{ds}$ from (6) are substituted,

$$\frac{1}{r_1}-\frac{1}{r}=\frac{-\frac{P_x}{EFr}-\frac{M_x}{EFr^2}+\frac{wt}{r}-\frac{M_x}{EI}+\frac{P_x}{EFr}+\frac{M_x}{EFr}-\frac{wt}{r}}{1-\frac{P_x}{EF}-\frac{M_x}{EFr}+wt},$$

which, when reduced, gives

$$\frac{1}{r_1}-\frac{1}{r}=-\frac{M_x}{EI}\frac{1}{\left(1-\frac{P_x}{EF}-\frac{M_x}{EFr}+wt\right)}. \quad . \quad . \quad . \quad . \quad (13)$$

---

* $-\frac{da+\varDelta da}{ds+\varDelta ds}+\frac{da}{ds}$ divided by ds

$$=\frac{-\frac{da}{ds}-\frac{\varDelta da}{ds}+\frac{da}{ds}\left(1+\frac{\varDelta ds}{ds}\right)}{1+\frac{\varDelta ds}{ds}}$$

$$=\frac{\frac{1}{r}-\frac{\varDelta da}{ds}-\frac{1}{r}-\frac{1}{r}\frac{\varDelta ds}{ds}}{1+\frac{\varDelta ds}{ds}}=-\frac{\frac{\varDelta da}{ds}+\frac{1}{r}\frac{\varDelta ds}{ds}}{1+\frac{\varDelta ds}{ds}}.$$

It is evident that $\frac{\Delta ds}{ds}$ must be a very small value, and when r is large as compared with the depth of the arch rib, the value of $\frac{1}{r}\frac{\Delta ds}{ds}$ becomes infinitely small, and, from (6^a),

$$\frac{1}{r_1}-\frac{1}{r}=-\frac{\Delta da}{ds}=-\frac{M_x}{EI}. \quad . \quad . \quad . \quad . \quad . \quad . \quad . \qquad (13^a)$$

When the arch is designed so that the center line of pressure coincides with the axis of the arch rib, M_x becomes 0 and $\frac{1}{r_1}=\frac{1}{r}$, or the radius of curvature remains the same. Under this condition the change in form results from an angular movement of the consecutive planes of section of the arch rib about the center of curvature. When the change of form is caused by compression, the axis of the arch is shortened. To balance this contraction in the two-hinged arch a change in the horizontal thrust must take place; in the arch with fixed ends (hingeless) a change in the horizontal thrust must take place, and a pair of forces must be created at each support, causing moments which will hold the ends of the arch in their fixed positions.

(*a*) CHANGE IN THE LENGTH OF THE COORDINATES OF THE AXIS OF A BEAM.—In Fig. IX the point C represents the point (x, y) of the axis of the arch, and Δx, Δy the change of position for this point. ds, dx, dy are the arc and the ordinates of the points A and C, which are infinitely close together, and Δds, Δdx, Δdy the changes in length of these ordinates. The plane of section at A makes an angular deflection $=\Delta a$, and this same angular deflection is assumed to take place at the point C; and the new position of the point C will be at A', and the line $A'C$ is the change of position.

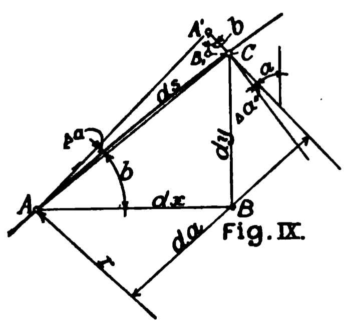

Fig. IX.

The ordinates of this change are $B_{,}C$ and $A'B_{,}$, and their lengths are determined from the similar triangles ABC and $A'B_{,}C$, and

$$A'C=-\Delta a ds, \quad B_{,}C=A'C\sin b, \quad \sin b=\frac{dy}{dx},$$

$$B_{,}C=-\Delta a ds\frac{dy}{ds}=-\Delta a dy, \quad B_{,}A'=A'C(-\cos b), \quad \cos b=\frac{dx}{ds},$$

$$A'B_{,}=\Delta a ds\frac{dx}{ds}=\Delta a dx.$$

An increase Δds in the length of the bar $AC(=ds)$ shifts the point A' in the direction of the coordinates the distances

$$\Delta dx = \Delta ds\frac{dx}{ds} \quad \text{and} \quad \Delta dy = \Delta ds\frac{dy}{ds};$$

and the total change of position of the point A' is

$$\Delta dx = -\Delta a dy + \Delta ds\frac{dx}{ds},$$

$$\Delta dy = \quad \Delta a dx + \Delta ds\frac{dy}{ds}.$$

These changes occur in each element of the arch axis, from a given point A as an origin; and the total change is obtained by summation of these expressions, in which $\int \Delta dx = \Delta x$ and $\int \Delta dy = \Delta y$.

$$\Delta x = -\int \Delta a dy + \int \frac{\Delta ds}{ds} dx,$$

$$\Delta y = \quad \int \Delta a dx + \int \frac{\Delta ds}{ds} dy.$$

The values for the point of origin are indicated by the subscript $_0$, and those for the point B by the subscript $_1$, and a partial integration gives

$$\left.\begin{aligned} \Delta x_1 - \Delta x_0 &= -\Delta a_1 y_1 + \Delta a_0 y_0 + \int_{s_0}^{s_1} \frac{\Delta da}{ds} y ds + \int_{s_0}^{s_1} \frac{\Delta ds}{ds} dx, \\ \Delta y_1 - \Delta y_0 &= \quad \Delta a_1 x_1 - \Delta a_0 x_0 - \int_{s_0}^{s_1} \frac{\Delta da}{ds} x ds + \int_{s_0}^{s_1} \frac{\Delta ds}{ds} dy. \end{aligned}\right\} . \qquad (14)$$

Equations (6) may be abbreviated to the following:

$$\frac{\Delta ds}{ds} = -\frac{P_x}{EF} - \frac{M_x}{EFr} + wt = -\frac{P'}{EF} + wt;$$

and

$$\frac{\Delta da}{ds} = \frac{P_x}{EFr} + \frac{M_x}{EFr^2} - \frac{wt}{r} + \frac{M_x}{EI} = \frac{P'}{EFr} - \frac{wt}{r} + \frac{M}{EI},$$

and

$$\Delta a_1 = \Delta a_0 + \int_{s_0}^{s_1} \frac{\Delta da}{ds} ds.$$

Substituting these values in (14),

$$\Delta x_1-\Delta x_0=-\Delta a_0 y_1+\Delta a_0 y_0-\int_{s_0}^{s_1}\frac{\Delta da}{ds}y_1 ds+\int_{s_0}^{s_1}\frac{\Delta da}{ds}y ds+\int_{s_0}^{s_1}\frac{\Delta ds}{ds}dx$$

$$=-\Delta a_0(y_1-y_0)-\int_{s_0}^{s_1}\frac{\Delta da}{ds}(y_1-y)ds+\int_{s_0}^{s_1}\frac{\Delta ds}{ds}dx,$$

and from this

$$\Delta x_1-\Delta x_0=-\Delta a_0(y_1-y_0)-\int_{s_0}^{s_1}\frac{M}{EJ}(y_1-y)ds$$
$$-\int_{s_0}^{s_1}\frac{P'}{EF}\left(\frac{y_1-y}{r}ds+dx\right)+wt\int_{s_0}^{s_1}\left(\frac{y_1-y}{r}ds+dx\right). \quad (15)$$

In the same manner is obtained

$$\Delta y_1-\Delta y_0=\Delta a_0(x_1-x_0)+\int_{s_0}^{s_1}\frac{M}{EJ}(x_1-x)ds$$
$$+\int_{s_0}^{s_1}\frac{P'}{EF}\left(\frac{x_1-x}{r}ds-dy\right)-wt\int_{s_0}^{s_1}\left(\frac{x_1-x}{r}ds-dy\right). \quad (16)$$

These equations may be simplified when the radius of curvature is very large as compared with the depth of the arch rib, which makes $P'=P$, and $J=I$. Also, the expressions for the temperature changes may be simplified very approximately to $wt(x_1-x_0)$ and $wt(y_1-y_0)$, which gives

$$\left.\begin{aligned}\Delta x_1-\Delta x_0&=-\Delta a_0(y_1-y_0)-\int_{s_0}^{s_1}\frac{M}{EI}(y_1-y)ds\\&\qquad-\int_{s_0}^{s_1}\frac{P}{EF}\left(\frac{y_1-y}{r}ds+dx\right)+wt(x_1-x_0),\\\Delta y_1-\Delta y_0&=\Delta a_0(x_1-x_0)+\int_{s_0}^{s_1}\frac{M}{EI}(x_1-x)ds\\&\qquad+\int_{s_0}^{s_1}\frac{P}{EF}\left(\frac{x_1-x}{r}ds-dy\right)+wt(y_1-y_0).\end{aligned}\right\} \quad (17)$$

3. **The Three-Hinged Arch.**—*Exterior Forces.*—From equation (12), Chapter I,

$$\mathfrak{M}_g-H_1 y=M_x. \quad . \quad . \quad . \quad . \quad . \quad . \quad . \quad . \quad (18)$$

Now, when $x=g$, or the distance from the line AB to the crown hinge y is equal to the rise f of the arch measured from the center

hinge to the springing line, $M_x=0$, as there can be no bending at the hinge, and

$$\mathfrak{M}_g=Hf, \quad \text{or} \quad H=\frac{\mathfrak{M}_g}{f}. \quad . \quad . \quad . \quad . \quad . \quad . \quad . \qquad (19)$$

When the abutment hinges are both at the same elevation, and the crown hinge is at the center of the span, of length l (see Fig. X), any vertical load K at the distance g from the left support (when $g<\frac{l}{2}$) will tend to exert a bending moment at the crown hinge

$$\mathfrak{M}_g=K\frac{g}{l}\,\frac{l}{2}=K\frac{g}{2},$$

and, from (19),

$$H=K\frac{g}{2}\,\frac{1}{f}=K\frac{g}{2f}. \quad . \quad . \quad . \quad . \quad . \quad . \quad . \quad . \qquad (20)$$

For $g>\frac{l}{2}$,

$$H=K\frac{l-g}{2f}, \quad . \quad . \quad . \quad . \quad . \quad . \quad . \quad . \quad . \quad . \qquad (20^a)$$

and for $g=\frac{l}{2}$,

$$H=K\frac{l}{4f}. \quad . \quad . \quad . \quad . \quad . \quad . \quad . \quad . \quad . \quad . \quad . \qquad (21)$$

When for the various values of g the corresponding values of H are plotted from a horizontal axis, the points thus obtained will

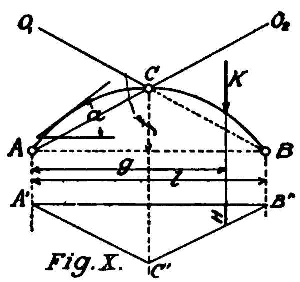

Fig. X.

form two straight lines (see Fig. X), whose point of intersection is located on the vertical through the center hinge.

The ordinate at this point of intersection is expressed by equation (21). The value of H for any position of a load K is then equal to the ordinate on the load vertical, measured between the axis $A'B'$ and the segments of the moment polygon $A'C'$ and $C'B'$.

Horizontal-Thrust Curve.—For the three-hinged arch this polygon is composed of two straight lines; later it will be shown that for the two-hinged and hingeless arches this polygon is composed of segments which are tangents to a curve. This broken line has been given the name "Horizontal-thrust Curve" for three-hinged, as well as for two-hinged and hingeless arches.

The value of H substituted in equation (18) gives the bending moment for a single load placed at the distance

$$\left.\begin{aligned} M_{x<g}&=K\frac{l-g}{l}x-Hy,\\ M_{x>g}&=K\frac{g}{l}(l-x)-Hy. \end{aligned}\right\} \quad . \quad . \quad . \quad . \quad . \quad . \quad (22)$$

Further, from equations (3) and (4), Chapter I $\left(P_x=V_1 \sin a +H_1 \cos a\right.$, and $S_x=V_1 \cos a-H_1 \sin a$, in which $\left.V_1=K\frac{g}{l}\right)$:

$$\left.\begin{aligned} P_{x<g}&=K\frac{l-g}{l}\sin a+H\cos a,\\ P_{x>g}&=-K\frac{g}{l}\sin a+H\cos a. \end{aligned}\right\} \quad . \quad . \quad . \quad . \quad (23)$$

$$\left.\begin{aligned} S_{x<g}&=K\frac{l-g}{l}\cos a-H\sin a,\\ S_{x>g}&=-K\frac{g}{l}\cos a-H\sin a. \end{aligned}\right\} \quad . \quad . \quad . \quad . \quad (24)$$

(*a*) Horizontal and Vertical Deflections. Effect of a Change in Temperature and a Horizontal Displacement of the Abutments.—A three-hinged arch is assumed to have its points of support at the same elevation. When the abutments shift a distance Δl, the span l of the arch is increased by this distance; also, a temperature change of $\pm t$ degrees is assumed to take place.

Equation (17) gives

$$\Delta x_1-\Delta x_0=-\Delta a_0(y_1-y_0)-\int_{s_0}^{s_1}\frac{M}{EJ}(y_1-y)ds-\int_{s_0}^{s_1}\frac{P_1}{EF}\left(\frac{y_1-y}{r}ds+dx\right) +wt\int_{s_0}^{s_1}\left(\frac{y_1-y}{r}ds+dx\right).$$

For a shifting of the abutments $M=0$ and $P=0$; and integrating the above equation for the half-arch, calling the total length of the arch axis B, and its length from the left support to the point (x, y) equal to s, for an arch whose axis is a circular arc, and f=rise of the arch,

$$\frac{\Delta l}{2}=-\Delta a_0 f\pm wt\left(\frac{B-l}{2}+\frac{l}{2}\right). \quad . \quad . \quad . \quad . \quad . \quad (25)$$

From this

$$\Delta a_0=-\frac{\Delta l}{2f}\pm wt\frac{B}{2f}.$$

For flat arches whose axes are not circular arcs,

$$\varDelta a_0 = -\frac{\varDelta l}{2f} \pm wt\frac{3+8k^2}{6k}, \quad . \quad . \quad . \quad . \quad . \quad . \quad . \quad (26)$$

in which $k=\frac{f}{l}$.

The horizontal displacement of a point (x, y) of the arch is then

$$\varDelta x = -\frac{\varDelta l}{2}\left(1-\frac{y}{f}\right) \pm wt\left(s\cos a - \frac{B}{2f}y\right),$$

and, from equation (16), the vertical displacement . . . . (27)

$$\varDelta y = -\frac{\varDelta l}{2}\frac{x}{f} \pm wt\left(s\sin a + \frac{B}{2f}x\right),$$

or, approximately, for flat arches,

$$\left.\begin{aligned} \varDelta x &= -\frac{\varDelta l}{2}\left(1-\frac{y}{f}\right) \pm wt\left(x-\frac{ly}{2f}\right), \\ \varDelta y &= -\frac{\varDelta l}{2}\frac{x}{l} \pm wt\left(y+\frac{lx}{2f}\right). \end{aligned}\right\} \quad . \quad . \quad . \quad . \quad . \quad (27^a)$$

For the deflection of the crown,

$$\varDelta f = -\frac{l}{4f}\varDelta l \pm wt\frac{Bl}{4f}. \quad . \quad . \quad . \quad . \quad . \quad . \quad . \quad (28)$$

(*b*) Deflections Caused by Loads.—The value of $\varDelta a_0$, which is the change in the angle a at the support A, is unknown in equations (15) and (16).

When B equals the total length of the arch, and $\varDelta a'_c$ the angular displacement at the crown hinge of the right half of the arch, by making the approximations $J=I$ and $P'=P$, (15) and (16) will give for the deflections of the crown hinge:

From the left support to the crown hinge:

$$(\varDelta x_1 = \varDelta x_c, \quad \varDelta x_0 = 0, \quad y_1 = f, \quad y_0 = 0).$$

$$\varDelta x_c = -\varDelta a_0 f - \int_0^{\frac{1}{2}B}\frac{M}{EI}(f-y)ds - \int_0^{\frac{1}{2}B}\frac{P}{EF}\left(\frac{f-y}{r}ds + dx\right). \quad (29)$$

From the crown hinge to the right support:

$$(\Delta x_1=0,\quad \Delta x_0=\Delta x_c,\quad y_1=0,\quad y_0=f,\quad \Delta a_0=\Delta a'_c).$$

$$-\Delta x_c=+\Delta a'_c f+\int_{\frac{1}{2}B}^{B}\frac{M}{EI}y\,ds+\int_{\frac{1}{2}B}^{B}\frac{P}{EF}\left(\frac{y}{r}ds-dx\right).$$

From the left support to the crown hinge:

$$(\Delta y_1=\Delta y_c,\quad \Delta y_0=0,\quad x_1=\tfrac{1}{2}l,\quad x_0=0).$$

$$\Delta y_c=\Delta a_0\frac{l}{2}+\int_0^{\frac{1}{2}B}\frac{M}{EI}\left(\frac{l}{2}-x\right)ds+\int_0^{\frac{1}{2}B}\frac{P}{EF}\left(\frac{l-2x}{2r}ds-dy\right).\qquad (30)$$

$$(\Delta y_1=0,\quad \Delta y_0=\Delta y_c,\quad x_1=l,\quad x_0=\tfrac{1}{2}l,\quad \Delta a_0=\Delta a'_c).$$

$$-\Delta y_c=\Delta a'_c\frac{l}{2}+\int_{\frac{1}{2}B}^{B}\frac{M}{EI}(l-x)ds+\int_{\frac{1}{2}B}^{B}\frac{P}{EF}\left(\frac{l-x}{r}ds-dy\right).$$

Add together now the first and second equations, also the third and fourth, and from the two equations thus obtained eliminate $\Delta a'_c$; then, after collecting the terms,

$$\Delta a_0=-\int_0^{B}\frac{M}{EI}\left(1-\frac{y}{2f}-\frac{x}{l}\right)ds$$
$$-\int_0^{B}\frac{P}{EF}\left[\left(1-\frac{y}{2f}-\frac{x}{l}\right)\frac{ds}{r}+\frac{dx}{2f}-\frac{dy}{l}\right].\quad . \quad . \quad (31)$$

For any form of loading the values of M and P are known, and Δa_0 can be solved from (31); substituting this value in (15) and (16) will give the horizontal and vertical displacements of any point (x, y) of the arch; or, when substituted in (29) and (30), it will give the horizontal and vertical displacements of the crown hinge for any form of loading.

Flat Parabolic Arch: Deflections Caused by a Single Load.—The equation of the parabolic arc is

$$y=\frac{4f}{l^2}x(l-x).$$

For a flat arch the assumptions can be made with sufficient accuracy that $ds=dx$, $r=\frac{l^2}{8f}$, and $P=\text{constant}=H$, for all sections of the arch. I and F are also assumed to be constant. For a single load at the distance $g<\frac{l}{2}$ from the support A, it follows from (31) and

(22), when substituting for the part of the arch from 0 to g, that $H=K\frac{g}{2f}$,

$$M_{x<g}=K\frac{l-g}{l}x-Hy=K\left(\frac{l-g}{l}x-\frac{g}{2f}y\right),$$

and for the part of the arch from g to l,

$$M_{x>g}=K\left(\frac{g}{l}(l-x)-\frac{g}{2f}y\right),$$

$$P=H=K\frac{g}{2f} \quad \text{and} \quad K\frac{g}{2f}y=K\left\{\frac{2g}{l^2}x(l-x)\right\},$$

and substituting in (31) for y its value $\frac{4f}{l^2}x(l-x)$,

$$1-\frac{y}{2f}-\frac{x}{l}=1-\frac{2fx(l-x)}{fl^2}-\frac{2x}{l}=1-\frac{3x}{l}+2\frac{x^2}{l^2},$$

$$\begin{aligned}\Delta a_0=&-\frac{K}{EI}\left[\frac{l-g}{l}\int_0^g x\left(1-\frac{3x}{l}+2\frac{x^2}{l^2}\right)dx+\frac{g}{l}\int_g^l (l-x)\left(1-\frac{3x}{l}+2\frac{x^2}{l^2}\right)dx\right.\\&\left.-\frac{2g}{l^2}\int_0^l x(l-x)\left(1-\frac{3x}{l}+2\frac{x^2}{l^2}\right)dx\right]\\&-\frac{K}{EF}\frac{g}{2f}\left[\frac{8f}{l^2}\int_0^l\left(1-\frac{3x}{l}+2\frac{x^2}{l^2}\right)dx+\int_0^l\left(\frac{dx}{2f}-\frac{dy}{l}\right)\right],\end{aligned}$$

or

$$\Delta a_0=\frac{Kg[l^3-5(l-g)^3]}{30EIl^2}-\frac{Kg(8f^2+3l^2)}{12EFf^2l}. \quad . \quad . \quad . \quad (32)$$

In the same manner is obtained the change in the angle a at the right support B:

$$-\Delta a_1=\frac{Kg[l^3-5g^3(l-g)^3]}{30EIl^2}-\frac{Kg(8f^2+3l^2)}{12EFf^2l}. \quad . \quad . \quad (33)$$

The deflections of any point (x, y) of the arch are obtained by substituting these equations in (15) or (16), which gives the following values:

for $x<\frac{l}{2}$, $<g$,

$$\Delta x=\frac{K}{EI}\frac{fx}{15l^4}[2g\{5(l-g)^3-l^3\}(l-x)-\{5l^2(2l-3x)\ ^*$$

$$-g(30l^2-55lx+16x^2)\}x^2]+\frac{K}{EF}\frac{gx}{6fl^4}\{16(l-2x)f^2+3l^3\}(l-2x), \quad (34)$$

$$\Delta y=\frac{K}{EI}\frac{x}{30l^2}[5x^2\{l^2-g(3l-x)\}+g\{l^3-5(l-g)^3\}]$$

$$+\frac{K}{EF}\frac{gx}{12f^2l^2}[16(3x-2l)f^2-3l^3]; \quad (35)$$

for $x<\frac{l}{2}$, $>g$,

$$\Delta x=\frac{K}{EI}\frac{fg}{15l^4}[-5g^2l^2(2l-g)+2xl(4l^3+15lg^2-5g^3)-2x^2(19l^3+15g^2l-5g^3)$$

$$+70l^2x^3-55lx^4+16x^5]+\frac{K}{EF}\frac{gx}{6fl^4}[16(l-2x)f^2+3l^3](l-2x), \quad (36)$$

$$\Delta y=\frac{K}{EI}\frac{g}{30l^2}[5g^2l^2-x(4l^3+15lg^2-5g^3)+15x^2l^2-15x^3l+5x^4]$$

$$+\frac{K}{EF}\frac{gx}{12f^2l^2}[16(3x-2l)f^2-3l^3]; \quad (37)$$

and for $x>\frac{l}{2}$

$$\Delta x=\frac{K}{EI}\frac{fg}{15l^4}[-l^5+2xl(6l^3-5g^2l+5g^3)-2x^2(21l^3-5g^2l+5g^3)$$

$$+70x^3l^2-55x^4l+16x^5]-\frac{K}{EF}\frac{g(l-x)}{6fl^4}\{16f^2(2x-l)+3l^3\}(2x-l), \quad (38)$$

$$\Delta y=\frac{Kg(l-x)}{30EIl^2}[l^3-5g^2(l-g)-5x(l-x)^2]$$

$$+\frac{Kg(l-x)}{12EFf^2l^2}[16(l-3x)f^2-3l^3]. \quad (39)$$

---

* These equations were developed by Melan.

The deflections of the crown hinge are ($x=\frac{1}{2}l$):

$$\Delta x_c=\frac{Kfg}{6EIl^2}(g^3+\tfrac{1}{8}l^3-g^2l), \quad \ldots \ldots \ldots \quad (40)$$

$$\Delta y_c=\frac{Kg}{60EIl}(5g^3+\tfrac{3}{8}l^3-5g^2l)-\frac{Kg(8f^2+3l^2)}{24EFf^2}. \quad \ldots \quad (41)$$

For the angular displacement at the crown hinge,—

left half of the arch:

$$\Delta a_c=\frac{Kg}{120EIl^2}(9l^3-60g^2l+20g^3)-\frac{Kg}{12EFf^2l}(3l^2-16f^2); \quad (42)$$

right half of the arch:

$$\Delta a'_c=\frac{Kg}{120EIl^2}(l^3+20g^2l-20g^3)+\frac{Kg}{12EFf^2l}(3l^2-16f^2). \quad (43)$$

Equations (34) to (43) are applicable only when $g<\frac{l}{2}$; the deflections caused by a load on the right half of the arch are obtained from the laws of symmetry.

When the load is at the center hinge,

$$\Delta x_c=0,$$

$$\Delta y_c=-\frac{Kl^3}{480EI}-\frac{Kl(8f^2+3l^2)}{48EFf^2}, \quad \ldots \ldots \quad (44)$$

$$\Delta a_c=-\Delta a'_c=-\frac{7Kl^2}{480EI}+\frac{K(16f^2-3l^2)}{24EFf^2}. \quad \ldots \quad (45)$$

The horizontal displacement of the crown is a maximum according to (40) when a load is placed at the distance $g\left(=\frac{l}{4}\right)$ from the support.

Any load placed on the left half of the arch deflects the crown towards the right, and *vice versa*.

When only the first member of equation (41) is considered,

$$\Delta y_c=0 \quad \text{when} \quad g \text{ (approximately)}=0.336l;$$

from which it follows that loads placed on the outer thirds of the span will cause the crown to rise, and that any loads on the middle third will cause it to sink.

(c) Special Equations. Flat Parabolic Arch (*Melan*).—Equations (32) to (45) will give the deflections for more than one load, or for a uniformly distributed load, by a summation of the results.

For a uniformly distributed load, however, these deflections may be obtained directly. Let D be the load per unit length, g_1 the distance (measured from the left support) which is covered by the load, and $g_1 < \frac{l}{2}$. Then

$$\Delta a_0 = -\frac{pg_1^2}{120EIl^2}[8l^3 - 20l^2g_1 + 15lg_1^2 - 4g_1^3] - \frac{pg_1^2(8f^2+3l^2)}{24EFf^2l}, \quad (46)$$

$$-\Delta a_1 = \frac{pg_1^2}{120EIl^2}[2l^3 - 5lg_1^2 + 4g_1^3] - \frac{pg_1^2(8f^2+3l^2)}{24EFf^2l}. \quad . \quad . \quad . \quad (47)$$

For the crown hinge

$$\Delta a_c = \frac{pg_1^2}{240EIl^2}[9l^3 - 30lg_1^2 + 8g_1^3] - \frac{pg_1^2(3l^2-16f^2)}{24EFf^2l}, \quad . \quad . \quad (48)$$

$$\Delta a'_c = \frac{pg_1^2}{240EIl^2}[l^3 + 10lg_1^2 - 8g_1^3] + \frac{pg_1^2(3l^2-16f^2)}{24EFf^2l}, \quad . \quad . \quad (49)$$

$$\Delta x_c = \frac{pg_1^2f}{480EIl^2}[5l^3 - 20lg_1^2 + 16g_1^3], \quad . \quad . \quad . \quad . \quad . \quad . \quad . \quad (50)$$

$$\Delta y_c = \frac{pg_1^2}{960EIl^2}[3l^3 - 20lg_1^2 + 16g_1^3] - \frac{pg_1^2(8f^2+3l^2)}{48EFf^2}. \quad . \quad . \quad (51)$$

When the loading extends from the left support to the right of the crown hinge and $g_1 > \frac{l}{2}$, the following equations are obtained:

$$\Delta a_0 = -\frac{p(l-g_1)^2}{120EIl^2}[2l^3 - 5(l-g_1)^2 + 4(l-g_1)^3]$$
$$-\frac{p(4lg_1 - l^2 - 2g_1^2)(8f^2+3l^2)}{48EFf^2l}, \quad . \quad . \quad (52)$$

$$-\Delta a_1 = \frac{p(l-g_1)^2}{120EIl^2}[-l^3 + 2l^2g_1 + 3lg_1^3 + 4g_1^3]$$
$$-\frac{p(4lg_1 - l^2 - 2g_1^2)(8f^2+3l^2)}{48EFf^2l}, \quad . \quad . \quad (53)$$

$$\Delta a_e = \frac{p(l-g_1)^2}{240EIl^2}[l^3 + 10l(l-g_1)^2 - 8(l-g_1)^3]$$

$$-\frac{p(4lg_1 - l^2 - 2g_1^2)(3l^2 - 16f^2)}{48EFf^2l}, \quad . \quad . \quad (54)$$

$$\Delta a'_e = \frac{p(l-g_1)^2}{240EIl^2}[9l^3 - 30l(l-g_1)^2 + 8(l-g_1)^3]$$

$$+\frac{p(4lg_1 - l^2 - 2g_1^2)(3l^2 - 16f^2)}{48EFf^2l}, \quad . \quad . \quad (55)$$

$$\Delta x_c = \frac{p(l-g_1)^2 f}{480EIl^2}[5l^3 - 20l(l-g_1)^2 + 16(l-g_1)^3], \quad . \quad . \quad . \quad (56)$$

$$\Delta y_c = \frac{p(l-g_1)^2}{960EIl}[3l^3 - 20l(l-g_1)^2 + 16(l-g_1)^3]$$

$$-\frac{p(4lg_1 - l^2 - 2g_1^2)(3l^2 + 8f^2)}{96EFf^2}. \quad . \quad . \quad (57)$$

The horizontal displacement of the crown hinge becomes a maximum when $g_1 = \frac{l}{2}$, or

$$\Delta x_c\,(\text{max.}) = \frac{pfl^3}{960EI}. \quad . \quad . \quad . \quad . \quad . \quad . \quad . \quad . \quad (58)$$

The crown hinge rises the most when the two end thirds of the span are loaded, which gives

$$\Delta y_c\,(\text{max.}) = \frac{37}{116{,}640}\frac{pl^4}{EI} - \frac{pl^2(3l^2 + 8f^2)}{216EFf^2}. \quad . \quad . \quad . \quad (59)$$

The greatest depression occurs at the crown hinge when the middle third of the span is loaded, which gives

$$-\Delta y_c\,(\text{max.}) = \frac{37}{116{,}640}\frac{pl^4}{EI} + \frac{5}{864}\frac{pl^2(3l^2 + 8f^2)}{EFf^2}. \quad . \quad . \quad (60)$$

CHAPTER VIII.

THE TWO-HINGED ARCH RIB.

(A CONTINUATION OF CHAPTER III.)

1. Horizontal Thrust.—From Equations (2) to (9) of Chapter I the end moments M_1 and M_2 are equal to zero, and the exterior forces are known, from which the value of H can be determined.

The equation of condition can be developed from (15) as follows:

$$\Delta x_1 - \Delta x_0 = -\Delta a_0(y_1 - y_0) - \int_{s_0}^{s_1} \frac{M}{EJ}(y_1 - y)ds - \int_{s_0}^{s_1} \frac{P'}{EF}\left(\frac{y_1 - y}{r}ds + dx\right)$$

$$+ wt \int_{s_0}^{s_1} \left(\frac{y_1 - y}{r}ds + dx\right).$$

In this equation I may be substituted for J. B = total length of arch.

In connection with Fig. IV, Chapter I, it was shown that a freely supported beam is changed into a two-hinged arch by thrusting the end A of the beam back into its original position by the application of a force H. The distance which the end A of the beam is moved is defined by the above equation, viz.:

$$\Delta l = \int_0^b \frac{M}{EI} yds + \int_0^l \frac{P'}{EF}\left(\frac{y}{r}ds - dx\right) - wt \int_0^l \left(\frac{y}{r}ds - dx\right). \quad (61)$$

Bearing in mind that $\frac{ds}{r} = da$ (see Figs. IX and XI), $y \sin da$ is the projection of y upon the curve, or, the angle being very small, the arc and the sine of the arc are equal, and the projection of y upon the curve is equal to yda. This value diminishes with an increase in the radius of curvature, and becomes zero for the straight line; and, whatever the radius, it is always equal to zero at the points of intersection of the curve with the x-axis; and for a curve in which $\frac{f}{l}$ does not exceed $\frac{1}{8}$, $y\frac{ds}{r} - dx = -ds \cos a$ $(dx = -ds \cos a)$.

Also, $P' = H\frac{ds}{dx} = \frac{H}{\cos a}$, since the direction of the force is approximately the same as that of the arch axis, and for flat arches the assumption is without error. In addition, the term in which P' appears expresses the influence of the secondary stress (axial force) on the horizontal thrust, which influence is in itself inconsiderable, and in practical engineering may be neglected.

An average area F_0 can be found from

$$\frac{B}{F_0} = \int_0^b \frac{ds}{F} = \frac{s_1}{F_1} + \frac{s_2}{F_2} + \dots *$$

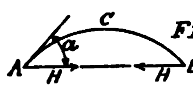

Fig. XI.

B is again the total length of the arch, F_1, F_2, etc., the average areas for the lengths s_1, s_2, etc., of the arch, and [according to Eq. (12), Chapter I] $\mathfrak{M} - Hy = M$ may be substituted, which gives

$$\Delta l = \int_0^b \frac{\mathfrak{M} y ds}{EI} - \int_0^b \frac{Hy^2 ds}{EI} - \int_0^l \frac{H}{EF} ds \cos a + wt \int_0^l ds \cos a.$$

In this equation $\int_0^l \frac{H}{EF} ds \cos a = \frac{HB}{EF_0} \cos a$ (see Fig. XI),

and $$wt \int_0^l ds \cos a = wt\, B \cos a;$$

substituting these values and solving for H gives

$$H = \frac{\int_0^b \frac{\mathfrak{M}}{I} y ds + EwtB \cos a - E\Delta l}{\int_0^b \frac{y^2 ds}{I} + \frac{B}{F_0} \cos a} \quad . \quad . \quad . \quad . \quad . \quad (62)$$

In the numerator of this equation the first term indicates the influence caused by a load, the second term the influence caused by a temperature change, and the third term the influence caused by a sliding or turning of the abutments.

For the semicircle the angle $a = 90$ degrees, and its $\cos = 0$; therefore no temperature stresses can take place in the semicircular arch.

Determination of the Integrals.—In the above equation the value of the moment of inertia is introduced:

$$I_{,} = I \cos a = I \frac{dx}{ds}, \quad . \quad . \quad . \quad . \quad . \quad . \quad . \quad . \quad (63)$$

* F, F_1, etc., are the sections at right angles to the arch axis.

which makes

$$\int_0^b \frac{\mathfrak{M}}{I} y\,ds = \int_0^l \frac{\mathfrak{M}}{I_,} y\,dx,$$

and

$$\int_0^b \frac{y^2 ds}{I} = \int_0^l \frac{y^2 dx}{I_,}.$$

Vertical Forces.—In Fig. XII the arch is divided into panels of an arbitrary length d. It is further assumed that the moment of inertia is constant in each panel and for the panel d_m the moment of inertia equals I_m, etc.; also that the two integrals of (62) can be resolved into progressions. Let d_0 be the average length of a panel; then

$$y = y_{m-1} + \frac{d_0}{d_m}(y_m - y_{m-1}), \quad . \quad . \quad . \quad . \quad . \quad . \quad . \quad (64)$$

$$\mathfrak{M} = \mathfrak{M}_{m-1} + \frac{d_0}{d_m}(\mathfrak{M}_m - \mathfrak{M}_{m-1}). \quad . \quad . \quad . \quad . \quad . \quad . \quad (65)$$

$\mathfrak{M}_{m-1}$ and $\mathfrak{M}_m$ are the moments at the points $m-1$ and m of a freely supported beam.

(The inferior prime in $I_,$ is omitted from the following equations, e.g., in place of $I_{,m+1}$ is written I_{m+1}.)

$$\frac{1}{I_m}\int_0^{d_m} \mathfrak{M} y\,dx = \frac{d_m}{6I_m}[\mathfrak{M}_{m-1}(2y_{m-1}+y_m) + \mathfrak{M}_m(2y_m+y_{m-1}). \quad (66)$$

$$\frac{1}{I_m}\int_0^{d_m} y^2 dx \ = \frac{d_m}{6I_m}[y_{m-1}(2y_{m-1}+y_m) + y_m(2y_m+y_{m-1}). \quad . \quad (67)$$

Introducing an average moment of inertia I_0 and an average panel length d_0, these equations give

$$\int_0^l \frac{\mathfrak{M} y\,dx}{I_,} = \frac{d_0}{6I_0}\Big[\ldots + \frac{d_m}{d_0}\frac{I_0}{I_m}\{\mathfrak{M}_{m-1}(2y_{m-1}+y_m) + \mathfrak{M}_m(2y_m+y_{m-1})\}$$

$$+\frac{d_{m+1}}{d_0}\frac{I_0}{I_{m+1}}\{\mathfrak{M}_m(2y_m+y_{m+1}) + \mathfrak{M}_{m+1}(2y_{m+1}+y_m)\}\ldots\Big]$$

$$= \frac{d_0}{6I_0}\Sigma_0^l \mathfrak{M}_m\Big[\frac{d_m}{d_0}\frac{I_0}{I_m}(2y_m+y_{m-1}) + \frac{d_{m+1}}{d_0}\frac{I_0}{I_{m+1}}(2y_m+y_{m+1})\Big] \quad . \quad (68)$$

and

$$\int_0^l \frac{y^2 dx}{I_,} = \frac{d_0}{6I_0}\Sigma_0^l y_m\Big[\frac{d_m}{d_0}\frac{I_0}{I_m}(2y_m+y_{m-1}) + \frac{d_{m+1}}{d_0}\frac{I_0}{I_{m+1}}(2y_m+y_{m+1})\Big]. \quad (69)$$

For brevity, let

$$v_m = \frac{d_m}{6d_0}\frac{I_0}{I_m}(2y_m + y_{m-1}) + \frac{d_{m+1}}{6d_0}\frac{I_0}{I_{m+1}}(2y_m + y_{m+1}). \quad . \quad . \quad (70)$$

Then

$$\int_0^l \frac{\mathfrak{M}y}{I_{\prime}}dx = \frac{d_0}{I_0}\Sigma_0^l \mathfrak{M}_m v_m, \quad . \quad . \quad . \quad . \quad . \quad . \quad (71)$$

and

$$\int_0^l \frac{y^2 dx}{I_{\prime}} = \frac{d_0}{I_0}\Sigma_0^l y_m v_m. \quad . \quad . \quad . \quad . \quad . \quad . \quad (72)$$

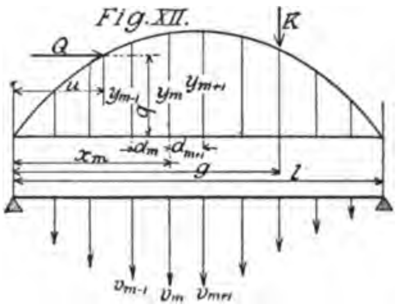

Fig. XII.

Under the influence of a single load at the distance g from the point of support A, the progressions in the foregoing equations can be expressed statically and determined graphically.

Let x_m indicate the abscissa of the point (x, y) (see Fig. XII). Then

$$\Sigma_0^l \mathfrak{M}_m v_m = K\left[(l-g)\Sigma_0^g \frac{x_m v_m}{l} + g\Sigma_g^l \frac{(l-x_m)}{l} v_m\right] = K\mathfrak{M}_g.^* \quad . \quad (73)$$

The values of v can be considered as loads acting at the panel points of a beam freely supported at the ends, and $K\mathfrak{M}_g$ is the moment in this beam caused by these loads at the vertical coinciding with the load line.

The values of $y_m v_m$ can be considered as loads v_m acting horizontally at the panel points at the distances y_m from the line AB; this is equivalent to a beam projecting from a wall and supporting the loads v at the distances y from the wall.

When the distances d are equal, equation (70) changes to

$$v_m = \frac{I_0}{6I_m}(2y_m + y_{m-1}) + \frac{I_0}{6I_{m+1}}(2y_m + y_{m+1}). \quad . \quad . \quad . \quad (70^a)$$

---

* The integrals of (71) and (72) are equivalent to the bending moment of a simple beam, which characteristic was first discovered and described by Mohr.

When the moment of inertia I is constant, this equation changes to

$$v_m = \tfrac{1}{6}(y_{m-1} + 4y_m + y_{m+1}). \quad . \quad . \quad . \quad . \quad . \quad (70^b)$$

When the panel lengths d are made small, these equations may be changed, without serious error, into

$$v_m = \frac{I_0}{I_m} y_m, \quad \text{or into} \quad v_m = y_m, \quad . \quad . \quad . \quad . \quad . \quad (70^c)$$

when the moment of inertia I is constant.

(a) Horizontal Forces.—A force Q acts in a horizontal direction at the distance q from the line AB, and the abscissa of its point of application is u. (See Fig. XII.)

In the following analysis the displacement of the abutments and the influence of a temperature change will not be considered. Equation (61) is applicable in this case. As before, the approximations $P' = \frac{H-Q}{\cos a}\Big]_{x=0}^{x=u}$ and $P' = \frac{H}{\cos a}\Big]_{x=u}^{x=l}$ are made, which give for the horizontal thrust at the right support B:

$$H_Q = \frac{\int_0^b \frac{\mathfrak{M}' y}{I} ds + \frac{Qu}{F_0}}{\int_0^b \frac{y^2 ds}{I} + \frac{B \cos a}{F_0}}. \quad . \quad . \quad . \quad . \quad . \quad (74)$$

Substituting therein the values of the integrals of (71) and (72), dividing by I_0, and multiplying by d_0, gives

$$H_q = \frac{\Sigma_0^l \mathfrak{M}'_m v_m + Q\frac{I_0 u}{F_0 d_0}}{\Sigma_0^l y_m v_m + \frac{B \cos a I_0}{F_0 d_0}}. \quad . \quad . \quad . \quad . \quad . \quad (75)$$

At the support A acts a force directed outward $= Q - H_q$.
For a horizontal force Q the moment is

$$\mathfrak{M}' = Qy, -Q\frac{q}{l}x\Big]_{x=0}^{x=u} \quad \text{and} \quad \mathfrak{M} = Q\frac{q}{l}(l-x)\Big]_{x=u}^{x=l},$$

which makes

$$\Sigma_0^l \mathfrak{M}'_m v_m = Q\Big[\Sigma_0^u y_m v_m - \frac{q}{l}\Sigma_0^u v_m x + \frac{q}{l}\Sigma_u^l v_m (l-x)\Big]$$

$$= Q\Big[\frac{q}{l}\Sigma_0^l (l-x) v_m - \Sigma_0^u (q-y) v_m\Big]. \quad . \quad . \quad . \quad (76)$$

In this equation $\frac{1}{l}\Sigma_0^l (l-x)v_m$ is equal to the vertical reaction at A of a beam acted on by the vertical loads v_m.

This reaction is easily obtained, and for a symmetrical arch is equal to $\frac{1}{2}\Sigma_0^l v_m$.

Now, suppose this reaction to act horizontally at A on a beam which is acted on by the forces v_m in a direction opposite to the reaction; then equation (76) is the difference between the moment caused by the reaction mentioned in this article and the moment of the forces v_m with reference to the horizontal line of action of the force Q.

General equations for temperature stresses, yielding of the abutments, and the computation of deflections will be found in Art. 2 (i) of this chapter.

2. Special Equations for Determining the Horizontal Thrust.—In place of abutments capable of resisting the horizontal thrust, the two end hinges may be connected by means of a tie-rod. This case is also solved by the general equation (61). Here Δl represents the stretch of the tie-rod, which must be capable of resisting the horizontal thrust, and when F_1 = area of the tie-rod,

$$\Delta l = \frac{H}{EF_1} l + \omega t l;$$

and this substituted in (62) gives

$$H_1 = \frac{\int_0^b \frac{\mathfrak{M} y}{I} ds + E\omega t(B \cos a - l)}{\int_0^b \frac{y^2}{I} ds + \frac{B \cos a}{F_0} + \frac{l}{F_1}}. \quad . \quad . \quad . \quad . \quad (77)$$

This tie-rod is quite often curved upward and hung to the arch by means of suspenders (see Fig. XIII).

Fig. XIII.

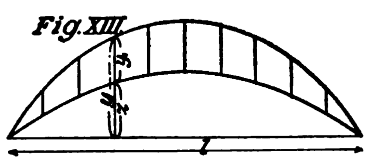

When, again, the approximation is made for flat arches that the secondary stress in the arch and in the tie-rod $(P) = H$, it then follows that

$$M = \mathfrak{M} - Hy + Hz = \mathfrak{M} - Hy'.$$

Further, if F_0 = average sectional area of the arch rib,
F_1 = sectional area of the tie-rod,
F_2 = " " " a suspender,
d = panel distance of suspenders,

$$H=\frac{\int_0^b \frac{\mathfrak{M}y'}{I}ds+Ewt(B\cos a-l_{,})}{\int_0^b \frac{y_{,}^2}{I}ds+\frac{B\cos a}{F_0}+\frac{l_{,}}{F_1}+\frac{1}{F_2}\Sigma_0^l\, y_{,}\left(\frac{\Delta^2 z}{d}\right)^2} \quad . \quad . \quad (78)$$

In this equation $l_{,}$ = length of curved tie-rod. If the curve is assumed to be a parabola, $l_{,}=l\left(1+\frac{16}{3}\frac{f_{,}^2}{l^2}\right)$, approx., in which $f_{,}$ = rise of tie-rod at center of span $=z_{\max}$. (See Fig. XIII.)

The substitution of (71) and (72) in this equation can be made when y' is inserted in place of y in (70).

The last term of the denominator indicates the influence of the stretch of the suspenders.

(*a*) Arches with Parabolic Axes.—It is here assumed that the moment of inertia of the arch rib increases from the crown to the support in the same ratio as the secant of the angle which the tangent to the arch axis makes with the horizontal:

$$I=I_0 \sec a,$$

where I_0 is the moment of inertia of the arch rib at the crown.

General Equations for any Curvature of the Arch Axis. In the following analysis the influence of the exterior forces only is analyzed, the influences of the secondary stresses, the temperature stresses, and sliding of the abutments being for the present neglected.

Under these conditions equation (61) reduces to

$$\int_0^b \frac{M}{EI}yds=0. \quad . \quad . \quad . \quad . \quad . \quad . \quad . \quad (79)$$

The assumption $I=I_0 \sec a$ gives, when $\sec a=\frac{ds}{dx}$,

$$I=I_0\frac{ds}{dx},$$

and I_0 is a constant, E is a constant, and both are eliminated from (77).

$$\int_0^l \frac{M}{EI}yds=\int_0^l \frac{M}{EI_0}y\frac{dx}{ds}ds=\int_0^l Mydx=0, \quad . \quad . \quad . \quad (79^a)$$

and substituting $\mathfrak{M}-Hy$ for M from (12), Chapter I, gives

$$\int_0^l \mathfrak{M} y dx - \int_0^l H y^2 dx = 0,$$

or

$$H = \frac{\int_0^l \mathfrak{M} y dx}{\int_0^l y^2 dx}; \quad . \quad . \quad . \quad . \quad . \quad . \quad . \quad . \quad (80)$$

and substituting the values of (71) and (72) for the integrals, gives

$$H = \frac{\Sigma_0^l \mathfrak{M}_m v_m}{\Sigma_0^l y_m v_m}. \quad . \quad . \quad . \quad . \quad . \quad . \quad . \quad . \quad (81)$$

In this equation $\Sigma_0^l \mathfrak{M}_m v_m$ is again equal to the value of equation (73), and when $\Sigma_0^l y_m v_m$ is made the unit of measurement,

$$H = \Sigma_0^l \mathfrak{M}_m v_m.$$

In the same manner is obtained, for a horizontal force Q,

$$H_Q = \frac{\Sigma_0^l \mathfrak{M}'_m v_m}{\Sigma_0^l y_m v_m}, \quad . \quad . \quad . \quad . \quad . \quad . \quad . \quad . \quad (82)$$

and substituting the values of equation (76) in (82) gives the horizontal thrust at the supports, remembering that $H_2 = Q - H_1$, that for the distance u the horizontal thrust in the arch equals H_1, and for the distance $(l-u)$ it equals H_2.

Equations (81) and (82) may be used for either the graphical or the analytical computation of the horizontal thrust, and are applicable for any curvature of the arch axis.

The reactions for the two-hinged arch are obtained in the same manner as those for a beam freely supported at the ends, and with the reaction and the horizontal thrust the component of any exterior force can be drawn or computed; or, with the assistance of equation (20), Chapter I, the ordinates of the intersection locus may be computed when M_1 and M_2 are each made equal to zero.

The equations developed in the preceding paragraphs show that the moment of inertia can vary materially before its influence will appreciably affect the horizontal thrust; and for this reason the assumption made at the beginning of this article—that $I = I_0 \sec a$—is applicable to most arch ribs in practice.

The labor involved in computing the stresses in the two-hinged arch would be considerably reduced if the horizontal thrusts or the intersection locus could be taken from a standard diagram, and simple corrections made thereto to render it applicable to the case under consideration.

For any curvature of the axis of the arch except the parabola, the analytical solution of this problem becomes very laborious and complicated; but for the parabola of unit span and unit rise, it is comparatively simple.

The Parabolic Arch.—For this purpose introduce into equation (79^a) the value of M expressed in ordinates of the components with reference to the line AB, and for y the ordinates of the parabola, as follows:

Equation (79^a) gives

$$\int_0^l Mydx=0,$$

and from Fig. 1, Chapter I,

$$M=y_{\prime}H=y_{\prime\prime}H-yH.$$

This value introduced in (79^a) gives

$$\int_0^l y_2Hydx-\int_0^l yHydx=0;$$

as H is a constant, it may be eliminated from the equation, and

$$\int_0^l y_2ydx=\int_0^l y^2dx. \quad . \quad . \quad . \quad . \quad . \quad . \quad (83)$$

Fig. XIV.

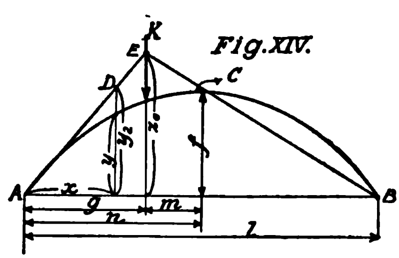

The application of the equation for the parabola is simplified, in this case, by taking the origin of coordinates at the center of the span, as shown in Fig. XIV.

In equation (83) the value of y_2 may be expressed in terms of z_0, as follows:

For the distance g, $\quad y_2 = z_0 \dfrac{x}{n-m}$;

For the distance $l-g$, $\quad y_2 = z_0 \dfrac{x}{n+m}$.

Also, the equation for the parabola is

$$y = \frac{fx}{n^2}(2n-x),$$

and introducing these values in (83) gives

$$\int_0^{2n} \frac{f^2x^2}{n^4}(2n-x)^2 dx = \int_0^{n-m} z_0 \frac{x}{n-m}\frac{fx}{n^2}(2n-x)dx + \int_{n-m}^{2n} z_0 \frac{x}{n+m}\frac{fx}{n^2}(2n-x)dx,$$

or

$$\int_0^{2n} \frac{f}{n^4}(2n-x)^2 dx = \int_0^{n-m} \frac{z_0}{n^2(n-m)}(2n-x)dx + \int_{n-m}^{2n} \frac{z_0}{n^2(n+m)}(2n-x)dx.$$

Integrating and solving for z_0 gives

$$z_0 = \frac{32n^2 f}{25n^2 - 5m^2}, \quad \ldots \ldots \ldots \quad (84)$$

or, if m is taken $= n-g$, $g = kl$, and $n = \frac{1}{2}l$,

$$z_0 = \frac{8}{5} f \frac{1}{1+k-k^2},$$

l being unity for horizontal measurements.

When f is unity for vertical measurements,

$$z_0 = \frac{8}{5}\frac{1}{1+k-k^2}, \quad \ldots \ldots \ldots \quad (85)$$

and the ordinates z_0 for successive values of g can be easily found and plotted, as in Fig. 14, Chapter III.

The same method is used to obtain the ordinates of the intersection locus for a horizontal force.

(*b*) Horizontal Forces.—From equation (78)

$$H=\frac{\int_0^l \mathfrak{M}' y dx}{\int_0^l y^2 dx},$$

and the value of $\mathfrak{M}'$ can be again expressed in ordinates of the components with reference to the line AB; for y the ordinates of the parabola are substituted.

From Fig. XV it follows that

$$-V_1=V_2=\frac{Qq}{l},$$

$$V_1 x_0 = H_1 q, \quad \text{or} \quad x_0=\frac{H_1}{V_1}q, \quad \text{or} \quad x_0=\frac{H_1}{Q}l;$$

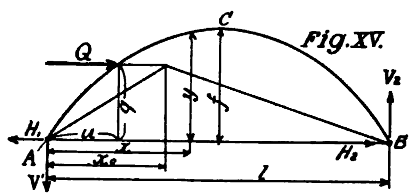

and when l is the unit of measurement for length,

$$x_0=\frac{H}{Q}. \quad \ldots \ldots \ldots \quad (86)$$

From equation (76)

$$\mathfrak{M}'=\Sigma_0^l Q\frac{q}{l}(l-x)-\Sigma_0^u Q(q-y), \quad \ldots \ldots \quad (86^a)$$

and this substituted in (80) gives

$$H=\frac{Q\frac{q}{l}\int_0^l (l-x)y dx - Q\int_0^u qy dx + \int_0^u Qy^2 dx}{\int_0^l y^2 dx},$$

or

$$\frac{H}{Q}=x_0=\frac{\frac{q}{l}\int_0^l (l-x)y dx - \int_0^u qy dx + \int_0^u y^2 dx}{\int_0^l y^2 dx}. \quad \ldots \quad (87)$$

$\int_0^l y^2 dx =$ twice the moment of the area ACB around the axis AB.

For the parabola, $\int y\,dx = \text{area} = \frac{2}{3}fl$, and the distance from the center of gravity of the area to $AB = \frac{2}{5}f$;

$$\therefore \int_0^l y^2 dx = \frac{8}{15}f^2 l.$$

Substituting for y the equation of the parabola

$$y = \frac{4f}{l^2}(lx - x^2) \text{ gives (see Fig XV)}$$

$$q = \frac{4f}{l^2}(lu - u^2), \quad \text{and} \quad u = kl, \quad q = 4f(k - k^2).$$

$$\frac{q}{l}\int_0^l (l-x)y\,dx = \frac{4fq}{l^3}\int_0^l (l-x)^2 x\,dx = 4flq\left(\tfrac{1}{2} - \tfrac{2}{3} + \tfrac{1}{4}\right) = \tfrac{1}{3}flq$$
$$= \tfrac{4}{3}f^2 l(k - k^2),$$

$$-q\int_0^u y\,dx = -\frac{4fq}{l^2}\int_0^u (lx - x^2)dx = -\frac{4fq}{l^2}u^2(l-u)$$
$$= -\tfrac{8}{3}f^2 l(3k^3 - 5k^4 + 2k^5),$$

$$+\int_0^u y^2 dx = \frac{16f^2}{l^4}\int_0^u x^2(l-x)^2 dx = \frac{16f^2}{l^4}\left(\frac{l^2u^3}{3} - \frac{lu^4}{2} + \frac{u^5}{5}\right)$$
$$= \tfrac{8}{15}f^2 l(10k^3 - 15k^4 + 6k^5),$$

and

$$\frac{H}{Q} = x_0 = \frac{\frac{4}{3}f^2 l(k-k^2) - \frac{8}{3}f^2 l(3k^3 - 5k^4 + 2k^5) + \frac{8}{15}f^2 l(10k^3 - 15k^4 + 6k^5)}{\frac{8}{15}f^2 l},$$

$$x_0 = \frac{k}{2}[5(1 - k - 2k^2 + 4k^3) - 8k^4]. \quad . \quad . \quad . \quad . \quad . \quad . \quad . \quad . \quad . \quad . \quad (88)$$

This equation has been plotted in Fig. 13 for a unit span equal to $\frac{1}{2}l$, and a unit rise equal to f.

(c) Temperature and Secondary Stresses. (*Parabolic Arch*).—Equation (61) shows that the secondary stress $\int_0^l \frac{P'}{EF}\left(\frac{y}{r}ds - dx\right)$ contributes its share towards Δl, as does also the temperature stress $wt\int_0 \left(\frac{y}{r}ds - dx\right)$.

These equations have the same form and can therefore be analyzed together.

Assuming again that for flat arches $\frac{y}{r}ds-dx=-ds\cos a=-dx$, gives [see equation (61)]

$$\int_0^l -\frac{P}{EF}dx=-\frac{P'}{EF_0}l=\varDelta x \quad . \quad . \quad . \quad . \quad . \quad . \quad . \quad (89)$$

and

$$\int_0^l wtdx=wtl=\varDelta x'. \quad . \quad . \quad . \quad . \quad . \quad . \quad . \quad . \quad (90)$$

Any exterior force acting on the arch shifts the hinge through a distance

$$\int_0^b \frac{M}{EI}yds=\varDelta x. \quad . \quad . \quad . \quad . \quad . \quad . \quad . \quad . \quad . \quad (90^a)$$

Now,

$$I=I_0\sec a=I_0\frac{ds}{dx},$$

and substituting this value in (90^a) gives

$$\int_0^l \frac{M}{EI_0}ydx=\varDelta x. \quad . \quad . \quad . \quad . \quad . \quad . \quad . \quad . \quad . \quad . \quad (91)$$

To shift the hinge back into position, a force H acts thereat, its moment arm for any point of the arch $=y$, and its bending moment $M=Hy$; these give for the secondary stress

$$\int_0^l \frac{H}{EI_0}y^2dx=-\frac{P'}{EF_0}l, \quad . \quad . \quad . \quad . \quad . \quad . \quad . \quad (91^a)$$

or

$$\frac{H}{I_0}\int_0^l y^2dx=-\frac{P}{F_0}l.$$

The value of $\int_0^l y^2dx$ has been found for the parabola$=\frac{8}{15}f^2l$; substituting this value in the previous equation gives

$$H=-\frac{15}{8}\frac{P'}{F_0}\frac{I_0}{fl}.$$

Now, P is the average stress in the arch rib, F_0 its average area, and $\frac{P}{F_0}=n$, which gives

$$H_n=-\frac{15}{8}\frac{nI_0}{fl}. \quad \ldots \ldots \ldots \quad (92)$$

Similarly, for the temperature stress,

$$H_t=\frac{15}{8}\frac{EI_0wt}{f^2}. \quad \ldots \ldots \ldots \quad (93)$$

Equations (89) to (93) are applicable in most cases which present themselves in practical bridge building.

Instead of the expression $\int -ds\cos a=\int -dx=-l$, the following should be substituted in the case of flat arches:

$$\int -ds\cos a=-B\cos a=l\left(1+\frac{8}{3}\frac{f^2}{l^2}\right)\left(1-8\frac{f^2}{l^2}\right)$$

$$=l\left(1-\frac{16}{3}\frac{f^2}{l^2}-\frac{64}{3}\frac{f^4}{l^4}\right),$$

or, approximately, $$=l\left(1-\frac{16}{3}\frac{f^2}{l^2}\right). \quad \ldots \ldots \ldots \quad (94)$$

This will insure greater accuracy, but will make equations (92) and (93) unnecessarily complicated; and for practical use equation (93) is sufficiently correct.

To determine the influence on the stresses in the arch caused by a shifting of the abutments, equation (91) can be used, letting Δx represent the amount of shifting, and substituting Hy for M, as follows:

$$\frac{H}{EI_0}\int_0^l y^2dx=\Delta x=\frac{H}{EI_0}\frac{8}{15}f^2l;$$

so that, if the abutment shifts a distance Δx,

$$H=\Delta x\frac{15EI_0}{8f^2l}. \quad \ldots \ldots \ldots \quad (93^a)$$

(*d*) CRESCENT-SHAPED TWO-HINGED ARCH. (Special Equations.)* —The general equation (61) is applicable to any form of arch rib.

This equation can be simplified when in the crescent arch (see Fig. XVI) the following conditions are satisfied:

h = height of arch rib;

y = ordinate of the arch axis;

$h = k_{,}y$, in which $k_{,}$ is a constant ratio between the ordinate of the axis and the height of the arch rib;

F = area of section of one flange at the crown;

a = angle of inclination of the axis of the arch to the horizontal;

F' = area of the flange section at the hinges $= F \sec a$;

I = moment of inertia, and

$$I = 2 \times (\tfrac{1}{2}h)^2 F' = \tfrac{1}{2}h^2 F \sec a = \tfrac{1}{2}k_{,}^2 y^2 F \sec a. \quad . \quad . \quad . \quad . \quad . \quad (94^a)$$

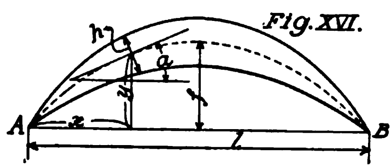

In this value for I the moments of inertia of the flanges around their own neutral axes have been neglected. Now h is largest at the crown and gradually decreases to zero at the hinges. In practice, however, this is not true, as, for reasons of construction, the arch rib rarely ends in points at the hinges. The assumption introduces an error which is on the safe side, and the stresses which are the result of the computation will be from 1 to 5 % larger near the hinges than the actual stresses in the structure. (Compare computation of the intersection locus with the deflections of the Douro Bridge.)

Neglecting for the present the secondary stresses, temperature stresses, and the shifting of the abutments, equation (61) reduces to

$$\int_0^l \frac{M}{EI} y\,ds = 0,$$

and substituting the value obtained for I gives

$$\int_0^l M \frac{dx}{y} = 0. \quad . \quad . \quad . \quad . \quad . \quad . \quad . \quad . \quad (95)$$

Vertical Load K.—From Fig. I, Chapter I,

$$M = y_{,}H = y_{,,}H - yH,$$

* These equations were developed by the author.

which, when substituted in (95), gives

$$\int_0^l Hy_{\prime\prime}\frac{dx}{y}=\int_0^l H\frac{y}{y}dx,$$

or

$$\int_0^l y''dx=\int_0^l ydx, \quad . \; . \; . \; . \; . \; . \; . \quad (95^a)$$

which means that the area of the triangle AEB is equal to the area between the arch axis and the chord AB (see Fig. XIV). For the parabolic arch axis,

$$\text{Area of parabola}=\tfrac{2}{3}fl,$$

$$\text{Area of triangle }=\tfrac{1}{2}z_0l;$$

$$\therefore\; z_0=\tfrac{4}{3}f. \quad . \; . \; . \; . \; . \; . \; . \; . \; . \; . \quad (96)$$

(*e*) Horizontal Load Q. (See Fig. XV.)—From equation (95),

$$0=\int_0^l M'\frac{dx}{y},$$

or

$$0=\int_0^l \mathfrak{M}'\frac{dx}{y}-Hy\frac{dx}{y},$$

and

$$H=\int_0^l \frac{\mathfrak{M}'dx}{yax}.$$

From equations (86) and (86^a),

$$\mathfrak{M}'=Q\frac{q}{l}(l-x)-Q(q-y),$$

which, when substituted for $\mathfrak{M}'$ in the last equation, gives

$$\frac{H}{Q}=x_0=\frac{\frac{q}{l}\int_0^l(l-x)dx-\int_0^u qdx+\int_0^u ydx}{\int_0^l ydx}. \quad . \; . \quad (97)$$

For a parabolic arch axis

$$\int_0^l ydx=\text{area of the parabola}=\tfrac{2}{3}fl,$$

and again introducing $y=\frac{4f}{l^2}(lx-x^2)$, $q=4f(k-k^2)$, and $u=kl$ * gives

$$\frac{q}{l}\int_0^l (l-x)dx=\tfrac{1}{2}ql=2fl(k-k^2),$$

$$\int_0^u qdx=qu=4fl(k^2-k^3),$$

$$\int_0^u ydx=\frac{4f}{l^2}\left(\frac{lu^2}{2}-\frac{u^3}{3}\right)=\tfrac{2}{3}fl(3k^2-2k^3);$$

and

$$\frac{H}{Q}=x_0=\frac{2fl(k-k^2)-4fl(k^2-k^3)+\tfrac{4}{3}fl(3k^2-2k^3)}{\tfrac{2}{3}fl}$$

$$=k(4k^2-6k+3). \quad \ldots \ldots \quad (98)$$

These values for x_0 have been plotted in Fig. 20 for a unit span $=l$ and a unit rise $=f$.

(*f*) Temperature and Secondary Stresses in the Crescent-Shaped Arch.—As obtained before in equation (90^a),

$$\int_0^l \frac{M}{EI}yds=\Delta x.$$

Substituting in this equation $ds=dx \sec a$, and for I its value in (94^a) gives

$$\int_0^l \frac{M}{E}\frac{2dx}{k^2yF}=\Delta x;$$

and substituting $M=Hy$ gives

$$\left.\begin{aligned}\int_0^l \frac{2H}{Ek^2F}dx&=\Delta x,\\ \text{or}\qquad \frac{2Hl}{Ek^2F}&=\Delta x,\end{aligned}\right\} \quad \ldots \ldots \quad (99)$$

and substituting for Δx its values from equation (89) or (90) gives for the temperature stress

$$H_t=\tfrac{1}{2}wtEk^2F; \dagger \quad \ldots \ldots \quad (100)$$

* u and l have the values given in Fig. XV.

† Before applying (99^a) and (100), see Art. 21 (*b*), Chap. III.

and for the secondary stress

$$H_n = -\tfrac{1}{2}nk^2F, \quad . \; . \; . \; . \; . \; . \; . \; . \quad (101)$$

in which n = average stress per square inch in the chord sections $= \frac{P}{F_0}$.

For a shifting of the abutments through a distance Δx, equation (99) gives

$$H = \Delta x \frac{Ek^2F}{l}. \quad . \; . \; . \; . \; . \; . \; . \; . \quad (99^a)$$

(*g*) SPECIAL EQUATIONS: *Arch with Full Web and Horizontal Upper Chord.*—The arch shown in Fig. XVII is composed of a web with chord angles and plates, $A_{,,}B_{,,}$ being the top chord and ACB

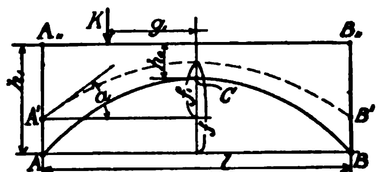

Fig. XVII.

the bottom chord. The horizontal thrust H is defined by equations (62), which can be reduced to a special case when the bottom chord ACB is a parabola. In the figure $A_{,}B_{,}$ is the neutral axis of the arch, and the moments of inertia at the crown and at the hinges are I_0 and $I_{,,}$ respectively. Also,

$$\left.\begin{aligned} m &= \frac{f'}{f}, \\ n &= \frac{h_{,} - h_0}{h_0}, \\ p &= \frac{I_{,} + I_0}{I_0} - \frac{2h_{,}}{h_0}, \end{aligned}\right\} \quad . \; . \; . \; . \; . \; . \; . \; . \quad (102)$$

and, approximately, when x is the distance from the section to the crown of the arch,

$$I'_x = I_0\left(1 + 8n\frac{x^2}{l^2} + 16p\frac{x^4}{l^4}\right).$$

Further,

$$A=m\left(8m\frac{f^2}{l^2}-1\right)-2n,$$

$$B=8m^3\frac{f^2}{l^2}+2nm\left(8m\frac{f^2}{l^2}-1\right)-4n^2+p,$$

$$C=16nm^3\frac{f^2}{l^2}+m(4n^2-p)\left(8m\frac{f^2}{l^2}-1\right)-4n(2n^2-p),$$

$$D=\tfrac{1}{3}-\tfrac{2}{5}m+\tfrac{1}{7}m^2+8m^2\frac{f^2}{l^2}(\tfrac{1}{5}-\tfrac{2}{7}m),$$

$$E=\tfrac{1}{5}+\tfrac{2}{7}m\left(4m\frac{f^2}{l^2}-1\right),$$

and $\frac{2g}{l}=k.$ $B=$ length of neutral axis.

These values substituted in equation (62) will give

$$H=\frac{\left\{\tfrac{1}{8}(1-k^2)+\tfrac{1}{48}A(1-k^4)-\tfrac{1}{120}B(1-k^6)+\tfrac{1}{224}C(1-k^8)\right\}K\frac{l}{f}+\frac{EI_0}{f^2l}wtB\cos a}{1-\tfrac{2}{3}m+\tfrac{1}{5}m^2+8m^2\frac{f^2}{l^2}(\tfrac{1}{3}-\tfrac{2}{5}m+\tfrac{1}{7}m^2)-2nD+(4n^2-p)E-\tfrac{4}{7}n(2n^2-p)+\frac{I_0B\cos a}{F_0f^2l}}. \quad (103)*$$

This equation (due to Melan) is also applicable to an arch rib with a parabolic axis and an arbitrary variation in its sectional area.

For example, for a constant moment of inertia $n=p=0$, and $m=1$.

For the crescent-shaped arch rib $m=1$, $n=-1$, $p=+1$, which will give

$$H=\frac{\left\{\tfrac{1}{8}(1-k^2)+[\tfrac{1}{48}(1-k^4)+\tfrac{1}{120}(1-k^6)+\tfrac{1}{224}(1-k^8)]\left(1+\frac{8f^2}{l^2}\right)\right\}K\frac{l}{f}+\frac{EI_0}{f\cdot l}wtB\cos a}{1+\frac{8}{3}\frac{f}{l^2}+\frac{I\cos a}{F_0f^2l}}. \quad (104)*$$

* In applying equations (103) and (104) the *location* of the arch axis $A'B'$ in Fig. XVII affects the result. It should be remembered that the ordinates of the arch axis are measured from the line AB; and for this reason the location of the axis should be verified from the finished design, and the necessary corrections made. Generally, it will be both easier and more correct to use the method described for the spandrel-braced two-hinged arch, in the computation of which the location of the arch axis does not enter.

Or, the equation for the crescent-shaped arch deduced by Schäffer may be applied, viz.:

$$H=\frac{\left\{(1+k)\log_e\frac{2}{1+k}+(1-k)\log_e\frac{2}{1-k}\right\}K\frac{l}{8f}+\frac{EI_0}{f^2l}wtB\cos a}{1+\frac{8}{3}\frac{f^2}{l^2}+\frac{I_0B\cos a}{F_0f^2l}}. \qquad (104^a)^*$$

The intersection locus can then be obtained from the general equation (20^a).

[Compare equations (103), (104), and (104^a) with (95^a) and (96), deduced by the author.]

Circular Arch Rib with Constant Moment of Inertia (Melan—see Fig. XVIII).—By substituting in equation (15) the exact values

$$P'=P\frac{M}{r},\quad \text{and}\quad y=r(\cos c-\cos a),\quad y_0=y_1=0,\quad \frac{y}{r}ds-dx=-ds\cos a,$$

$$P=H\cos c+V\sin c,\quad \text{and}\quad \frac{I}{Fr^2}=n,\quad \text{and}$$

$$H=\frac{[\sin^2a-\sin^2c+2\cos a(\cos c-\cos a)-2(1+n)\cos a(a\sin a-c\sin c)]K+2\frac{EI}{r^2}(2wtra\cos a-\Delta l)}{2[a-3\sin a\cos a+2(1+n)a\cos^2a]} \qquad (105)$$

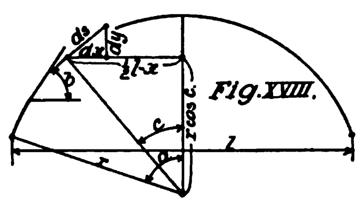

For the semicircle,

$$a=\frac{\pi}{2},\quad \text{and}\quad H=\frac{\cos^2c}{\pi}K-\frac{2EI\Delta l}{r^3\pi}. \quad . \quad . \quad . \quad . \quad (106)$$

The equation of the intersection locus follows from (20^a):

$$z=\frac{Kr(\sin a^2-\sin c^2)}{2H\sin a}, \quad . \quad . \quad . \quad . \quad . \quad . \quad . \quad . \quad . \quad (107)$$

* Equation (104^a) is not as convenient to apply as equation (95^a). (Compare with the computations of the Douro Bridge, Art. 18, Chap. III.)

and for the semicircle:

$$z_0=\frac{\pi r}{2}, \quad . \quad . \quad . \quad . \quad . \quad . \quad . \quad . \quad . \quad (107^a)$$

and for this special case the intersection locus is a straight line.

For a uniformly distributed load on the semicircular arch,

$$H_{\text{total}}=\frac{4}{3\pi}Pr. \quad . \quad . \quad . \quad . \quad . \quad . \quad . \quad . \quad (107^b)$$

(*h*) Correction of the Intersection Locus of the Parabolic Arch Rib Whose Moment of Inertia is Expressed by the Equation $I=I_0$ sec a, to Make It Applicable to an Arch of Arbitrary Curvature.—When secondary and temperature stresses are neglected and the abutments are fixed in position, the general equation (83) is

$$\int y_2 y dx=\int y^2 dx \quad \text{(see Fig. XIV).}$$

The center of gravity of the strip ydx is at the distance $\frac{1}{2}y$ from AB, and is also distant y_3 from the point D, or

$$y_2=y_3+\tfrac{1}{2}y,$$

and equation (83) can be written

$$\int_0^l y_3 y dx+\int_0^l \tfrac{1}{2}y^2 dx=\int_0^l y^2 dx,$$

or

$$\int_0^l y_3 y dx=\int_0^l \tfrac{1}{2}y^2 dx, \quad . \quad . \quad . \quad . \quad . \quad . \quad . \quad . \quad . \quad (108)$$

which means that the moment of the area ACB with respect to the axis AB is equal to its moment with respect to the axis AEB.

To show the influence of equation (108) on the intersection locus, the arch $AC'B$ has been drawn in Fig. XIX. The rise of this arch and also one-half the span are each equal to unity. The center of gravity of the area $AC'B$ is at p, and of the area $AC'D$ at $p_{,}$.

In the figure the arc $AC'B$ is a semicircle. When the load is placed at f the component of the load is fB, passing through the point e, and the distance Dp is equal to the distance pe.

When the load is placed at I, the component is equal to the line

AI. This line passes through the point g, and the distance $hp_{,}$ is equal to the distance $p_{,}g$.

The line ACB is the equivalent parabola, i.e., the area ACB is equal to the area $AC'B$.

The center of gravity of the area ACB is at P, and that of ACD is at P'.

When the load is placed at F, the component of this load is the line FB. This line passes through the point E, and the distance DP is equal to PE.

When the load is placed at I, the component of this load is the line AI passing through the point G, and the distance HP' is equal to $P'G$.

Now the distance pP is practically one-fourth of the distance

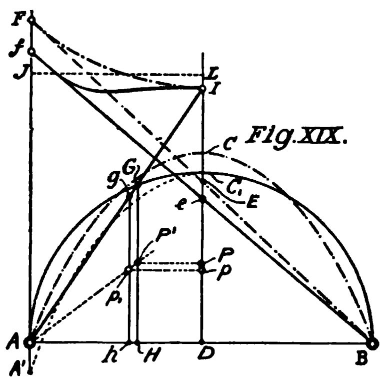

$CC_{,}$, or the distance eE is equal to one-half the distance $CC_{,}$, and Ff is equal to CC'.

The point $p_{,}$ may be approximately located by the following construction: Draw a line $pp_{,}$ parallel to AB, and also the line AP'; the point of intersection of these two lines is very close to the center of gravity of the area $AC_{,}D$. From this it follows that the points g and G must be situated on the same straight line which passes through the point A. (From similar triangles, $gh:Ah=GH:AH=ID:AD$.)

For the semicircular arch two points, f and I, of the intersection locus are thus found.

In Fig. XIX the line $A'C'$ is the equivalent parabola AC, drawn so that the crowns of the parabola and of the semicircle coincide, and by the foregoing it can be proved that the difference between the vertical ordinates of the lines fI and FI is nearly equal to the difference between the vertical ordinates of the lines AC' and $A'C'$.

The same can be demonstrated analytically by applying equations (71) and (72).

For arches in which the rise does not exceed one-tenth of the span, this correction may be neglected without affecting the practical

accuracy of the computation. The correction, as indicated in Fig. 14*a*, will produce an intersection locus which is substantially true, even for arches of large rise.

To understand this a comparison will be made with a semicircular arch. The latter, with a constant moment of inertia, has for an intersection locus a straight line, $z_0 = \frac{\pi r}{2}$ [see Eq. (107^a)], or, for a rise = 1,

$$z_0 = 1.57 = \text{line } JL. \quad . \quad . \quad . \quad . \quad . \quad . \quad . \quad (109)$$

In practice, however, the arch has a smaller moment of inertia at the crown than towards the haunches, and the intersection locus should dip below the straight line at the center, and rise above it at the ends.

The intersection locus of Fig. 14 is for a parabolic arch whose moment of inertia increases in the ratio $I = I_0 \sec a$, which means that the moment of inertia for an equivalent semicircular arch near the haunches is disproportionately large. The equivalent parabola has a rise of 1.1775. The line FI is the intersection locus, z_0 at the center of span = 1.507, and at the ends

$$z_0 = 1.884. \quad . \quad . \quad . \quad . \quad . \quad . \quad . \quad . \quad (109^a)$$

Equations (109) and (109^a) give the two extreme values.

Now, equations (71) and (72) will give for a well-designed semicircular arch values of the ordinates z_0 of the intersection locus = 1.51 at the center and 1.698 near the ends.

From this it is seen that the maximum error in the corrected ordinates of the intersection locus is 2 per cent. at the abutments and zero at the crown. A much larger error than 2 per cent. could be made at the abutments without showing any error in the stresses in the arch, and the correction described in Art 1 (*a*), Chap. III, gives the true intersection locus.*

(*i*) Temperature Stresses. General Equations.—The horizontal thrust caused by a change in temperature of t degrees is obtained from equation (62) when $\mathfrak{M}$ and Δl are both made equal to zero.

For steel (meter and ton units) $E = 22{,}000{,}000$, $w = 0.00001240$ for 1° C., and $Ew = 273$; and for $t = \pm 30°$ C.,

$$Ewt = \pm 8{,}190,$$

* In making these corrections let the crowns of the parabola and of the arch axis coincide, and let the parabola intersect the points A or B of the arch axis; then measure the differences on the horizontal ordinates from the arch axis, and plot them in the same direction from the intersection locus.

which, substituted in (62), gives

$$H_t = \pm 8{,}190 \frac{I_0 B \cos a}{d_0 \Sigma_0^l y_m v_m + \dfrac{I_0 B \cos a}{F_0}}, \quad . \quad . \quad . \quad (110)$$

and for the flat parabola, approximately,

$$H_t = \pm 8{,}190 \frac{15}{8f^2} \frac{I_0}{1 + \dfrac{15}{8} \dfrac{I_0}{F_0 f^2}}. \quad . \quad . \quad . \quad . \quad . \quad (110^a)$$

Stresses Caused by the Shifting of the Abutments.—In equation (62) $\dfrac{\mathfrak{M} y ds}{I} = 0$, and $EwtB \cos a = 0$; and shifting of the abutments causes a horizontal thrust

$$H = \frac{-E\Delta l}{\displaystyle\int_0^b \frac{y^2 ds}{I} + \frac{B \cos a}{F_0}} = \frac{-E\Delta l I_0}{\displaystyle\int_0^b \frac{I_0}{I} y^2 ds + \frac{I_0 B \cos a}{F_0}},$$

or

$$H = \frac{-E\Delta l I_0}{W}. \quad . \quad . \quad . \quad . \quad . \quad . \quad . \quad . \quad . \quad . \quad . \quad . \quad (110^b)$$

$$W = \int_0^l \frac{I_0}{I} y^2 ds + \frac{I_0 B \cos a}{F_0}.$$

(*j*) Deflections in Two-Hinged Arches—General Equations.—Equation (16) or (17) will give the angular displacement at the hinges; for the total length of a symmetrical arch,

$$\Delta y_, - \Delta y_0 = 0, \quad x_, - x_0 = l, \quad x_, - x = l - x,$$

and the total length of the arch $= B$, which gives

$$\Delta a_0 = -\frac{1}{l} \int_0^B \frac{M}{EI} (l - x) ds - \frac{1}{l} \int_0^B \frac{P}{EF} \left\{ (l - x) \frac{ds}{r} - dy \right\} + wta.$$

Again,

$$\cos a = \frac{dx}{ds}, \quad I' = I \cos a = I \frac{dx}{ds},$$

and

$$a = \frac{B}{2r} = \int \frac{ds}{2r} = \int \frac{dx}{2r \cos a}$$

$$= \int \frac{l}{l} \frac{dx}{2r \cos a} = \frac{1}{l} \int \frac{(l - x) dx}{r \cos a} - \frac{1}{l} \int \frac{(\frac{1}{2} l - x) dx}{r \cos a}.$$

From similar triangles (see Fig. XVIII)

$$\frac{\frac{1}{2}l-x}{r\cos a}=\frac{dy}{dx},$$

and

$$\frac{\frac{1}{2}l-x}{r\cos a}dx=dy,$$

which, when substituted in the equation for Δa_0, gives

$$EI_0\Delta a_0=-\frac{1}{l}\int_0^l\frac{MI_0}{I_,}(l-x)dx-\frac{1}{l}\int_0^l\frac{PI_0}{F}\frac{(l-x)dx}{r\cos a}+\frac{1}{l}\int_0^l\frac{PI_0}{F}dy$$
$$+Ewt\frac{I_0}{l}\int_0^l\frac{(l-x)dx}{r\cos a}-Ewt\frac{I_0}{l}\int_0^l dy.$$

If in this equation is substituted the value of

$$M\frac{I_0}{I_,}+\frac{I_0}{r\cos a}\left(\frac{P}{F}-Ewt\right)=\text{o}, \quad . \quad . \quad . \quad . \quad . \quad (111)$$

it will be transformed into

$$EI_0\Delta a_0=-\frac{1}{l}\int_0^l\text{o}(l-x)dx-\frac{I_0}{l}\int_{x=0}^{x=l}\left(\frac{P}{F}-Ewt\right)dy, \quad . \quad . \quad (112)$$

and this value substituted in (17) gives

$$-EI_0\Delta y=\frac{x_,}{l}\int_0^l\text{o}(l-x)dx-\int_0^{x_,}\text{o}(x_,-x)dx+C_1. \quad . \quad (113)$$

$$EI_0\Delta x=\frac{y_,}{l}\int_0^l\text{o}(l-x)dx-\int_0^{x_,}\text{o}(y_,-y)dx+C_2, \quad . \quad (114)$$

and
$$\left.\begin{aligned}C_1&=-\frac{x_,}{l}I_0\int_{x=0}^{x=l}\left(\frac{P}{F}-Ewt\right)dy+I_0\int_{y_0}^{y_,}\left(\frac{P}{F}-Ewt\right)dy,\\ C_2&=\frac{y_,}{l}I_0\int_{x=0}^{x=l}\left(\frac{P}{F}-Ewt\right)dy-I_0\int_{x_0}^{x_,}\left(\frac{P}{F}-Ewt\right)dx.\end{aligned}\right\} \quad . \quad (115)$$

The expressions for C_1 and C_2 indicate the influence of a change in length of the arch axis upon the deflection of the arch.

The approximation $\frac{P}{F}=\frac{H}{F_0}$ does not cause any appreciable error;

F_0 is the average sectional area of the arch axis, and this introduced in the second term of equation (112) gives

$$\frac{I_0}{l}\int_{x=0}^{x=l}\left(\frac{P}{F}-Ewt\right)dy=I_0\left(\frac{H}{F_0}-Ewt\right)y_{,,}$$

and equations (115) change into

$$\left.\begin{aligned}C_1&=\ \ I_0\left(\frac{H}{F_0}-Ewt\right)y_{,,}\\C_2&=-I_0\left(\frac{H}{F_0}-Ewt\right)x_{,}.\end{aligned}\right\} \quad . \quad . \quad . \quad . \quad . \quad (115^a)$$

The values of $\mathfrak{o}$ under the integral signs may be considered as forces with which the horizontal projection of the arch is loaded, and $\frac{1}{l}\int_0^l \mathfrak{o}(l-x)dx$ [from equation (112)] is then the vertical reaction $\mathfrak{O}_A$ of these loads at the left support, the second part of the equation being a constant and negligible.

In equation (113) $\frac{x'}{l}\int_0^l \mathfrak{o}(l-x)dx$ is then the positive bending moment M_0 caused by the vertical reaction $\mathfrak{O}_A$ at the point $(x_{,}, y_{,})$, and $\int_0^{x_{,}} \mathfrak{o}(x_{,}-x)dx$ is the negative bending moment at that point of the vertical forces $\mathfrak{o}$ between the support and the point (x', y').

In equation (114) the first term is the positive bending moment M_0 of this same force $\mathfrak{O}_A$, when considered as acting horizontally, and the second term is the negative bending moment of the forces $\mathfrak{o}$ acting horizontally between the support and the point $(x_{,}, y_{,})$; and equations (112), (113), and (114) can be written (subscripts $_v$ and $_h$ indicating vertical and horizontal, respectively):

$$EI_0\Delta a_0=\mathfrak{O}_A, \quad . \quad . \quad . \quad . \quad . \quad . \quad . \quad . \quad (112^a)$$

$$-EI_0\Delta y=M_{0v}+C_1, \quad . \quad . \quad . \quad . \quad . \quad . \quad . \quad (113^a)$$

$$EI_0\Delta x=M_{0h}+C_2. \quad . \quad . \quad . \quad . \quad . \quad . \quad . \quad (114^a)$$

These equations permit either graphical or analytical computations of the deflections. The radius of curvature of the arch axis is usually very large, as compared with the dimensions of the arch rib, and $\mathfrak{o}$ may be made equal to the bending moment M of the arch rib reduced by $\frac{I_0}{I_{,}}$; and the deflection of the arch resulting from the change in length of the axis of the arch can be neglected, which makes C_1 and C_2 equal to zero. $-\Delta y$ is the ordinate of a recip-

rocal polygon which is drawn from a force polygon with the pole distance EI_0, this reciprocal polygon being the reduced moment area $M\frac{I_0}{I}$.

To make the computation, the value of $\mathfrak{o}$ in (111) can be expressed as follows by substituting for M its value $\mathfrak{M}-Hy$:

$$\mathfrak{o}=H\left[\left(\frac{\mathfrak{M}}{H}-y\right)\frac{I_0}{I_{\prime}}+c\right]; \quad . \quad . \quad . \quad . \quad . \quad (116)$$

$$c=\left(1-\frac{EF_0wt}{H}\right)\frac{I_0}{F_0r\cos a}. \quad . \quad . \quad . \quad . \quad . \quad (117)$$

The values of M_{0_v} and M_{0_h} of (113^a) and (114^a) can each be represented by the difference in the ordinates of two reciprocal polygons. The loads for the construction of one polygon are expressed by the value $\frac{\mathfrak{M}}{H}\frac{I_0}{I}+c$, and are obtained by drawing the moment polygon from a force polygon of the single load with a pole distance H, reducing the ordinates of this polygon in the ratio $\frac{I_0}{I_{\prime}}$, and adding to these ordinates the value of c. The latter value is so small that it is usually neglected.

The loads for the construction of the other polygon are expressed by the value $y\frac{I_0}{I_{\prime}}$, and are obtained by reducing the crdinates of the arch axis in the ratio $\frac{I_0}{I_{\prime}}$; and the polygon drawn with these values is the horizontal-thrust curve previously mentioned* [see Equations (70^c), (71), (72), and (81), and also Art. 3, Chap. VII].

---

* These ordinates of the horizontal-thrust curve are the loads on a simple beam, from which another moment polygon results. For the parabolic axis and $I_0=I\sec a$:

$$m_x=\frac{l-x}{l}\int_0^x xydx+\frac{x}{l}\int_x^l (l-x)ydx=\frac{fx}{3l^2}(x^3-2lx^2+l^3),$$

$$\int_0^l\frac{I_0}{I}y^2ds=\int_0^l y^2dx=\frac{8}{15}f^2l, \quad B\cos a=l\left(1-\frac{16}{3}\frac{f^2}{l^2}\right),$$

and for $$x=\tfrac{1}{2}l, \quad m_x=\tfrac{5}{48}fl.$$

(See Douro Bridge, Art. 20, Chap. III, and Chap. VI.)

Equations (113) and (113^a) are the same as the one which is deduced directly from the elastic deflection for the simple beam, viz., $\frac{d^2y}{dx}=\frac{M}{EI}dx$, which may be graphically computed; and the deflection curve of the arch is computed in the same manner as that of a simple beam, viz., it is the moment polygon of a simple beam, the loads for its construction being equal to the ordinates of the moment polygon resulting from the loads which cause the deflection.

(*k*) Deflections Caused by Changes in Temperature.—In equation (111) the value of M is the moment of the horizontal thrust caused by a change in temperature, or

$$M = H_t y \frac{I_0}{I_\prime} = H_t o_{\prime\prime}$$

and this value of $o_\prime$ substituted in equation (113) gives

$$-EI_0 \Delta y = H_t m_x + C_1, \quad . \quad . \quad . \quad . \quad . \quad . \quad . \quad (118)$$

where m_x is the ordinate of the horizontal-thrust curve at the point x. From equation (115^a), when $H = H_t$ and the arch is a parabola with a constant moment of inertia,

$$-C' = 2\left(Ewt - \frac{H_t}{F_0}\right) I_0 y, \text{ approx.}, \quad . \quad . \quad . \quad . \quad (119)$$

or

$$EI_0 \Delta y = H_t m_x + 2\left(Ewt - \frac{H_t}{F_0}\right) I_0 y. \quad . \quad . \quad . \quad . \quad (120)$$

(*l*) Deflection of the Crown Caused by a Yielding of the Abutments.—An increase from l to $l + \Delta l$ gives

$$\Delta y = -\frac{\Delta l}{W}\left(m_x - 2\frac{I_0}{F_0} y\right), \quad . \quad . \quad . \quad . \quad . \quad (121)$$

when

$$W = \int_0^l \frac{I_0}{I} y^2 ds + \frac{I_0 B \cos a}{F_0} \quad \text{[see also Equation } (110^b)\text{]}.$$

CHAPTER IX.

THE HINGELESS ARCH (CONTINUATION OF CHAPTER IV).

1. General Equations.—INFLUENCE OF A SINGLE VERTICAL LOAD.—In the hingeless arch the ends of the arch are rigidly held in position as explained in Chapter I. In this arch the supports may have the same or different elevations; but in the deduction of the following equations the assumption is made that the curvature of the arch axis is such that its vertical center line coincides with the center of the span.

Equations (16) and (17) are applicable in this case by extending the integration over the total length of the arch when $\Delta a_1 = 0$ (which indicates the fixed position of the ends of the arch).

The coordinate axes are drawn so that the vertical axis coincides with the center line of the span and the horizontal axis is parallel with the line joining the ends of the arch axis. It is further assumed that $J = I$ and $P' = P$, and the influences of a shifting of the abutments or of a change in temperature are neglected for the present.

Equations (16) and (17) then read

$$\left.\begin{aligned} \Delta a_{,} = 0 &= \int_0^B \frac{M}{EI} ds + \int_0^B \frac{P}{EFr} ds, \\ 0 &= \int_0^B \frac{M}{EI} y ds + \int_0^B \frac{P}{EF}\left(\frac{y}{r} ds - dx\right), \\ 0 &= \int_0^B \frac{M}{EI} x ds + \int_0^B \frac{P}{EF}\left(\frac{x}{r} ds + dy\right). \end{aligned}\right\} \quad . \quad . \quad (122)$$

The factors whose values are dependent on P are small as compared with those whose values depend on M, and the assumption may be made that $P = H$, and that $F =$ an average value F_0.

The following reductions can be made, which give very close approximations:

$$\int_0^B \frac{P}{EFr} ds = \frac{HB}{EFr}, \quad \int_0^B \frac{P}{EF}\left(\frac{y}{r} ds - dx\right) = -\frac{Hl}{EF_0},$$

$$\int_0^B \frac{P}{EF}\left(\frac{x}{r} ds + dy\right) = 0.$$

Further, $\cos a = \frac{dx}{ds}$, and $I_{,} = I \cos a$,

in which a = the angle which the axis makes with the *horizontal.*

These values substituted in the former equations give

$$\left.\begin{aligned} &\int_{-\frac{l}{2}}^{+\frac{l}{2}} \frac{M}{I_{,}} dx + \frac{HB}{F_0 r_0} = 0, \\ &\int_{-\frac{l}{2}}^{+\frac{l}{2}} \frac{M}{I_{,}} y dx - \frac{Hl}{F_0} = 0, \\ &\int_{-\frac{l}{2}}^{+\frac{l}{2}} \frac{M}{I_{,}} x dx = 0. \end{aligned}\right\} \quad \ldots\ldots \quad (123)$$

(*a*) Vertical Forces.—As described in Chapter I, M is the bending moment in the arch, which is represented by the distance (FG in Fig. XX) from the equilibrium polygon to the axis of the arch multiplied by the pole distance, which, from the very nature of its construction, is equal to H; or

$$M = H \times FG = H(FL - GJ - JL) = \mathfrak{M} - H(y + e).$$

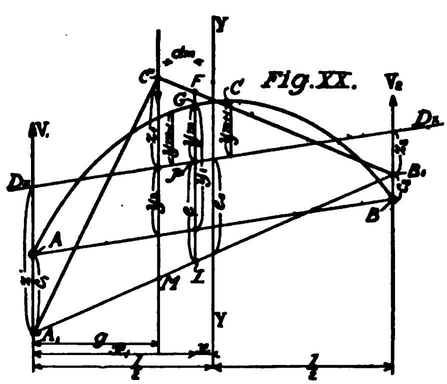

$\mathfrak{M}$ indicates again the moment of the simple beam, and $e = e_0 + \frac{c_2 - c_1}{l} x$, so that

$$M = \mathfrak{M} - Hy - He_0 - H\frac{c_2 - c_1}{l} x. \quad \ldots\ldots \quad (124)$$

For brevity these values are indicated as follows:

$$H=H, \quad X_1=H\frac{c_2-c_1}{l}, \quad \text{and} \quad X_2=He_0, \quad . \quad . \quad . \quad (125)$$

which, when substituted in (124), give

$$M=\mathfrak{M}-Hy-X_1x-X_2. \quad . \quad . \quad . \quad . \quad . \quad . \quad (126)$$

Further, from the symmetry of the arch axis with respect to the vertical axis,

$$\int_{-\frac{l}{2}}^{+\frac{l}{2}}\frac{xdx}{I_{\prime}}=0, \quad \text{and} \quad \int_{-\frac{l}{2}}^{+\frac{l}{2}}\frac{xydx}{I_{\prime}}=0,$$

and the axis D_x can be drawn so that

$$\int_{-\frac{l}{2}}^{+\frac{l}{2}}\frac{ydx}{I_{\prime}}=0. \quad . \quad . \quad . \quad . \quad . \quad . \quad . \quad (127)$$

Substituting the value of (126) in (123) gives

$$\int_{-\frac{l}{2}}^{+\frac{l}{2}}\left(\frac{\mathfrak{M}}{I_{\prime}}dx-\frac{X_2}{I_{\prime}}dx\right)+\frac{HB}{F_0r_0}=0,$$

$$\int_{-\frac{l}{2}}^{+\frac{l}{2}}\left(\frac{\mathfrak{M}}{I_{\prime}}ydx-\frac{H}{I_{\prime}}y^2dx\right)-\frac{Hl}{F_0}=0,$$

$$\int_{-\frac{l}{2}}^{+\frac{l}{2}}\left(\frac{\mathfrak{M}}{I_{\prime}}xdx-\frac{X_1}{I_{\prime}}x^2dx\right)=0.$$

Solving these equations for H, X_1, and X_2 gives

$$H=\frac{\int_{-\frac{l}{2}}^{+\frac{l}{2}}\frac{\mathfrak{M}}{I_{\prime}}ydx}{\int_{-\frac{l}{2}}^{+\frac{l}{2}}\frac{y^2dx}{I_{\prime}}+\frac{l}{F_0}}, \quad . \quad . \quad . \quad . \quad . \quad . \quad (128)$$

$$X_1=\frac{\int_{-\frac{l}{2}}^{+\frac{l}{2}}\frac{\mathfrak{M}}{I_{,}}xdx}{\int_{-\frac{l}{2}}^{+\frac{l}{2}}\frac{x^2dx}{I_{,}}}, \quad . \quad . \quad . \quad . \quad . \quad . \quad . \quad . \qquad (129)$$

$$X_2=\frac{\int_{-\frac{l}{2}}^{+\frac{l}{2}}\frac{\mathfrak{M}}{I_{,}}dx+\frac{HB}{F_0r}}{\int_{-\frac{l}{2}}^{+\frac{l}{2}}\frac{dx}{I_{,}}}. \quad . \quad . \quad . \quad . \quad . \quad . \qquad (130)$$

The values of the integrals can be determined in the same manner as was explained for the two-hinged arch (see Art. 1, Chap. VIII). The arch is divided into panels of the lengths d_m, d_{m-1}, d_{m+1}, etc., an average panel length is assumed $=d_0$, and an average moment of inertia I_0, which gives

$$v_m=\frac{d_m}{6d_0}\frac{I_0}{I'_m}(2y_m+y_{m-1})+\frac{d_{m+1}}{6d_0}\frac{I_0}{I'_{m+1}}(2y_m+y_{m+1}), \qquad (131)$$

$$v_m'=\frac{d_m}{6d_0}\frac{I_0}{I'_m}(2x_m+x_{m-1})+\frac{d_{m+1}}{6d_0}\frac{I_0}{I'_{m+1}}(2x_m+x_{m+1}), . \qquad (132)$$

$$v''_m=\frac{1}{2}\frac{d_m}{d_0}\frac{I_0}{I'_m}+\frac{1}{2}\frac{d_{m+1}}{d_0}\frac{I_0}{I'_{m+1}}, \quad . \quad . \quad . \quad . \quad . \quad . \quad . \quad . \quad . \qquad (133)$$

or, with sufficient accuracy,

$$v'_m=x_mv''_m; \quad . \quad . \quad . \quad . \quad . \quad . \quad . \qquad (134)$$

and these values substituted in equations (128), (129), and (130) give

$$H=\frac{\Sigma_0^l\mathfrak{M}_mv_m}{\Sigma_0^ly'_mv_m+\frac{I_0l}{F_0d_0}}, \quad . \quad . \quad . \quad . \quad . \quad . \quad . \qquad (135)$$

$$X_1=\frac{\Sigma_0^l\mathfrak{M}_mv'_m}{\Sigma_0^lx_mv'_m}, \quad . \quad . \quad . \quad . \quad . \quad . \quad . \quad . \quad . \qquad (136)$$

$$X_2=\frac{\Sigma_0^l\mathfrak{M}_mv''_m+H\frac{I_0B}{F_0d_0r}}{\Sigma_0^lv''_m}. \quad . \quad . \quad . \quad . \quad . \quad . \qquad (137)$$

The location of the axis DD is obtained from (127), viz.:

$$y_2=\frac{\int \frac{I_0}{I_,}y'dx}{\int \frac{I_0}{I_,}dx}=\frac{\Sigma_0^l y'_m v''_m}{\Sigma_0^l v''_m}. \quad . \quad . \quad . \quad . \quad . \quad (138)$$

When the moment of inertia is a constant, y_2 is the height of a parallelogram of the length AB whose area is equal to the area ACB.

Under the influence of a single unit load the above values can be expressed statically, as follows:

$$\Sigma_0^l \mathfrak{M}_m v_m=\frac{l-g}{l}\Sigma_0^g x'_m v_m+\frac{g}{l}\Sigma_g^l (l-x'_m)v_m=\mathfrak{M}_v^*,$$

which is the bending moment of a simple beam supporting the vertical loads v_m.

The values for $\Sigma_0^l \mathfrak{M}_m v'_m$ and $\Sigma_0^l \mathfrak{M}_m v''_m$ can be expressed in the same manner, and the graphical or analytical solution of the problem becomes very simple.

When the values of H, X_1, and X_2 are known, the vertical reactions V_1 and V_2 can be computed. If the points of support A and B have the same elevation (see Chap. I),

$$\left.\begin{aligned} V_1&=K\frac{l-g}{l}+\frac{M_2-M_1}{l}=\mathfrak{V}_1+H\frac{c_2-c_1}{l}=\mathfrak{V}_1+X_1,\\ \text{and}\qquad V_2&=\mathfrak{V}_2-X_1. \end{aligned}\right\} \quad . \quad (139)$$

$\mathfrak{V}_1$ and $\mathfrak{V}_2$ are the vertical reactions of a simple beam.

The location and direction of the components are defined by equations (135) and (139), and from these the tangent curves are derived. These equations also define the intersections of the components on the load lines, which, in turn, define the intersection locus.

(*b*) Influence of a Single Horizontal Load [see equations (75) and (76)].—When a horizontal load Q acts on the arch (see Fig. XX[a]), and when the vertical ordinate of its point of application $=q$, and its horizontal ordinate measured from $A=u$, then

$$H_h=\frac{\Sigma_0^l \mathfrak{M}'_m v_m+Q\frac{I_0 u}{F_0 d_0}}{\Sigma_0^l y_m v_m+\frac{I_0 l}{F_0 d_0}}, \quad . \quad . \quad . \quad . \quad . \quad (135^a)$$

* For explanation, see Art. 1, Chap. VIII.

$$X_{1_h}=\frac{\Sigma_0^l \mathfrak{M}'_m v'_m - Q\frac{I_0 q}{F_0 d_0}}{\Sigma_0^l x_m v'_m}, \quad . \quad . \quad . \quad . \quad . \quad . \quad . \quad . \quad (136^a)$$

$$X_{2_h}=\frac{\Sigma_0^l \mathfrak{M}'_m v''_m + H\frac{I_0 B}{F_0 d_0 r_0} - Q\frac{I_0 u}{F_0 d_0 r_0}}{\Sigma_0^l v''_m}. \quad . \quad . \quad . \quad (137^a)$$

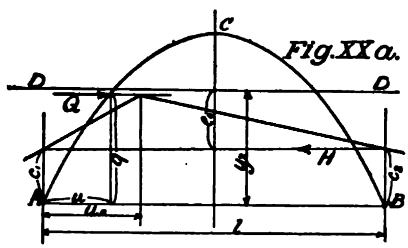

In these equations H_h is the horizontal thrust at B which is exerted inward towards the center

The bending moments at the abutments are equal to

$$M_1=Hc_1 \quad \text{and} \quad M_2=Hc_2.$$

Now,
$$c_1=y_2-e_0-\left(\frac{c_2-c_1}{2}\right),$$

so that
$$Hc_1=Hy_2-He_0-H\frac{c_2-c_1}{2}\frac{l}{l},$$

and, from equation (125),

$$\left.\begin{aligned} M_1&=Hy_2-X_2-X_1\frac{l}{2}. \\ \text{Similarly,} \qquad M_2&=Hy_2-X_2+X_1\frac{l}{2}. \end{aligned}\right\} \quad . \quad . \quad . \quad . \quad . \quad . \quad (140)$$

(*c*) Special Equations. Moment of Inertia a Constant.—When the variation in the moment of inertia of a hingeless arch is relatively small, $I_{\prime}=I \cos a$ can be safely assumed as a constant, and when the panels are made equal [see equations (131), (132), and (133)],

$$v_m=\tfrac{1}{6}(y_{m-1}+4y_m+y_{m+1}).$$

If the panel lengths are sufficiently short,

$$v_m = y_m;$$

further,
$$v'_m = x_m$$

and
$$v''_m = 1.$$

When the above assumptions are introduced in equation (137) the first term of the numerator indicates the moment of a uniformly distributed load when the panel lengths d_0 represent the unit load.

The reactions at A or B are then equal to $\frac{1}{2}l$, and the bending moment $= \frac{1}{2}lg - \frac{1}{2}g^2 = \dfrac{g(l-g)}{2}$.

The second term is a constant $= C$.

The denominator is simply equal to l, and

$$X_2 = K\frac{g(l-g)}{2l} + C,$$

$$C = \frac{HI_0B}{F_0lr};$$

and when this value which represents the secondary stress is neglected,

$$2He_0 = K\frac{g(l-g)}{l} = 2X_2, \quad . \quad . \quad . \quad . \quad . \quad (141)$$

which is equal to the ordinate on the load line of a simple moment polygon for the force K, when this polygon is drawn from a force polygon with a pole distance equal to H.

In the same manner is obtained

$$X_1 = \frac{\int_{-\frac{l}{2}}^{+\frac{l}{2}} \mathfrak{M}x\,dx}{\int_{-\frac{l}{2}}^{+\frac{l}{2}} x^2dx} = K\frac{g(l-g)}{l}\,\frac{(l-2g)}{l^2} = 2X_2\frac{l-2g}{l^2}.$$

The denominator of this equation is equal to $\dfrac{l^3}{12}$. The numerator, according to equation (136), can be represented by a beam ACB (see Fig. XXI) loaded with the positive load ACD and the negative load BCD'. (It should be remembered that the vertical axis from which x is measured is located at the center of the span.)

The vertical reaction at $A=\frac{1}{12}l^2$, and ($K=1$) its positive bending moment is $\frac{1}{12}gl^2$.

The bending moment is then equal to the moment of the reaction at A *minus* the moment of the area $ADEF$, which bending moment is equal to

$$\tfrac{2}{3}g\times\tfrac{1}{2}g^2+\tfrac{1}{2}g\times g(\tfrac{1}{2}l-g)=\{\tfrac{1}{3}g^3+\tfrac{1}{4}g^2(l-2g)\}K,$$

or
$$\Sigma_0^l\mathfrak{M}_m v'_m=\frac{K}{12}gl^2-\{\tfrac{1}{3}g^3-\tfrac{1}{4}g^2(l-2g)\}K$$

and
$$\frac{\Sigma_0^l\mathfrak{M}_m v'_m}{\Sigma_0^l x_m v'_m}=K\frac{\{gl^2-4g^3-3g^2(l-2g)\}12}{12l^3}$$

$$=K\frac{g(l-g)}{l}\,\frac{(l-2g)}{l^2}=2X_2\frac{l-2g}{l^2}.$$

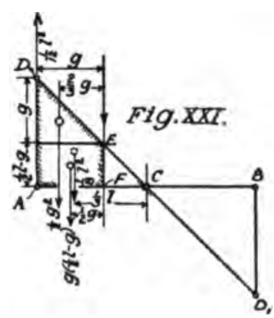

Fig. XXI.

From (125), $\quad X_1=H\dfrac{c_2-c_1}{l}\quad$ and $\quad X_2=He_0;$

so that
$$H\frac{c_2-c_1}{l}=2He_0\frac{l-2g}{l^2},$$

or
$$\frac{c_2-c_1}{2}=e_0\frac{l-2g}{l}, \qquad (142)$$

from which c_2-c_1 and e_0 can be found analytically or graphically.

Further, substituting the value of X_1 in equation (139) gives

$$V_1=\mathfrak{V}_1+X_1=K\frac{(l-g)^2(l+2g)}{l^3}, \qquad (143)$$

$$V_2=\mathfrak{V}_2-X_2=K\frac{g^2(3l-2g)}{l^3}; \qquad (144)$$

and, referring to Fig. XX, c_1, c_2, and e_0 are now known, and, as explained before, $C'M=2e_0$; all the other factors which are needed for the construction of the moment polygon are also known.

It may be observed that the vertical reactions in equations (143) and (144) correspond to the vertical reactions of a straight beam which is fixed at the ends and has a constant moment of inertia.

The ordinate z_0 measured from the axis D_x is then

$$z_0=\frac{K}{H}\frac{g(l-g)}{l}-e_0-\frac{c_2-c_1}{l}\left(\frac{l}{2}-g\right),$$

and substituting the values obtained for e_0 and (c_2-c_1) therein gives

$$z_0=8\frac{H}{K}\frac{e_0^2}{l}. \qquad (145)$$

Further, $$z_1=e_0+\frac{e_2-e_1}{2}=2\frac{l-g}{l}e_0,$$

or $$z_1=\frac{g(l-g)^2}{l^2}\frac{K}{H}=\frac{1}{2}\frac{l}{g}z_0, \qquad (146)$$

and the bending moments at the supports are

$$M_1=-H(z_1-y_2)=-K\frac{g(l-g)^2}{l^2}+Hy_2, \qquad (147)$$

$$M_2=-H(z_2-y_2)=-K\frac{g^2(l-g)}{l^2}+Hy_2. \qquad (148)$$

When the influence of the secondary stresses is neglected and the moment of inertia is a constant, equations (123) can be expressed by the following law, first enunciated by Winkler (see Fig. XX, in which D_xD_x and YY are the axes of origin):

The area ACB = area $A'C'B'$, or $\int Mdx=0$.

The moment of the area ACB = the moment of the area $A'C'B'$ with respect to two arbitrary axes, or $\int Mydx=0$ and $\int Mxdx=0$, from which it follows that the two areas ACB and $A'C'B'$ must have the same center of gravity with reference to the horizontal axis.

Winkler's Law.—For a fixed arch with a nearly uniform cross-section, that line of pressure is the true one for which the sum of the squares of its deviations from the axis of the arch is a minimum.

This law can also be derived from the theorem of least work, viz.:

$\mathfrak{A} = \int \frac{M^2}{EI_{\prime}} dx + \int \frac{P^2}{EF} ds =$ minimum; or, with the above assumptions,

$$\mathfrak{A} = \int M^2 dx = \text{minimum}.$$

(*d*) The Construction of the Components of a Vertical Load K is then a simple operation. The horizontal-thrust curve acb in Fig. XXI^a is drawn, and the intensity of K for this curve is found in the same manner as described in Chapter IV, Art. 5, etc., for the Syra Valley Bridge. The axis D_x is found from area $ABGG_1$ = area ACB.

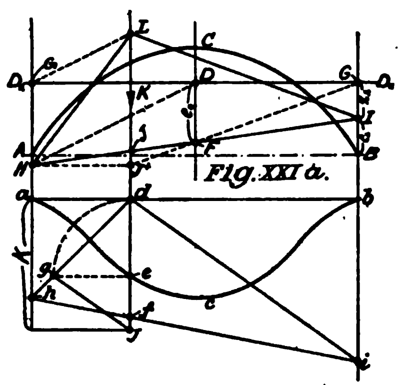

Fig. XXI a.

When the load K is placed as indicated in Fig. XXI^a, the horizontal thrust is equal to the ordinate de, and with this ordinate as a pole distance and the load K as the force, the force polygon dgJ is drawn, and from this the moment polygon dhi; the ordinate df is then equal to $2e_0$ [see equation (141)].

One half of df is then plotted from the axis D_x on the center line, giving the point F, and a line GF is drawn to an intersection with the load line, giving the point J'. Through this point the line HJ' is drawn parallel to AB, which gives the point H, and drawing the line HF, its prolongation will produce the point I on the right-hand vertical; the line HI is the true closing line of the moment polygon and the distance AH plus the distance IB is equal to $c_2 - c_1$. {See equation (142). In this case c_1 is negative and $-c_1 = -(-c_1) = +c_1$.}

To obtain the point L of the intersection locus, the line G_1L is drawn parallel to a line which joins the point D and the point H. This construction follows from the equation $LJ = 2e_0$ and also from (145), (146), etc.

(*e*) Special Equations.—*The Moment of Inertia a Constant, and the Curve of the Arch Axis that of a Flat Parabola* ($I=I_0 \sec a$).—In Fig. XXII ACB is the axis of a parabolic arch, and the area of $AA'BB'=\frac{2}{3}fl=$ area ACB, and the line $A'B'$ is the axis D_x.

The equation of the parabola is again

$$y_{,}=\frac{4f}{l^2}x(l-x), \quad y=y_{,}-\tfrac{2}{3}f=\frac{4f}{l^2}x(l-x)-\tfrac{2}{3}f, \qquad \text{and} \qquad I=\text{a constant.}$$

Introducing these values into equation (128) gives

$$H=\frac{15}{4}\frac{g^2(l-g)^2}{fl^3}\frac{K}{1+\dfrac{45}{4}\dfrac{I}{F_0f^2}} \quad . \quad . \quad . \quad . \quad . \quad . \quad (149)$$

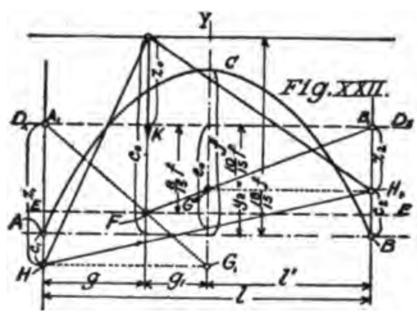

The vertical reactions at the supports are obtained from equations (143) and (144).

From (145),

$$z_0=\frac{8}{15}f\left(1+\frac{45}{4}\frac{I}{F_0f^2}\right) \quad . \quad . \quad . \quad . \quad . \quad . \quad . \quad (150)$$

From (146),

$$\left.\begin{aligned} z_1&=\frac{1}{2}\frac{l}{g}z_0, \\ z_2&=\frac{1}{2}\frac{l}{l-g}z_0. \end{aligned}\right\} \quad . \quad . \quad . \quad . \quad . \quad . \quad . \quad . \quad (151)$$

These three equations are sufficient to compute the intersection locus and the tangent curves. The term $\frac{45}{4}\frac{I}{F_0f^2}$ expresses the influence of the secondary stress, and when this is neglected,

$$z_0=\tfrac{8}{15}f, \quad . \quad . \quad . \quad . \quad . \quad . \quad . \quad . \quad . \quad . \quad . \quad . \quad . \quad . \quad (150^a)$$

or

$$c_0=z_0+y_2=\tfrac{8}{15}f+\tfrac{2}{3}f=\tfrac{6}{5}f, \quad . \quad . \quad . \quad . \quad . \quad . \quad . \quad . \quad . \quad (152)$$

which is the ordinate for the intersection locus and is a straight line.

$$c_1=-z_1+y_2=-\frac{1}{2}\,\frac{l}{g}z_0+\frac{2}{3}f=\frac{2}{15}\,\frac{f}{g}(5g-2l);$$

and, again substituting $g=kl$,

$$c_1=\frac{2}{15}f\frac{5k-2}{k} \quad \text{and} \quad c_2=\frac{2}{15}f\frac{3-5k}{1-k}. \qquad (153)$$

From these equations the intersection locus and tangent curves are drawn in Fig. 24 for a rise $f=1$ and a span $l=2$.

Horizontal Force.—Parabolic Arch with a Constant Moment of Inertia $I=I_0 \sec a$.—Following the same procedure as before,

$$c_1=\frac{2k(1-k)^2(2-7k+8k^2)}{1+k^2[-15+50k-60k^2+24k^3]}f, \qquad (154)$$

$$c_2=\frac{2(1-k^2)(3-9k+8k^2)}{15-50k+60k^2-24k^3}f, \qquad (155)$$

$$u_0=l[1-\tfrac{1}{2}(3-12k+24k^2-16k^3)]. \qquad (156)$$

In these equations $k=\frac{u}{l}$ (see Fig. XX[a]), and from them the intersection locus and tangent curves have been drawn in Fig. 31.

Equations (151) may be expressed in ordinates which are measured from the axes D_x and Y (see Fig. XXII). Then

$$\left.\begin{aligned} z_1&=\frac{8}{15}f\left(\frac{l'}{l'-g'}\right), \\ z_2&=\frac{8}{15}f\left(\frac{l'}{l'+g'}\right), \end{aligned}\right\} \qquad (151^a)$$

and putting these equations in the form

$$z_1:\tfrac{8}{15}f=l':l'-g',$$

indicates the method for constructing the components of a vertical load to be as follows:

An axis EE is drawn parallel to DD at the distance $\frac{8}{15}f$, and the lines $A_{,}F$ and $B'F$ are drawn, $A_{,}F$ being prolonged to an intersection with the axis Y; the points G and $G_{,}$ are then transferred to H' and H, and $AH=c_1$ and $BH'=c_2$.

(*f*) INFLUENCE OF A CHANGE IN TEMPERATURE AND A YIELDING OF THE ABUTMENTS.—Equations (16) and (17) are again applicable when t=change in temperature, and Δl=the increase in the span caused by a shifting of the abutments; and with the simplifications previously given,

$$\int_{-\frac{l}{2}}^{+\frac{l}{2}}\frac{M}{I_{,}}dx+(H-EF_0wt)\frac{B}{F_0r_0}=0, \quad . \quad . \quad . \quad . \quad (157)$$

$$\int_{-\frac{l}{2}}^{+\frac{l}{2}}\frac{M}{I_{,}}ydx-(H-EF_0wt)\frac{l}{F_0}=E\Delta l, \quad . \quad . \quad . \quad (158)$$

$$\int_{-\frac{l}{2}}^{+\frac{l}{2}}\frac{M}{I_{,}}xdx=0. \quad . \quad . \quad . \quad . \quad . \quad . \quad . \quad . \quad . \quad . \quad (159)$$

From equation (126), when $\mathfrak{M}=0$,

$$M=-Hy-X_1x-X_2,$$

and the horizontal axis D_x is again so chosen that

$$\int_{-\frac{l}{2}}^{+\frac{l}{2}}\frac{ydx}{I_{,}}=0 \quad \text{and} \quad c_1=c_2.$$

These values substituted in the above equations give

$$H_t=\frac{Ewtl-E\Delta l}{\int_{-\frac{l}{2}}^{+\frac{l}{2}}\frac{y^2dx}{I_{,}}+\frac{l}{F_0}}, \quad . \quad . \quad . \quad . \quad . \quad . \quad . \quad (160)$$

$$X_1=0,$$

$$X_2=\frac{HB-EF_0wtB}{F_0r\int_{-\frac{l}{2}}^{+\frac{l}{2}}\frac{dx}{I_{,}}}. \quad . \quad . \quad . \quad . \quad . \quad . \quad . \quad . \quad . \quad (161)$$

Substituting equations (131) to (133) in (160) and (161) gives

$$H_t=\frac{EI_0wtl-EI_0\Delta l}{d_0\left(\Sigma_0^l y_mv_m+\frac{I_0l}{F_0d_0}\right)}, \quad . \quad . \quad . \quad . \quad . \quad . \quad (162)$$

$$X_2=\frac{I_0BH-EF_0wt}{F_0d_0r\Sigma_0^l v''_m}. \quad . \quad . \quad . \quad . \quad . \quad . \quad . \quad . \quad (163)$$

In equation (163) the denominator is very large as compared with the numerator, and no serious error is committed when the assumptions are made that

$$X_2 = Hz_0 = 0, \quad \text{or} \quad z_0 = 0,$$

and that H_t of (162) is located on the axis D_x.

For the parabolic arch axis with a moment of inertia $I_r = I \sec a$ the value of

$$\int_{-\frac{l}{2}}^{+\frac{l}{2}} y^2 dx = \tfrac{4}{45} f^2 l,$$

in which y is measured from the axis D_x, and equation (160) or (163) becomes

$$H_t = \frac{45}{4f^2} \frac{EI_0 wt - EI_0 \frac{\Delta l}{l}}{1 + \frac{45}{4} \frac{I_0}{F_0 f^2}}; \quad . \quad . \quad . \quad . \quad . \quad (164)^*$$

and introducing from equation (150),

$$\frac{15}{8} \frac{z_0}{f} = 1 + \frac{45}{4} \frac{I_0}{F_0 f^2} \quad \text{(see Fig. XXII)}$$

gives

$$H_t = \frac{6EI_0 wt}{z_0 f} - \frac{6EI_0 \Delta l}{z_0 f l}. \quad . \quad . \quad . \quad . \quad . \quad (165)\dagger$$

The first term gives the horizontal thrust caused by a temperature change, and the second the horizontal thrust caused by a yielding of the abutments.

(*g*) DEFLECTIONS.—The deflections are again derived from the fundamental equations (15), (16), and (17). The analysis is iden-

---

* When in (164) the secondary stress is neglected, the equation becomes

$$H_t = \frac{45EI\,wt}{4f^2}. \quad . \quad . \quad . \quad . \quad . \quad . \quad . \quad . \quad . \quad . \quad (164^a)$$

When the secondary stress in the arch is assumed to act in the same manner as a decrease in temperature, this equation gives the value for H_s when $\frac{n}{E}$ is substituted for wt;

or

$$H_s = \frac{45nI}{4f^2}. \quad . \quad . \quad . \quad . \quad . \quad . \quad . \quad . \quad . \quad . \quad (164^b)$$

† For the application of equation (165) see Art. 8 (*b*), Chap. IV., Syra Valley Bridge.

tical with that described for the two-hinged arch, and it differs only from that of the hingeless arch in that the value of the ordinates y of the arch axis are measured from the axis D_x, and that there is no angular movement at the supports of the hingeless arch. Here $\Delta a_0=0$, or, in Equation (112[a]),

$$EI_0\Delta a_0=\mathfrak{D}_A=0.$$

Equation (111) may be expressed in the same manner:

$$M\frac{I_0}{I_t}+\frac{I_0}{r\cos a}\left(\frac{P}{F}-Ewt\right)=\circ. \quad . \quad . \quad . \quad . \quad . \quad (166)$$

Again, for equations (113[a]) and (114[a]),

$$-EI_0\Delta y=M\circ_v+C_1, \quad . \quad . \quad . \quad . \quad . \quad . \quad (167)$$

$$EI_0\Delta x=M\circ_h+C_2. \quad . \quad . \quad . \quad . \quad . \quad . \quad (168)$$

In these equations M represents the bending moment caused by the forces $\circ$, their vertical or horizontal directions being indicated by the inferiors v and h, respectively.

From equations (115)

$$C_1=I_0\int_{y_0}^{y_1}\left(\frac{P}{F}-Ewt\right)dy, \quad \text{and} \quad C_2=-I_0\int_{x_0}^{x_1}\left(\frac{P}{F}-Ewt\right)dx,$$

or, substituting H for P,

$$C_1=I_0\left(\frac{H}{F_0}-Ewt\right)y_1, \quad . \quad . \quad . \quad . \quad . \quad . \quad (169)$$

$$C_2=-I_0\left(\frac{H}{F_0}-Ewt\right)x_1. \quad . \quad . \quad . \quad . \quad . \quad (170)$$

In equation (166), M is the bending moment in the arch axis at the point (x_1, y_1), and when the moment polygon is obtained from a force polygon with a pole distance equal to H, this equation may be written

$$\frac{\circ}{H}=\left(m\frac{I_0}{I_t}+c\right), \quad . \quad . \quad . \quad . \quad . \quad . \quad . \quad . \quad . \quad . \quad (171)$$

and

$$c=\left(1-\frac{EwtF_0}{H}\right)\frac{I_0}{F_0 r\cos a}. \quad . \quad . \quad . \quad . \quad . \quad (172)$$

The difference between the two-hinged and the hingeless arch in the matter of computing deflections is that in the two-hinged arch the deflections are taken as the difference between the ordinates of two moment polygons, while in the hingeless arch the ordinates of one moment polygon are used.*

In these equations the influence of a change in temperature on the deflections is given.

It is often desirable, however, to determine this deflection separately, and equation (120) may be employed for this purpose, viz.:

$$EI_0\Delta y = H_t m_x + 2\left(Ewt - \frac{H_t}{F_0}\right) I_0 y_, \quad . \quad . \quad . \quad . \quad (173)$$

In this equation H_t is obtained from the general equations (160) or (162), or, when the axis of the arch is a parabola, from (165).

For all practical purposes, equation (165) is sufficiently accurate for any arch.

m_x is again the ordinate of the horizontal-thrust curve at the point x, and $y_,$ the ordinate of the axis from the line AB.

Deflection of the Crown Caused by a Shifting of the Abutments.—To obtain this deflection, equation (121) may be used [see also equation (135)]:

$$\left.\begin{aligned} \Delta y &= -\frac{\Delta l}{W}\left(m_x - 2\frac{I_0}{F_0}y_,\right), \\ \text{and} \qquad W &= \int_0^b \frac{I_0}{I} y^2 ds + \frac{I_0}{F_0}\frac{l}{d_0}. \end{aligned}\right\} \quad . \quad . \quad . \quad . \quad . \quad (174)$$

In this equation m_x is again the ordinate of the horizontal-thrust curve at the point x, and $y_,$ the ordinate of the arch axis measured from the line AB (at the crown $y_, = f$).

---

* See foot-note on page 284.

CHAPTER X.

ARCHED FRAMEWORKS.

ANALYSIS OF THE DISPLACEMENT THEORY FOR THE DETERMINATION OF STRESSES IN ARCHES.

1. Horizontal Thrust (adapted from Müller-Breslau and Melan).—Fig. XXIII shows an arched framework which is held in place by a hinge at B, but is free to slide horizontally at A. Under the influence of the load K the structure deflects and the point A will slide outward. The stresses in the members caused by this load will be those of a simple girder and they are indicated by P.

A horizontal force H is applied at A, pushing it back to its former position. The stresses in the structure caused by this force will be called u for a horizontal thrust $=1$, or Hu for the force H.

Fig. XXIII.

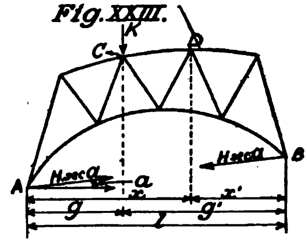

The intensity of this force in the direction of AB will be equal to $H \sec a$, and the total stress in the members will be equal to

$$S=P+Hu. \qquad (175)$$

These stresses cause changes in the length of the members of the structure, and when the length of one member $=s$, its area $=F$, and the modulus of elasticity $=E$,

$$\text{change in length}=\Delta s=\frac{sS}{EF}. \qquad (176)$$

The work performed by the interior stresses in causing this elongation is, from (175) and (176),

$$\mathfrak{L}=\tfrac{1}{2}\Sigma\Delta sS=\tfrac{1}{2}\Sigma\frac{sS^2}{EF};$$

and when $\frac{s}{F}=z$,

$$\mathfrak{L}=\frac{1}{2E}\Sigma zS^2. \quad . \quad . \quad . \quad . \quad . \quad . \quad . \quad . \quad . \quad . \quad (177)$$

As a simple girder the horizontal displacement of the point A under the influence of the load K would be equal to Δl, and when A is forced to its original position,

$$-\Delta l \cos a=\frac{d\mathfrak{L}}{d(H \sec a)}, \quad \text{or} \quad -\Delta l=\frac{d\mathfrak{L}}{dH}. \quad . \quad . \quad . \quad (178)$$

Differentiating equation (177) and substituting in (178) gives

$$-\Delta l=\frac{1}{E}\Sigma zS\frac{dS}{dH}; \quad . \quad . \quad . \quad . \quad . \quad . \quad (179)$$

differentiating (175) gives $\frac{dS}{dH}=u$ (P being a constant), and substituting this in (179) gives

$$-E\Delta l=\Sigma zSu=\Sigma zPu+H\Sigma zu^2; \quad . \quad . \quad . \quad . \quad (179^a)$$

and from this

$$H=-\frac{\Sigma zPu+E\Delta l}{\Sigma zu^2}. \quad . \quad . \quad . \quad . \quad . \quad . \quad . \quad . \quad . \quad (180)$$

The displacement Δl of the point A can be expressed in a different manner:

A load K applied at the point X will cause a displacement $=K_x g_{xa}$, and a force equal to 1 sec a applied at A will cause a displacement g_{aa}.

The force H, therefore, will cause a displacement Hg_{aa}, and

$$-\Delta l=\Sigma K_x g_{xa}+Hg_{aa},$$

from which

$$H=-\frac{\Sigma K_x g_{xa}+\Delta l}{g_{aa}}. \quad . \quad . \quad . \quad . \quad . \quad . \quad (181)$$

From equations (180) and (181),

$$\left.\begin{aligned}\Sigma zPu&=E\Sigma K_x g_{xa},\\ \text{and} \qquad \Sigma zu^2&=Eg_{aa}.\end{aligned}\right\} \quad . \quad . \quad . \quad . \quad . \quad . \quad . \quad (182)$$

From this it follows that the values under the summation signs in equation (180) are equal to the horizontal displacements at A multiplied by E, these displacements being caused by the vertically acting load K and by the horizontally acting force H.

When a change in temperature occurs at the same time, Δl must be—according to (179^a)—

$$-E\Delta l=\Sigma zPu+H\Sigma zu^2+\Sigma Ewtsu. \quad . \quad . \quad . \quad . \quad (183)$$

When only the temperature change takes place, $P=0$, or

$$-E\Delta l=H_t\Sigma zu^2+\Sigma Ewtsu,$$

from which

$$H_t=-\frac{E\Delta l+\Sigma Ewtsu}{\Sigma zu^2}. \quad . \quad . \quad . \quad . \quad . \quad . \quad . \quad (184)$$

The temperature change is assumed to take place uniformly in the whole structure, or

$$\Sigma wtsu=wt\Sigma su.$$

If in a framework, which is considered as a free body, two opposed forces of unit intensity respectively act at the panel points A and B (distant apart $s_{,}$) and in the direction of the line joining these two panel points, these forces will cause stresses u' in the members s of the framework which are expressed by the equation

$$\Sigma u's+s_{,}=0. \quad . \quad . \quad . \quad . \quad . \quad . \quad . \quad . \quad . \quad . \quad (185)$$

This is known as the law of Mohr, who first stated it.

Now in this case $s_{,}=AB=l\sec a$ and u are the stresses in the members caused by the forces $1 . \sec a$ in the direction AB, from which it follows that

$$u'=u\cos a=\frac{u}{\sec a}, \quad \Sigma u's=\Sigma\frac{us}{\sec a}, \quad \text{and} \quad s_{,}=l\sec a;$$

and these values substituted in (185) give

$$\Sigma us=-l\sec^2 a,$$

and this substituted in (184) gives

$$H_t = -\frac{E(\Delta l - wtl \sec^2 a)}{\Sigma zu^2} \quad . \quad . \quad . \quad . \quad . \quad . \quad . \quad (186)$$

Equations (180) and (181) determine the horizontal thrust caused by vertical loads, and (184) and (186) the horizontal thrust caused by temperature changes. In equation (186) $\sec a = 1$ when the two hinges are located in a horizontal plane.

To obtain the influence line of the horizontal thrust for vertical forces, a unit load should be placed successively at the different panel points of the structure, and for each position the stresses u caused by this load in the members of the structure should be computed.

The simplest way is to assume a unit vertical reaction and a unit horizontal thrust to act at the hinge A, and to compute the stresses for each in the members of the structure, the first causing the stresses s'', and the second the stresses u.

When the load is placed at a panel point which is distant x from A and x' from B, and the arch is symmetrical with respect to the vertical axis which passes through the crown, the horizontal thrust can be expressed as follows:

$$H_x = \frac{l\Sigma_0^x zs''u + x\Sigma_x^{x_1} zs''u}{l\Sigma_0^l zu^2} \quad . \quad . \quad . \quad . \quad . \quad . \quad (187)$$

In this equation Σ_0^x includes all the members between A and the point x, $\Sigma_x^{x_1}$ includes all the members between the point x and the point which is symmetrical with x on the opposite side of the crown of the arch.

For the graphical computation of H equation (181) gives for the influence of a vertical load K,

$$H = \frac{Kg_{xa}}{g_{aa}},$$

and, as explained before, g_{xa} represents the horizontal projection of the displacement of the point A which is caused by a vertical force $K=1$, and g_{aa} the horizontal projection of the displacement of A caused by a force $=1 \sec a$ acting in the direction of the chord AB.

Maxwell's law proves that the displacement of A in the direction of AB, which is caused by a unit vertical force, must be equal to the vertical deflection of the loaded panel point caused by a unit force acting in the direction of the chord at A. This law will give the influence line of H from the vertical deflections of the panel points.

Various methods may be used to determine these displacements or deflections, some being accurate and others close approximations.

(a) COMPUTATION OF DEFLECTIONS IN THE TWO-HINGED ARCH.—In Fig. XXIII a vertical force equal to 1 causes a horizontal thrust $=H_g$ at C. To find the deflection Δ_y at the panel point D caused by this force $=1$ at C, it is assumed that this unit force acts at D and causes stresses in the members $=s''_x$, the framework being considered as a simple beam freely supported at A and B. Now, $S=K(s''_g+H_g u)$ and is caused by a force K applied at the point C, and the changes in length of the members of the framework $=\frac{z}{E}S$. The principle of the equality of the external and internal work gives the equation

$$\Delta y \,.\, 1=\Sigma\frac{zSs''_x}{E}=\frac{K}{E}(\Sigma zs''_g s''_x+H_g\Sigma zus''_x)$$

and
$$\Delta y=\frac{K}{E}\left(\frac{\Sigma zs''_g s''_x}{H_g}+\Sigma zus''_x\right)H_g. \quad . \quad . \quad . \quad . \quad (188)$$

Now, $s''_x=-H_x u$ gives

$$\Sigma zus''_x=-H_x\Sigma zu^2,$$

and
$$\Delta y=\frac{K}{E}(\Sigma zs''_g s''_x-H_g H_x\Sigma zu^2). \quad . \quad . \quad . \quad . \quad . \quad (189)$$

H_g and H_x are determined by equation (187).

$\Sigma zs''_g s''_x$ is determined by assuming a vertical reaction at A and computing the stresses s'' caused by this reaction in the members of the framework, which gives

$$\left.\begin{aligned} &\text{for } g<x: \quad \Sigma zs''_g s''_x=\frac{x'g'}{l^2}\Sigma^g_0 zs^2{}_{\prime\prime}+\frac{x'g}{l^2}\Sigma^x_g zs^2{}_{\prime\prime}+\frac{xg}{l^2}\Sigma^l_x zs^2{}_{\prime\prime};\\ &\text{“} \quad g>x: \quad \Sigma zs''_g s''_x=\frac{x'g'}{l^2}\Sigma^x_0 zs^2{}_{\prime\prime}+\frac{xg'}{l^2}\Sigma^g_x zs^2{}_{\prime\prime}+\frac{xg}{l^2}\Sigma^l_g zs^2{}_{\prime\prime}.\end{aligned}\right\}(190)$$

For a full load the deflection of the crown can be found with sufficient accuracy by taking the average value of the deflections at all the panel points. Let the panels be of the same width, K the load at the panel points, n the number of panels, S the load stresses in the members of the framework caused by unit loads

at all the panels, and the deflection curve a parabola; then, from the equation for the equality of the internal with the external work,

$$\Delta y_c = \frac{3}{2}\frac{K\Sigma zS^2}{nE}. \quad . \quad . \quad . \quad . \quad . \quad . \quad . \quad . \quad . \quad (191)$$

The horizontal displacement Δx of the panel point D caused by a vertical load K at C is

$$1 \times \Delta x = \Sigma \frac{z}{E} S_0 u',$$

or

$$\Delta x = \frac{P}{E}(\Sigma z\mathfrak{s}''_0 u' + H_0 \Sigma zuu'). \quad . \quad . \quad . \quad . \quad (192)$$

Here u' represents the stresses in the members of a freely supported framework caused by a horizontal unit force acting at the panel point D.

(*b*) Deflections Caused by a Change in Temperature and Yielding of the Abutments.—To determine the vertical deflection at D (Fig. XXIII),

$$\Delta y_t = \Sigma \mathfrak{s}''_x \left(wts + \frac{z}{E} H_t u \right) = wt\Sigma \mathfrak{s}\mathfrak{s}''_x + \frac{Htzu\mathfrak{s}''_x}{E}.$$

Substituting the value of H_t from Equation (184) gives

$$\Delta y_t = wt\Sigma \mathfrak{s}\mathfrak{s}''_x - \frac{\Delta l + wt\Sigma \mathfrak{s}u}{\Sigma zu^2} \cdot \Sigma zu\mathfrak{s}''_x = wt\Sigma \mathfrak{s}\mathfrak{s}''_x - (wt\Sigma \mathfrak{s}u + \Delta l)H_x, \quad (193)$$

in which, as before,

$\mathfrak{s}$ = length of the members of the framework;
H_x = horizontal thrust caused by the unit vertical force at D.

From Mohr's law, $\Sigma \mathfrak{s}u = -l \sec^2 a$ and $\Sigma \mathfrak{s}\mathfrak{s}''_x = 0$, which changes the above equation for the deflection at D to

$$\Delta y_t = \frac{H_t}{E}\Sigma zu\mathfrak{s}''_x = \pm (wtl \sec^2 a - \Delta l)H_x.$$

The horizontal deflection of the point D caused by a change in temperature is

$$\Delta x_t = \Sigma u'\left(wts + \frac{z}{E}H_t u\right) = wt\Sigma u's + \frac{H_t \Sigma zuu'}{E},$$

or

$$\Delta x_t = \pm wt\Sigma u's \pm (wtl \sec^2 a - \Delta l)\frac{\Sigma zuu'}{\Sigma zu^2}. \quad . \quad . \quad . \quad . \quad (194)$$

In the graphical computation the object is to determine the horizontal and vertical deflections of the panel point D. The influence lines correspond to the deflection curves for a vertical or horizontal unit force acting at D.

The computation can be performed by means of a Williot Diagram, or of force and moment polygons which are derived from the deflection angles.

(c) Deflections of the Three-Hinged Spandrel-Braced Arch.—The determination of these deflections is divided into two parts (see Fig. XXIV).

First, the top chord of the arch is assumed to be continuous at the crown, which changes the three-hinged into a two-hinged arch subjected to the horizontal thrust of a three-hinged arch; and no angular movement can take place at the crown hinge.

When, however, the connection in the top chord is broken, an angular movement will occur at the crown hinge, and the two deflections thus obtained are added, giving the total deflection of the three-hinged arch.

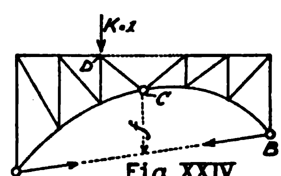

Fig. XXIV.

As a three-hinged arch the stresses in the members caused by a force $K=1$ are

$$S = s''_x + \mathfrak{H}_x u.$$

$\mathfrak{H}_x$ is then the horizontal thrust in the three-hinged arch caused by the vertical unit force K at D.

The angular movement at the crown, viz., $a_c = 0$.

These stresses have the tendency to cause a horizontal displacement at A towards the center, which may be determined from

$$g_a = \Sigma zSu = \Sigma z\mathfrak{s}''u + \mathcal{H}_x \Sigma zu^2.$$

Now,

$$\Sigma z\mathfrak{s}''u = -H_x \Sigma zu^2,$$

or

$$g_a = (\mathcal{H}_x - H_x)\Sigma zu^2 = (\mathcal{H}_x - H_x)g_a,$$

where H_x is the horizontal thrust in the two-hinged arch, and g_a the horizontal displacement of the two-hinged arch at the support caused by a unit horizontal force applied at A.

This horizontal displacement g_a cannot take place if the abutment hinges are fixed in position. When, however, the top chord is broken so that the crown hinge is free to move, the angular displacement of the crown hinge is expressed by

$$a_c = \frac{g_a}{f} = (\mathcal{H}_x - H_x)\frac{g_a}{f}. \quad . \quad . \quad . \quad . \quad . \quad . \quad (195)$$

INDEX.

PAGE

Abutments 227
  deflections in Douro Bridge caused by yielding of 99
  of hingeless arch, yielding of 158, 298
Arch
  concrete, stresses in the sections of... 179
  masonry, stresses in the section of.... 179
  reinforced concrete, determination of the section of 180, 187
  three-hinged flat parabolic, deflections of 250–256
  type, determination of 218
  wind stresses in 207
Arch bridge, live load for 212
Arches, dimensions of existing (tables), 231, 239
Arch rib
  change of form, analysis of 244
  hingeless arch, form of.............. 101
  hingeless arch, depth at crown....... 105
  solid, stresses in................... 175
  three-hinged...................... 22
Axial force 7

Bar subjected to compression and bending, stresses in................. 170
Beams
  bending moments and shearing forces in 199
  change in length of coördinates of axis of curved...................... 246
  longitudinal stresses in.............. 202
Bending and compression, stresses in bar subjected to................ 170
  moments in beams 199
Bridges, impact coefficients for......... 216

Column formulas
  Gordon's.......................... 196
  Johnson's 192, 197

PAGE

Column formulas
  reinforced-concrete 191
  steel............................ 196
  stone 191
  wood 196
Components 7
Compression and bending, stresses in bar subjected to 170
Concentrated load
  three-hinged braced arch............ 36
  three-hinged masonry arch 31
Concrete arch, stresses in the section of a. 179
Conjugate pressure on the masonry arch 118
Crescent-shaped arch (roof-truss)..... 77–82
Crescent-shaped roof-truss............. 77
  dead load 78
  snow load 79
  standard diagram for 77
  stresses, summary of 83
  temperature stresses................ 80
  tie-rods, stresses in 82
  wind pressure...................... 81
Crescent-shaped two-hinged arch
  computation of horizontal thrust in 78, 82
  horizontal forces 273
  secondary stress 275
  special equations for............ 272, 277
  temperature stresses................ 274
  vertical forces...................... 272
Curved beam, change in length of coördinates of axis 246

Dead load
  crescent-shaped roof-truss 78
  steel arch bridge 211
  three-hinged braced arch............ 14
Deflection angles (two-hinged arch)..... 60
Deflections
  and stresses in the three types of arches, comparison of........... 220

PAGE

Deflections
  Douro Bridge 92–99
  hingeless arch 159, 301
  three-hinged arch 67, 250–256
  three-hinged arch (displacement theory) 308
  two-hinged arch................. 92–99
    due to yielding of abutments...... 285
    from loads (displacement theory)... 306
    from temperature and yielding of abutments (displacement theory). 307
    general equations for 281
  two-hinged spandrel-braced arch 64
Depth of arch rib at crown, hingeless masonry arch................. 105
Dimensions of existing arches (tables), 231, 234
Displacement theory
  three-hinged arch 308
  two-hinged arch
    deflections...................... 306
    horizontal-thrust................. 302
    temperature stress................ 305
Division lines........................ 10
Douro Bridge
  deflections caused by
    horizontal forces 96
    secondary stress.................. 95
    temperature changes 97
    vertical forces................... 92
    yielding of abutments............. 99
  horizontal forces 90
  horizontal-thrust curve, construction of 85

Earth pressure and dead load, resultant of, for hingeless arch 123
Eccentricity of a force compared to its magnitude..................... 177
Elastic theory, application of 3
Electric railway bridges, live loads for (Table XV)..................... 215

Flat parabolic arch, three-hinged, deflections of 250–256
Forces of the arch, exterior............ 1
  relation between exterior forces and interior stresses 239

Highway bridges, live loads for (Table XIV)......................... 214
Hingeless arch
  arch rib, form of 101
  change of form..................... 124
  components, graphical construction of (vertical force, parabolic arch, constant moment of inertia)..... 295
  constant moment of inertia of........ 291

PAGE

Hingeless arch
  dead load and earth pressure, resultant of......................... 123
  deflections 159, 301
    caused by shrinkage of masonry, temperature or yielding of abutments 163, 299
  depth at crown.................... 105
  earth pressure and dead load, resultant of 123
  erection of........................ 159
  horizontal forces 290
  horizontal thrust, computation of 129
  intersection locus and tangent curves construction of.................. 145
    general method for determining 126
  line of pressure, analytical computation of......................... 154
  live loads.......................... 109
  masonry arch
    change of form, influence of 124
    dead loads........................ 106
    depth at crown.................... 105
    earth pressure and dead load, resultant of 123
    horizontal forces................. 118
    live loads........................ 109
    temperature and secondary stresses. 111
  moment of inertia of, special equations for constant 296
  preliminary dimensions 145
  secondary stresses.................. 111
    elimination of.................... 141
  standard diagram
    construction of................... 126
    correction of 147, 153
      application of corrections........ 151
    horizontal forces 121
    vertical forces................... 104
  Syra Valley Bridge 126
  temperature stresses 111, 156, 298
  variable moment of inertia, elimination of......................... 142
  vertical forces..................... 286
  vertical loads 106, 286, 290
    analytical computation of 108
  yielding of abutments 158, 298
Horizontal forces
  crescent-shaped arch................ 273
  Douro Bridge........................ 90
    deflections in 96
  hingeless arch 118, 290
  Syra Valley Bridge 140
  two-hinged arch 262, 268, 273
  two-hinged arch rib 41, 262
Horizontal thrust
  comparison of values obtained by various methods for two-hinged arch.......................... 89

PAGE
Horizontal thrust
computation of
crescent-shaped two-hinged arch
due to dead load ... 78
due to snow load ... 78
due to wind ... 81
in tie-rods ... 82
hingeless arch
horizontal forces ... 122, 290
moment of inertia a constant ... 291
temperature ... 111, 298
vertical forces ... 106, 129, 134, 286
yielding of abutments ... 298
special equations
Balet ... 272
horizontal forces ... 273
Melan ... 275
Schäffer ... 277
secondary stress ... 275
temperature ... 274
vertical forces ... 272
three-hinged arch rib ... 23
of masonry ... 30, 33
three-hinged spandrel-braced arch ... 15
two-hinged arch (displacement theory)
temperature ... 305
vertical and horizontal forces ... 302
two-hinged arch, general method
horizontal forces ... 90
temperature ... 91–98
yielding of abutments ... 99
two-hinged arch rib ... 40, 46, 258
due to temperature changes ... 40
two-hinged arch with parabolic axis
horizontal forces ... 268
temperature and secondary stress 269
vertical forces ... 264
two-hinged spandrel-braced arch. 53, 62
special equations for (Melan) ... 275
Syra Valley Bridge ... 129, 134
Horizontal-thrust curve
Douro Bridge ... 85
two-hinged arch ... 85–90
computation of ... 85

Impact coefficients for bridges (Table XVI) ... 216
Inertia, moment of ... 212
Intersection locus ... 8
hingeless arch
construction of ... 145
general method for determining ... 126
of masonry ... 126, 141
two-hinged arch ... 279
computation of ... 84–90
two-hinged spandrel-braced arch ... 56

Line of pressure ... 7

PAGE
Line of pressure
hingeless arch, analytical computation of ... 145
hingeless masonry arch ... 154
Line of resistance ... 8
Live loads
arch bridge ... 212
electric railway bridges (Table XV) ... 215
highway bridges (Table XIV) ... 214
hingeless arch ... 109
three-hinged arch ... 16
Live-load stresses
three-hinged braced arch ... 16
three-hinged masonry arch ... 31
two-hinged arch rib (steel shape) ... 47
Longitudinal stresses in beams ... 202

Masonry arch
stresses in the section of ... 179
three-hinged ... 29–31
Masonry arch (hingeless) ... 105–124
average moment of inertia, determination of ... 127
conjugate pressure on ... 118
deflections ... 159, 163
erection ... 159
intersection locus
correction of ... 141
determination of ... 126
line of pressure, analytical computation of ... 154
preliminary dimensions ... 145
standard diagram for ... 121
application of (corrected) ... 151, 153
correction of ... 147
tangent curves, correction of ... 141
determination of ... 126
temperature stresses in ... 156
yielding of abutments of ... 158
Masonry arch rib, three-hinged
concentrated load ... 31
live load ... 31
stresses in extreme fibers ... 34
Materials, strength of ... 206
temperature coefficients for ... 217
Moment of inertia ... 242
Moment of inertia (average)
hingeless masonry arch ... 127
Syra Valley Bridge ... 127
Moment of inertia (constant), hingeless arch ... 291
Moment of inertia (variable)
elimination of, in hingeless arch ... 142
two-hinged arch ... 75
Moment polygon
Syra Valley Bridge ... 137

Parabola, construction of, by tangent method ... 25

PAGE

Parabolic arch
three-hinged flat, deflections of, 250, 252, 256
two-hinged 264, 269
Permissible stresses in mild steel 199
Piers, intermediate 229
Pressure, line of 7

Reinforced beams, longitudinal stresses in 202
Reinforced-concrete arch
determination of the section of a.. 180, 187
stresses in 180, 182, 187
Resistance, line of 8
Rolled-steel shape, two-hinged arch made from a 42, 45
Roof-truss
crescent-shaped 77, 83
three-hinged spandrel-braced 20

Secondary stress
crescent-shaped arch 275
deflections in Douro Bridge caused by 95
hingeless arch 111
elimination of 141
Shear, maximum 10
Shearing forces in beams 199
Shrinkage of masonry, deflections of hingeless arch due to 163, 299
Snow load, crescent-shaped roof-truss... 80
Spandrel-braced three-hinged arch 13
Spandrel-braced two-hinged arch.. 51, 56-70
Special equations for two-hinged arch, 263, 272, 275, 277
Standard diagram
crescent-shaped two-hinged arch (roof-truss) 77
hingeless arch
construction of (general method)... 126
correction of 147, 153
correction of (application) 151
horizontal forces 121
vertical forces 104
hingeless masonry arch 147, 151, 153
two-hinged arch 38
construction of (general method)
horizontal forces 90
vertical forces 87
correction of 38, 56, 277, 280
horizontal forces 38
vertical forces 38
two-hinged crescent-shaped arch, vertical and horizontal forces 77
two-hinged spandrel-braced arch 56
Steel arch bridge, dead load of 211
Steel, permissible stresses in mild 199
Strength of materials 206

PAGE

Stresses
and deflections in the three types of arches, comparison of 220
distribution of, over section of steel shape 50
in a bar subjected to compression and bending 170, 174
in a concrete or masonry arch 179
in a crescent-shaped roof-truss 83
in a reinforced-concrete arch 180, 182, 187
in a solid arch rib 175
in a three-hinged braced arch
concentrated load 31
live load 16
in a three-hinged spandrel-braced arch 13
in a two-hinged arch, due to yielding of abutments 99
in beams, longitudinal 202
in extreme fibers of arch 34
in mild steel, permissible 199
in reinforced beams, longitudinal 202
maximum and minimum in an arch . 9, 11
Syra Valley Bridge
analytical solution, general 138
average moment of inertia, determination of 127
curvature (Table IX) 169
horizontal forces 140
horizontal thrust
analytical computation 134
graphical computation of 129
moment polygon, construction of 137
secondary stress, variable moment of inertia and curvature (Table VII) 167
standard units used in correction of standard diagram 169
variable moment of inertia and curvature (Table VIII) 167

Tangent curves 8
hingeless arch
construction of 145
general method for determining 126
hingeless masonry arch 126, 141
Temperature changes, deflections in Douro Bridge caused by 97
Temperature coefficients for materials... 217
Temperature stresses
crescent-shaped arch 274
hingeless arch 111, 156, 298
three-hinged arch, deflections due to.. 250
two-hinged arch 97
two-hinged arch rib 39
(steel shape) 48
two-hinged spandrel-braced arch 57
Three-hinged arch 13, 248
dead load 14

PAGE

Three-hinged arch
deflection of 67, 308
deflections
displacement theory of. 308
due to loads 251
due to temperature changes 250
due to yielding of abutments 250
of flat parabolic arch (Melan's equations). 256
(single load) 252
live load 16
spandrel-braced, stresses in 13
stresses, analytical computation of. . . . 18
Three-hinged arch rib. 22
flange stresses. 22
horizontal thrust, computation of 23
summary of stresses 27
web stresses 25
Three-hinged arch rib (masonry) 29
concentrated load 31
horizontal thrust, computation of . . 30, 33
live-load stresses 31
Three-hinged braced arch
analytical computation of stresses 18
dead-load stresses 14
live-load stresses 16
stresses due to loads 16, 31
Three-hinged spandrel-braced arch, horizontal thrust, computation of. . . . 15
Three-hinged spandrel-braced roof-truss 20
Tie-rods, crescent-shaped roof-truss. 82
Two-hinged arch 36
crescent-shaped roof-truss 77–83
deflections
approximate method for computing 42
caused by horizontal forces. 96, 306
caused by secondary stress 95
caused by temperature changes 97
caused by vertical forces. 92, 306
caused by yielding of abutments, 99, 285, 307
(displacement theory of) 306
general equations for 281
Douro Bridge 84, 99
horizontal forces 262, 268, 273
horizontal thrust. 258
computation of (displacement theory) 302, 305
computation of (general method), 90, 91, 98, 99
horizontal-thrust curve, construction of
horizontal forces 90
vertical forces. 85
integrals, determination of. 259
intersection locus
computation of
horizontal forces (general method) 90
vertical forces (general method). . 84
correction of. 279

PAGE

Two-hinged arch
special equations. 263
Balet 272
Melan. 275
Schäffer. 277
standard diagram
construction of 87, 90
correction of 38, 56, 277, 280
horizontal forces 38
vertical forces. 38
stress analysis of 39
stresses in crescent-shaped. 272–275
temperature and secondary stress 269
temperature stresses. 97
displacement theory 305
general equations 274, 280
vertical forces 260, 272
with parabolic axis, computation of horizontal thrust in 264, 269
with variable moment of inertia. 75
yielding of abutments of (general equations) 281, 285
Two-hinged arch rib
horizontal forces 41, 262
horizontal thrust in, computation of, 40, 46, 258
standard diagram for 38
stress analysis of 39
summary of stresses in. 28
temperature and secondary stresses. . 39
vertical forces. 260
Two-hinged arch rib (rolled-steel shape)
distribution of stresses over section. . . 50
example of. 42, 45
live-load stresses 47
temperature stresses. 48
Two-hinged crescent-shaped arch
computation of horizontal thrust in 78, 82
special equations for. 272–277
standard diagram, vertical and horizontal forces. 77
Two-hinged spandrel-braced arch. 51
deflection angles 60
deflections of 64
example of 70
horizontal thrust in 53, 62
special equations for computing (Melan) 275
intersection locus, construction of 56
standard diagram, correction of 56
temperature stresses, computation of . 57
Williot Diagram. 53
with curved upper chord 59
Type of arch, determination of. 218

Vertical forces
crescent-shaped arch. 272
deflections in Douro Bridge caused by 92

PAGE
Vertical forces
hingeless arch...................... 286
two-hinged arch............... 260, 272
Vertical loads on hingeless arch 106, 286, 290
analytical computation of........... 108

Williot Diagram (two-hinged arch)..... 53
Wind girder
in cylindrical surface of arch......... 209
under floor system, resisting all wind pressure...................... 207
Wind pressure on crescent-shaped roof-truss.......................... 81
Wind stress in arches................. 207

Yielding of abutments
deflections in Douro Bridge caused by. 99
deflections of three-hinged arch...... 251
of hingeless arch............... 158, 298
deflections due to............ 163, 299
of two-hinged arch (general equations), 281, 285